THE

# American Journal of

# ANATOMY


MANAGING EDITOR

DONALD DUNCAN

The University of Texas
Medical Branch
Galveston Texas

ASSOCIATE EDITORS

Burton L. Baker
University of Michigan

Sam L. Clark, Jr.
Washington University

C. P. Leblond
McGill University

Richard J. Blandau
University of Washington

Don W. Fawcett
Harvard University

Harland W. Mossman
University of Wisconsin



VOLUME 113

JULY SEPTEMBER NOVEMBER 1963

PUBLISHED BY

THE WISTAR INSTITUTE OF ANATOMY AND BIOLOGY

PHILADELPHIA PA

# CONTENTS

## No. 1 JULY 1963



## No. 2 SEPTEMBER 1963

# Blood Vessels of the Chicken's Uterus (Shell Gland)[1]

S. L. FREEDMAN AND P. D. STURKIE
*Physiology Section, Department of Poultry Science*
*Rutgers, the State University, New Brunswick, New Jersey*

Barkow (1829) in his study of the cloacal blood supply of several avian species, detailed the pelvic branches of the aorta. Kaupp ('18) and Mauger ('41) also investigated the circulatory pattern of these same arteries but neither study is as well documented as that of Barkow.

The vascular supply of the avian oviduct has received scant anatomical attention, but Barkow (1829), Stresemann ('27) and Mauger ('41) did provide information on this point. It is the purpose of this report to describe in detail the major arteries and veins of the hen's pelvis with special emphasis on the uterine (shell gland) blood vessels. A new nomenclature is presented to correlate with the findings of this study.

## MATERIALS AND METHODS

Dissections were conducted on 86 laying White Leghorn hens. Visualization of the blood vessels was facilitated by the injection of colored latex solutions into the arteries and veins.

Red latex was introduced into the arterial circulation through the aorta, and the venous circulation received blue latex via both the femoral and coccygeo-mesenteric veins. The latex solutions were delivered through polyethylene catheters secured to their respective blood vessels. Latex was withdrawn into a 10 ml plastic syringe attached to an appropriate catheter and manually propelled into the blood vessel. Pressure was maintained on the syringe until the latex injection was completed on the posterior portion of the oviduct. To prevent the media from escaping, catheters were removed after the blood vessels were ligated. Specimens were submerged in a bath of running water until the latex solidified. Details of the latex injection procedure are given by Freedman ('62).

## RESULTS

The circulatory pattern representative of the majority of dissections is presented in figures 1 and 2. Deviations from the vascular distribution ascertained in this study have been shown by Freedman ('62).

The major arterial branches of the aorta in the uterine region of the oviduct are illustrated in figure 1. The sciatic arteries arise from the descending aorta at the level of the middle lobes of the kidneys and course laterally to pass between the middle and posterior lobes of each kidney. Two renal arteries originate from each sciatic artery as it passes through the parenchyma of the kidney (fig. 2 C and D). One of these arteries supplies the middle lobe of the kidney and the other supplies the posterior lobe.

A third blood vessel, the hypogastric artery, arises at the origin of the two renal arteries from the left sciatic artery (fig. 2, E). This artery, which supplies the utero-isthmus region of the oviduct, will be discussed more fully in the section of this paper concerning the uterine vasculature.

The continuation of the aorta, caudal to the origin of the sciatic arteries, is termed the middle sacral aorta. The unpaired posterior mesenteric artery originates from the middle sacral aorta, at the caudal border of the posterior lobes of the kidneys. Just caudad to the origin of the posterior mesenteric artery, the aorta has its final bifurcation, giving rise to the internal iliac arteries. The aorta continues toward the tail on the ventral surface of the lumbosacral and coccygeal vertebrae and is designated as the middle coccygeal aorta.

The internal iliac arteries are branches of the middle sacral aorta that arise within 1.5 cm of the origin of the posterior

[1] Paper of the Journal Series, New Jersey Agricultural Experiment Station, Department of Poultry Science, supported by NSF Grant (G-13137).

mesenteric artery The internal iliac ar teries course obliquely toward the tail and bifurcate into two branches on the ventral surface of lumbosacral vertebra 14 The artery that courses medially from the bifurcation is designated the pelvic artery and the artery that courses laterally the pudendal artery

The pudendal artery courses obliquely across the ventral surface of the depressor

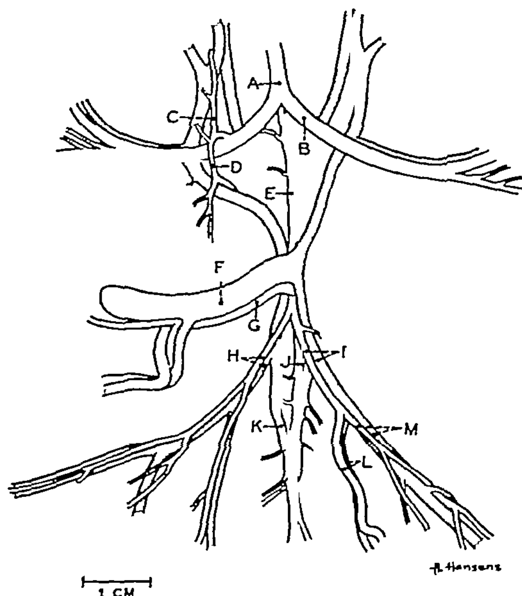



Fig. 1 Ventral view of the vascular system of the pelvic region, after surrounding tissue has been dissected way The arterial system is represented by white and the venous system by black.

*Abbreviations*

A, Aorta
B, Left sciatic artery
C, Right middle renal artery
D Right posterior renal artery
E, Middle sacral *aorta*
F Coccygeo-mesenteric vein
G Posterior mesenteric artery
H Right internal iliac artery and vein
I, Left internal iliac artery and vein
J Middle coccygeal aorta
K, Right coccygeal vein
L, Left pelvic artery and vein
M, Left pudendal artery and vein

coccygeus muscle and bifurcates at the lateral border of this same muscle. The lateral branch of the pudendal artery courses with the pudendal nerve through the pelvic cavity to the border of the ilium, continues caudally medial to the semimembranous muscle, and emerges in the cloacal region between the levator ani and cruralis caudalis muscles. At its termination this artery supplies the cloacal muscles, posterior abdominal wall muscles, anus skin, and fat deposits of the cloacal region.

The medial branch of the pudendal artery traverses the lateral border of the depressor coccygeus muscle and courses toward the posterior body wall. Before this artery exits from the abdominal cavity it divides into two branches the first is a lateral branch that terminates in the body wall dorsolateral to the cloaca. The other branch follows the contour of the urostilus and supplies the rectrices.

The pelvic artery courses ventromedially from the bifurcation of the internal iliac artery and travels in apposition with and

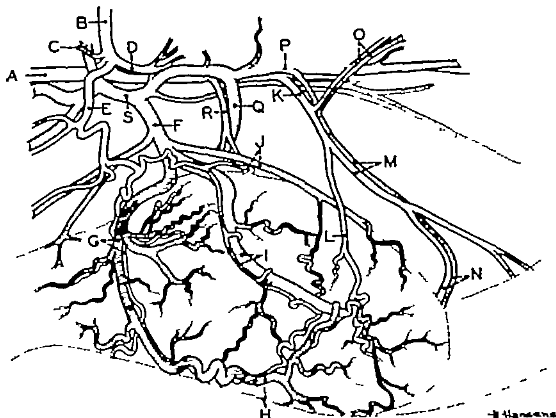



Fig. 2 Lateral view of the blood vessels to the uterine portion of the hen oviduct. The arterial system is in white and the venous system is shaded. Drawn to scale.

**Abbreviations**

A, Aorta
B Left sciatic artery
C, Left middle renal artery
D Left posterior renal artery
E, Hypogastric artery
F Hypogastric vein
G Anterior uterine artery and vein
H, Inferior uterine artery and vein
I, Lateral uterine artery and vein
J Superior uterine artery and vein
K, Left internal iliac artery
L, Middle uterine artery
M, Left pelvic artery and vein
N Posterior uterine artery and vein
O Left pudendal artery and vein
P Coccygeal vein
Q, Coccygeo-mesenteric vein
R, Posterior mesenteric artery
S, Left renal revehens (efferent) vein

mesenteric artery The internal iliac arteries course obliquely toward the tail and bifurcate into two branches on the ventral surface of lumbosacral vertebra 14 The artery that courses medially from the bifurcation is designated the pelvic artery and the artery that courses laterally the pudendal artery

The pudendal artery courses obliquely across the ventral surface of the depressor

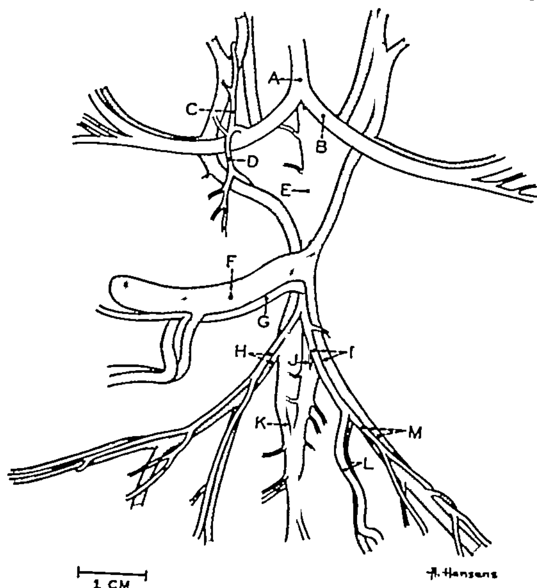



Fig. 1 Ventral view of the vascular system of the pelvic region, after surrounding tissue has een dissected away The arterial system is represented by white and the venous system by black.

*Abbreviations*

Aorta
Left sciatic artery
Right middle renal artery
Right posterior renal artery
Middle sacral aorta
Coccygeo-mesenteric vein

G, Posterior mesenteric artery
H, Right internal iliac artery and vein
I, Left internal iliac artery and vein
J Middle coccygeal aorta

K, Right coccygeal vein
L, Left pelvic artery and vein
M Left pudendal artery and vein

second possible exception is the hypogastric vein, which is the largest blood vessel draining the shell gland. The anterior lateral, and superior uterine veins anastomose to form this vein which empties into the revehens vein of the left kidney The hypogastric vein drains the region supplied by the hypogastric artery but does not coincide with the identical pathway of the artery

## DISCUSSION

The blood vessels of the pelvic region have previously received some attention as a corollary of other studies for example the investigation of ovarian vascularization in the hen by Nalbandov and James (49) Barkow's (1829) all-but-forgotten study presents some detailed reports of the arterial supply of the cloaca. We cannot agree, however with Barkow's report of blood being supplied to the uterus from both sides of the body The 16 uterine arteries named by Barkow cannot be interpreted without a diagram, which does not accompany his report. Kaupp ('18) has named several more arteries and veins than can be ascertained from his photographs. Also, the posterior mesenteric artery has been incorrectly shown by Kaupp ('18 fig 61B) as originating bilaterally Mauger's (41) study of the oviductal circulation was too schematic to be useful in physiological investigations. However his figure 2 shows the origin of the anterior middle and posterior uterine arteries without indicating that they supply the shell gland. Bradley and Grahame ('60) have used the term hypogastric to denote several different blood vessels. In an effort to avoid ambiguity and to give each blood vessel a separate and suitable designation, the premise advocated by Schreiber ('60) has been adopted. Each artery vein, and nerve that travels in juxtaposition is similarly named. Since the blood vessels have received various names in the literature (tables 1 and 2) the less-conflicting terminology proposed to the autonomic and peripheral nerves by Freedman ('64) is the basis for the nomenclature of the blood vessels.

The major branches of the aorta are similarly named (table 1) whereas the arteries of the posterior lumbosacral and coccygeal region are variably named, if identified at all. The final bifurcation of the descending aorta in the chicken has been termed either the internal iliac or hypogastric arteries. There has been a great deal of confusion over this designation, since two texts on the anatomy of the fowl (Kaupp, 18 and Bradley and Grahame '60) have given these vessels several names. Also these same terms have been used for blood vessels of the kidneys.

In man, the hypogastric and internal iliac arteries and veins are synonymous. Since the hen has a distinct hypogastric nerve, the blood vessel accompanying the nerve is also designated hypogastric. Hence the arteries originating from final bifurcation of the aorta will be given the alternative designation of internal iliac arteries. The two arteries that arise from the bifurcation of each internal iliac artery and the accompanying vein are named for the nerves that they accompany The lateral branch is termed the pudendal artery and the medial branch the pelvic artery

The venous drainage from the shell gland poses an intriguing problem since the direction of blood flow in the coccygeomesenteric vein has not been firmly established. The blood from the uterus may flow into the coccygeo-mesenteric vein and away from the kidneys or flow along with blood supplied by a renal portal system and traverse the efferent renal vein.

Changes in the uterine blood flow of the hen during egg formation have been reported by Hunsaker ('59) The physiological mechanisms governing the blood supply of the shell gland deserve more attention in view of the possible connection of the uterine veins and the renal portal system in the hen.

## SUMMARY

The blood vascular pattern of the chicken's uterus has been studied in 86 White Leghorn hens. Gross dissections were facilitated by the injection of colored latex into the arteries and veins.

The major branches of the aorta and their corresponding veins in the uterine region of the oviduct, were also studied. A new nomenclature is presented [illegible]

TABLE 1

*Arteries of the chicken's pelvic region*

| Nomenclature of Freedman and Sturkie | Barkow (1856) | Kaupp (1918) | Magee (1941) | Nalbandov and James (1949) | Bradley and Grahame (1960) |
|---|---|---|---|---|---|
| Sciatic | Ischiadic | Ischiadic | Sciatic | Sciatic | Sciatic |
| Middle sacral | Sacralis media | Sacralis media | Middle sacral | Caudal | Middle sacral |
| Posterior mesenteric | Mesenterica posterior | Posterior mesenteric | Posterior mesenteric | Posterior mesenteric | Caudal mesenteric |
| Middle coccygeal | Median coccygeal and coccygea communis | Median coccygeal | | | |
| Hypogastric | Designation not clear | Described but not named | Described but not named | | Designated but not named |
| Internal iliac | Hypogastric | Pudenda communis and hypogastric | Internal iliac | Internal iliac | Hypogastric |
| Pelvic | Internal iliac | Hemorrhoidalis intima | | | |
| Pudendal | Rami musculares of hypogastric | Pudenda externa | | | |

TABLE 2

*Veins of the chicken's pelvic region*

| Nomenclature of Freedman and Sturkie | Kaupp (1918) | Stresemann (1927) | Gordeuk and Grundy (1950) | Hunsaker (1959) | Bradley and Grahame (1960) |
|---|---|---|---|---|---|
| Coccygeo-mesenteric | Coccygeo-mesenteric | Coccygeo-mesenteric | Coccygeo-mesenteric | | Coccygeo-mesenteric |
| Hypogastric | | Described but not named | | Described but not named | Described but not named |
| Internal iliac | Iliaca interna, coccygea and hypogastric | Hypogastrica | Coccygea | | Internal iliac |
| Pelvic | Pudenda | | Pudenda and cutanea | | Pudendal and cutaneus |
| Pudendal | Cutanea publica | | | | |
| Coccygeal | Coccygea | | | | |

Not differentiated as to which vessel was the pelvic and which was the pudendal.

attempt to reconcile the disparity of terms previously used for these blood vessels and also to include the new blood vessels identified.

Blood is supplied to the hen's uterus by three arteries, all of which originate from the left side of the body. The hypogastric artery, a branch of the left sciatic artery, provides the anterior portion of the uterus. The hypogastric artery bifurcates into an anterior uterine and superior uterine artery. Lateral and inferior uterine arteries originate from the anterior uterine artery on both surfaces of the uterus. The venous system and its modifications from the arterial pattern are described and discussed.

## LITERATURE CITED

Barkow H. 1829. Anatomisch-physiologische Untersuchungen vorzüglich über das Schlagadersystem der Vögel. Arch. f. Anat. U Physiol. (Meckel'). 305–496.

Bradley O. C., Revised by T. Grahame. 1960. The Structure of the Fowl. 4th Edition. Oliver and Boyd, Edinburgh and London.

Freedman, S. L. 1962. Innervation and blood vessels to the uterus of the chicken. Doctoral dissertation, Rutgers University.

Freedman, S. L., and P. D. Sturkie. 1964. Extrinsic nerves of the chicken uterus (shell gland). In press.

Gordeuk, S., Jr., and M. L. Grundy. 1950. Observations on circulation in the avian kidney. Am. J. Vet. Res., *11*: 256–259.

Hunsaker, W. G. 1959. Blood flow and calcium transfer through the uterus of the chicken. Doctoral dissertation, Rutgers University.

Kaupp, B. F. 1918. Anatomy of the Domestic Fowl. W. B. Saunders Co., Philadelphia and London.

Mauger, H. M., Jr. 1941. The autonomic innervation of the female genitalia in the domestic fowl and its correlation with the aortic branching. Am. J. Vet. Res., 2: 447–452.

Nalbandov, A. V. and M. F. James. 1949. The blood-vascular system of the chicken ovary. Am. J. Anat., 85: 347–378.

Schreiber, J. 1960. Problems of veterinary anatomical nomenclature. Brit. Vet. J. *116*: 1–14.

Stresemann, E. 1927. Handbuch der Zoologie. Volume VII, Part 2. Walter de Gruyter and Co., Berlin and Leipzig.

# Morphogenetic Studies of the Rabbit

## XXXII. QUALITATIVE SKELETAL VARIATIONS INDUCED BY THE AC GENE (ACHONDROPLASIA)

D. D. CRARY AND P B SAWIN
*Roscoe B Jackson Memorial Laboratory Bar Harbor Maine*

An exhaustive examination of the pathology of the various tissues and organs of recessive lethal achondroplasia (*ac*) in the rabbit, made by Pearce and Brown in 45 (Brown and Pearce, 45 Pearce and Brown, 45a, 45b) failed to reveal evidence to account for the anomaly Histologically the skeleton showed the abnormalities of the long bones to be similar to those of chondrodystrophies in other species. Other references to skeletal changes were broad and general. Roentgenographic study of newborn animals was made but, due to the low calcium content of bone at this age and the retarded development of *acac* animals, it failed to reveal all the defects induced by this gene. More recently in a collection of alizarin stained specimens derived from stock (AC) obtained from the Rockefeller Institute in '53 we have noted a number of effects not previously described. The present paper deals with the qualitative aspects of the gene and discusses them in relationship to localization of effect and to a possible interpretation of the primary gene action.

### MATERIALS AND METHODS

Animals used in this investigation were 339 new born *acac*s ranging in age from 28 to 35 days postcopulation (pc) and 237 phenotypically normal (*Ac*) animals of the same race and age. Alizarin stained skeletons of each were examined under a dissecting scope for ossification of elements, relative degree of development of each vertebral formula, and any abnormalities that might exist.

Pearce and Brown reported a preponderance of females in their sample. Our first observations, based on external genitalia seemed to confirm this. However examination of gonads showed no significant departure from expected equality It is assumed therefore, that the earlier discrepancies were due to the relative immaturity of the specimens.

### OBSERVATIONS

In phenotypically normal (*Ac*) rabbits born at term (31 days pc) all of the primary ossification centers of the bones except carpals and most tarsals are ossified and well developed (fig 9) In addition to the primary centers all animals examined had epiphyses of the distal femur, proximal tibia proximal and distal humerus and 62% had that of proximal femur By 32 days pc all other epiphyses of the major long bones except that of proximal fibula may be present. This is somewhat in advance of races III and X (Crary and Sawin, 49) in which only the first four mentioned epiphyses appear before 34 to 36 days. However the order of appearance is essentially the same. The tibia and fibula are fused for the distal two-thirds of their length Fusion of vertebral centra with neural arches has been initiated only from vertebra 28 or 29 on.

Normal animals of the AC race possess 26 presacral vertebrae (7 cervical 12 thoracic and 7 lumbar) and from 15 to 18 caudal vertebrae Variation from this pattern occurs as in increase in rib number at the thoracolumbar border in only 5% of the animals with the extra pair of ribs very poorly expressed. By contrast, other races may show a well developed

---

This investigation was supported (in part) by PHS research grant C881C from the National Cancer Institute, National Institutes of Health, Public Health Service, and in part by grant from the American Cancer Society The authors wish to express their appreciation to Eugene Farrin and Adelaide Concerne for their assistance in the preparation of specimens and illustrations.

## LITERATURE CITED


Arey L. B 1954 Developmental Anatomy 6th ed. W B Saunders Co., Philadelphia.

Backman, G 1934 Die Abhängigkeit morphologischer Variationen von Differenzierungs und Wachtumsgradienten Anat. Anz., 78 78–87

Behrle F C., D M. Gibson and H C. Miller 1951 Role of hyaline membranes blood, exudate edema fluid and amniotic sac contents in preventing expansion of the lungs of new born inf ts. Pediatrics, 7 782–792.

Briggs, J N and Georgina Hogg 1958 Peri n tal pulmonary pathology Ibid., 22 41–48.

Brown, W H and Louise Pearce 1945 Hereditary achondroplasia in the rabbit. I. Physical appearance and general f atures. J Exp. Med., 82 241 260.

Bruce J A. 1941 Time and order of ppearance of ossific tion centers and their development in the skull f the rabbit. Am. J Anat., 68 41–67

Carter T C. 1954 The genetics f luxate mice. IV Embryology J Genet., 52: 1–35

Chang, T K. 1949 Morphological study on the skeleton of the Ancon sheep. Growth., 13 269–297

Child, C. M. 1925 The physiological significance of the cephalocaudal differential in vertebrate dev lopment. Anat. Rec 31 369–383.

Crary D. D and P B Sawin 1949 Morphogenetic tudies of the rabbit. VI. Genetic fac tors influencing the ossific tion pattern of the limbs. Genetics, 34 508–523

——— 1955 Morphogenetic studies of the rabbit. XIV Manifestations of regional growth t onset of vertebral ossification. J Heredity 46 183–189

——— 1957 Morphogenetic studies of the rabbit. XVIII. Growth of ossification centers f the vertebral centra d ring the twenty-first day Anat. Rec 127 131 150

Crary D D P B Sawin nd N ncy Atkinson 1958 Morphogenetic studies of the rabbit. XXI. The nature of disproportionate dwarfism induced by the DA gene revealed by the early fetal ossification pattern. Am. J Anat., 103 69–97

Crew F A. E. 1924 The bulldog calf contribution to the study of achondroplasia. Proc Roy Soc. Med., 17 39–58.

Curry G. A. 1959 Genetical and developmental studies on droopy-eared mice. J Embryol. and Exp. Morphol., 7 39–65.

Danforth, C. H. 1930 Numerical variations and homologies in vertebrae Am. J Phys Anthrop., 14 463–481

Dwight, T 1901 Description of the human spines showing numerical variation in the Warren Museum of the Harvard Medical School. Mem. Bost. Soc. N t. Hist., 5 237–312.

Forsthoefel P F 1959 The embryological development of the skeletal effects of the luxoid gene in the mouse including its interaction with the luxate gene. J Morph., 104 89–141

Green, E. L. 1941 Genetic and non-genetic factors which influence the type of the skeleton in an inbred strain of mice. Genetics 26 192–222.

Green, M. C. 1951 Further morphological effects of the short ear gene in the house mouse. J Morph., 88 1 22.

——— 1955 Luxoid — a new hereditary leg and foot abnormality in the house mouse. J Heredity 46: 91–99.

Grüneberg, H. 1943 Congenital hydrocephalus in the mouse se of spurious pleiotropism. J Genet., 45 1 21.

Hoof Diane 1959 The effects of the achondroplasia (ac) gene on the skull development in the rabbit. Student thesis, The Jackson Laboratory Bar Harbor Maine

Hull Inez B. 1947 Morphogenetic studies of the rabbit. IV The inheritance of developmental patterns of rib ossification. J Exp. Zool 105 173–197

Huxley J S. 1932 Problems of Relative Growth. Lincoln MacVe gh, London. Dial Press, N Y

Knöbcke F 1929 Bemerkungen zur Wirbelsäule des Chondrodystrophen. Beitr z. path. Anat. u. z. allg. P th., 81 547–567

Kühne K. 1931 Die Vererbung der Variationen der menschlichen Wirbelsäule. Zeit. Morph. u. Anthr 30 1 221

Landauer W 1931 Untersuchungen über das Krüperhuhn. II. Morphologie und Histologie des Skelets insbesondere des Skelets der langen Extremitätenknochen. Zeitschr für mikros. anat. Forschung 25 115–180.

——— 1934 Studies on the creeper fowl. VI. Skeletal growth. Bull. 193 Conn. State College Storrs, Conn.

——— 1935 A lethal m tation in dark Cornish fowl. J Genet., 31 237 242.

——— 1940 The nature of disproportionate dwarfism with special reference to fowl. Sigma XI Quarterly 28 1–10.

Lipsett, J C. 1941 Disproportionate dwarfism in Amblystoma. J Exp. Zool., 86 441–459

O'Rahilly R. 1951 Morphological patterns in limb deficiencies and duplications. Am. J. Anat., 89 135–191

——— 1956 Developmental deviations in the carpus and the tarsus. Clin. Orthoped., 10 9–18.

P tten, A. R. 1937 A comparison of the glycine content of the proteins of normal and chondrodystrophic chick embryos t different stages of development. J Nutrition, 13 123–130.

Pearce Louise and W H. Brown 1945a Hereditary achondroplasia in the rabbit. II. Pathologic aspects. J Exp. Med., 82 261 280.

——— 1945b Hereditary achondroplasia in the rabbit. III. Genetic aspects, general considerations. Ibid., 82: 281 295.

Rudolph A. M., J E. Drorbaugh, A. M. Auld, A. J Rudolph A. S. Nadas, C. A. Smith and J P H bbell 1961 Studies on the circulation in the neonatal period. The circulation in the respiratory distress syndrome. Pediatrics, 27 551–566.

Sawin, P B. 1937 Preliminary studies of hereditary variation in the axial skeleton of the rabbit. Anat Rec., 69 407–428.

——— 1945 Morphogenetic studies of the rabbit. I. Regional specificity of hereditary factors affecting homoeotic ariations in the axial skeleton. J Exp. Zool., *100*: 301–329
Sawin, P B and D D Crary 1956 Morphogenetic studies of the rabbit. XVI. Quantitative racial differences in ossification pattern of the vertebrae of embryos as an approach to basic principles of mammalian growth. Am. J Phys. Anthrop., *14*. 625–648.
——— 1957a Morphogenetic studies of the rabbit. XVII. Disproportionate adult size induced by the DA gene. Genetics, 42 72–91
——— 1957b Bipartite centra at onset of ossification in two races of rabbits. Abstract. Anat. Rec., *127* 362.
Sawin, P B., and Inez B. Hull 1946 Morphogenetic studies of the rabbit. II. Evidence of regionally specific hereditary factors influencing the extent of the lumbar region. J Morph., 78 1 26.
Sawin, P B D. D. Crary and Judith Webster 1959 Morphogenetic studies f the rabbit. XXIII. The effects of the dachs gene DA (chondrodystrophy) upon linear and lateral growth of the skeleton as influenced in time. Genetics, 44. 609–624
Sawin, P B Mary Ranlett and D D Crary 1962 Morphogenetic studies of the rabbit. XXIX. Accessory ossification centers at the occipito-vertebral border in the dachs rabbit. Am. J Anat., *111* 239–257
Stockard, C. R. 1941 The genetic and endocrine basis for differences in form and behavior Wistar Inst. Anat. and Biol. Phila.
Tanner J M., and P B. Sawin 1953 Morphogenetic studies of the rabbit. XI. Genetic differences in the growth of the vertebral column and their relation to growth and development in man. J Anat., 87 54–65.
Thompson, D'A. W 1948 On Growth and Form. University Press, Cambridge. MacMillan Co., New York.
Zwilling, E. 1956 Reciprocal dependence of ectoderm and mesoderm during chick embryo limb development. Amer N t., 90 257–265.

## LITERATURE CITED


Arey L. B. 1954 Developmental Anatomy 6th ed. W. B. Saunders Co., Philadelphia.

Backman, G. 1934 Die Abhängigkeit morphologischer Variationen von Differenzierungs und Wachtumsgradienten. Anat. Anz., 79 78–87

Behrle F. C., D. M. Gibson and H. C. Miller 1951 Role of hyaline membranes, blood, exudate edema fluid and amniotic sac contents in preventing expansion of the lungs of new born infants. Pediatrics 7 782–792.

Briggs J. N. and Georgia Hogg 1958 Perinatal pulmonary pathology. Ibid., 22 41–48.

Brown W. H., and Louise Pearce 1945 Hereditary achondroplasia in the rabbit. I Physical appearance and general features. J. Exp. Med., 82 241 260.

Bruce J. A. 1941 Time and order of appearance of ossification centers and their development in the skull of the rabbit. Am. J. Anat., 68 41–67

Carter T. C. 1954 The genetics of luxate mice IV Embryology J. Genet., 52 1–35.

Chang, T. K. 1949 Morphological study on the skeleton of the Ancon sheep. Growth., 13 269–297

Child, C. M. 1925 The physiological significance of the cephalocaudal differential in vertebrate development. Anat. Rec. 31 369–383.

Crary D. D. and P. B. Sawin 1949 Morphogenetic studies of the rabbit. VI. Genetic factors influencing the ossification pattern of the limbs. Genetics, 34 508–523.

——— 1955 Morphogenetic studies of the rabbit XIV Manifestations of regional growth t onset of vertebral ossification. J. Heredity 46 183–189

——— 1957 Morphogenetic studies of the rabbit. XVIII. Growth of ossific tion centers of the vertebral centra during the twenty first day Anat. Rec 127 131 150

Crary D. D. P. B. Sawin and Nancy Atkinson 1958 Morphogenetic studies of the rabbit. XXI. The nature of disproportionate dwarfism induced by the DA gene revealed by the early fetal ossification pattern. Am. J. Anat., 103 69–97

Crew F. A. E. 1924 The bulldog calf contribution to the study of achondroplasia. Proc. Roy Soc. Med., 17 39–58

Curry G. A. 1959 Genetical and developmental studies on droopy-eared mice J. Embryol. nd Exp Morphol., 7 39–65.

Danforth C. H. 1930 Numerical variations and homologies in vertebrae. Am J Phys. Anthrop., 14 463–481

Dwight, T. 1901 Description of the human spines showing numerical variation in the Warren Museum of the Harvard Medical School. Mem. Bost. Soc. N t. Hist 5 237–312.

Forsthoefel, P. F. 1959 The embryological development of the skeletal effects of the luxoid gene in the mouse including its interaction with the luxate gene. J. Morph., 104 89–141

Green, E. L. 1941 Genetic and non-genetic factors which influence the type of the skeleton in an inbred strain of mice. Genetics 26 192–222.

Green, M. C. 1951 Further morphological effects of the short ear gene in the house mouse. J. Morph., 88 1 22.

——— 1955 Luxoid — a new hereditary leg and foot abnormality in the house mouse. J. Heredity 46 91–99

Grüneberg H. 1943 Congenital hydrocephalus in the mouse a case of spurious pleiotropism. J. Genet., 45 1 21

Hoof Diane 1959 The effects of the achondroplasia (ac) gene on the skull development in the rabbit. Student thesis The Jackson Laboratory Bar Harbor Maine

H. B. Inez B. 1947 Morphogenetic studies of the rabbit. IV. The inheritance of developmental patterns of rib ossification. J. Exp. Zool., 105 173–187

Huxley J. S. 1932 Problems of Relative Growth. Lincoln MacV agh, London. Dial Press N. Y.

Knötzke F. 1929 Bemerkungen zur Wirbelsäule des Chondrodystrophen. Beitr. z. path. Anat. u. z. allg. Path., 81 547–567

Kühne K. 1931 Die Vererbung der Variationen der menschlichen Wirbelsäule Zeit. Morph. u. Anthr 30: 1 221

Landauer W. 1931 Untersuchungen über da Krüperhuhn. II. Morphologie und Histologie des Sk lets insbesondere des Skelets der langen Extremitätenknochen. Zeitschr für mikros anat. Forschung., 25 115–180

——— 1934 Studies on the creeper fowl. VI. Skeletal growth. Bull. 193 Conn. State College Storrs Conn.

——— 1935 A lethal mutation in dark Cornish fowl. J. Genet., 31 237–242.

——— 1940 The nature of disproportionate dwarfism with special reference to fowl. Sigma XI Quarterly 28 1–10.

Lipsett, J. C. 1941 Disproportionate dwarfism in Amblystoma. J. Exp. Zool., 86 441–459

O'Rahilly R. 1951 Morphological patterns in limb deficiencies and duplications. Am. J. Anat., 89 135–191

——— 1956 Developmental deviations in the carpus and the tarsus. Clin. Orthopaed 10 9–18.

P tten, A. R. 1937 A comparison of the glycine content of the proteins of normal and chondrodystrophic chick embryos t different stages of development. J. Nutrition, 13 123–126.

Pearce Louise, and W. H. Brown 1945a Hereditary achondroplasia in the rabbit. II. Pathologic aspects. J. Exp. Med., 82: 261 280.

——— 1945b Hereditary achondroplasia in the rabbit. III. Genetic aspects, general considerations. Ibid., 82: 281 295.

Rudolph, A. M. J. E. Drorbaugh, A. M. Auld, A. J. Rudolph, A. S. Nadas, C. A. Smith and J. P. H. bbell 1961 Studies on the circulation in the neonatal period. The circulation in the respiratory distress syndrome Pediatrics, 27 551–566.

Sawin, P. B. 1937 Preliminary studies of hereditary variations in the axial skeleton of the rabbit. Anat. Rec., 69 407–428.

——— 1945 Morphogenetic studies of the rabbit. I. Regional specificity of hereditary factors affecting homoeotic ariations in the axial skeleton. J Exp Zool., *100* 301–329

Sawin, P B., and D. D. Crary 1956 Morphogenetic studies of the rabbit. XVI. Quantitative racial differences in ossification pattern of the vertebrae of embryos as an pproach to basic principles of mammalian growth. Am. J Phys. Anthrop., *14* 625–646.

——— 1957 Morphogenetic studies of the rabbit. XVII. Disproportionate adult size induced by the DA gene. Genetics *42*: 72–91

——— 1957b Bipartite centra t onset of ossification in two races of rabbits. Abstract. Anat. Rec., *127* 362.

Sawin, P B and Inez B Hull 1946 Morphogenetic studies of the rabbit. II. Evidence of regionally specific hereditary factors influencing the extent of the lumbar region. J Morph., *78*: 1 26.

Sawin, P B., D. D Crary and Judith Webster 1959 Morphogenetic studies of the rabbit. XXIII. The effects of the dachs gene [illegible] drodystrophy) upon linear and [illegible] of the skeleton as influenced [illegible] netics, *44* 609–624.

Sawin, P B Mary Hamlett and [illegible] 1962 Morphogenetic studies of [illegible] XXIX. Accessory ossification [illegible] occipito-vertebral border in the [illegible] Am. J Anat., *111* 239–25[illegible]

Stockard, C. R. 1941 The genetic [illegible] crine basis for differences in form [illegible] havior Wistar Inst. Anat. and Bi[illegible]

Tanner J M., and P B Sawin 19[illegible] genetic studies of the rabbit. XI. [illegible] ferences in the growth of the [illegible] and their relation to growth and [illegible] in man. J Anat., *87* 54–65.

Thompson D'A. W 1948 On Growth and Form. University Press, Cambridge [illegible] lan Co New York.

Zwilling, E. 1956 Reciprocal [illegible] ectoderm and mesoderm during [illegible] limb development. Amer Nat., [illegible]

## PLATE 1

### EXPLANATION OF FIGURES

1 Newborn acac bowing minim m presacral ossification comparable t 21 day fetus in figure 5 and minimum tail ossification. Not proportionately greater width of centr than in normal fetuses I this and the following acac nimals.

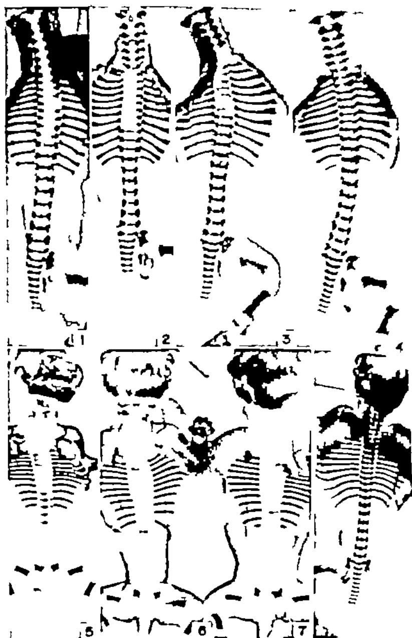
2 Newborn acac showing minimum presacral ossification as in figure 1 but with w ll ossified tail. Note gap in tail ossification and reduced n mbe f presacral ertebra Compare with figure 13.

3 Newborn acac showing median amount of ossification with some tendency tow rd tail g p. It compares with 21 day fetus in figure 6 except for tail. Note bipartit centra on vertebrae 5–20 16.

4 Newborn acac bowing maximum of ossification. It compares well with 23 d y fetus in figure 8 Note that tail is ossified throughout. Note reduction in twelfth pair of ribs and slight craniad shift in sacral attachment. Compare with figure 13.

5–7 Range of ossific tion of normal 21 day fetuses. Note "in tandem bipartite centrum of vertebra 20 in figure 7 The first pair of ribs for thi fetu has not yet ossified. The last pair is thirteenth pair (on vertebra 20) not reduced twelfth.

8 Average ossification of normal 23 d y fetus.


1
2
3
4
5
6
7

## PLATE 3

EXPLAN TION FIGU

15 Sternum f normal (*Ac*) newborn.

16–18 Variation in ossific tion of ternum f newborn *acac* animals. Note f ion of sternebrae 4 and 5 i figure 16 which show the m xim m n mber of sternebrae ossified. Compare with ternum of 3 day fetus in figure 8

19 H nd limb of normal (*A* ) newborn. Not fusion of tibia and fibula for distal two-third of their length. Note also that all metat rsal nd phalanges re ossified, a re epiphyses of distal femu and proximal tibia.

20 Hind limb of newborn *acac* showi g tibia and fibula unfused. Not minimal ossification of metatarsal and phalanges and b- sence f epiphyses in this and the following three figures.

21 Hind limb of newborn *acac* showing f sion of tibia and fibula beginning t the distal end.

22 Hind limb of newborn *acac* showing fusion of tibi nd fibul beginning i the middle Both end of the bones are still free

23 Hind limb of newborn *acac* showing rel tively normal f sion of tibia and fibula.

24 Forelimb of normal (*A* ) newborn. Note shape of cromion proc es of sc pula. Note also that metacarpal and phalanges are well ossified as are epiphyses f proximal and distal humerus and proximal ulna.

25 Forelimb of newborn *acac* howing relativ ly normal acromion process. Note deficient ossification of metacarpal and phalanges and lack of epiphyses in this and the following figures.

26 Forelimb f newborn *acac* showing thin acromion process which ha buckled upon itself

27 28 Forelimbs of newborn *acac* animals showing cromion processes which hav bent at right angles. Note greater foreshortening of radi nd ulna in figure 28


15
16
17
18
19
20
21
22
23
24
25
26
27
28

Direct observation of a seminiferous cycle can only be achieved by continuous observation of one site in the testis A more feasible method of almost equivalent validity is based on the assumption that spermatogenesis is an irreversible process allowing the stages which are observed in different parts of the testis to be arranged in sequence. The rat simplifies the process further by a fascinating correlation between phase-lag in the cycle and distance from the termination of the tubule in the rete testis This secondary phenomenon allows successively earlier stages of the cycle to be studied by following the individual tubule distally If this seminiferous wave is complete with a total length of 17.28 mm and is located in a rat whose seminiferous cycle follows the findings of Clermont, Leblond and Messier ('59) in being completed in 12 days each micron of distance along the tubule will be equivalent to one minute of time and our 10 μ cross sections record ten minutes of history

METHODS

A spectrum of methods was used in the course of this investigation ranging from paraffin embedding through squash-staining of enzymatically dissociated tubules to cannulation of individual tubules with removal of their contents by suction or pressure Only those methods which contributed materially to the results included in this paper will be detailed here

The paraffin embedded tissue was cut into sections 10 μ thick a compromise between a thickness sufficient to capture a complete Sertoli cell and the thinness requisite for good microscopic observation and photography For many of the preparations the tubules were excised in parallel groups which were then attached to flat slips of plastic to preserve their orientation during further procedures This resulted in suitably long lengthwise sections and even more important adequate areas of the tangential cuts which are too frequently neglected in testicular studies

The most comprehensive visualization of the Sertoli cells was obtained by the direct silver method (Elftman '52) more generally employed for the Golgi apparatus After the completion of the silver formalin and hydroquinone formalin steps, the tissue was placed overnight in either 15% formalin or in Bouin's solution Subsequent to sectioning and substitution of gold for the silver PAS staining and Harris hematoxylin were used together or separately

Fixation overnight in dichromate-sublimate (Elftman '57) followed by paraffin embedding, allowed the phospholipids to be stained with Sudan black B By preceding the application of the Sudan black with the Feulgen reaction counterstaining of the nuclei in a contrasting color was achieved when desired and the addition of periodic acid oxidation after the HCl incubation added the virtues of PAS staining

General cytological preservation was most adequate after fixation in Bouin's fluid overnight Nuclear detail was brought out by either the Feulgen reaction iron hematoxylin or Harris hematoxylin. Combining one of these with the PAS procedure brought out the acrosome structure and especially after permanganate oxidation the Sertoli cell cytoplasm and the cell boundaries Combining PAS staining with iron hematoxylin according to the method developed for the pituitary (Elftman '60) allowed both the classic and the more recent criteria of sperm maturation to be followed on the same slide. Aldehyde fuchsin staining after permanganate oxidation was applied with or without accompanying PAS staining

*Pattern of Sertoli cell distribution*

The dominant role played by the Sertoli cells in the spatial organization of the seminiferous epithelium is apparent in figure 1 which shows a 10 μ section of a tubule prepared by the direct silver method. The plane of section encountered this tubule as it was bending resulting in a transverse section of one portion modulating into a tangenital section further to the left.

The cross-section portion of the figure exhibits the typical arrangement of acrosome-stage 3 The immature spermatids, each with its Golgi apparatus showing as a black dot, are piled vertically above the basal layer The maturing spermatozoa have their heads attached to the Sertoli



Fig. 1 Section through curved portion of rat seminiferous tubule (× 200) prepared by the direct silver method followed by PAS and Harris hematoxylin. Thickness 10 μ. In the lower right of the figure the tubule is cut in cross-section and the Sertoli cells may be seen rising from their nuclei located on the basal membrane to make contact with the maturing spermatozoa towards the lumen. The Sertoli trunks are surrounded by spermatids, each with black Golgi body associated with gray acrosomic vesicle. Further towards the left the section becomes increasingly tangential to the tubule showing the orderly ground plan of Sertoli cell distribution with the germ cells arranged around the Sertoli cells. Acrosome-stage 3.

cytoplasm at various levels above the basement membrane with their cytoplasm, including residual granules near the lumen. The trunks of the Sertoli cells can be followed towards the lumen from the triangular nuclear region on the basement membrane.

As seen in the cross-section of the tubule, the Sertoli trunks appear to be spaced at variable distances from each other Sometimes the space is wide enough to accomodate three spermatids usually only two less frequently slightly more than one. This variability in spacing is more apparent than real, as may be seen by studying the region of the tubule which is cut tangentially Here the Sertoli trunks appear as dark cross-sections arranged in a highly regular pattern. When this pattern is intersected by cross-sections of the tubule, which would be perpendicular to the plane of the figure in this region, slight differences in the orientation of the section would result in different spacing of the Sertoli trunks included in the section An easy way to study this effect is to take a semi-transparent sheet of plastic such as a slightly exposed photographic film, and cut a slit in it 2 mm wide, which represents 10 μ at the magnification of figure 1 This slit may then be laid over the tangential part of figure 1 and the effect of different orientations studied.

Further details concerning the pattern of Sertoli cell distribution, as seen in tangential sections, are illustrated in figures 2–4 of plate 1 In figure 2 the tubule is in acrosome-stage 13 with a few older primary spermatocytes in diakinesis showing at the lower edge of the figure where the tubule was cut at a higher level. The basal layer of primary spermatocytes is in the zygotene stage and is conspicuously arranged in rings. This arrangement is not fortuitous; each of the rings is organized around one Sertoli cell at its center recognizable through the p of a dark nucleolus in an otherwise spicuous nucleus.

...age number of spermatoc... in ... is six, with variations ... number due largely to

Direct observation of a seminiferous cycle can only be achieved by continuous observation of one site in the testis. A more feasible method of almost equivalent validity is based on the assumption that spermatogenesis is an irreversible process allowing the stages which are observed in different parts of the testis to be arranged in sequence. The rat simplifies the process further by a fascinating correlation between phase-lag in the cycle and distance from the termination of the tubule in the rete testis. This secondary phenomenon allows successively earlier stages of the cycle to be studied by following the individual tubule distally. If this seminiferous wave is complete with a total length of 17.28 mm and is located in a rat whose seminiferous cycle follows the findings of Clermont, Leblond and Messier ('59) in being completed in 12 days, each micron of distance along the tubule will be equivalent to one minute of time and our 10 μ cross sections record ten minutes of history.

### METHODS

A spectrum of methods was used in the course of this investigation, ranging from paraffin embedding through squash-staining of enzymatically dissociated tubules to cannulation of individual tubules with removal of their contents by suction or pressure. Only those methods which contributed materially to the results included in this paper will be detailed here.

The paraffin embedded tissue was cut into sections 10 μ thick, a compromise between a thickness sufficient to capture a complete Sertoli cell and the thinness requisite for good microscopic observation and photography. For many of the preparations the tubules were excised in parallel groups which were then attached to flat slips of plastic to preserve their orientation during further procedures. This resulted in suitably long lengthwise sections and even more important adequate areas of the tangential cuts which are too frequently neglected in testicular studies.

The most comprehensive visualization of the Sertoli cells was obtained by the direct silver method (Elftman '52) more generally employed for the Golgi apparatus. After the completion of the silver formalin and hydroquinone-formalin steps, the tissue was placed overnight in either 15% formalin or in Bouin's solution. Subsequent to sectioning and substitution of gold for the silver, PAS staining and Harris hematoxylin were used together or separately.

Fixation overnight in dichromate-sublimate (Elftman '57) followed by paraffin embedding allowed the phospholipids to be stained with Sudan black B. By preceding the application of the Sudan black with the Feulgen reaction counterstaining of the nuclei in a contrasting color was achieved when desired and the addition of periodic acid oxidation after the HCl incubation added the virtues of PAS staining.

General cytological preservation was most adequate after fixation in Bouin's fluid overnight. Nuclear detail was brought out by either the Feulgen reaction, iron hematoxylin or Harris hematoxylin. Combining one of these with the PAS procedure brought out the acrosome structure and, especially after permanganate oxidation, the Sertoli cell cytoplasm and the cell boundaries. Combining PAS staining with iron hematoxylin according to the method developed for the pituitary (Elftman '60) allowed both the classic and the more recent criteria of sperm maturation to be followed on the same slide. Aldehyde fuchsin staining after permanganate oxidation was applied with or without accompanying PAS staining.

#### *Pattern of Sertoli cell distribution*

The dominant role played by the Sertoli cells in the spatial organization of the seminiferous epithelium is apparent in figure 1, which shows a 10 μ section of a tubule prepared by the direct silver method. The plane of section encountered this tubule as it was bending, resulting in a transverse section of one portion modulating into a tangential section further to the left.

The cross-section portion of the figure exhibits the typical arrangement of acrosome-stage 3. The immature spermatids, each with its Golgi apparatus showing as a black dot, are piled vertically above the basal layer. The maturing spermatozoa have their heads attached to the Sertoli



Fig. 1 Section through curved portion of a rat seminiferous tubule (× 200) prepared by the direct silver method followed by PAS and Harris hematoxylin. Thickness 10 µ. In the lower right of the figure the tubule is cut in cross-section and the Sertoli cells may be seen rising from their nuclei located on the basal membrane to make contact with the maturing spermatozoa towards the lumen. The Sertoli trunks are surrounded by spermatids, each with black Golgi body associated with gray acrosomic vesicle. Further towards the left the section becomes increasingly tangential to the tubule showing the orderly ground plan of Sertoli cell distribution with the germ cells arranged around the Sertoli cells. Acrosome-stage 3.

cytoplasm at various levels above the basement membrane with their cytoplasm, including residual granules near the lumen. The trunks of the Sertoli cells can be followed towards the lumen from the triangular nuclear region on the basement membrane.

As seen in the cross-section of the tubule, the Sertoli trunks appear to be spaced at variable distances from each other Sometimes the space is wide enough to accomodate three spermatids, usually only two less frequently slightly more than one This variability in spacing is more apparent than real, as may be seen by studying the region of the tubule which is cut tangentially Here the Sertoli trunks appear as dark cross-sections arranged in a highly regular pattern. When this pattern is intersected by cross-sections of the tubule, which would be perpendicular to the plane of the figure in this region, slight differences in the orientation of the section would result in different spacing of the Sertoli trunks included in the section. An easy way to study this effect is to take a semi-transparent sheet of plastic, such as a slightly exposed photographic film, and cut a slit in it 2 mm wide which represents 10 µ at the magnification of figure 1 This slit may then be laid over the tangential part of figure 1 and the effect of different orientations studied.

Further details concerning the pattern of Sertoli cell distribution, as seen in tangential sections are illustrated in figures 2–4 of plate 1 In figure 2 the tubule is in acrosome-stage 13 with a few older primary spermatocytes in diakinesis showing at the lower edge of the figure wh the tubule was cut at a, higher basal layer of primary in the zygotene stage and is arranged in rings. This not fortuitous each of the ganized around one Sertoli center recognizable through the of a dark nucleolus in an otherw spicuous nucleus.

The average number of sperma in each ring is six, with variations and below this number due largely

plane of section. But this does not mean that there are six times as many basal *primary spermatocytes in this layer as* there are Sertoli cells. Each spermatocyte belongs to two rings, being shared so to speak, by two neighboring Sertoli cells with *one of which it may have closer* affiliation in a manner similar to the elec tron pairs in chemical valency

There is consequently one Sertoli cell for each three primary spermatocytes of the basal layer This exceeds the esti mates made by investigators primarily interested in the germ cells The reason is not hard to find. If a slit 6 mm wide representing a 10 μ section is oriented over figures 2–4 it will be found to be surprisingly easy to avoid including Sertoli cells with the customary thinner sections *the recognizable portions of the Sertoli* cells are even more elusive.

The arrangement of the basal layer of primary spermatocytes around the Sertoli cells is a basic determinant for the distri bution of the more mature germ cells. As the primary spermatocytes grow in size they have no room to move sideways but must gain space further from the basement memebrane this they accomplish by forming two layers with faceted bound ..es (fig 6) When the two maturation have been completed the sper ..tids are arranged in four zig zagged ..yers (figs. 8–10 1) A tangenital section through any one of these layers will consequently include on the average as many spermatids as there were basal pri mary spermatocytes

Tangential sections of seminiferous tu*bules at acrosome-stage 3 are shown in* figures 3 and 4 The dark cross-sections of the Sertoli trunks and the maturing sper matozoa attached to them are arranged in regular pattern The number of sper matids surrounding each Sertoli trunk is the expected six, with some increase when the plane of section encounters more than one layer of spermatids.

One striking feature of the Sertoli cell sections in both figures 3 and 4 is the number which exhibit three prongs. Since an equitable distribution of the spermatids among the Sertoli cells could be achieved by having each Sertoli cell attached to three spermatids in each of the four layers, these prongs may very well indicate a connection between the Sertoli cell and *each alternate spermatid of the six which* surround it.

*The Sertoli cell cycle*

The relation of the Sertoli cell to the germ cells and the changes in this relation during the cycle of the seminiferous epithelium can be studied best in sections which include as much as possible of the trunk of the Sertoli cell Such sections may be either transverse or longitudinal with respect to the tubule but must be nearly perpendicular to the basement membrane the angle of inclination being that of the Sertoli trunk. Only such sections represent properly the functional units of the testis this orientation is rarely achieved *in sections employed for germ cell study* Since the Sertoli trunk is under no obligation to be linear and its arborizations must reach each of the germ cells with which it is associated even a 10 μ section is incapable of capturing the complete cell.

A convenient starting point is afforded by acrosome-stage 7 represented in figures 5 and 11 This stage precedes the release of the maturing spermatozoa and it can be seen in figure 5 that the Sertoli cell trunks continue beyond the spermatids to retain their connection with the spermatozoa In figure 11 and more clearly in figure 5 transverse branches of the Sertoli trunk are seen to make close contact with the spermatids Although there is reason to believe that physical contact is effectuated earlier (figs. 3 and 4) the emphasis here is on the fact that the Sertoli cell is *prepared to take charge of a new generation* of spermatids before it has finished its obligations to the predecessors. The radial course of the Sertoli trunk from the basement membrane outside of which the vascular supply is located to the interior of the tubule where cellular transformations of momentous significance must be energized certainly suggests a well-engineered channel of communication.

Much cellular detail which is not of immediate importance for our present discussion may be seen in these sections, even in the photomicrographs with close scrutiny and it is worthwhile to digress slightly to point out some of them. In fig-

ure 5 the basal layer of cells contains not only the triangular cell bodies of the Sertoli cells but also spermatogonia and early *spermatocytes. The next layer* contains primary spermatocytes with pachytene chromatin and a Golgi apparatus staining weakly with periodic-acid-Schiff The spermatids show their acrosome configuration and, more faintly the centrioles. The almost-mature spermatozoa show vivid nuclei and residual granules In figure 11 the Golgi apparatus forms black dots in the spermatids. At this stage it has separated from the acrosome vesicle which can be seen less distinctly in the photograph than in the original preparation.

After the maturing spermatozoa have relinquished *their connections* with the Sertoli cells, the spermatids accelerate their maturation. Their continued dependence on the Sertoli cells is evident in figure 6 (acrosome-stage 11) and *figure* 12 (acrosome-stage 12) The Sertoli trunks connecting the spermatids with the basal membrane, furnish the pathway which guides the migration of the spermatid nuclei. In figure 6 the distance separating these nuclei from the basement membrane has been increased by the growth of the primary spermatocytes which has necessitated their disposition in two layers. The distance separating the spermatid nuclei from the periphery of the tubule is rapidly diminished by their migration along the Sertoli cell pathway In figure 12 they are closer to the membrane and in figure 7 (acrosome-stage 14) they have almost reached it. One might readily imagine that this proximity to vascular supply is related to a competition for nurture between meiosis and spermatid maturation.

When the meiotic divisions which are in progress in figure 7 have been completed, each primary spermatocyte has given rise to four spermatids. These are arranged in four layers, the boundaries between which are not planes but are characterized by the facets which allow similar cells to be packed with minimal surface area With this packing of spermatids the maturing spermatozoa tend to move away from the basal membrane as in figure 8 (acrosome-stage 3) but the Sertoli cell to which they are attached *retains its connection* with its nucleus in the basal layer The Sertoli trunk is angulated to conform with the packing requirements of the spermatids and its internal structure reveals characteristic granules as well as slender fibrils both of which *may* also be seen in figure 6.

Once more the maturing spermatozoa migrate towards the periphery of the tubule, again almost reaching the basal membrane in figure 13 (acrosome-stage 4) and figure 9 (acrosome-stage 5) The trunks of the Sertoli cells are less angulated at this stage suggesting that the presence of the elongate heads of the immature spermatozoa may assist the Sertoli cells with which they are associated in withstanding the packing pressures of the surrounding spermatids. The Golgi apparatus of the spermatids is clearly evident as dense black dots in figure 13. It is still osculating with the acrosomic vesicle the granule of which is also visible. In figure 9 the acrosome is in a distinctly later stage *of* development and the Sertoli nuclei and the basal layer of primary spermatocytes show to better advantage.

The final emigration of the maturing spermatozoa *from* the basal membrane towards the lumen is well under way in figures 10 and 11 and is nearer completion in figure 5 All of these figures represent *acrosome-stage* 7 a stage which is disproportionately long in comparison with the other stages of this nomenclature. As the immature spermatozoa ascend, the nuclei *of the Sertoli* cells rise with them (fig. 10), assuming momentarily a position similar to that which they occupy permanently in some mammals. In this elevated position they *no longer* exhibit the pyramidal shape which would seem to be impressed on them by physical factors present in the basal layer The cell as a whole does not *migrate, only the* nucleus the trunk of the cell, including a distinctive fibril which is shown in figure 10 retains its anchorage in the basal layer

With *the return of* the Sertoli nuclei to their basal position the Sertoli cell once more assumes the configuration of figure 5 and it is ready to repeat its cycle the germ cells which surround spermatic generation younger tha with which we started. The Serto *is co-extensive* with the cycle of th

## PLATE 1

### EXPLANATION OF FIGURES

Photomicrograph of 10 μ sections of rat seminiferous tubules.

Figs. 2–4 Tangential section (× 600) After Bouin fixation the tissue for figure 2 was stained with Harris hematoxylin, that for figures 3 and 4 with aldehyde fuchsin PAS and hematoxylin after permanganate oxidation.

2 Section at the level of the Sertoli nuclei, acrosome-stage 13. The basal primary spermatocytes are arranged in rings around the Sertoli cells which have an inconspicuous nucleus except for the characteristic punctate nucleolus. Note that the rings of spermatocytes are shared by adjacent Sertoli cells. A few primary spermatocytes of the previous generation lying at a higher level are present at the lower edge of the figure

3–4 Section nearer the lumen acrosome-stage 3. The trunks of the Sertoli cells, darkly stained are arranged with striking regularity so that each is surrounded by an average of six spermatids. Three prongs extend from each Sertoli trunk, suggesting attachment to alternate spermatids in the ring. This is especially clear in the upper right hand corner of figure 4

Figs. 5–10 The Sertoli cell cycle in cross-section (× 400) The tissue was fixed in Bouin fluid and stained with aldehyde fuchsin PAS and Harris hematoxylin after permanganate oxidation except for figure 5 which received only PAS and hematoxylin.

5 The spermatids show secure attachment to the Sertoli cell trunks which ascend from the nuclear region on the basal membrane towards the lumen where the almost-mature spermatozoa are still connected with them. Acrosome-stage 1 to 7

6 The rapidly maturing spermatids have an avenue of communication with the periphery of the tubule through the somewhat enlarged Sertoli trunks in which granules and slender longitudinal fibrils are present. The primary spermatocytes have enlarged sufficiently to necessitate packing in two layers. Acrosome-stage 11

7 The nuclei of the spermatids have migrated closer to the basal membrane and meiosis is in progress. Acrosome-stage 14

8 The spermatids resulting from meiosis occupy four layers seemingly crowding the maturing spermatozoa away from the basal membrane with which they remain connected by the Sertoli cells. Acrosome-stage 2.

9 The heads of the maturing spermatozoa again approach the basal membrane closely guided in their migration by the Sertoli trunk. Acrosome-stage 5.

10 The maturing spermatozoa are well on their way to the lumen with the Sertoli cell nuclei following in their wake. Acrosome-stage middle 7 This configuration is followed shortly by that of figure 5, in which the Sertoli cell nuclei have regained a basal position

Figs. 11 13 The Sertoli cell as shown by the direct silver method. (× 400) Subsequent Bouin fixation, gold replacement, PAS and Harris hematoxylin staining.

11 The dimensions of the Sertoli cells are delineated more clearly by the direct silver method since it produces deeper staining of the Sertoli cytoplasm. The Golgi apparatus of the spermatids appears as deep black dots in the spermatids. It has just lost contact with the acrosomic vesicle which is gray in the photograph. Acrosome-stage 7

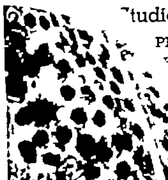
12 The Golgi apparatus of the spermatids has migrated into their cytoplasm near the lumen. Large primary spermatocytes are located around the Sertoli trunks basally Acrosome-stage 12.

13 The staunch trunks of the Sertoli cells are separated by spermatids in which the Golgi apparatus is still in tangential contact with the acrosomic vesicles. Acrosome-stage 4

# "tudies on the Skin

## PHOSPHATASES DURING THE
## HE SKIN IN THE RAT[1]

HIMOTO AND KAZUO OGAWA
f Anatomy Kyoto University School of Medicine



was applied. The sections were incubated in the substrate medium at 37 C for 2 to 2½ hours.

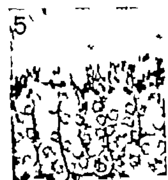
The effect of various pHs (8.2, 9.2, and 10 0) on the activity of alkaline phospha ises was tested with 2% sodium β-glyc phosphate as substrate as well as with ral other substrates, such as 0.2% se 1 phosphate (G-1 P) 0.2% glu- phosphate (G-6-P) and 0.2" fruc hosphate (F-6-P) using adult rats s embryos of the fourteenth day n

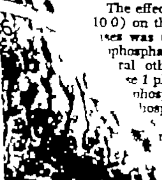
*mical demonstration of acid* (AC P) Gomori's lead ace Gomorim '50) was used to on-specific acid phospha- ctions were incubated in dium for 30 to 60 min-

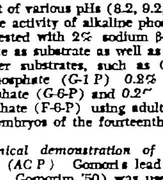
ous pHs (4 4 5.2 and activity was also ob- ts and embryos in gestation.

*tration of tripoly- xametaphospha* od (Berg '60) olyphosphate aphosphate however consistent re then d orig ation tain

te

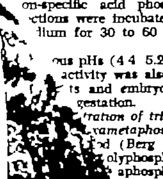


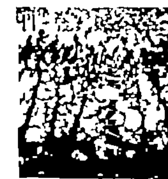
















# Histochemical Studies on the Skin

## I THE ACTIVITY OF PHOSPHATASES DURING THE HISTOGENESIS OF THE SKIN IN THE RAT[1]

KEN HASHIMOTO AND KAZUO OGAWA
*Department of Anatomy Kyoto University School of Medicine*
Kyoto Japan

There are very few practically no detailed histochemical studies on the distribution of phosphatases in the rat skin through its organogenesis from embryonic stage although there have been several fairly extensive studies on the distribution of the phosphatases in the adult human and animal skins (Montagna, 47 Montagna and Hamilton, 47 Fisher and Glick, 47 Spier and Martin, '50 Hardy '52 Moretti and Mescon, '56 Kopf '57 Braun-Falco '58 Moretti et al. '60) There are however a few studies on phosphatases in embryos other than rat (Moog 44 Johnson and Bevelander 46)

The present study deals with the distribution and activity of alkaline acid, poly and meta-phosphatases in the rat skin, and further a chronological follow up of these enzymes from embryonic to adult stage.

### MATERIALS AND METHODS

*Animals* Nine embryos (3 embryos each at the seventh, fourteenth, and eighteen day of gestation) 2 new-born rats three hours after birth, 1 rat 10 days old, 1 rat 15 days old, and 5 adult rats of the Wistar strain, weighing approximately 100 g, were used in the present investigation.

Rats were killed by a blow on the neck without anesthesia. Hair was cut. Skin specimens taken from the back were cut into small square pieces and immediately fixed in ice-cold 10% neutral formalin for 30 minutes. In the case of embryos skin was removed from the back while they were still alive.

Frozen sections, approximately 20 microns in thickness, were made and used for various enzymatic studies.

*Histochemical demonstration of alkaline phosphatases (AL.P )* Gomori's modified calcium cobalt method (Gomori '52) was applied. The sections were incubated in the substrate medium at 37 C for 2 to 2½ hours.

The effect of various pHs (8.2 9.2, and 10 0) on the activity of alkaline phosphatases was tested with 2% sodium β-glycerophosphate as substrate as well as with several other substrates such as 0.2% glucose-1-phosphate (G-1 P) 0.2% glucose-6-phosphate (G-6-P) and 0.2% fructose-6-phosphate (F-6-P) using adult rats as well as embryos of the fourteenth day of gestation

*Histochemical demonstration of acid phosphatase (AC P ).* Gomori's lead acetate method (Gomorim '50) was used to demonstrate non-specific acid phosphatases. Frozen sections were incubated in the substrate medium for 30 to 60 minutes at 37 C.

The effect of various pHs (4 4 5.2 and 6 0) on the enzyme activity was also observed using adult rats and embryos in their fourteenth day of gestation.

*Histochemical demonstration of tripolyphosphatase (TPP) and hexametaphosphatase (HMP).* Berg's method (Berg, '60) was first used with tripolyphosphate $Na_5P_3O_{10}$, and sodium hexametaphosphate $(NaPO_3)6$ as substrates. Since however the results of staining were inconsistent with this method, the media were then prepared by the second method used originally by Berg ('55) for the demonstration of inorganic polyphosphatase to obtain more consistent results.

As was done in the cases of alkaline and acid phosphatases, the effect of various pHs (3.2, 4.2, 4 4 4 8 and 5 4) on the enzymatic activity was tested in adult

[1] This investigation was supported by grants from the Rockefeller Foundation (GA-MNS-[illegible]), the Dome Chemicals Inc., New York, N. Y and the Daly Laboratories, Inc., South Norwalk, Conn.
Present address Boston Dispensary Department of Dermatology Tufts University School of Boston, Mass.



Fig. 6 Adult rat ALP stain pH 9.2. Cell or cell remnant of medullae of hairs are stained black due to metallic sulfide × 150.

staining reaction than the middle layer (stratum intermedium) (fig. 7). In the stratum germinativum there were occasional congregations of large-sized cells which stained strongly. They seemed to represent the anlagen of the primary epithelial germ cells (fig. 8).

*In the 14-day-old embryo* the epidermis especially the basal layer, primary epithelial germs at bulbous peg stage and a number of connective tissue cells including mast cells showed an enzymatic activity (fig. 9). The advancing border of the primary epithelial germs stained most intensely as well as the papillae in it (fig. 10).

*In the 18-day-old embryo* the anlagen of the sebaceous glands and the bulge appeared and showed enzyme reactions (fig. 11). Other elements which showed the enzymatic activity in younger specimens continued to be reactive.

*In the new-born rats* the distribution and reaction intensity of the enzyme did not show any significant change from those of the younger specimens.

*In the 5-day-old rats* the staining characteristics were same as in younger specimens except that occasionally weakly stained fibers of premature arrector pili muscles appeared.



Fig. 7 Seven-day-old embryo. ACP stain, pH 5.2. Strongly reactive outer layer (periderm) and inner layer (stratum germinativum) and less strongly reactive middle layer (stratum intermedium) of the epidermis are demonstrated. × 600.



Fig. 8 Seven-day-old embryo. ACP stain, pH 5 2. High magnification of stratum germinativum. Congregations of intensely reactive large cells, the anlagen of the primary epithelial germs, along the lower border of the stratum germinativum are demonstrated. × 1,500.

In the 10-day-old and adult rats arrector pili muscles became more strongly reactive, while the other staining characteristics remained the same as in the younger specimens. However the staining intensity in each reactive organ diminished to some extent in comparison with that of embryo specimens. The resting hair follicles showed an enzymatic activity in the epithelial sacs dermal papillae upper portion of the follicles and in the epidermis although the reaction intensity was decreased in these elements (fig 12)

*Tripolyphosphatase (TPP) and hexametaphosphatase (HMP).* The distribution and activity of TPP was essentially very similar to those of AL.P., not only in the adults but also in embryos (table 1) and those of HMP were limited to the sebaceous glands, hair bulbs dermal papillae and in addition, the capillaries dermal muscles and mast cells were stained depending on the pH used (table 2)

*Others* PFAS was positive in capillaries hair follicles as a whole and diffusely in the epidermis. The plasmal reaction was positive in sebaceous glands capillaries epidermis and in the hair follicles, especially in the epithelial germs in 14-day-old embryos. Sudan IV was positive in sebaceous glands and epidermis; in addition, there were positive spots and

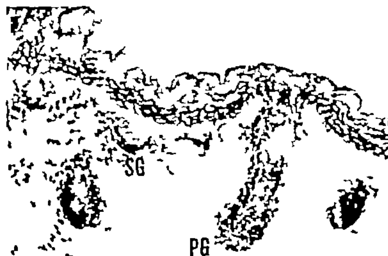



Fig. 9 Fourteen-day-old embryo. ACP stain, pH 5 2. Primary epithelial germs (PG) epidermis esp. the basal layer mast cells and connective tissue cells are shown to be reactive. Advancing border of primary epithelial germs and that of secondary epithelial germs (SG) which are just emerging, are strongly reactive. × 150.

Alkaline phosphate in addition to its role in hydrolysis of phosphatase mono-esters in the digestive tract probably plays an important part in the absorption of sugar from the intestine and the reabsorption of glucose in the kidney tubules (Cantarow and Schepartz, '54) Burstone ('58) demonstrated AL.P in the Golgi apparatus which is said to be associated with the functions of absorption and excretion (Palay '58) Recently Ogawa et al. ('60 '61) observed in the astrocytes and fibroblasts cultured *in vitro* using the kitten cerebellum that the Golgi apparatus of these cells was positive for AL.P Egar ('53) observed the increased permeability of the capillaries of the adrenals after administration of sodium to the pregnant rats.

From the above it is possible to surmise that the AL.P intervenes in the adjustment of the permeability of the cell membrane and also the exchange of substances through it. Mölbert et al ('60) could identify AL.P in cell membrane in the kidney by means of electron microscopy to support the above assumption. In our study however it was difficult to decide the exact localization of AL.P in the cells

Melczer and Deme ('43) observed the Golgi apparatus in the peripheral cells of the sebaceous gland acini to diminish and finally disappear as they became mature in the center and it is of great interest that in our study the AL P in its highest concentration in the peripheral cells diminished towards the center of the acini

In cell cultures. AL P is found in Golgi apparatus but also in the lysosomes (de Duve '56) which take neutral red in supravital stain (Ogawa et al. '60) The lysosomes are known to consist of phospholipoprotein and in this connection it is possible to discuss the role which AL P might play in phospholipid metabolism, but more detailed studies are expected It is assumed that AL P plays a part in the transphosphorylation in the tissue especially in the young metabolically active parts but there has been no pertinent study on this subject.

*Acid phosphatase (AC P)* As for AC P it was found that the enzyme was distributed in the organs such as sebaceous gland and epidermis in which the lipid especially the phospholipid, content was high Hooyman ('32) found that the basal layer of the epidermis had a phospholipid content comparable with that of the glandular organs of the body and it decreased appreciably during keratinization. Montagna ('56) found an abundant amount of phospholipid in the sebaceous cells at all stages of maturation in the rat.

The plasmal reaction performed by us revealed a positive reaction in the sebaceous gland epidermis matrix, and papilla and this distribution is in conformity to that of AC.P These findings suggest some intimate correlationship between AC.P and phospholipid. Another evidence that the AC P is involved in phospholipid metabolism is found in the positive reaction of lysosomes for AC.P (de Duve '56 Ogawa et al '60 '61) which is phospholipoprotein.

Another possible role which AC P might play is found in the metabolism of phosphate attached to nucleic acid (Moretti et al '56) but this point can not be taken without further elucidation of the subject.

*Tripolyphosphatase (TPP) and hexametaphosphatase (HMP)* Berg et al. ('60) found the distribution of TPP to be similar to that of AL P in the small intestines and attributed the same functional roles to it absorption and excretion through the intestinal epithelium In our study TPP showed a similar distribution to AL.P., and it is assumed that this enzyme should have similar functions to those of AL P in the skin. The metabolic role of HMP is not clear but must have similar functions to those of TPP and AL.P

*Enzymatic activities during histogenesis.* The essential distribution of all phosphatases studied in the present investigation was not different between embryonic and adult stages in the rat skin as soon as the particular organ which is reactive for the particular enzyme or enzymes later in the adult stage appeared in the course of histogenesis it showed positive reaction for that enzyme or enzymes However in embryos the staining reaction of each reactive element was generally much more intense than in adults The bulge appeared first in the 18-day-old embryo and continued to be reactive until it disap-

peared in the course of the maturation of the hair follicle.

*Specific requirement of pH and substrate for enzymatic activities* In all enzymes studied in the present investigation, it was found that fairly wide ranges of pHs, lower and higher optimal ones detected satisfactorily the enzymatic activities In ALP all the substrates used demonstrated a similar distribution of enzyme activity irrespective of the substrates used. Thus the faculative requirement of these enzymes for pHs and substrates indicates that the enzymes studied are of rather non specific nature.


SUMMARY

1 The activity and distribution of alkaline, acid, poly and meta-phosphatases with various substrates and pHs were followed chronologically from embryonic to adult stage in the rat.

2 The essential distribution of these enzymes in embryos was not different from that in adults. However in embryos the staining reaction of each reactive element was generally much more intense than in adults

3 The main sites of alkaline phosphatase activity at all stages were the capillaries, sebaceous glands, and less constantly the papillae and hair bulbs. The reaction of the musculus arrectores pilorum, dermal muscles and connective tissue cells depended largely on the substrate used and pHs tested. The epidermis stained deepest in basal and subcorneal layers.

4. Acid phosphatase was strongly reactive in the epidermis, especially the basal layer and in the lower portion of hair follicles up to the keratogenous zone and often also further along the outer root sheath continuously to the basal layer of the epidermis. Papillae hair matrices sebaceous glands especially the peripherally located generative cells and the arrector pili muscles were constantly stained Capillaries became reactive at high pHs (pHs 5.2–6.0)

5 The activity and distribution of tri-polyphosphatase was essentially similar to those of alkaline phosphatase in that capillaries, sebaceous glands hair matrices papillae and epidermis were stained

6. The activity and [illegible] of [illegible] metaphosphatase were [illegible] in the [illegible] baceous glands, hair [illegible] and [illegible] The capillaries, dermal [illegible] and [illegible] cells were stained depending on the [illegible] used.

7 There were no [illegible] differences in the activity and distribution of the [illegible] line phosphatases whether [illegible] phates or β-glycerophosphate was [illegible] substrate.



ACKNOWLEDGMENTS

The authors are greatly indebted to Professor M. Okamoto and Dr. [illegible] Department of Anatomy School of Medicine Kyoto University for their many valuable suggestions and to Professor [illegible] Department of Dermatology [illegible] University School of Medicine for his critical review of the manuscript.


LITERATURE CITED


Berg, G. G. 1955 Histochemical [illegible] tion of acid inorganic polyphosphatase Histochem. Cytochem., 3 22–31.

——— 1960 Histochemical demonstration of acid trimetaphosphatase and [illegible] phatase. Ibid., 8 92–101.

Berg, G. G., and J [illegible] 19[illegible] [illegible] metaphosphatase as an adaptive [illegible] absorbing epithelial. Histochemical [illegible] Eleventh Annual Meeting, April, [illegible]

Braun-Falco, O. 1958 The biology of [illegible] Growth. Ed. by W Montagna and R. A. [illegible] Academic Press Inc., New York. Chap 4 [illegible]

Burstone, M. S. 1958 The relationship between fixation and techniques for histochemical localization of hydrolytic enzymes. J Histochem Cytochem., 6 322.

Cantarow A., and B. Schepartz 1954 Biochemistry W B. Saunders Co., Philadelphia Chap 7 231

de Duve, C., B. C. Pressman, R. J Gianetto, [illegible] Wattiaux and F Appleman 1955 Tissue fractionation studies. 6. Intracellular distribution patterns of enzymes in rat-liver tissue Biochem. J 60 604–617

Egar W W Gottesleben and M. Tietke 19[illegible] Über das Verhalten der alkalischen und sauren Phosphatase bei funktioneller Belastung der Nebenniere. Virchows Arch., 324 172–1[illegible]

Fisher, L., and D. Glick 1947 Histochemistry XIX. Localization of alkaline phosphatase in normal and pathological human skin. Proc. Soc. Exp. Biol. Med., 66 14–18.

Gomori, G. 1950 An improved histochemical technique for acid phosphatase. Stain Technol., 25 81–85.

——— 1952 Microscopic Histochemistry Chicago Univ Press, Chicago.

Hardy M. H. 1952 The histochemistry of hair follicles in the mouse. Am. J Anat., 90 [illegible] 329.

Horstman, E., and A. Dabelow 1957 Handbuch der Mikroskopischen Anatomie des Menschen. Ed. by W v Möllendorf and W Bargman. Springer Verlag, Berlin. Vol. 3 Part 3 Chap. VI, 160.

Johnson, P L., and G. Bevelander 1946 Glycogen and phosphatase in the developing hair Anat. Rec., 95 193–199

Kooyman, D J 1932 Lipid of the skin. Arch. Derm. Syphil. 25 444–450.

Kopf A. W 1957 The distribution of alkaline phosphatase in normal and pathologic skin. Arch. Derm 75: 1–37

Melczer N and S. Deme 1943 Beiträge zur Tätigkeit der menschlichen Talgdrüsen. I. Histologisch nachweisbar chemische Veränderungen während der Talgerzeugung. Dermatologica 86 24–36.

——— 1943 Beiträge zur Tätigkeit der menschlichen Talgdrüsen. II. Rolle und Formveränderungen des Golgi-Apparetes der Talkproduktion. Arch. Derm. U Syphil., 183 388–395.

Montagna, W 1947 Histochemistry of the sebaceous glands of the rat. Anat. Rec., 97 356.

——— 1956 The Structure and Function of Skin. Academic Press Inc., New York.

Montagna, W., and J B. Hamilton 1947 Histochemical analysis of the sebaceous glands of the hamster Fed. Proc., 6 166–167

Molbert, E. R. G., F Duspiva and O. H. von Deimling 1960 The demonstration of alkaline phosphatase in the electron microscope J Biophys. Biochem. Cytol., 7 387–390

Moog, F 1944 Localizations of alkaline and acid phosphatases in the early embryogenesis of the chick. Biol. Bull., 86 51–80.

Moretti, G., and H. Mescon 1956 Histochemical distribution of acid phosphatase in normal human skin. J Histochem. Cytochem., 4 247–253.

Moretti, G., K. Adachi and R. A. Ellis 1960 Regional differences in acid phosphatase and tween esterase activity in the epidermis of the chimpanzee and the macaque. Ibid., 8 237–241.

Ogawa K., N Mizuno, K. Hashimoto and M. Okamoto 1960 Cytochemistry of cultured neural tissue. III. Additional staining techniques with special references to lysosomes. Proc. Dpt. Anat. Schl. Med., Kyoto Univ 4: 1–15.

Ogawa, K., N Mizuno and M. Okamoto 1961 Lysosomes in cultured cells. J Histochem. Cytochem., 9 202.

Palay S. L. 1958 Frontiers in Cytology Ed. by S. L. Palay Yale Univ Press, New Haven. Chap. 11 305–342.

Pinkus, H. 1958 The Biology of Hair Growth. Ed by W Montagna and R. A. Ellis. Academic Press Inc., New York. Chap 1 1–32.

Spier H. W and K. Martin 1950 Histochemische Untersuchungen über die Phosphomonoesterasen der Haut mit Hinweis auf Befunde bei Hauterkrankungen. Arch. klin. exp. Dermat., 202 120–152.

Sumner J B and F Somers 1943 Chemistry and Methods of Enzymes. Academic Press Inc., New York.

# The Structure of Intermediate Vascular Pathways in the Spleen of Rabbits[1]

LEON WEISS

*Department of Anatomy The Johns Hopkins University School of Medicine Baltimore Maryland*

It is likely that the major functions of the red pulp and marginal zone are clearance and modification of certain hemal elements. Damaged erythrocytes aged erythrocytes (Weiss, '62) Foà Kurloff cells (Nadel, '52) lymphocytes from the thymus (Fichtelius, '60) granulocytes in shock and in hibernation, thorium dioxide and other colloidal matter in plasma (Weiss, '62) endotoxin, are examples of elements cleared by the spleen. In some instances as granulocytes of animals in shock and plasmal thorium dioxide, these functions are shared with the liver other parts of the reticuloendothelial system, and even the lungs and kidneys. In other cases, as the Foà-Kurloff cell and lymphocytes produced in the thymus, the spleen s role in sequestration may be more selective. Nice discriminations exist moderately damaged erythrocytes are selectively removed from the circulation by the spleen severely damaged erythrocytes, by the liver and reticuloendothelial system as a whole (Jandl and Kaplan, '60 Winkelman, Wagner McAfee and Morley '60)

Once cleared from the blood, the trapped elements meet varied fates. Impaired erythrocytes are phagocytized Lymphocytes and monocytes may undergo transformation into plasma cells and macrophages. Other cells may remain stored varying lengths of time and re-enter the circulation morphologically unchanged (Knisely '36)

It is likely that the intermediate circulation of the spleen, including the marginal zone splenic sinuses, splenic cords and arterial terminations clears blood and provides the staging for subsequent transformation and phagocytosis The marginal zone is an irregular vascular space which surrounds white pulp and into which many terminal arterial vessels empty Thus, after its intra-arterial injection, India ink in the spleen is most evidently present in the marginal zone (Mills '26 Snook, '58) Splenic cords are vascular spaces in the red pulp proper lying between splenic sinuses and communicating with them through mural apertures. They receive many arterial endings. Like sinuses, cords are lined by reticular cells which are considered phagocytic and cytopoietic (Maximow and Bloom, '57) Unlike that of sinuses the cordal lumen is usually divided into communicating spaces by slender branches of cordal reticular cells and by strands of extracellular reticulum, and these luminal spaces are often crowded with lymphocytes, monocytes, plasma cells and macrophages.

This paper presents observations by electron microscopy upon cords and sinuses of normal rabbit spleens and of rabbit spleens after the administration of Thorotrast. Its objectives are to define intermediate vascular pathways through the spleen, to describe the cytology of reticular cells comprising cords and sinuses, and to relate these findings to the spleen s capacity to clear blood.

## *A note on the use of the terms reticulum basement membrane and reticular cell*

The term *reticulum* was employed by Mall (1888) to designate slender extracellular argyrophilic fibers in liver spleen and other organs. He further characterized them in relation to their resistance to digestion and their solubility in a variety of reagents. These fibers are associated with cytoplasmic processes of reticular

[1] This work supported by Grant Heme C3373 (C1) of the United States Public Health Service.
Senior Investigator — Public Health Service.

cells. These cytoplasmic processes may be designated as *cellular reticulum* and the argyrophilic fibers as *extracellular* or *fibrous reticulum* or *reticulum* alone.

By electron microscopy each of the argyrophilic fibers in red pulp may have two components: true fibers and a ground material in which these fibers are embedded. It is possible that the ground material masks many more fibers than appear present (see observations below) or that like soluble collagen, it may be fibrous or amorphous depending upon such factors as pH and tonicity (Gross '59) Moreover the argyrophilia of the reticulum consisting primarily of ground substance is one finding which suggests that ground material and not fibers is responsible for binding silver (see Weiss '59 and '62, and Cohen Weiss and Calkins '60 for further discussion)

The extracellular reticulum of red pulp may be divided into several sections: the basement membrane and surrounding reticulum of arterial vessels the fenestrated basement membrane common to a sinus and contiguous cord the reticulum of cords the reticulum associated with veins of the pulp and with trabeculae. These components are portions of a continuous system of extracellular connective tissues.

That reticulum surrounding splenic sinuses possesses major transverse components joined by slighter longitudinal strands On surface view this reticulum gives the appearance of a net investing the sinus. The fibers of this net are in fact, not fibers at all but a continuous sheet of extracellular ground substance ensheathing the sinus containing fibers and perforated by large regularly spaced fenestrations. These fenestrations reduce the sheath of extracellular connective tissue to slender continuous strands like the lines outlining the squares of a chessboard Therefore this portion of the splenic reticulum appears best designated as a fenestrated basement membrane a designation employed by Bennett, Hampton and Luft ('60) Since reticular cells lining a sinus lie on the obverse surface of this basement membrane and reticular cells lining a cord lie on the reverse surface I consider this membrane common to cord and sinus.

The term *reticular cell* is used to designate those cells associated with reticular fibers comprising the substantive fixed morphological elements in splenic sinuses, splenic cords and marginal zones and possessing, as described below a characteristic disposition and distinctive cytological features.

## MATERIALS AND METHODS

The spleen was obtained from 16 adult male albino New Zealand rabbits weighing 3–6 kg Six of the animals were given 0 5 ml/kg Thorotrast (Heyden Chemical Co. N Y ) at 37 C intravenously either five minutes or one hour before splenectomy

In most cases the spleen was removed under surgical anesthesia without any effort to keep the blood in the organ In a few instances the vascular pedicle was clamped and tied and then the whole organ put in fixative. After about an hour the superficial blackened part was removed cut into blocks about 2 mm³ fixed another half hour and dehydrated

In a few cases a rabbit was killed by about 200 mg sodium pentobarital (4 ml Nembutal, Abbott) intravenously and then allowed to remain undisturbed 20–30 minutes or enough time to allow its blood to clot. Then the spleen was taken out, cut into blocks and fixed This material, prepared to avoid major redistribution or loss of the blood cells during its removal and cutting into blocks proved as well preserved as fresh spleen

The tissue was fixed in 1% osmium tetroxide buffered to pH 7 35 by veronal acetate buffers to which 0.25 gm/25 ml sucrose was added It was then dehydrated in ethyl alcohol and embedded according to the routine of Richardson, Jarett and Finke ('60) in araldite obtained through the New York Society of Electron Microscopists. Some blocks intended for thicker sections to be studied by light microscopy were embedded in methacrylate (Weiss, '57)

After sectioning with a Caracas diamond knife (48 angle) in a Porter Blum microtome the sections were mounted on grids coated with celloidin and carbon

Most of these grids were placed section surface down, on one of the following staining solutions at room temperature: 1% uranyl acetate for two hours (Watson, '58) 1% phosphotungstic acid for ten minutes, lead hydroxide (Method A of Karnovsky '61) for ten minutes. They were rinsed in distilled water after staining, and dried.

The sections were studied in a Siemens Elmskop I.

OBSERVATIONS

From study by light microscopy of sections 2–3 µ in thickness, cut from methacrylate-embedded blocks, several observations of red pulp may be emphasized in addition to those described in earlier papers. It was seen again that a fundamental property of the red pulp is the wall common to a sinus and cord. This wall consists of a median fenestrated basement membrane covered, on its obverse surface by reticular cells lining the sinus and on its reverse surface by reticular cells lining the cord.

The luminal content of sinuses varies considerably from place to place. Some segments of sinuses contain blood of the same apparent composition as in most systemic vessels. Others contain only plasma or a disproportionately large number of lymphocytes and monocytes. Plasma cells and macrophages are commonly present in sinuses, even in normal animals given no Thorotrast.

Cords and marginal zone also vary considerably in content and dimension from place to place. In general lymphocytes and monocytes are present in higher proportion to granulocytes and erythrocytes than in systemic blood. An occasional striking finding is the presence of a large irregular cleft filled with coagulated plasma and a few cells. The cellular content of cords varies from place to place moreover particularly with regard to the number and proportions of free macrophages, plasma cells and erythrocytes.

Not *uncommonly free* cells are observed in an aperture in the wall common to a sinus and cord. Such cells presumably in transit, are dumb-bell shaped an expanded portion in the sinus an expanded portion in the cord and a constricted mid-zone in the aperture (see fig. 15)

In many places in both cords and sinuses, plasma is more coarsely granular than in both extra-splenic systemic vessels and most vessels in the spleen, which suggests plasma proteins are more concentrated in such places (see figs. 5 and 11)

*Reticular cells in sinuses*

Under the electron microscope reticular cells lining sinuses may present a cuboidal shape in cross-section, but this shape appears readily modified by such occurrences as pressure of contiguous cells, pinocytosis or vacuolization at the cell surface, and large phagocytic or other inclusions (see for example figs. 2 3 and 8) These lining cells are attached only to the basement membrane. They are free of attachment to vicinal lining cells and, in fact plasma, thorium dioxide and free cells likely in passage are often insinuated between lining cells separating them by a considerable distance (figs. 2, 3 5 9 and 11)

Reticular cells lining sinuses generally contain moderate concentrations of RNP particles mitochondria, Golgi membranes, and endoplasmic reticulum — but it is not unusual to observe cells with large clusters of mitochondria or with high concentrations of RNP particles. Indeed cytoplasmic vacuoles apparently associated with endoplasmic reticulum are highly characteristic of reticular cells (figs. 6, 8 and 10) These are usually filled with a clear material — even with Thorotrast about. The vacuoles are of different size but are often quite large and in suitable preparations continuity with the outer nuclear membrane and with the plasma membrane is evident. Occasionally the membranes bounding these vacuoles are studded with RNP granules as in figure 10 The vacuoles may contain material resembling the substance of basement membrane.

The most distinctive characteristic of reticular cells — both of sinus and cord — is a *concentration of cytoplasmic material* deeply stained with uranyl acetate (see, especially figs. 3 4 7 8, 11 and 16) In both sinal and cordal reticular cells this material tends to lie near the extracellular reticulum — although this tendency is more pronounced in cordal cells.

Large clear vacuoles bounded by mem brane continuous with the cell membrane and with the outer nuclear membrane while not restricted to reticular cells were highly characteristic of them. Occasionally these vacuoles contained thorium dioxide or other phagocytized material. Of interest in refernce to the recent report of cartilage matrix in vacuoles of chon drocytes (Sheldon and Kimball '62) is the presence of material resembling the ground substance of basement membrane within some of these vacuoles. Particles of RNP were commonly observed studded upon the bounding membranes

A highly distinctive characteristic of reticular cells in the red pulp of rabbit spleen are concentrations of granular material faintly stained with lead hydrox ide or osmium tetroxide but deeply stained with uranyl acetate These concentrations may contain several components. They contain material resembling basement membrane and often particles which appear to be RNP particles. In some in stances a filamentous component was present similar to the cytoplasmic fila ments sometimes observed in reticular cells and in arterial endothelium (Weiss '62) The disposition of this material within a cell is striking. In reticular cells lining sinuses they account for the basal striations of light microscopy (Mollier 11 Jolly and Chevalier 09) They appear related to the cytoplasmic web stained by successive treatment with tannic acid phosphomolybdic acid and amido black as described by LeBlond Puchtler and Cler mont ('60) The aggregations in this material however and that from human spleen fixed in osmium tetroxide and embedded in methacrylate are stained in the periodic acid-Schiff reaction Even in sinal reticular cells and more markedly in cor dal reticular cells, this material is present in close physical relation to the reticu lum A component of the material can resemble the dense layer of basement membrane as seen in other organs but rarely present in the red pulp of spleen It is of interest that in his study of rat lymph nodes Han ('61) noted the rough ER most highly developed within attenuated cell processes surrounding fibers

*Phagocytes and free cells*

Macrophages lymphocytes monocytes and plasma cells are commonly present in *cords and sinuses. It* is noteworthy that the corpuscular content of blood in the spleen is different from that of the systemic circulation. Macrophages plasma cells and other cell types not usually considered blood cells are present in the lumen of sinuses. They are also present in the blood of the splenic vein and are likely filtered from the blood in the circulation of the liver and the lungs Within cords free cells are nestled between the processes of reticular cells. Lymphocytes and monocytes in cords and sinuses may be sequestered from the circulation. Yet the blood is not their only likely source. *There is evidence from studies of* runt disease that lymphocytes migrate to the red pulp from the white pulp (Congdon and Makinodan '61) Reticular cells considered multipotential, may undergo transformation into lymphocytes and monocytes and account for some of those in cords and sinuses.

It is difficult to evaluate the capacity of *reticular cells to become phagocytic. After* the moderate stimulus provided by Thorotrast phagocytes loaded with thorium dioxide were quickly evident. But in cells identifiable as reticular cells by their association with reticular fibers their possession of granular concentrations (vide supra) and their location few phagocytic vacuoles were discovered and these were small or moderate in size It is likely however that some cordal reticular cells, notably those deep in the cords rather than those immediately subjacent to a sinus became phagocytic. This conclusion is supported by the close association of such phagocytic cells with reticulum and the general similarity of their cytoplasm to that of well defined reticular cells. However granular cytoplasmic concentrations stained with uranyl acetate were absent from these phagocytes.

It is evident that many macrophages are free cells because they may be observed free in the sinal lumen (see figs. 6 and 13 of an earlier paper — Weiss '59) Such free macrophages in sinuses or in cords

may be derived from monocytes or perhaps lymphocytes cleared from blood or emigrated from white pulp. Or they may be derived from reticular cells become freed of the extracellular reticulum and phagocytic. Yet it is difficult to establish any given cordal macrophage as free and not a phagocytic reticular cell fixed to reticulum since only a small portion of a reticular cell's surface may be fixed to extracellular reticulum and, so large are these cells, this portion is likely out of field.

In lymph nodes and spleen of rats studied by electron microscopy Han ('61) found reticular cells associated with fibers had no demonstrable phagocytic capacity In lymph nodes of rabbits, however Sorenson ('60 '61) observed by electron microscopy reticular cells which had phagocytized colloidal gold.

*Organization of the intermediate circulation*

Reticular cells of cords differ from those of sinuses in their conformation. Sinal reticular cells are shaped like tapering rods their long axis parallel to the long axis of the sinus. Cordal reticular cells branch. Those lying upon the reverse surface of the basement membrane common to cord and sinus extend slender processes along the basement membrane and into the lumen of the cord. These processes are associated with extracellular reticulum, the former with the basement membrane the latter with cordal reticulum Since this is the prevailing pattern of reticular cell conformation my hypothesis that cords represent collapsed sinuses (Weiss '57) is no longer tenable. The cords are vascular spaces however (vide infra) their close relationship demonstrable experimentally (Weiss, '59)

It is clear from the observations of Mills ('26) of MacNeal, Otani and Patterson ('27) of Snook ('58) of this study and earlier ones (Weiss, '59 '62) that several circulatory pathways exist in the red pulp Arterial terminations end in different places. Most empty into the marginal zone Many end in the cords some few end in direct connection with sinuses. Moreover as Snook has shown and I can confirm, arterial endings may end in several different ways in the cords of rabbits. Each of these variations surely constitutes a variation in blood flow Further terminating arterial vessels may differ in size. Some are of arteriolar size and possess cytological adventitial elements. Others are slender structures of capillary size. They may open by a slit-like penetration of basement membrane associated with microvilli, or the opening may be broad The height of the terminating endothelium is typically high but is subject to variation as first emphasized by MacNeal Otani and Patterson ('27)

The number of direct connections of artery to sinus appears small Sinuses receive blood from cords. The blood passes across the sinal wall, through the fenestrated basement membrane and between the reticular cells lining the sinus Yet as MacNeal Otani and Patterson ('27) and Snook ('58) have emphasized it is possible that the circulation into the sinuses may achieve the directness of arterial-sinal communication despite arterial endings terminating in a cord. Indeed my observations support the liklihood that such arrangements exist. It is not unusual to find a small arterial orifice lying in a cord directed at a fenestration in the basement membrane common to that cord and a sinus. The orifice, smaller than the fenestration in breadth may be only 5 μ from the wall of the sinus and the cordal reticular lining cell retracted or absent from the cordal surface of the basement membrane in that vicinity Thus passage from such an arterial vessel to a sinus is blocked only by sinal lining cells which meet across the opening in the basement membrane. Now passage across the wall of a sinus from cordal lumen into sinal lumen offers no more resistance to the passage of blood cells than passage through a terminating arterial vessel, since the arterial endothelium is usually high and effaces the arterial lumen as the sinal lining cells touching side to side, cover the fenestration in the basement membrane. In fact it is not uncommon to encounter blood cells in the wall of a sinus presumably in transit through the wall.

Among the differences consequent on differences in the charact[illegible] terminating arterial vessels are diff[illegible] of flow The direct artery-sinu[illegible]

*Large clear vacuoles bounded by* membrane continuous with the cell membrane and with the outer nuclear membrane while not restricted to reticular cells, were highly characteristic of them. Occasionally these vacuoles contained thorium dioxide or other phagocytized material. Of interest in refernce to the recent report of cartilage matrix in vacuoles of chondrocytes (Sheldon and Kimball '62) is the presence of material resembling the ground substance of basement membrane within some of these vacuoles. Particles of RNP were commonly observed studded upon the bounding membranes

A highly distinctive characteristic of reticular cells in the red pulp of rabbit spleen are concentrations of granular material faintly stained with lead hydroxide or osmium tetroxide but deeply stained with uranyl acetate These concentrations may contain several components They contain material resembling basement membrane and often, particles which appear to be RNP particles. In some instances a filamentous component was present similar to the cytoplasmic filaments sometimes observed in reticular cells and in arterial endothelium (Weiss '62) The disposition of this material with in a cell is striking. In reticular cells ... sinuses they account for the basal striations of light microscopy (Mollier 11 Jolly and Chevalier 09) They appear related to the cytoplasmic web stained by successive treatment with tannic acid phosphomolybdic acid and amido black as described by LeBlond Puchtler and Clermont (60) The aggregations in this material however and that from human spleen fixed in osmium tetroxide and embedded in methacrylate are stained in the periodic acid-Schiff reaction Even in sinal reticular cells and more markedly in cordal reticular cells, this material is present in close physical relation to the reticulum. A component of the material can resemble the dense layer of basement membrane as seen in other organs but rarely present in the red pulp of spleen It is of interest that in his study of rat lymph nodes, Han ('61) noted the rough ER most highly developed within attenuated cell processes surrounding fibers

*Phogocytes and free cells*

Macrophages lymphocytes, monocyt and plasma cells are commonly pres cords and sinuses. It is notewor the corpuscular content of bl spleen is different from th temic circulation. Macr cells and other cell ty sidered blood cells lumen of sinuses Th in the blood of the spl likely filtered from the blo lation of the liver and the lu cords free cells are nestled l processes of reticular cells. Lym and monocytes in cords and sinu be sequestered from the circulation the blood is not their only likely sou There is evidence from studies of ru disease that lymphocytes migrate to the red pulp from the white pulp (Congdon and Makinodan, '61) Reticular cells, considered multipotential, may undergo transformation into lymphocytes and monocytes and account for some of those in cords and sinuses.

It is difficult to evaluate the capacity of reticular cells to become phagocytic. After the moderate stimulus provided by Thorotrast phagocytes loaded with thorium dioxide were quickly evident. But in cells identifiable as reticular cells by their association with reticular fibers their possession of granular concentrations (vide supra) and their location few phagocytic vacuoles were discovered and these were small or moderate in size. It is likely however that some cordal reticular cells, notably those deep in the cords rather than those immediately subjacent to a sinus, became phagocytic. This conclusion is supported by the close association of such phagocytic cells with reticulum and the general similarity of their cytoplasm to that of well defined reticular cells However granular cytoplasmic concentrations stained with uranyl acetate were absent from these phagocytes

It is evident that many macrophages are free cells because they may be observed free in the sinal lumen (see figs. 6 and 13 of an earlier paper — Weiss '59) Such free macrophages in sinuses or in cords,

may be derived from monocytes or perhaps lymphocytes cleared from blood or emigrated from white pulp Or they may be derived from reticular cells become freed of the extracellular reticulum and phagocytic. Yet it is difficult to establish any given cordal macrophage as free and not a phagocytic reticular cell fixed to reticulum since only a small portion of a reticular cell's surface may be fixed to extracellular reticulum and, so large are these cells this portion is likely out of field.

In lymph nodes and spleen of rats studied by electron microscopy Han ('61) found reticular cells associated with fibers had no demonstrable phagocytic capacity In lymph nodes of rabbits, however Sorenson ('60 '61) observed, by electron microscopy reticular cells which had phagocytized colloidal gold.

*Organization of the intermediate circulation*

Reticular cells of cords differ from those of sinuses in their conformation. Sinal reticular cells are shaped like tapering rods, their long axis parallel to the long axis of the sinus. Cordal reticular cells branch. Those lying upon the reverse surface of the basement membrane common to cord and sinus extend slender processes along the basement membrane and into the lumen of the cord. These processes are associated with extracellular reticulum, the former with the basement membrane the latter with cordal reticulum. Since this is the prevailing pattern of reticular cell conformation my hypothesis that cords represent collapsed sinuses (Weiss '57) is no longer tenable The cords are vascular spaces however (vide infra) their close relationship demonstrable experimentally (Weiss, '59)

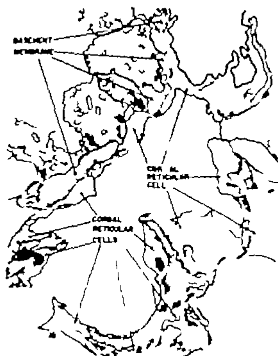
It is clear from the observations of Mills ('26) of MacNeal, Otani and Patterson ('27) of Snook ('58) of this study and earlier ones (Weiss '59 '62) that several circulatory pathways exist in the red pulp Arterial terminations end in different places. Most empty into the marginal zone. Many end in the cords, some few end in direct connection with sinuses. Moreover as Snook has shown and I can confirm, arterial endings may end in several different ways in the cords of rabbits. Each of these variations surely constitutes a variation in blood flow Further terminating arterial vessels may differ in size Some are of arteriolar size and possess cytological adventitial elements. Others are slender structures of capillary size They may open by a slit-like penetration of basement membrane associated with microvilli, or the opening may be broad. The height of the terminating endothelium is typically high but is subject to variation as first emphasized by MacNeal, Otani and Patterson ('27)

The number of direct connections of artery to sinus appears small. Sinuses receive blood from cords. The blood passes across the sinal wall through the fenestrated basement membrane and between the reticular cells lining the sinus. Yet as MacNeal, Otani and Patterson ('27) and Snook ('58) have emphasized, it is possible that the circulation into the sinuses may achieve the directness of arterial-sinal communication despite arterial endings terminating in a cord. Indeed my observations support the liklihood that such arrangements exist. It is not unusual to find a small arterial orifice lying in a cord directed at a fenestration in the basement membrane common to that cord and a sinus. The orifice smaller than the fenestration in breadth may be only 5 μ from the wall of the sinus and the cordal reticular lining cell retracted or absent from the cordal surface of the basement membrane in that vicinity Thus passage from such an arterial vessel to a sinus is blocked only by sinal lining cells which meet across the opening in the basement membrane Now passage across the wall of a sinus from cordal lumen into sinal lumen offers no more resistance to the passage of blood cells than passage through a terminating arterial vessel since the arterial endothelium is usually high and effaces the arterial lumen as the sinal lining cells touching side to side cover the fenestration in the basement membrane. In fact it is not uncommon to encounter blood cells in the wall of a sinus, presumably in transit through the wall.

Among the differences consequent on differences in the character of terminating arterial vessels are different rates of flow The direct artery-sinus connections and

# PLATE 5

### EXPLANATION OF FIGURE




5 This field includes portions of a contiguous sinus and cord. The *lining cells of the sinus are cut near cross section, are attached to the basement membrane but are free of attachment to contiguous lining cells.* The slender sinal lining cell which does not touch on the lumen is likely the tapering end of a cell.

These lining cells display a great deal of surf ce activity and their cytoplasm contains conspicuous, clear vacuoles. Note the surface of the topmost cell. Note too, the basal concentrations of a material deeply stained with uranyl cetate. There are moderate and variable concentrations of RNP particles present throughout the cytoplasm. Note the mitochondria of varied size having poorly developed cristae.

The subjacent cord contains erythrocytes and phagocytes. The cordal urf ce of the basement membrane is covered by the cytoplasm f reticular cells. *Over most of this surface the* cytoplasmic cover is very thin. In the right upper portion of the plate the nucleus of a cordal reticular cell *is prese t. The perinuclear cytoplasm is relatively voluminous.* Cordal reticular cells contain organelles similar to those lining sinuses. M terial tained with uranyl acetate similar to the basal material in sinal lining cells, is present in the cytoplasm lying gainst the basement membrane and in the cytoplasmic processes extending into the cordal lumen. Here, too, this material is usually close gainst the extracellular connective tissue. The strands of reticulum *subdividing the cordal lumen are clothed by thin layer of reticular cell cytoplasm.* In places, some of the cordal lumen is evident but most of it is filled by phagocytes, erythrocytes, and other free cells.

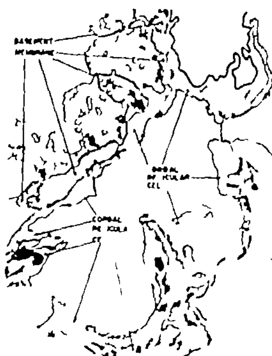
Thorium dioxide is present extracellularly in the cordal lumen and between sinal lining cells. Some is present within reticular cells, usually bounded by membrane. Many large vacuoles containing thorium dioxide are present in phagocytes. None is in th basement membrane

× 27,000



## PLATE 5

EXPLANATION OF FIGURE




5. Thi fi ld includes portions of ontiguou inus and ord The lining c ll of the inu re cut near ros section t attached to the basement membrane but are free of tt chment to contiguou lining cell The slender sin l lining cell which does not touch on the lumen l lik ly the t peri g end of c ll. These lini g ll di pl y great de l f rl c activity nd their ytopl m cont ins conspicuou clear vacuoles Not the urface of the topmost c ll Not ion the basal oncent tion of materi l deeply t i ed with u yl cet t There re moder te nd v ri ble oncen t tion f RNP p ticles present throughout the ytopl m Note the mitochond i f v ied size having poorly dev loped crista

Th bjacent ord ontains eryth rocytes nd ph gocytes The cordal urf of the basement membrane i overed by the ytopl sm of reticula c lls. Ove most of thi surfac the cytopl smic cover is very thin In the right upper portion of the pl te the nucleu of a cordal reticular cell i p ese t. The perinucle cyto pl m i rel tively vol minous. Cor d l reticul ll cont in org nelles imila t those lini g al se M t ri l t ined with uranyl acet t imila t the basal m teri l i al l lini g ll is p esent in the cytoplasm lying g inst the basement memb ne and i the ytopl mic processes extendi g i t the cord l l men. Here too, thi mat l l is lly close g in t the extrac llular connective tissu Th stra de of reticu lum subdividi g the ord l l me re lothed by thin l yer of reticula cell cytopl sm In places some of the cord l l men i evident but most of it i filled by ph gocytes eryth rocytes and other free ell

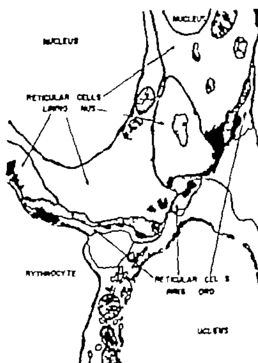
Thori m dioxide is present ext acell l ly i th cord l lume and betwee inal lining c ll Some i present within reticular ll u lly bou ded by membr ne M y l rge acuoles cont ining thori m dioxide re prese t in ph gocytes None i i the basement membrane

× 27,000



## PLATE 6

EXPLANATION OF FIGURE




6 This preparation which includes part of the wall of si us and cord is stained with lead hydroxide. The cytoplasmic concentrations deeply stained with uranyl acetate re unstained or lightly stained here RNP particles in cytoplasm and nucleus are moderately deeply stained. The basement membrane between the sinal reticular cells, above and the cordal reticular cells, below is un tained.

The small wedge-shaped sinal cell is probabl cut across its tapered end. Mitochondria and membranous systems of the reticular cells are noteworthy Mitchondria display considerable pleomorphism. The nature of the nuclear membranes well shown.

× 28,000


7

## PLATE 7

### EXPLAN TION OF FIGURE

7 Here two reticula cells in the wall of sinus are cut longitudinally and the longitudinal disposition of the basal gra ular material may be seen This material, stained with uranyl acetate accounts for the longitudinal basal striations of sinal lining cells. Note that the basement membrane — a portion is at the right lower corner — is unstained. Compare with figures 10 and 11

× 22,000



## PLATE 8

### EXPLAN TION OF FIGURE

8 A slender portion of cord, running from left to right, occupies the center f the plate It consist only of a portion of cordal cell and on the right, cordal lumen. Above and below this cordal tissue separated from it by basement membrane are portions of the lining cells of sinuses

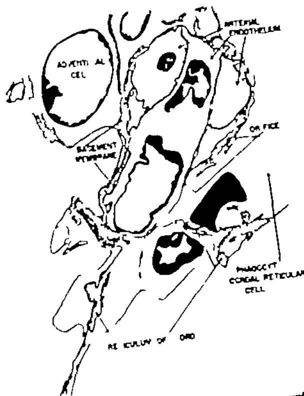
The cordal cell is noteworthy for large clear vacuoles. They represent dilated portion of the endoplasmic reticulum and, in places, the membrane bounding these vacuoles are studded with RNP granules. Note on the right, the cordal lumen continuou with the deep indentations of the plasma membrane Compare with figures 5 and 10. Thorium dioxide, given five minutes before splenectomy is in the cordal lumen and included with some cytopl smic vacuoles. Note the dense granular concentrations deeply tained by uranyl acet te They are in close proximity to the basement membrane. In places filamentou or a granular character may be observed. N ar the upper margin of the pl te on the right, are two m sses of thi material one in the sinal lining cell, the other in portion of the cordal cell which presents on the lumen of the sinus. In these masses both granular and filamentous components may be observed. Note the filamentous haracter evident in portions of the basement membrane At the middle of the left margin note the interesting oval formation constituting centriole It is surrounded by dense uranyl *acetate-stained material similar to that noted above. Similar formation* are present at the lower margin of the plate

× 39,000



PLATE 12

EXPLAN TION OF FIGURE



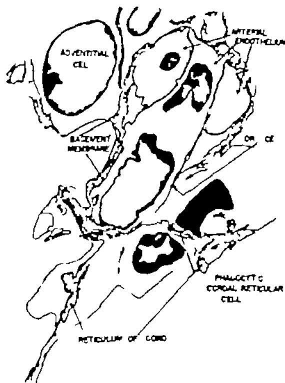

13 Thi field is in cord. Most of the pl te is occupied by small terminal rterial vessel. The vessel i outlined long much of it perim eter by a well-developed basement membrane continuous with that extra cellular connective tissue surrounding its rather slight adventitial le-ments. The basement membrane is defective in one place and here a slender luminal slit may be followed to the outside of the vessel. A portion of an endothelial cell present i the cord The endothelium is high, and effaces the lumen. The vessel is closely surrounded by cells of the cord Pressed against its orifice is the ectoplasm of phagocytic cell containing phagocyted erythrocyte. It is likely th t this phagocyte is reticular cell attached to the cordal reticulum. Contrast this vessel with the patulous one in figure 11 The tracing presents larger field than in the plate. The region of the orifice i enlarged figure 14

× 12,000



## PLATE 12

### EXPLANATION OF FIGURE




13 This field in cord. Most of the plate is occupied by small terminal arterial vessel. The vessel is outlined along much of its perimeter by well-developed basement membrane continuous with that extracellular connective tissue surrounding its rather slight adventitial lements. The basement membrane is defective in one place and here a slender luminal slit may be followed to the outside of the vessel A portion of an endothelial cell presents to the cord. The endothelium is high, and effaces the lumen. The vessel is closely surrounded by cells of the cord. Pressed against its orifice is the ectoplasm f phagocytic cell containing phagocyted erythrocyte It is likely that this phagocyte is a reticular cell ttached to the cordal reticulum. Contrast this vessel with the patulous one in figure 11 The tracing presents larger field than in the plate The region of the orifice is enlarged as figure 14

X 12,000

# Effects of Respiratory Inhibitors on Development of the Down Feather[1]

C. WARD KISCHER AND HOWARD L. HAMILTON[2]
*Department of Zoology and Entomology Iowa State University Ames Iowa*

The close association of alkaline phos-hatase and ribonucleic acid in the devel-ping down feather and the possible func-ons of these substances in differentiation ave been discussed by Koning and Hamil-n ('54) They demonstrated a gradient attern of alkaline phosphatase localized the pulp next to a high concentration of NA in epidermal regions of morphogen-is and differentiation. Later they found at when the phosphatase was inactivated y beryllium, which competes with mag-esium for a place on the enzyme mole-le, the synthesis of RNA in the epi-ermis was diminished, and little further orphogenesis occurred (Hamilton and oning, '56)

Similar results were obtained by Fabiny '59) through the use of Versene and 2-thienylalanine. By adding the chelat g compound, Versene to tissue cultures f developing down feathers he demon-rated an inactivation of alkaline phos-hatase and a concomitant decrease of NA in the epidermis. He concluded that e effect on RNA limited the synthesis of roteins and, hence curtailed morphogen-is. β-2-thienylalanine was used as a spe-fic *inhibitor* of the epidermal component f the feather and was thought to (a) pre-ent the release of RNA from the nucleolus the cytoplasm, or (b) antagonize the tilization of RNA during synthesis of pep-des and proteins.

Gibley and Hamilton ('63) found that rotic acid, isoguanine sulfate and 8-aza uanine inhibited the activity of the hosphatase and appeared to upset the metabolism of RNA. Their most striking bservations were (1) the occurrence of arge vacuolated nucleoli within the epi ermis in cultures treated with orotic acid t levels inhibiting phosphatase and (2) nlarged nucleoli and an apparent *increase* of RNA in tissues treated with 8-azagua-nine at concentrations which increased the reaction for phosphatase. Their conclu-sions supported the theory that alkaline phosphatase and RNA are interrelated in promoting morphogenesis of the feather with phosphatase supplying nutrients from pulp to epidermis and RNA functioning as a precursor for structural proteins such as keratin.

In contrast to alkaline phosphatase which seems directly connected with mor phogenesis, other enzymes such as suc-cinic dehydrogenase and cytochrome oxi-dase, are of more general occurrence and diffuse distribution throughout the tissue (Koning and Hamilton, '54) These too are enzymes important in the supply of sources of energy to cell and tissue, but are of a more fundamental type essential to the survival of cells, because they are directly concerned with basic respiratory requirements.

Heretofore, no work had been done on the effects of respiratory inhibitors on the morphogenesis of the down feather The present study was undertaken, therefore to test what effects the well-known respira-tory poisons sodium fluoride 2,4-dinitro-phenol, iodoacetate, and sodium cyanide might have on organogenesis.

## MATERIALS AND METHODS

Bilaterally-paired pieces of skin were re-moved under sterile conditions from the dorsal midline of chick embryos between stages 29 and 33 (6–8 days Hamburger

[1] This investigation was supported in part by research grant, RG-3813 (C7), from the Division of General Medical Sciences, National Institutes of Health, U. S. Public Health Service, and by the Industrial Science Research Institute of Iowa State University

Present address Department of Biological Sciences, Illinois State Normal University Normal, Illinois.

[2] Present address Department of Biology University of Virginia Charlottesville, Virginia.

and Hamilton, '51). One member of each pair was placed in a tissue culture of the hanging-drop type containing an aliquot of test solution, while the other piece was placed in a control culture containing an equivalent amount of either Pannett-Compton saline or 0.9% NaCl solution (Hamilton and Koning, '56).

The test chemical was weighed in a clean dry test tube. Sodium fluoride was sterilized in the autoclave before dissolving in sterile Pannett-Compton solution. 2,4-dinitrophenol and iodoacetate were dissolved in Pannett-Compton solution, while sodium cyanide was dissolved in 0.9% NaCl. Each non-sterile solution was then passed through a Seitz filter into a previously-sterilized test tube. In each case, with the exception of sodium cyanide, the original solution constituted the stock from which lower concentrations were prepared by dilution with the appropriate saline. Sodium cyanide solutions were prepared fresh prior to each culture period. Control cultures for the latter chemical received 0.9% NaCl, while all other controls received Pannett-Compton solution. The cultures were incubated from two to five days at 37.5 C. Certain pairs were then fixed in cold acetone and processed as whole mounts for the demonstration of alkaline phosphatase by Gomori's method ('46). Other pairs were fixed in cold absolute alcohol containing 5% glacial acetic acid, embedded, sectioned at 7 μ, and stained with 0.05% toluidine blue in 5% ethyl alcohol. Some sections were incubated in a 1 mg/ml solution of ribonuclease in distilled water for three hours at 59 C, while the corresponding controls were incubated for the same length of time in distilled water alone, before staining with toluidine blue. Areas which lost their basophilia after treatment with the enzyme were presumed to have contained ribonucleic acid.

## RESULTS

The concentrations of the chemicals ranged from 140 μg/ml in the case of sodium fluoride to 0.1 μg/ml for 2,4-dinitrophenol. The data recorded from the living cultures are given in table 1. Columns four and six summarize the data by giving ratios of treated value to control value for total growth of cultures and number of feathers respectively. Values for over-all growth were calculated from the ratio of (total diameter of treated culture minus 1 mm)/(total diameter of control culture minus 1 mm), since each piece of tissue started its growth in culture as an explanted fragment of approximately 1 mm. T/C values for feathers were determined from counts of the total number of feathers differentiating in treated and control cultures (column 5). In either case, a T/C value greater than 1.0 indicates stimulation, and less than 1.0 indicates inhibition, by the concentration of each chemical compound given in column one.

Each of the test chemicals inhibited feather development and over-all growth at the higher concentrations. In no instance do the data give evidence for significant stimulation of growth.

*Sodium fluoride* inhibited most cultures at a concentration of 140 μg/ml. Even with complete inhibition of feathers, the growth of the tissue was not completely inhibited, but the reaction for phosphatase was lacking (figs. 1 and 2). In others small accumulations of phosphatase indicated partial organization of feathers (figs. 3–4). Normally ribonucleic acid occurs in heavy concentration within the cytoplasm of epidermal cells, especially in those which lie next to the phosphatase-active pulp and particularly against the basement membrane. In sections stained for RNA, the cultures treated with 140 μg/ml showed feather loci with less RNA in the epidermis. The dermis appeared separated from the epidermis lateral to the main bulk of the pulp (figs. 15–16).

*2,4-dinitrophenol*, at concentrations of 8⅓ μg/ml, 16⅔ μg/ml and 33⅓ μg/ml, inhibited feathers partially to nearly completely (figs. 9–10). Growth of the treated cultures and the amount of phosphatase activity paralleled development of the feathers. Sections stained for RNA showed differential inhibition of the dermis (figs. 17–18). The epidermis appeared normal and there was no reduction in RNA at lower levels of inhibition.

*Iodoacetate* prevented the development of feathers at concentrations of 6¼ μg/ml, 12½ μg/ml and 25 μg/ml, even though growth of the tissue continued. At

TABLE 1

*Effects of respiratory inhibitors on the development of feathers*

| Chemical and concentration | Total number: Embryos | Total number: Tissue pairs | Average diameter: Control culture | Average diameter: Treated culture | T/C values for growth | Average number of feathers: Control culture | Average number of feathers: Treated culture | T/C values for number of feathers |
|---|---|---|---|---|---|---|---|---|
| μg/ml | | | mm | mm | | | | |
| Sodium fluoride | | | | | | | | |
| 140 | 11 | 59 | 4.26 | 2.55 | 0.48 | 4.50 | 0.80 | 0.18 |
| 70 | 10 | 42 | 4.30 | 3.78 | 0.84 | 3.34 | 2.45 | 0.73 |
| 35 | 10 | 58 | 4.33 | 3.95 | 0.89 | 4.07 | 4.43 | 1.09 |
| 17.50 | 2 | 10 | 3.53 | 3.51 | 0.95 | 3.60 | 3.10 | 0.86 |
| 8.75 | 2 | 15 | 3.72 | 3.88 | 1.06 | 2.74 | 2.74 | 0.95 |
| 2,4-dinitrophenol | | | | | | | | |
| 50 | 1 | 7 | 2.83 | 1.47 | 0.94 | 4.00 | 0.00 | 0.00 |
| 33.33 | 6 | 56 | 3.33 | 1.94 | 0.40 | 4.85 | 0.21 | 0.04 |
| 16.67 | 5 | 29 | 3.44 | 3.16 | 0.89 | 4.72 | 1.59 | 0.34 |
| 8.33 | 4 | 29 | 4.13 | 3.94 | 0.94 | 3.55 | 2.34 | 0.66 |
| 4.16 | 8 | 50 | 3.88 | 3.78 | 0.96 | 4.85 | 4.55 | 0.94 |
| 3.33 | 2 | 12 | 3.02 | 2.68 | 0.84 | 2.33 | 1.33 | 0.57 |
| 2.08 | 2 | 14 | 4.00 | 4.11 | 1.04 | 3.64 | 2.79 | 1.04 |
| 1.04 | 1 | 6 | 4.28 | 4.01 | 0.92 | 8.50 | 7.00 | 0.82 |
| 0.50 | 9 | 60 | 3.92 | 3.63 | 0.90 | 3.24 | 3.49 | 1.08 |
| 0.33 | 2 | 9 | 4.42 | 4.94 | 1.15 | 4.12 | 4.33 | 1.05 |
| 0.25 | 2 | 13 | 4.75 | 4.72 | 0.99 | 3.62 | 3.77 | 1.04 |
| 0.17 | 4 | 28 | 3.24 | 3.38 | 1.05 | 3.82 | 4.10 | 1.07 |
| 0.10 | 14 | 85 | 3.50 | 3.51 | 1.00 | 3.36 | 3.34 | 0.99 |
| Iodoacetate | | | | | | | | |
| 25 | 3 | 17 | 4.52 | 1.01 | 0.00 | 4.12 | 0.00 | 0.00 |
| 12.50 | 4 | 23 | 3.62 | 2.12 | 0.42 | 4.73 | 0.34 | 0.07 |
| 6.25 | 7 | 50 | 3.09 | 2.43 | 0.68 | 3.55 | 0.78 | 0.22 |
| 3.12 | 3 | 19 | 3.67 | 3.52 | 0.98 | 4.26 | 4.16 | 0.98 |
| 1.56 | 1 | 5 | 3.74 | 3.53 | 0.92 | 4.40 | 4.80 | 1.09 |
| Sodium cyanide | | | | | | | | |
| 125 | 2 | 16 | 4.90 | 1.03 | 0.01 | 4.72 | 0.00 | 0.00 |
| 62.50 | 4 | 28 | 4.28 | 1.66 | 0.30 | 4.60 | 0.18 | 0.04 |
| 33.33 | 3 | 20 | 4.61 | 2.10 | 0.58 | 5.20 | 2.10 | 0.40 |
| 16.67 | 8 | 53 | 3.89 | 3.06 | 0.72 | 4.45 | 3.41 | 0.77 |
| 8.33 | 3 | 17 | 4.46 | 3.26 | 0.65 | 5.06 | 5.34 | 1.04 |

all inhibitory levels the reaction for phosphatase was light or absent (figs. 5–8). Serial sections of feathers from inhibited cultures revealed that RNA was reduced or absent at the basement membrane, even though the thickness of the epidermis compared favorably with the controls (figs. 19–20).

*Sodium cyanide.* The reaction for alkaline phosphatase, the development of feathers, and total growth of the tissue all were correlated inversely with the concentration of cyanide (table 1). At lower levels, the phosphatase was active (figs. 11–12) but at higher concentrations (62½–125 μg/ml) phosphatase was reduced and feather loci were poorly organized (figs. 13–14). Sections revealed much reduction of RNA along the basement membrane (figs. 21–22). Degeneration of the mesenchyme of the locus was prominent.

### *Evidences of field organization*

*Orientation of fibroblasts.* A common phenomenon in both control and treated cultures was the presence of radially-oriented fibroblasts at the feather base (fig. 23). The pattern was often more apparent in treated cultures at lower concentrations of chemicals because the fibroblasts were more deeply stained than in controls. Typically the fibroblasts were oriented in curvilinear paths radiating from the base of the feather in a fashion reminiscent of

## PLATE 1

### EXPLANATION OF FIGURES

1 Control explant f skin from the back of an embryo of stage 29 Note the intense reaction for phosphatase in the pulp of each feather immediately below the growing epidermal tip. × 60

2 The corresponding bilateral half of the piece of tissue shown in figure 1 grown in the presence of sodium fluoride (140 µg/ml of mixed culture medium) The growth of the feathers has been completely inhibited and the phosphatase reaction is absent. × 60.

3 Control explant of skin from an embryo of stage 29 showing normal feathers and an intense phosphatase reaction within the feather germs. × 60.

4 The corresponding bilateral half of the piece of tissue shown in figure 3, grown in the presence of sodium fluoride (140 µg/ml) Note the small concentrations of phosphatase reaction and lack of feather outgrowths. × 60.

5 Control explant of skin from the back of an embryo of stage 32 showing the strong reaction for phosphatase within the feather germs. × 60.

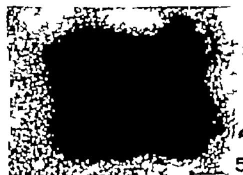
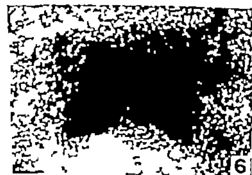
6 The corresponding bilateral half of tissue shown in figure 5 grown in the presence of iodoacetate (6¼ µg/ml) Although the phosphatase reaction is present, the feathers are not well formed. × 60.

7 The edge of a control piece of tissue, showing adjacent fibroblasts aligned parallel to the border of the epidermis. Note the intense phosphatase reaction within the nuclei. × 600.

8 The edge of the corresponding bilateral half of the piece of tissue shown in figure 7 The tissue was grown in the presence of 2,4-dinitrophenol (33⅓ µg/ml) Note the random orientation of the bordering fibroblasts and the reduced phosphatase reaction. × 600







## PLATE 1

### EXPLANATION OF FIGURES

1 Control explant of skin from the back of an embryo of stage 29 Note the intense reaction for phosphatase in the pulp of each feather immediately below the growing epidermal tip. × 60.

2 The corresponding bilateral half of the piece of tissue shown in figure 1, grown in the presence of sodium fl oride (140 µg/ml of mixed culture medium) The growth of the feathers has been completely inhibited and the phosphatase reaction is bsent. × 60.

3 Control explant of skin from an embryo of stage 29 showing normal feathers and an intense phosphatase reaction within the feather germs. × 60.

4 The corresponding bilateral half of the piece of tissue shown in figure 3, grown in the presence of sodium fluoride (140 µg/ml) Note the small concentrations of phosphatase reaction and lack of feather outgrowths. × 60.

5 Control explant of skin from the back of an embryo of stage 32 showing the strong reaction for phosphatase within the feather germs. × 60.

6 The corresponding bilateral half of tissue shown in figure 5, grown in the presence of iodoacetate (6¼ µg/ml) Although the phosphatase reaction is present, the feathers are not well formed. × 60.

7 The edge of control piece of tissue showing adjacent fibroblasts aligned parallel t the border of the epidermis. Note the intense phosphatase reaction within the nuclei. × 600.

8 The edge of the corresponding bilateral half of the piece of tissue shown in figure 7 The tissue was grown in the presence of 2,4-dinitrophenol (33⅓ µg/ml) Note the random orientation of the bordering fibroblasts and the reduced phosphatase reaction. × 600.

# A Study of Bone Resorption and the Osteoclast Problem by Stain Historadiography[1]

FEDOR BOHATIRCHUK
*Department of Anatomy University of Ottawa Ottawa, Canada*

During the last two or three decades investigators have been reconsidering the morphological and pathological problems of bone resorption in general and of osteoporosis in particular Most take the view that the disappearance of bone during resorption of any kind is the result of the simultaneous destruction of the two mat rices of bone — organic and inorganic (i.e., mineral, Pritchard, Eastoe, '56); in other words bone cannot lose the mineral matrix alone it must lose also the organic matrix (Nordin, '61) In addition the majority view holds that bone destruction is caused directly or indirectly by a specialized multinucleated giant cell, i.e., the osteoclast (Weidenreich '30; Kroon, '54; McLean, '55 Hancox, '56) Only a few authors (Howell, 1891 Arey '20; Jaffe '30) admit the possibility of calcium loss from bone through some other channels as yet uncertain. Bohatirchuk ('60) showed that the calcium impoverishment of normal aging bones can proceed without destruction of the organic matrix (so-called halisteresis) and he found only a few osteoclast-like cells in areas of atrophic aging bone.

An explanation of these controversies is best given in the saying of Frost ('60) most histologic work on this disease (meaning osteoporosis, F B ) has been carried out on decalcified sections. The folly of concluding *anything* about bone mineral from such material is obvious yet conclusions are tacitly and routinely made. Until undecalcified material is studied we have no right to assume there would be nothing there if such material were examined.

Since the data cited above (Bohatirchuk, '60) were obtained by a new method (Bohatirchuk, '57) for the study of undecalcified bone it is thought to be of interest to discuss briefly the improved technique of this method and to report the results therefrom in some cases of experimental bone resorption and in some of human material.

## MATERIAL AND METHOD

Stain historadiography (Bohatirchuk, '57 '61) was the principal method used. In its application to the study of bone the method consists of five stages (a) embedding in plastic blocks the undecalcified bone with some surrounding soft tissue; (b) serial cutting of the blocks in sections 10 μ and thinner (c) radiography of the sections with x rays 1 0 and 1.2 Å on a fine grain emulsion, (d) histological coloring of the same radiographed sections (without disembedding) and (e) the alternate study microscopically of the colored specimen and its historadiograph mounted on the same slide juxtaposed or superimposed. In some cases only the first three stages (i.e. historadiography or microradiography) were used. The technique of historadiography is described by many authors (Cosslett et al., '57 '60) and therefore will not be discussed here.

Ward's bioplastic (Rochester N Y U S A.) was used for embedding after the method described elsewhere (Bohatirchuk, '57 '61) Embedding in plastic requires precise timing of the various procedures in order to get blocks of requisite hardness. Frequent change of knives was a necessary condition for obtaining fine sections. Coloring was performed with safranin-fast green (Böhm-Oppel) thionine-picric acid (Schmorl), thionine-eosin, thionine fast green Although calcium-containing tissues in general are also col

[1] This work was supported by grant AM [illegible]-03 of the National Institutes of Health, Public Health Service, U.S.A. and partly by the James Picker Foundation, Canada and U.S.A.

identical conditions. It should be mentioned that the intensity of radiation from the x-ray target was not always uniform: one part of the field being sometimes more illuminated than another. It was necessary to bear this possibility in mind in making conclusions about calcium content. Hence, only bone images having similar blackness of nearby background were compared in serial historadiographs.

Besides changes in x ray absorption in all affected bones the local morphological signs typical of calcium impoverishment or bone destruction were also taken into consideration.

The morphological change was considered to be typical if it was present in about 75% of all specimens of a group. The approximate percentage of other findings is mentioned with their description.

The identification of a histological structure in which calcium was supposedly present was performed in a comparative study of serial historadiographs and their colored replicas. This identification of calcified structures in colored specimens was sometimes difficult because extra-bone calcium grains remained usually unstained and might then be distinguished only by their high refractive index.

For reasons which will be explained later the term multinucleated giant cell is preferred to osteoclast.

RESULTS

*Disappearance of calcium from the organic matrix — bone atrophy — halisteresis*

The general calcium impoverishment in bones of the affected extremity is conspicuous between the eighth and tenth day after the start of either type of experiment of group A, in a few cases even earlier (figs. 1 2) At this time no local morphological changes are apparent in either the historadiograph or colored specimen within the limits of magnification used, i.e. a true halisteresis is observed in this initial stage Local histological and historadiographical changes similar to those typical for the sixth or seventh decades of human life appear in experimental bones at the third week. Then, besides the general halisteresis mentioned above the much more pronounced local calcium deficiency appears in some areas. These areas are seen in spongy bone on the periphery of the narrow and concave parts of bone trabeculae close to the ends of fusing trabeculae and within bone canals and intraosseous lacunae. Such an area in a case of complete decalcification, appears in historadiograph black and without structure while the colored specimen shows here a stratified fibrous structure, sometimes with osteocytes present in former intraosseous lacunae (figs. 3 4 5 6) In cases of incomplete decalcification the historadiograph shows an area of decreased x ray absorption, usually between fusing trabeculae. In a few cases it is possible to distinguish separate calcium remnants here in the shape of grains or islands (figs. 7 8)

The sign of "bone powdering described by us as typical for aging bone atrophy in humans, is encountered in approximately 25% of experimental animals, starting at the fifth or sixth week. This sign is characterized by the appearance even at low magnification, of many separated calcium grains in places where one expects to find a solid inorganic matrix (fig 9)

The peculiar enlargement of intraosseous lacunae and bone canals is conspicuous in a sign called by us "bone sieving" (fig 10) The affected bone appears in historadiograph to be pierced like a sieve by numerous black holes of different shapes and sizes. The colored specimen of the same section shows osteocytes with in enlarged lacunae bone marrow cells and blood vessels within widened Haversian and Volkmann canals. The "bone sieving usually appears at the fifth or sixth week after the start of the experiment. Such a sign has not so far been reported in human bone atrophy (Bohatirchuk, '60)

The calcium impoverishment may occasionally be seen in historadiographs of some separate calcified fibers. At the fifth week of experiments of group A it is observed in nearly all animals. Such fibers appear spotty in historadiographs if seen even with 120 × or 180 × i.e. black gaps become visible between calcium-denuded and calcium impregnated parts of the fiber (fig 11) These changes are similar

——— 1960 X-Ray Microscopy and X-Ray Microanalysis. Second Symposium. Elsevier Publ. Amsterdam, New York.

Easton, J E. 1956 The Organic Matrix of Bone. Biochemistry and Physiology of Bone. Ed. by G. H Bourne. Academic Press, New York. Chap IV 81 107

Frost, H. M. 1960 Osteoporosis a Hard Look. J. of Am. Geriatr Soc., VIII: 568–571

Ham, A. W and W R. Harris 1956 Repair and Transplantation of Bone. Biochemistry and Physiology of Bone. Ed. by G. H. Bourne. Academic Press New York. Chap XVI 475–505.

Hancox N M. 1956 The Osteoclast. Biochemistry and Physiology of Bone. Ibid., VIII: 213–247

H wthorn, S. R. 1929 Multinucleated Giant Cells. Arch. Path., 7 651–712.

Howell, W H. 1891 Observ tions upon the Occurrence, Structure and Function of the Giant Cells of the Marrow J Morph., IV 117–130.

Jaffe L. 1930 The Resorption of Bone. Arch. Surg 20 355–371.

Jowsey J 1960 Age Changes in Human Bone. Clin. Orthoped., 17 210–218.

Kroon, D. B. 1954 The Bone Destroying Function of Osteoclasts. (Kölliker' Brush Border) Acta Anat., 21 1–18.

Lacroix, P., and R. Ponlot 1958 Remarques sur l'histopathologie de l'ostéoporose post-traumatique. Acta medica Belgica. Parmi les travaux dédiés au Prof. M. P Gérard. Pp. 1 29.

McLean, F., and M. Urist 1955 Bone. An Introduction to the Physiology of the Skeletal Tissue. The University of Chicago Press. Chicago.

Myers, H., J. Waterman, R. Black and V Flanagan 1959 The Relative Number of Osteoclasts in Normal and Rachitogenic Gottinges Pig Mandibular Condyles. Anat. Rec., 133: 487–499

Nordin, B E. C. 1961 The Pathogenesis of Osteoporosis. Lancet, May 13: 1011–1015.

Pritchard, J J 1956 General Anatomy and Histology of Bone. Ed. by G. H. Bourne. Academic Press, New York. Chap. I 1 27

Tonna, E. A. 1960 Osteoclast and the Aging Skeleton A Cytological, Cytochemical and Autoradiographic Study Anat. Rec., 137: 251–262.

——— 1960 Periosteal Osteoclasts Skeletal Development and Aging. Nature 4710 405–407

Urist, M. 1962 Osteoporosis. Annual Review of Medic., 13 273–286.

Weidenreich, F 1930 Das Knochengewebe. Handbuch der Mikroskopischen Anatomie des Menschen. Ed. W v Möllendorf Julius Springer Verlag, Berlin. 391–520.

## PLATE I

### EXPLANATION OF FIGURES

All the reproductions of microphotographs found in this work present the colors of original macroradiographs or historadiographs. Thus the maximum white color corresponds to the maximum amount of calcium, the maximum black to its bsence.

1–2 Magnified macroradiographs, rabbit, both calcanei, 10 μ sections, 10 kv both t 15 × L (left foot) control. R. (right foot) tenth day after the application of plaster of Paris cast.

The initial stage of general calcium impoverishment. Right calcaneus ppears blacker i.e., less absorbing x-rays than the left one.

Note Compare only those parts of bone which have approximately the same blackness of back ground. These as well as other results are verified in serial historadiographs.

3 Colored specimen rabbit calcaneus, four weeks after the application of plaster of Paris cast, 10 μ, thionine-eosine, 150 ×

4 Historadiograph of sections 3, 8 kv 150 ×

Arrows in both colored specimen and historadiograph indicate the whole decalcified zone. One arrow (second from below) points out the area where remnants of calcium are seen. Note that the above zone is present in all serial historadiographs on the same place
ther whitish spots (on the left side of historadio-
ry pe, size and position in serial historadio-
ay images of bone marrow structures at


L
1


R
2


3


4

——— 1960 X-Ray Microscopy and X-Ray Microanalysis. Second Symposium. Elsevier Publ. Amsterdam, New York.

Eastoe, J E. 1956 The Organic Matrix of Bone Biochemistry and Physiology of Bone Ed. by G. H. Bourne. Academic Press New York. Chap. IV 81–107

Frost, H. M. 1960 Osteoporosis a Hard Look. J of Am. Geriatr. Soc., VIII: 565–571.

Ham A. W and W R. Harris 1956 Repair and Transplantation of Bone. Biochemistry and Physiology of Bone. Ed. by G H. Bourne. Academic Press, New York. Chap. XVI 475–505.

Hancox, N M. 1956 The Osteoclast. Biochemistry and Physiology of Bone Ibid., VIII 213–247

Hawthorn, S. R. 1929 Multinucleated Giant Cells. Arch. Path., 7 651–713.

Howell, W H 1891 Observations upon the Occurrence Structure and Function of the Giant Cells of the Marrow J Morph., IV 117–130.

Jaffe L. 1930 The Resorption of Bone Arch. Surg., 20 355–371

Jowsey J 1960 Age Changes in Human Bone. Clin. Orthoped., 17 210–218.

Kroon, D. B 1954 The Bone Destroying Function of Osteoclasts. (Kölliker's Brush Border) Acta Anat., 21 1–18.

Lacroix P and R. Ponlot 1956 Remarques sur l'histopathologie de l'ostéoporose post-traumatique. Acta medica Belgica. Parmi les travaux dédiés au Prof M. P Gérard. Pp. 1 29.

McLean, F., and M. Urist 1955 Bone. An Introduction to the Physiology of the Skeletal Tissue. The University of Chicago Press. Chicago.

Myers, H., J Waterman, R. Black and V Flanagan 1959 The Relative Number of Osteoclasts in Normal and Rachitogenic Guinea Pig Mandibular Condyles. Anat. Rec., 133: 487–499

Nordin B E. C. 1961 The Pathogenesis of Osteoporosis. Lancet, May 13 1011–1015.

Pritchard, J J 1956 General Anatomy and Histology of Bone. Ed. by G. H. Bourne. Academic Press, New York. Chap. I: 1 27

Tonna, E. A. 1960 Osteoclast and the Aging Skeleton A Cytological, Cytochemical and Autoradiographic Study Anat. Rec., 137 251–269

——— 1960 Periosteal Osteoclasts, Skeletal Development and Aging. N ture 4710: 405–407

Urist, M. 1962 Osteoporosis. Annual Review of Medic., 13 273–286.

Weidenreich, F 1930 Das Knochengewebe. Handbuch der Mikroskopischen Anatomie des Menschen. Ed. W v Möllendorf. Julius Springer Verlag, Berlin. 391 520.

## PLATE 1

### EXPLANATION OF FIGURES

All the reprod ctions of microphotographs found in this work present the colors of original macroradiographs or historadiographs. Thus the maximum white color corresponds to the maximum amount of calcium, the maximum black to its absence.

1 2 M gnified macroradiograph rabbit, both calcanei, 10 μ sections, 10 kv both at 15 × L. (left foot) control. R. (right foot) tenth day after the application of plaster of Paris cast.

The initial stage of general calcium impoverishment. Right calcaneu appears blacker i.e., less absorbing x-rays than the left one.

Note Compare only those parts of bone which have pproximately the same blackness of background. These as well as other results are verified in serial historadiographs.

3 Colored specimen rabbit calcaneus, four weeks after the pplication of plaster of Pairs cast, 10 μ, thionine-eosine, 180 ×.

4 Historadiograph of sections 3 8 kv 180 ×

Arrows in both colored specimen and historadiograph indicate the whole decalcified zone. One arrow (second from below) points out the area where remnants of calcium are seen. Note that the above zone is present in all serial historadiographs on the same place whilst other slightly whitish spots (on the left side of historadiograph) vary in their shape, size and position in serial historadiographs. They present x-ray images of bone marrow structures t different levels.


L
1


R
2


3


4

——— 1960 X-Ray Microscopy and X-Ray Microanalysis. Second Symposium. Elsevier Publ. Amsterdam, New York.

Eastoe, J E. 1956 The Organic Matrix of Bone. Biochemistry and Physiology of Bone. Ed. by G. H. Bourne. Academic Press, New York. Chap IV 81–107

Frost, H. M. 1960 Osteoporosis a Hard Look. J of Am. Geriatr Soc., VIII 568–571.

Ham A. W., and W R. Harris 1956 Repair and Transplantation of Bone. Biochemistry and Physiology of Bone. Ed. by G H. Bourne. Academic Press, New York. Chap. XVI 475–505.

Hancox, N M. 1956 The Osteoclast. Biochemistry and Physiology of Bone. Ibid., VIII 213–247

Hawthorn, S. R. 1929 Multinucleated Gi... Cells. Arch. Path., 7 651–713.

Howell, W H. 1891 Observations upon the Occurrence, Structure and Function of the Giant Cells of the Marrow J Morph., IV 117–130.

Jaffe L. 1930 The Resorption of Bone. Arch. Surg., 20: 355–371

Jowsey J 1960 Age Changes in Human Bone. Clin. Orthoped., 17 210–218.

Kroon, D B. 1954 The Bone Destroying Function of Osteoclasts. (Kölliker's Brush Border) Acta Anat., 21 1–18

Lacroix, P., and R. Ponlot 1958 ... sur l'histopathologie de l'os... traumatique. Acta medica ... travaux dédiés au Prof. ...

McLean F., and M. Urist ... troduction to the ... Tissue. The U... Chicago.

Myers, H., J ... gan 195... clasts ... Fig ... 48...

N...

——— ... Der ... 407

Urist, M. ... of Medic.,

Weidenreich, ... Handbuch der ... Menschen. Ed. ... Springer Verlag, ...

## PLATE 1

### EXPLANATION OF FIGURES

All the reproductions of microphotographs found in this work present the colors of original macroradiographs or historadiographs. Thus the maximum white color corresponds to the maximum amount of calcium, the maximum black to its absence.

1–2 Magnified macroradiographs, rabbit, both calcanei, 10 μ sections, 10 kv both at 15 × L. (left foot) control. R. (right foot) tenth day after the application of plaster of Paris cast.

The initial stage of general calcium impoverishment. Right calcaneus appears blacker i.e., less absorbing x-rays than the left one.

Note Compare only those parts of bone which have approximately the same blackness of back ground. These as well as other results are verified in serial historadiographs.

3 Colored specimen, rabbit calcaneus, four weeks after the application of plaster of Pairs cast, 10 μ, thionine-eosine, 180 ×.

4 Historadiograph of sections 3, 8 kv 180 ×

Arrows in both colored specimen and historadiograph indicate the whole decalcified zone. One arrow (second from below) points out the area where remnants of calcium are seen. Note that the above zone is present in all serial historadiographs on the same place whilst other slightly whitish spots (on the left side of historadiograph) vary in their shape, size and position in serial historadiographs. They present x-ray images of bone marrow structures at different levels.


5


6


7


8


9


10

## PLATE 2

### EXPLAN TION OF FIGURES

5 Colored specimen, rabbit tibia, three weeks after severing the Achilles tendon 10 μ thionine-eosine, 180 ×

6 Historadiograph of section 5 10 kv 180 × Arrows point out a large band of completely decalcified tissue on the surface of trabecula (structureless black in historadiograph) Fibrillar structure of decalcified tissue and several lacunae with osteocytes are seen within the decalcified zone.

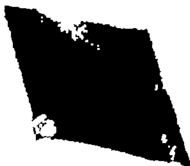
7 Colored specimen rabbit calcaneus, five weeks after the application of plaster of Paris cast 10 μ, Schmorl, 320 ×

8 Historadiograph of section 7 10 kv 120 × A large decalcified zone is evident between fusing ends of two trabeculae. A small bone rest (arrow) is seen within the decalcified tissue.

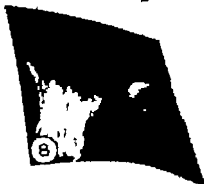
9 Historadiograph, rabbit calcaneus five weeks after the application of plaster of Paris cast, 10 μ, 10 kv Arrow points out the area of powdered bone 180 ×

10 Historadiograph, rabbit calcaneus five weeks after the application of plaster of Paris cast, 10 μ, 10 kv Several enlarged intraosseous lacunae with irregular outlines are typical for "bone sieving. 240 ×


5




7


8


9


10

## PLATE 2

EXPLANATION OF FIGURES

5 Colored specimen, rabbit tibia three weeks after severing the Achilles tendon, 10 μ thionine-eosine 180 ×

6 Historadiograph of section 5 10 kv 180 × Arrows point out a large band of completely decalcified tissue on the surface of trabecula (structureless black in historadiograph) Fibrillar structure of decalcified tissue and several lacunae with osteocytes are seen within the decalcified zone.

7 Colored specimen, rabbit calcaneus, five weeks after the application of plaster f Paris cast, 10 μ, Schmorl, 320 ×

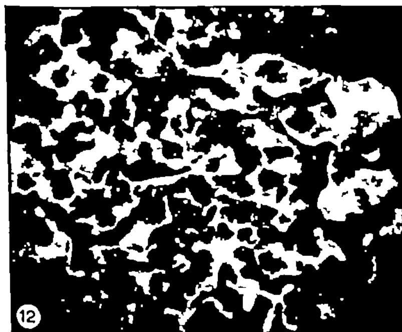
8 Historadiograph of section 7 10 kv 120 × A large decalcified zone is evident between fusing nds of two trabeculae. A small bone rest (arrow) is seen within the decalcified tissue.

9 Historadiograph rabbit calcaneus, five weeks after the application of plaster of Paris cast, 10 μ, 10 kv Arrow points out the area of powdered bone 180 ×

10 Historadiograph rabbit calcaneus, five weeks after the pplication of plaster of Paris cast, 10 μ, 10 kv Several enlarged intraosseous lacunae with irregular outlines are typical for "bone sieving. 240 ×

PLATE 3



## PLATE 3

### EXPLANATION OF FIGURES

11 Historadiograph, rabbit calcaneus, five weeks after the application of plaster of Paris cast 10 μ, 10 kv Arrow indicates several bone fibers of which calcium impregnated parts (white dots) alternate with calcium denuded ones (black gaps) Similar fibers are seen in other parts of historadiograph. 180 ×

12 Historadiograph, human vertebra male 79 10 μ 10 kv Newly organized trabeculae in Paget's disease (late stage) are covered with Howship's lacunae There are many small trabeculae with irregular outlines separated one from another 80 ×


13


14


15



('58) state that such fibers terminate bilaterally in both the ventromedial and dorsomedial nuclei. Nauta ('61) however states that none of the fibers in the stria terminalis reach these areas. In addition, all the studies of the amygdala in the monkey describe degenerated fibers extending to the thalamic nuclei. These have not been seen in either the cat or rabbit. Such differences can be explained in part by the variations in the size and position of the lesions and the staining techniques employed. However some must certainly reflect species variations.

It was felt that there was still much to be learned concerning the efferent pathways of the amygdala and their sites of termination. Thus an experimental study of the basal and lateral nuclei of the amygdala in cat was undertaken.

## MATERIALS AND METHODS

Forty-three adult cats ranging in weight from 2.5 to 5 kg were used in this series of experiments. In 27 cats an attempt was made to place the lesion in the right lateral nucleus and in 16 cats in the right basal nucleus. The following procedure was carried out on each cat.

The animal was anaesthetized with an intraperitoneal injection of 40 mg of Nembutal per kg body weight. Using a Labtronics stereotaxic apparatus a glass insulated silver electrode was inserted into either the lateral or basal nucleus and coagulation carried out with a Blendtome electro-surgical unit. To reach the lateral nucleus the electrode was inserted either vertically or obliquely on an angle of from 60° to 70° to the horizontal in the frontal plane. To reach the basal nucleus it was inserted either vertically or on an angle of 55°. In the latter instance however the electrode was not orientated in the frontal plane but at an angle to it. Thus the electrode coursed through the cortex and external capsule to the amygdala in an inferior medial and posterior direction.

The post-operative course was, in most cases, uneventful. Slight transient edema of the conjunctiva was occasionally encountered.

On the tenth post-operative day the animal was anaesthetized and intracardiac perfusion carried out by introducing 400 ml of 0.85% saline solution followed by 400 ml of 10% formalin into the left ventricle. The brain was then removed and stored in ten times its own volume of 10% formalin for at least eight weeks. Serial frozen sections were cut in either the frontal or sagittal plane and stained by the Nauta-Gygax technique. The cresylecht violet stain was used to determine the extent of the lesion and to verify the location of the preterminals.

## OBSERVATIONS

Both the lesion and the Nauta-Gygax staining were satisfactory for purposes of analysis in 13 brains. All lesions were fusiform in shape and approximately 2 mm × 2 mm × 2.5 mm in size. In every brain except no. 1 and 43 the electrode tract was identified passing through the cortex and external capsule and in a few it passed through the inferior tip of the claustrum as well. In those brains with lesions in the basal nucleus the tract also coursed through the medial part of the lateral nucleus. The electrode was inserted vertically in brains no. 1 and 43. Thus the tracts in these two brains pass through cortex and internal capsule. More inferiorly they pass through the lentiform nucleus in no. 1 and through the optic tract in no. 43.

### *Lateral nucleus. Cats no. 1, 6, 7, 8, 21, 25*

The lesions in brains no. 1, 8, 21 and 25 are illustrated in figures 1 to 4. In nos. 1 and 25 the lesion is confined to the lateral nucleus. In nos. 8 and 21 there is slight encroachment upon the periamygdaloid cortex, and in nos. 6, 7 and 8 the lesion is touching the lateral border of the basal nucleus. Moreover in no. 6 the lesion extends minimally into the inferior tip of the putamen and the lateral part of the central nucleus.

Two main efferent pathways from the lateral nucleus were identified. The smaller of the two was seen in frontal sections in brains no. 6, 7, 8 and 21 as a thin flat band of fibers coursing superiorly and medially from the lateral nucleus through the central nucleus to a position just inferior to the ansa lenticularis (fig. 9). From here it continues in an inferomedial

direction between the ansa lenticularis and the optic tract to join the medial forebrain bundle at the level of and slightly anterior to the ventromedial nucleus of the hypothalamus. The preterminals of these fibers are scattered throughout the lateral hypothalamus (fig 10) and an occasional fiber could be identified in the medial forebrain bundle as far posteriorly as the mammillary nucleus.

In no. 1 a few fibers dorsomedial to the lesion were observed coursing medially to approach the inferior aspect of the ansa lenticularis. They could not be traced further however because here they mingled with degenerated fibers from the vertical electrode tract.

The pathway could not be identified with certainty in no. 25 but as the tract is thin and flat it would be difficult to identify in the sagittal sections made of this brain.

The second much larger pathway of the lateral nucleus is the longitudinal association bundle of Johnston, a band of fibers located just dorsal to the border between the basal and lateral nuclei. Degenerated fibers course superiorly and medially to enter the lateral aspect of this bundle (figs 11, 12) They continue anteriorly to the level of the optic chiasma. Here they begin to fan out diffusely in an anteromedial direction. At the level of and just anterior to the anterior commissure their preterminals were identified in the medial half of the anterior amygdaloid area and the lateral preoptic region (fig. 13) This pathway was seen in each of the six brains.

Short intra-amygdaloid fibers were seen in the immediate vicinity of every lesion coursing into the basal nucleus and terminating there.

Basal nucleus *Cats no 29 32 37 40 43*

The lesions in cats no. 37 40 and 43 are illustrated in figures 5–7 In nos 29 32 and 37 the lesion is almost completely confined to the lateral half of the basal nucleus. There is only a slight encroachment on the cortical nucleus just inferior to the basal nucleus. The lesion in no 40 is in the central part of the basal nucleus and just touches the central nucleus superiorly In no. 43 it occupies the medial half of the basal and the superior third of the medial nucleus

Two main efferent pathways from the basal nucleus were identified. From the superior and medial aspect of every lesion a great number of degenerated fibers course superiorly Many form small compact bundles (fig. 14) As they approach the upper margin of the nucleus they branch like a Y into two pathways The great majority course laterally to join the medial aspect of the longitudinal association bundle. A few turn medially to enter the stria terminalis (fig. 15) In no 40 where the lesion was more centrally placed, the contribution to the stria terminalis was larger than in nos. 29 32 and 37 (fig 16)

The fibers in the longitudinal association bundle continue anteriorly and slightly medially to the level of the optic chiasma. Here they show a partial division into lateral and medial components. The medial shows the greatest number of fibers in nos. 40 and 43 the brains in which the lesion was placed more medially This bundle curves anteromedially beneath the internal capsule and the majority of its fibers terminate in the medial two-thirds of the preoptic region (fig. 17) and the bed nucleus of the anterior commissure. A few continue into the commissure but they could not be identified on the contralateral side.

The lateral component courses more gradually in a medial direction ventral to the medial bundle, and terminates in the lateral two-thirds of the preoptic region, the bed nucleus of the anterior commissure and the substantia innominata.

The smaller pathway of the basal nucleus is as mentioned above, the stria terminalis. In nos. 29 32, 37 and 40 degenerated fibers were followed in the stria to its point of division into its various components. A few fibers terminate here in the bed nucleus of the tract (fig. 16) while others continue in the supracommissural component to the bed nucleus of the anterior commissure

In no 43 where the lesion involves the medial half of the basal nucleus and the superior third of the medial nucleus the degeneration in the stria terminalis

much more dense Some of these fibers end in the bed nucleus of the stria terminalis but most of them continue anterior to the anterior commissure in the supracommissural bundle. Their preterminals are scattered in the anteroinferior part of the nucleus of the anterior commissure the medial preoptic region, and the anterior nucleus and most rostral part of the ventromedial nucleus of the hypothalamus.

In brains no. 29 37 40 and 43 short fibers could be followed from the vicinity of the lesions to their termination in the lateral nucleus.

*Lateral and basal nuclei. Cats* no 34 36

The lesion in cat no. 36 is illustrated in figure 8 In both brains the lesion occupies the more inferior part of the medial half of the lateral nucleus and the lateral half of the basal nucleus. In each there is a very slight invasion into the cortical nucleus at the most caudal limit of the lesion.

Most of the degenerated fibers course superiorly to enter the central part of the longitudinal association bundle. The contribution from the basal nucleus is heavier than that from the lateral. The fibers continue anteriorly to the level of the optic chiasma. Here they become more diffuse as they continue rostrally in an anteromedial direction (figs. 19 20) Their preterminals were identified at the level of the anterior commissure in the medial half of the anterior amygdaloid area and the lateral and intermediate preoptic region.

A few fibers course from the medial aspect of the lesion to enter the stria terminalis. They terminate in the bed nucleus of this tract. In addition, in no 36 a few fibers course medially from the lateral nucleus through the central nucleus and continue just inferior to the ansa lenticularis to join the medial forebrain bundle.

DISCUSSION

*Stria terminalis*

In agreement with the studies of Johnston ('23) Humphrey ('36) Fox ('40) and others, the basal nucleus has been found to be one of the nuclei contributing to the supracommissural component of the stria terminalis. Ban and Omukai ('59) report that in the rabbit it also sends fibers to the preoptic component. In this investigation of the cat no such contribution could be identified. Fox ('43) however did observe degeneration in the preoptic component in two cat brains where the lesion involved both the basal and central nucleus. The central nucleus must have been the site of origin of these fibers. It is interesting to note that the preoptic component varies not only in its composition but also in size. In the cat it is small (Fox, '40) but in the rabbit it is quite large (Young, '36) Ban and Omukai ('59) traced it as far as the preoptic region. In the cat fibers from the basal nucleus reach this area via the longitudinal association bundle.

In the rabbit the supracommissural component projected to the bed nuclei of the stria terminalis and anterior commissure the septal area, and the rostral part of the ventromedial nucleus of the hypothlamus (Ban and Omukai, '59) In the cat, fibers from the lateral and central part of the basal nucleus were seen to terminate only in the bed nucleus of the stria terminalis and anterior commissure while fibers from the medial nucleus and possibly from the most medial part of the basal end in the anterior hypothalamus and the most rostral part of the ventromedial nucleus. This provides an anatomical basis for Gloor's observation ('55) that in the cat short latencies are recorded in the ventromedial nucleus of the hypothalamus only on stimulation of the corticomedial division of the amygdala. No degeneration extended into the septal area in the cat.

In their investigation of the temporal lobe in the monkey Adey and Meyer ('52) and Adey et al. ('58) reported that amygdalofugal fibers coursing in the stria terminalis end in the region of the anterior commissure and the ventromedial dorsomedial and periventricular nuclei of the hypothalamus. The lesions in these studies involved most of the amygdala and the temporal pole cortex. Nauta ('61) who made much more discrete lesions that were almost completely confined to the basolateral complex of the monkey has

not confirmed these observations. He found that the degenerated fibers in the stria terminalis terminated just rostral to the ventromedial nucleus in the medial preoptic nucleus, the anterior hypothalamus and the nucleus supraopticus diffusus. He stressed that no preterminals were identified in the ventromedial nucleus itself even in one brain in which the stria terminalis had been completely severed. While there is evidence then that fibers from the basal nucleus of the rabbit and from the most medial part of the basal nucleus of the cat terminate here it is most unlikely that such fibers are present in the monkey

As in the studies of Johnston ('23) in the opossum Fox ('40 43) in the cat, and Ban and Omukai ('59) in the rabbit, no fibers from the lateral nucleus of the cat were observed entering the stria terminalis. This supports the observation of Gloor ('55) that only long latencies could be recorded in the stria on stimulation of the lateral nucleus. Here again however there may be species differences as Humphrey ('36) observed a few such fibers in the bat and Lauer ( 45) saw them in the monkey

*Anterior commissure*

In studies of normal material fibers have been described coursing from the lateral and basal nuclei into the posterior limb of the anterior commissure by way of the external capsule (Young, '36 Humphrey '36 Fox, 40 Lauer 45) Ban and Omukai ('59) have been able to trace such fibers into the anterior commissure but have not been able to follow them to the opposite amygdala. The present investigation provides no additional information concerning this pathway in the cat as in all but two brains the electrode tract passed through the external capsule

*Ventral amygdalofugal pathways*

The longitudinal association bundle of Johnston is the main ventral amygdalofugal pathway for both the lateral and basal nuclei in the cat. It is first seen as a distinct oval bundle at the level of the posterior limit of the medial amygdaloid nucleus As reported by Fox ( 40) it courses anteriorly dorsal to the junction of the basal and lateral nuclei and ventral to the central nucleus. The contribution of the basal nucleus to the pathway is considerably greater than that of the lateral. In addition the fibers from the lateral nucleus are probably more thinly myelinated as Fox ( 43) was unable to stain them by the Marchi technique At the level of the optic chiasma the bundle curves medially and its fibers become more diffusely scattered. Those fibers arising in the lateral nucleus terminate in the medial half of the anterior amygdaloid area and the lateral preoptic region.

In those brains in which the lesion involved only the basal nucleus (Cats no. 29 32, 37 40) the degenerated fibers in the longitudinal association bundle showed a partial division into lateral and medial components. This was also observed by Fox ( 43) in his Marchi study He stated that the lateral component disappeared on the superior surface of the basal nucleus while the medial coursed medialward, inferior to the internal capsule. In one normal brain Fox ( 43) traced these fibers to the bed nucleus of the stria terminalis. In the present investigation the lateral component was observed to course medially inferior to the medial component, to terminate in the lateral two-thirds of the preoptic region the bed nucleus of the anterior commissure and the substantia innominata. The medial component formed a more distinct bundle that coursed immediately inferior to the internal capsule and continued medially to terminate in the medial two-thirds of the preoptic region and the bed nucleus of the anterior commissure

It is interesting to note that in the preoptic region there is some indication of a lateromedial point to point distribution of fibers arising in the basolateral complex.

Gloor ('55) has reported that on stimulation of the basolateral complex short latencies are recorded in the medial and lateral preoptic regions. These impulses probably reach the preoptic region through the longitudinal association bundle.

Nauta ('61) tentatively identified the longitudinal association bundle in the monkey but did not separate it from the more diffuse medially directed ventral amygdalofugal system. Possibly the longitudinal association bundle is more compact in the

## PLATE 2

### EXPLANATION OF FIGURES

Photomicrographs of sections stained by the N uta-Gygax technique.

9 Cat no. 6. Degenerated fibers of passage from the lateral amygdaloid nucleus coursing just inferior to the ansa lenticularis. × 900.

10 Cat no. 6. Degenerated preterminals in the lateral hypothalamus. × 900.

11 Cat no. 1 Degenerated fibers coursing superiorly and medially from the lesion to enter the longitudinal association bundle. × 900.

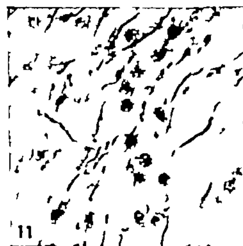
12 Cat no. 25 A bundle of degenerated fibers coursing superiorly to join the longitudinal association bundle. Sagittal section. × 575.

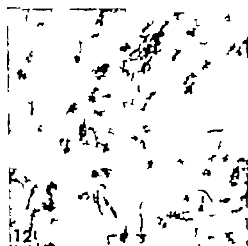
13 Cat no. 7 Degenerated preterminals in the lateral preoptic region. × 900.

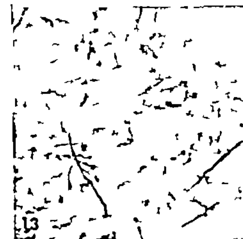
14 Cat no. 37 Bundles of degenerated fibers coursing superiorly from the lesion. × 575.


9


10


11


12


13


14

# Seasonal Changes in Body Weight, Reproductive Organs Pituitary Adrenal Glands Thyroid Gland, and Spleen of the Belding Ground Squirrel (*Citellus beldingi*)

STURGIS McKEEVER
*Department of Zoology University of California, Davis*

The genus Citellus is widely distributed in the Nearctic and Palearctic regions and consists of a large number of hibernating species. Studies of endocrine size and function in relation to reproductive and seasonal cycles have been reported for several species, but no such studies have been made of *Citellus beldingi*. This paper reports the results of a study of the species in Lassen County northeastern California.

The range of the belding ground squirrel covers northeastern California, eastern and central Oregon, southwestern Idaho and northern and central Nevada. In northeastern California it inhabits meadows and sagebrush (*Artimisia tridentata*) flats and rocky areas adjoining meadows where succulent vegetation is available. In such areas the animals live in colonies of varying size and density Burrows may be closely spaced, and two or more animals frequently enter the same burrow Individuals may be found scattered over areas occupied by open ponderosa pine (*Pinus ponderosa*) and sagebrush types.

The animals eat grasses and sedges in early spring but a little later in the season, flowers account for approximately 10% of their food. In July the diet consists of 10% seed and bulbs, 45% grasses and sedges and 45% flowers. Insects are eaten at all seasons but account for less than 1% of the diet.

The period of seasonal activity varies. At 4,500 ft elevation in the Great Basin area the animals become active in early March and remain active until early July At 5 600 ft elevation, they do not become active until late March or early April, but remain active until late July or early August. In areas with heavy snowfall, the animals emerge from hibernation later and some remain active until late August. In general, emergence is correlated with the average time when the grasses and sedges begin growth in the spring, and termination of activity is correlated with the time when food plants become dry In years of heavy snowfall, the animals may emerge while snow is two to three feet deep but the snow melts rapidly and food is soon available After the animals estivate they do not emerge from their burrows until the next spring.

Breeding takes place very soon after the animals emerge from hibernation, for most animals are sexually active when they emerge or become so within a few days. The animals breed only once each year

## METHODS

Specimens were collected at Susanville (4,500 ft elevation) Black's Mt. Experimental Forest (5 600 ft elevation) and Norvell Flat (5 700 ft elevation) by either shooting or live trapping. Live-trapped animals were killed within eight hours of capture by constricting the lungs.

All animals were weighed to the nearest 0 1 gm. Adrenals pituitary thyroid, spleen, and reproductive organs were removed from each animal and placed in fixative. Bouin s fixative was used for tissues which were to be examined histologically and 10% formalin was used for all other tissues. The tissues were later cleaned and weighed to the nearest 0 1 mg on a Mettler Precision Balance. Relative weight of the pituitary spleen and thyroid and of paired adrenals, ovaries testes and seminal vesicles, was computed as the

In cooperation with the Southwest Forest and Range Experiment Station, United States Forest Service Berkeley California.

ratio of tissue weight in milligrams per gram body weight. Stomach weight was subtracted from body weight before these computations were made.

Reproductive activity of males was determined by the method described by Jameson ('50) Females were considered to be sexually active if they (1) were pregnant, (2) were lactating, (3) had an enlarged uterus (4) had recent placental scars or (5) had enlarged mammae

Animals collected from 1958–61 were included in computations of the variation in relative weight of glands from females of different reproductive classes. Only those animals collected in 1960–61 from areas of approximately the same elevation were included in computations of seasonal variation in gland size.

Pituitaries were sectioned at 5 μ and stained with periodic acid-Schiff reagent, iron hematoxylin and orange G All other tissues were sectioned at 7 μ and stained with either Pasini s stain or hematoxylin and eosin.

Activity of the pituitary was subjectively determined on the basis of size, abundance and degree of staining of Schiff-positive basophils. The degree of activity was indicated by a scale ranging from one for small widely scattered, weakly-stained basophils to six for numerous large intensely-stained cells.

Activity of the thyroid was determined by measuring the height of the epithelial cells with an ocular micrometer at 750 ×

Width of each of the three zones of the adrenal cortex was measured with an ocular micrometer at 70 × on a median section of the adrenal. The percentage width of each zone with respect to the total width of the cortex, was computed from these data.

## OBSERVATIONS

Most specimens were collected on or near Black s Mountain Experimental Forest. There, some animals emerged from hibernation the last week of March and by the second week of April all animals had emerged. At the latter date all males had greatly enlarged testes and seminal vesicles, and females were in early stages of pregnancy

Males fought vigorously during the breeding season, and over 90% of the animals had cuts on the head and shoulders. Many of the cuts were infected, but practically all healed within three weeks.

The earliest that young were observed above ground was May 25 By late July most adults and juveniles had estivated and by mid-August less than 1% of the animals were active. The change in numbers was conspicuous, for the animals were easily observed on meadows which had been grazed by livestock.

*Body weight.* Adult males and females maintained approximately the same body weight through June but in July males averaged almost 40 gm heavier than females. Weight gain was slow during May but thereafter accelerated in both sexes. By July the animals had approximately doubled their April weight (fig. 1) Subcutaneous and body cavity fat deposits were extremely heavy (fig. 27) Since most animals had estivated by August, the sample for that month was small however males collected in August averaged 60 gm lighter than July specimens.

In contrast to the gain in weight by belding ground squirrels during May the arctic ground squirrel, *C undulatus* lost weight at this time (Hock, '60) However arctic ground squirrels emerged from hibernation in mid-April, when no food was available.

Weights of juvenile males and females paralleled each other with males only slightly heavier than females. The graphic data show a decrease in the rate of gain during August. However specimens were collected only during the first two weeks of August, and if plotted accordingly would show approximately the same rate of gain as July specimens. Despite the fact that juveniles gained approximately 100 gm in six weeks, they entered estivation approximately 100 gm lighter than adults.

Stomach weight increased in both sexes and age groups from the time the animals became active until they estivated (table 1) This probably indicated a proportionate increase in total food consumption.

*Testes and seminal vesicles* In adult males testes and seminal vesicles were of maximum size in April when 70% of the

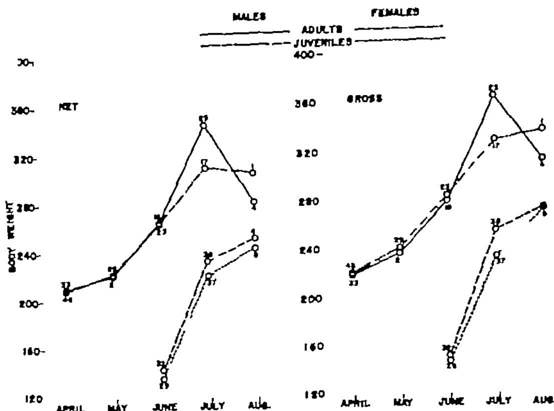



Fig. 1 Average monthly body weight in grams of *Citellus beldingi*. Net weight equals gross weight minus weight of the stomach and its contents. Figures at each point represent sample size.

TABLE 1

*Average monthly weight in grams of stomachs and stomach contents of Citellus beldingi. The number of specimens is shown in parenthesis.*

| Month | Adult males | Adult females | Juvenile males | Juvenile females |
|---|---|---|---|---|
| April | 9.2(33) | 11.4(46) | — | — |
| May | 15.8(24) | 17.8(29) | — | — |
| June | 14.2(18) | 18.3(23) | 7.9(38) | 10.9(29) |
| July | 18.3(25) | 18.2(17) | 20.6(38) | 11.1(37) |
| August | 30.0(4) | 20.0(1) | 20.1(4) | 27.9(8) |

animals were sexually active. By May when all males were sexually quiescent, both glands were extremely atrophied; testes were one-sixth and seminal vesicles were less than one-third the relative and gross size of April specimens (fig. 2). Involution was less rapid in June but testes reached minimum gross and relative size during this month. In July testes were double their June gross weight, and showed some increase in relative size despite the rapid increase in body weight. A similar increase in size of testes just before hibernation occurred in the California ground squirrel *C. beecheyi* (Tomich, '59). In the arctic ground squirrel, testes began to enlarge before hibernation and continued to increase during the winter; spermatids became evident just before emergence from hibernation (Hock, '60). Mayer and Bernick ('59) worked with the same species and found indications that no sexual

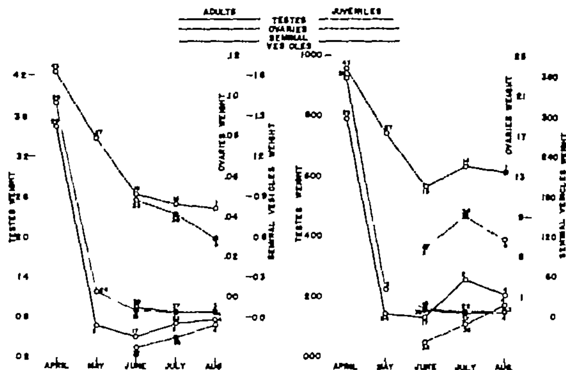


Fig. 2 Average monthly weight of reproductive organs of *Citellus beldingi*. Weights on the left graph are in milligrams per gram body weight; those on the right graph are actual weights in milligrams. Figures at each point represent sample size.

development took place during hibernation development took place just prior to entering hibernation and immediately after emergence.

In four adult male belding ground squirrels collected during August, testes decreased in gross weight but increased in relative weight. Seminal vesicles continued to decrease slightly in both relative and gross size during July but increased slightly in August.

Testes and seminal vesicles of juveniles varied in both relative and gross weight in a pattern similar to that exhibited by adult glands except that in August the testes of juveniles increased while adult testes decreased in gross size

Adult seminal vesicles were so involuted in late summer that they could not be distinguished from juvenile glands in either gross or microscopic features. Testes of juveniles had straight or smoothly curved blood vessels on the surface in contrast to testes of non-active adults which had very convoluted vessels. Microscopically testes of adults differed from those of juveniles in that tubules of adults had a larger lumina and less densely packed epithelial cells.

*Ovaries* Ovaries of adults were largest in April than decreased rapidly in size through June to less than half their maximum size. Gross size of adult ovaries was least in June and increased in July Relative size decreased during July and August (fig. 2) Hock ('60) was unable to determine whether ovaries of the arctic ground squirrel increased in size before hibernation, but found that ovarian follicles continued to grow slowly through the winter When the animals emerged from hibernation, follicles were ready to rupture as soon as copulation occurred.

Since ovary size is correlated with reproductive activity the following observations of belding ground squirrels are pertinent. Seven per cent of the 46 females collected during April and of 29 collected in May failed to show any sign of sexual activity Of the sexually active animals collected in April, 81% were pregnant and 19% had enlarged uteri. Seven per cent

of sexually active animals collected in May were pregnant, and 93% were lactating. Twenty-three adult females were collected in June and 35% were sexually active. Of the sexually active animals, 63% were lactating, 12% had enlarged uteri and 25% had enlarged mammae and had just ceased lactating. The only sexually active female collected during July was lactating. Litter size varied from 3 to 10 and averaged 7.1 for 37 pregnant animals and 7.0 for placental scar counts of 63 animals. Howell ('38) found that litter size varied from 4 to 12, with an average of 8.

From the foregoing, it is apparent that the ovaries involuted rapidly during the lactation and post-lactation periods. Histologically the decrease was correlated with a sharp decrease in size of many atretic follicles and a progressive decrease in size of corpora lutea cells (figs. 22–24).

Ovaries of juveniles decreased in relative size from June through August, but gross size increased in July and decreased in August. Although gross weight of juvenile ovaries was only one-half to two-thirds that of adult ovaries collected at the same time relative weight was only slightly less.

*Adrenal glands.* Adrenals of adult males and females were approximately the same size when the animals emerged from hibernation (fig. 3). They attained maximum size in both sexes in May when adrenals of females were approximately 20% larger than those of males. Male adrenals were, therefore, largest one month after the breeding season; the same rela-

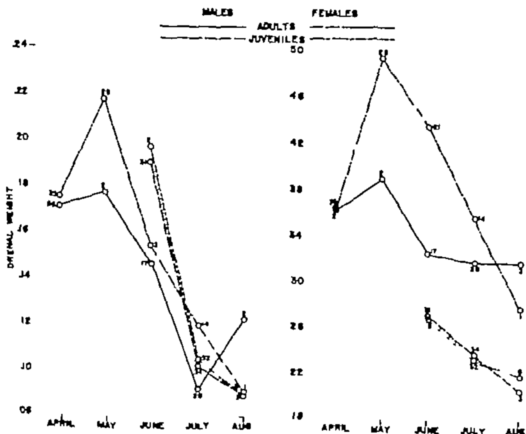



Fig. 3 Average monthly weight of paired adrenal glands of Citellus beldingi. Weights on the left graph are in milligrams per gram body weight; those on the right graph are actual weights in milligrams. Figures at each point represent sample size.

tionship was found in the California ground squirrel *C beecheyi* (Tomich 59) Adrenals of both sexes of the belding ground squirrel decreased sharply in gross and relative weight during June and female glands continued to decrease at approximately the same rate during July and August. The relative weight of adult male adrenals continued to decline sharply during July but increased in August. Gross weight declined only slightly during these months.

According to Deane and Lyman ('54) the adrenals are larger in males than in females of hibernating species with the exception of the prairie dog Cynomys However with the exception of August, when only three adult specimens were obtained, adrenals of female belding ground squirrels were consistently heavier than those of males.

Adrenal glands of juveniles of both sexes followed an almost parallel sharp decline in relative and gross weight during July and August. The decline in gross weight was particularly interesting because body weight was increasing rapidly at that time. In *C beecheyi*, relative adrenal weight of juveniles increased as the season progressed, particularly in males until the animals started storing fat (Tomich, '59)

In the belding ground squirrel an essentially constant relationship prevailed between adrenal weight and body weight at adrenal weights higher than 160 mg/gm. Below this value there was an inverse relationship between body weight and adrenal weight for both sexes and both age groups (fig 4) The change in relationship probably resulted from the beginning of fat deposition Hughes and Mall ('58) found that adrenal weight de-

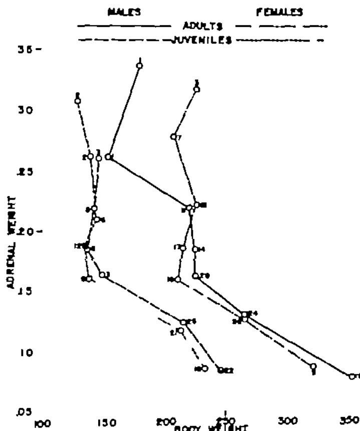



Fig 4 Relationship of weight of paired adrenal glands in milligrams per gram body weight to body weight in grams of 333 specimens of *Citellus beldingi*.

creased as the amount of fat increased in the deer (*Odocoileus hemionus columbianus*)

Relative weights of adrenal glands of four classes of reproductively active females were compared. Adrenals of lactating animals were significantly larger ($P < 0.05$) than those from any other class (table 2) Maximum adrenal enlargement during the period of lactation is contrary to the response found in *C tridecemlineatus* (Mann, '16; Foster '34) and in *C beecheyi* (Tomich, '59); in these species the adrenals attained maximum size during pregnancy and involuted after parturition. However the adrenals of laboratory rats (Andersen and Kennedy '33) of guinea pigs (Hartman and Brownell 49) and of the big brown bat, *Eptesicus f fuscus* (Christian, '53) were of maximum size during the period of lactation.

Histological examination of the adrenals showed that the relative width of the zona glomerulosa was approximately the same in the various age and reproductive classes of both sexes. Width of the zona reticularis was greatest and width of the zona fasciculata least in sexually active animals (fig. 5) A similar enlargement of the reticularis during the breeding season was reported by Zalesky ('34) for *C tridecemlineatus* but the outer sub-zone of elongated vacuolated cells described by Zalesky was not evident in *C beldingi*.

Adrenals of sexually active males were characterized by a distinct glomerulosa and an indistinct transition from fasciculata to reticularis. The inner reticularis was slightly vascularized and contained a few pyknotic nuclei. In some specimens, vacuoles were present in the outer fasciculata. Glands from animals which were badly cut from fighting frequently had necrotic areas in the glomerulosa and/or fasciculata (figs. 10 and 11). Such necrosis was not observed in animals which had no

TABLE 2

*Weights in milligrams per gram body weight of endocrine glands and spleen of sexually active female Citellus beldingi*

| Characteristics | | Condition of sexual activity: Pregnant | Lactating | Uterus enlarged | Mammae enlarged |
|---|---|---|---|---|---|
| **Pituitary** | | | | | |
| Number examined | | 39 | 29 | 13 | 2 |
| Mean weight ± S.E. | | 0.0193 ± 0.0008 | 0.0188 ± 0.0008 | 0.0197 ± 0.0015 | 0.0170 0.0000 |
| Extreme weights | min. | 0.011 | 0.010 | 0.006 | 0.017 |
| | max. | 0.030 | 0.027 | 0.035 | 0.017 |
| **Adrenal glands** | | | | | |
| Number examined | | 32 | 34 | 13 | 2 |
| Mean weight ± S.E. | | 0.1701 ± 0.007 | 0.2162 ± 0.010 | 0.1653 ± 0.014 | 0.1875 ± 0.001 |
| Extreme weights | min. | 0.097 | 0.125 | 0.104 | 0.186 |
| | max. | 0.263 | 0.335 | 0.277 | 0.189 |
| **Thyroid gland** | | | | | |
| Number examined | | 16 | 14 | 7 | 0 |
| Mean weight ± S.E. | | 0.1411 ± 0.010 | 0.1333 ± 0.009 | 0.1832 ± 0.014 | |
| Extreme weights | min. | 0.070 | 0.062 | 0.131 | |
| | max. | 0.209 | 0.186 | 0.243 | |
| **Spleen** | | | | | |
| Number examined | | 36 | 33 | 11 | 2 |
| Mean weight ± S.E. | | 3.7793 ± 0.1699 | 3.5282 ± 0.2023 | 4.2557 ± 0.3418 | 3.4670 ± 0.2790 |
| Extreme weights | min. | 1.962 | 1.967 | 2.914 | 3.088 |
| | max. | 6.000 | 6.679 | 5.896 | 3.846 |

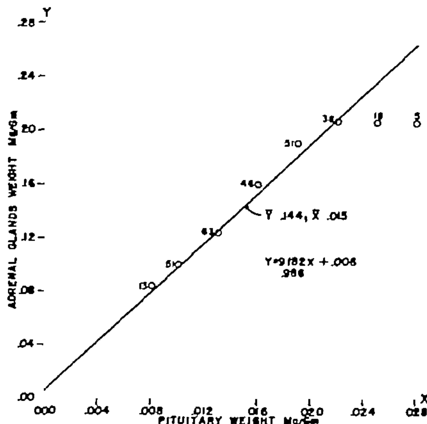



Fig. 7 Regression of Y on X for X range from .006 to .023 for 263 specimens of *Citellus beldingi*. The 23 specimens with X values of .025 and .028 were not included in computations of the regression line.

weight every month except August, when male glands were slightly larger in relative size than those of females. This contrasts with *C. tridecemlineatus* in which gross weight of the male pituitary was greater than that of the female from February through May but did not differ the remainder of the year (Hoffman and Zarrow '38a). However in relative weight the female gland was heavier than that of the male.

TABLE 3

*Seasonal change in activity of the anterior pituitary of Citellus beldingi. Activity was subjectively graded from 1 to 6, based upon PAS staining reaction.*

| Month | Adult males | Adult females | Juvenile males | Juvenile females |
|---|---|---|---|---|
| April | 3.6 | 5 | — | — |
| May | 6.0 | 5.5 | — | — |
| June | 3.3 | 4.5 | 2.3 | 3.5 |

*Thyroid gland.* The thyroid decreased in relative size from the time the animals came above ground until July with the exception of an increase in thyroid size in adult males during May (fig. 8). This is contrary to the findings of Zalesky ('35) for *C. tridecemlineatus* in which the thyroid maintained a maximum weight phase through the breeding season and into late summer and early autumn. In July the gland was the same size in both sexes and both age groups of *C. beldingi*. In the small sample collected during August, thyroids of adult males and juvenile females decreased in size, while glands of adult females and juvenile males enlarged.

In sexually active females the thyroid was largest in animals with enlarged uteri. Thyroids of these specimens were significantly larger than those from lactating adults ($P < 0.05$) but did not differ sig

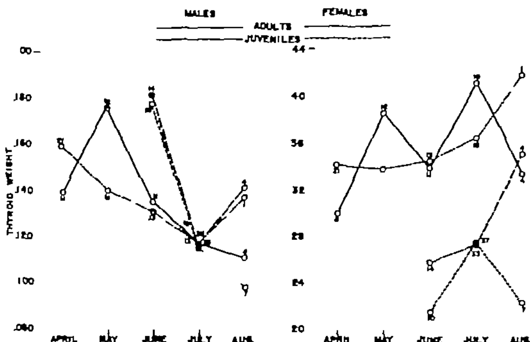



Fig. 8. Average monthly weight of the thyroid of *Citellus beldingi*. Weights on the left graph are in milligrams per gram body weight; those on the right graph are actual weights in milligrams. *Figures at each point represent sample size.*

nificantly from glands of pregnant animals.

Gross size of thyroids from adult females decreased slightly in May and then increased through August. In adult males the thyroid alternately increased and decreased in size maximum size was attained in July. Glands of juvenile males increased in size during July and August, whereas thyroids of juvenile females enlarged in July and decreased in size in August.

An increase in thyroid activity is, in general indicated by an increase in height of the epithelial cells lining the follicles (Maximow and Bloom, 48). For *C. beldingi*, seasonal changes in thyroid cell

TABLE 4

*Seasonal changes in height of epithelial cells of the thyroid gland of Citellus beldingi*

| Month | Adult males | Adult females | Juvenile males | Juvenile females |
|---|---|---|---|---|
| April | 8.16 | 7.17 | — | — |
| May | 9.70 | 9.76 | — | — |
| June | 6.59 | 8.77 | 9.95 | 7.94 |
| July | — | 7.04 | 6.34 | — |

height were similar to changes in relative weight of the thyroid, except that, in adult females cell height increased to a maximum during May (table 4) whereas thyroid weight decreased that month. Thus, maximum activity occurred in lactating animals. The seasonal change in cell height was approximately the same as that reported for *C. tridecemlineatus* (Hoffman and Zarrow '58b).

*Spleen.* The relative weight of the spleen followed the same trends from April through July as relative thyroid weights spleens of adult females decreased in size throughout the period, while those of males enlarged immediately after the breeding season and then atrophied (fig. 9). Spleens of juveniles decreased during July; the decrease was much greater in females than in males. In the specimens collected during August, spleens from males were larger and those from females smaller than in July specimens. There was no significant difference in spleen size of four classes of sexually active females (table 2).

## PLATE 1

### EXPLANATION OF FIGURES

*Adrenal glands*

10 Gland of a sexually active male. Necrotic areas are present in the glomerulosa. Transition from the fasciculata to reticularis is indistinct. H & E. × 280.

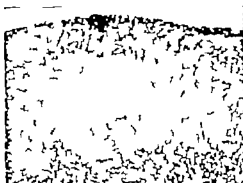
11 Gland of a sexually active male with necrotic areas in the inner fasciculata. Pasini. × 280.

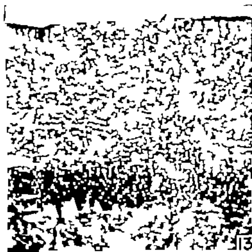
12 Gland of sexually quiescent male collected in May Enlarged, vacuolated cells in the outer fasciculata and some compaction of cells in the reticularis are characteristic. Pasini. × 280.

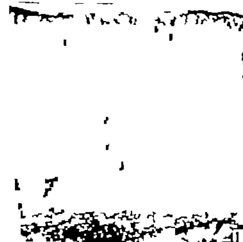
13 Gland of a sexually quiescent adult male collected in July A reticularis composed of cells which h ve little cytoplasm, and sharp transition between fasciculata and reticularis are characteristic of glands of adult males at this season. H & E. × 280.

14 Adrenal of an 87-gm juvenile male collected in late May The glomerulosa is distinct but poorly developed. Cells of the fasciculata are small and the transition from fasciculata to reticularis is indistinct. H & E. × 280.

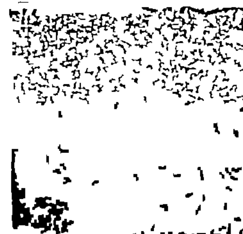
15 Adrenal of 173-gm juvenile male collected in late June. Compared with the 87-gm animal, the glomerulosa is better developed, and the transition from fasciculata to reticularis is more distinct. Pasini. × 280.


10


13


11







## PLATE 3

### EXPLANATION OF FIGURES

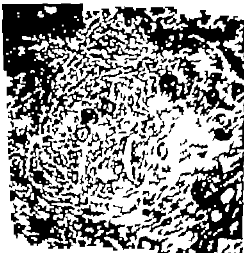
22–24 Ovaries of pregnant (22) lactating (23) and post lactating (24) females, showing progressive decline in size of atretic follicles and in cells of the corpora lutea. × 280.

25 Ovary of juvenile female, illustrating the small size of the follicles compared to those of the post-lactating adult. × 280

26 Seminal vesicles of a sexually quiescent adult, illustrating the degree of atrophy of the gland. × 280.

27 Body cavity and subcutaneous f t deposits in balding ground squirrel which was ready for hibernation


22


25


23


26


24


27

was under no 1 coverslips with H. S R. medium. For counting cells a ruled reticle was inserted in a 10 × wide field ocular of the binocular microscope and used with a 43 × achromatic objective To reduce the inclusion of tangential slices only the cells showing the entire circumference of the nuclear membrane and containing a central dominant nucleolus were counted in the affected field of each section. Each field was again scanned with the 63 × apochromatic objective, to tally the cells containing definitely swollen mitochondria. The control field was then scanned for evidence of retrograde reaction. Estimates of mitochondrial size were made with a calibrated reticle in a 15 × compensating eyepiece and with a 97 × fluorite objective

## OBSERVATIONS

*Normal cells* In mature normal facial motor neurons the mitochondria (stained red by basic fuchsin) appear rod-like to filamentous in form This shows up particularly well in the dendrite bases where the mitochondria tend to be oriented parallel to the cell membrane (figs. 8–10) Occasional forked or branched forms are seen (fig 10) More centrally in the soma a greater diversity of form exists that includes more small spherules and short rods. Nevertheless the final impression gained is that most of the mitochondria are actually filamentous in form, for examination at varying focal levels indicates that many of these short rods or spherules are the result of oblique or transverse slices through longer filaments (figs. 8 and 15) The range in apparent length (ca. 0 5–5 0 μ) therefore is partly an artifact related to the thinness and plane of section. This makes the assessment of mitochondrial length extremely difficult. In most cases it is next to impossible to distinguish a true end from a cut end of a given mitochondrion or to identify with certainty the discontinuity of two separate filaments which may be oriented end to end. On the other hand, the *thickness* of the apparent spherules and rods as well as of the filaments appears quite uniform (ca. 0.3–0 5 μ) Variations in this are at the margin of precision in ocular measurements with the light microscope (i.e 0 3 μ, Gage. 47)

In general within the animal series and methods used for this study there are no overt differences in mitochondrial form or size that can be attributed to normal differences in age (figs 6–9 10 13 and 16) This excludes any possible differences based on average segment length or thickness which otherwise might be derived from a close statistical analysis Even in the facial neurons of the newborn animal, the mitochondria are mature in their characteristics although they are more randomly distributed than in older cells Apparently with the enlargement of Nissl bodies at later ages the mitochondria come to lie between them and are pressed into a new orientation (fig. 8)

*Reactive changes Twenty-five and twenty day operatives* When the facial nerves are severed in hamsters of 25 and 20 days postnatal age, mitochondrial swelling is observed in about 15 — 25% of the neurons on the affected side four days after the operation as well as at the end of all the longer postoperative periods studied (table 1) The definitely swollen particles throughout the series range from about 0.5 μ to 1 5 μ in diameter representing a many fold increase in volume over the norm The greater the lapse of time after operation the more pronounced is the swelling (compare figs. 11 and 12) Many of the swollen particles in a cell appear single while others appear to involve a portion of a mitochondrion, resulting in a "balloon effect with an attached "tail" of normal thickness.

Total cell swelling is evident a *few days* after operation (cf also LaVelle and LaVelle '58a, '58b) This decreases with time, however so that in the latest postoperative ages the cells appear somewhat smaller than normal sometimes even shrunken, although they may contain the enormously swollen fuchsin stainable bodies. No signs of the retrograde reaction, including mitochondrial or somal swelling, were detected in the unoperated nuclear fields of the opposite side throughout the entire series.

*Fifteen and seven day operatives* After the facial nerves are severed at these ages, mitochondrial swelling is not detected four days after the operation. It does become evident when the postoperative animals

TABLE 1

*Each postoperative age represents one to three animals.*

0 refers to animals in which no mitochondrial swelling appears postoperatively + refers to animals in which mitochondrial swelling appears postoperatively on the affected side. A figure in parentheses below + refers to the percentage of cells in the affected nucleus showing swollen mitochondria. About 200–600 cells (depending on age) throughout the affected nucleus of a single animal at each indicated age were counted, using each fifth section. These figures are intended to be indicative only The low percentage for the 39 days old postoperative probably is related to the relatively low survival rate for cells after operation at seven days postnatal age. The time of inceptive swelling of mitochondria, regardless of time of operation, lies between 24 and 29 days of age.

| Age at Operation | Age at Killing: 11 | 13 | 15 | 19 | 20 | 21 | 22 | 24 | 25 | 26 | 29 | 30 | 31 | 32 | 39 | 46 | 50 | 56 |
|---|---|---|---|---|---|---|---|---|---|---|---|---|---|---|---|---|---|---|
| 7 → | 0 | 0 | 0 | 0 | 0 | 0 | 0 | | | + (4%) | | + | | | + (6%) | | | |
| 15 – | | | | 0 | 0 | 0 | 0 | | + (7%) | | | | + | | | + (26%) | | |
| 20 | | | | | | | | + (22%) | + | + | | | + | | | | + (37%) | |
| 25 | | | | | | | | | | | + (13%) | + | + | + | | | | + (23%) |

reach the respective postnatal ages of 24 and 28 days and thereafter (table 1; figs. 5 13–18) The cytological aspects of the swollen mitochondria, when they do appear are similar to those induced in the older operatives but are not accompanied by cell swelling. No signs of a retrograde reaction were detected on the unoperated side of any of the animals

In postoperative animals killed before the appearance of mitochondrial swelling, the affected neurons show retrograde signs such as eccentric nuclei with folded or thickened membranes but without somal swelling. This is in sharp contrast to the results found in the 25 or 20 day operatives, where four days after operation the affected cells show both mitochondrial and somal swelling in addition to the other retrograde signs. It should be noted that for the purpose of optimum comparison, the four day interval between operation and killing was chosen as the shortest postoperative span because by then a pronounced retrograde reaction is obtained for most cells after operation at all ages, while cell degeneration in the youngest operatives is limited to a few initial stages

After nerve section at seven days, approximately 40% of the affected cells survive the postoperative periods studied after section at 15 days 90% survive (cf. LaVelle and LaVelle '58b) The surviving cells therefore continue to develop and do not show the definite signs of mitochondrial swelling until after they pass through the late period of maturation. In table 1 are indicated the approximate percentages of these cells showing swollen mitochondria at different postoperative ages.

*Effects of fixation.* Perfusion with Regaud's fixative in general resulted in even penetration of tissue with excellent preservation of mitochondria. Perineuronal shrinkage spaces (not to be confused with patent lumina of capillaries) were rare either in the nuclear fields

studied or in adjacent regions of the sections (figs. 1 and 2) Proper fixation resulted in cells with clearly demarcated mitochondria and with perisomal boundaries in close apposition to the surrounding neuropil. The possibility of confusing one artifact for another arose. The cover slips on a few slides had been pressed down too tightly during mounting, resulting in fracture lines in the sections. Some of these lines extending around neurons gave the impression of perineuronal spaces. This artifact avoided by proper mounting procedure, apparently stems from the thinness of the sections and the fragility of material fixed in Regaud's fluid.

Occasional hyperchromic cells stained with aniline blue were seen in sections from animals of different ages. These occurred singly or in small isolated clusters of two or three cells, with no apparent predilection for the facial nuclear areas. A few were in close proximity to well fixed cells. Some of these cells appeared shrunken and tended to be associated with the fracture lines that appeared in a few slides (figs. 3 and 4) The significance of the seeming disposition of the spaces around these cells is uncertain. Mitochondria appeared variously clumped or condensed in some hyperchromic cells but normally distributed in others, with no evident relationship to the presence or absence of perineuronal spaces In the affected nuclear fields where mitochondrial swelling appeared in well fixed neurons, occasional hyperchromic cells were found which also contained swollen mitochondria. Mitochondrial swelling was observed however only in the cells of the affected nuclear groups which had reached an age when such swelling was elicited as a result of axon section. This is interpreted as corroborative evidence that the induced swelling is a direct effect of the operation as influenced by age and is not wholly obscured even in hyperchromic cells which perhaps represent a fixation artifact.

In the present instance, hyperchromic cells are few in number and do not materially affect the experimental results obtained. Nevertheless the question raised by the presence of such cells is a recurring one in the neuroanatomical literature and is further referred to in the discussion in regard to the preëminent problem of fixation of nervous tissue for cytological studies.

## DISCUSSION

Mitochondrial swelling in hamster facial neurons can be elicited by injury only after the cells have attained a definitive period in their development. Thus after axon severance at 7 15 or 20 days postnatal age, swollen mitochondria are observed when the postoperative animals reach about 25 days postnatal age. In other words, surviving neurons sectioned at the earlier ages continue their development and ultimately enter the period when they undergo the mature reaction pattern.

Our evidence indicates that the final steps in neuronal maturation are not readily detectable as a sequence of normal cytological changes but instead are reflected in the differential way the cell reacts to injury Although our emphasis here is on overt reactive changes, studies stressing very minute changes as with the electron microscope and/or at earlier ages might be revealing in regard to the normal sequence. However with electron microscopy Hess ('55) could not use mitochondria in normal spinal ganglia of postnatal guinea pigs as an index to aging. In the earlier phases of neurogenesis of some lower vertebrates intra-mitochondrial differences have been observed with the electron microscope (cf Novikoff, '61) A few reports on stained nervous tissue in some other animals have noted age differences in mitochondrial length and shape (cf Cowdry '18 and Andrew '56) Nevertheless, the whole picture of normal developmental changes is complicated by the great range of variability of nervous tissue from different animals of different ages as exposed to different technical procedures particularly fixation, which is discussed later in this paper

In earlier studies (LaVelle and LaVelle, '58a, '58b '59 LaVelle and Smoller '60) using dyes for nucleic acid and protein axon section at 20 days or later resulted in a diffuse type of chromatolysis in the neuronal cytoplasm accompanied by nucleolar nuclear and somal swelling; after section at 15 days or earlier a focal type of chromatolysis resulted which was never

accompanied by somal swelling. From the standpoint of operation time, the transition period for differentiating these effects appears to span the five-day interval extending from 15 to 20 days of age. The mitochondrial reaction, however, unlike somal swelling, develops latently after operation at the early ages. Of interest is our recent observation that the period from onset to near completion of myelination in the nuclear field and genu of the facial neurons of the hamster extends from seven to 25 days postnatal age (LaVelle, '62). The differential pattern of the retrograde reaction, therefore, discriminates phase differences in what otherwise appears as a smooth continuum in normal cytomorphological maturation.

It has been suggested (Bodian, '50; Flexner, '50) that the retrograde reaction may represent in some respects a reversion to an embryonic type or level of metabolism. This is true in terms of certain quantitative values, but perhaps not so in terms of a reassumption of a former level of integration. Our evidence indicates that the reversion is not along the same lines back toward the same primitive condition (cf. LaVelle, '58a, '59; LaVelle and Smoller, '60, in terms of the reaction regarding the nucleolus and Nissl substance). Similarly and more simply stated in the present instance, mitochondrial swelling in the mature injured cells is not a reversion to the younger condition since normal immature cells do not have swollen mitochondria; nor do they react to injury in the same fashion as the mature cell. Therefore, whatever the line of retrogression may be in the injured mature cell, the term "embryonic" may not be apropos.

Large neurons are usually involved when somal swelling is an accompaniment of the mature retrograde reaction (cf. Barr and Hamilton, '48; LaVelle and Smoller, '60). On the other hand, it is quite possible that a different reaction pattern might be consistent with some other neuronal type. Large neurons do not predominate numerically, and among neuronal types there is an extensive gradation in cytological complexity of certain components commonly associated with protein synthesis. For example, various mature neuronal types may be serially grouped, according to the relative differentiation of their nucleolar apparatuses and amounts of Nissl material, to correspond generally with different developmental stages of a neuron highly developed in this respect (LaVelle, '56). Such a grouping indicates that the cytologic system for protein synthesis has not attained the full developmental potential in different adult neuronal types and that the degree of advancement varies from type to type. This raises the question, therefore, as to whether the retrograde pattern in adult neurons having an "incompletely" developed organelle system for synthetic activity would be "mature" in character or would parallel that shown by earlier developmental stages of "better" endowed neurons. Differences in the reaction pattern of adult neurons might thus reflect efficiency levels of biosynthetic activity developmentally attained in parallel with organelle structure.

Perhaps a similar corollary exists for neuronal mitochondria. Mitochondrial increase in size in mature neurons after axon section has been observed for the toad by Luna ('13) and to some degree for the rat by Hartmann ('48, '49) and for the rabbit by Hudson et al. ('61). As with the hamster, large neurons with abundant Nissl substance and a highly developed nucleolar apparatus were studied. According to Thurlow ('17) the ratio of mitochondrial number to cytoplasmic volume varies with neuronal types. Variations in mitochondrial form in different mature neurons have also been reported (Nicholson, '16; Andrew, '56) but it is uncertain as to their consistency relevant to cell type within a given animal. Certainly more experimental and normal data are needed to establish such a consistency. It should be pointed out, however, that mitochondrial shape, size and number appear to be roughly consistent for a given cell type among different tissues in an organism (cf. Novikoff, '61).

As yet there is no uniformity of evidence from the literature to support a satisfactory interpretation of the phenomenon of mitochondrial swelling noted in the hamster series. Of relevance is Williams' report ('61) that isolated mitochondria from newborn rat liver are more resistant

## PLATE 1

### EXPLANATION OF FIGURES

Facial motor nerve cells of the golden hamster Basic fuchsin-aniline blue stain for mitochondria (which stain red) Figures one to four are × 645.

1 24 days postnatal age. Control side.

2 24 days postnatal age. Experimental side, operated on at 20 days. Swollen mitochondria are evident. Perfusion fixation with Regaud" fluid in the manner described results in the absence of perineuronal and perivascular spaces.

3 24 days postnatal age. Experimental side, operated on at 20 days. The cell at left is swollen, in early stage of reaction. At right is hyperchromic cell (intense staining with aniline blue) What may be a retraction space (or "fracture line ) is noticeable at the right and lower boundaries of this cell.

4 24 days postnatal age. Control side. A normal cell and a hyper chromic, apparently shrunken cell are close to each other The latter cell, deeply stained with aniline blue, is bounded by "shrinkage space.

Facial motor cells in figures five to nine are × 1,200. Basic fuchsin-aniline blue stain for mitochondria (which stain red)

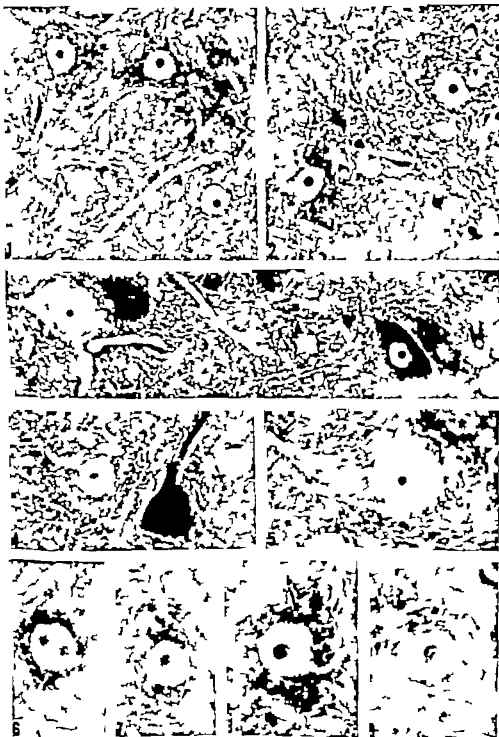
5 25 days postnatal age. Operated on t 15 days. Swollen mitochondria are first pparent when the 15-day operatives reach this age. The focal level was djusted so that the dumbbell" shaped, swollen mitochondrion (see arrow) could be seen in the dendrite.

6 7 days postnatal age. Normal cell.

7 15 days postnatal age. Normal cell.

8 20 days postnatal ge Normal cell. The disposition of mitochondria between Nissl bodies (lightly stained with aniline blue) can be seen in upper right region of cell. The orientation of the cell is such that the mitochondria are cut transversely in the lower left portion of the cytoplasm and appear as small fuchsin-stained dots or granules. = Nissl bodies. b = mitochondria.

9 50 days postnatal age. Normal cell



# Differentiation of First and Second-set Grafts of Neonatal Testis Ovary Intestine and Spleen Implanted Beneath the Kidney Capsule of Adult Albino Rat Hosts[1]

ANNYE CANNADY BUCK
*Department of Zoology The University of Michigan, Ann Arbor Michigan*

Recent work on the mechanisms governing success or failure of transplanted vertebrate tissues has been increasingly influenced by the concept of transplantation immunity While autografts are commonly successful, homografts and heterografts usually degenerate or are sloughed after a short period of toleration by the host (Gibson and Medawar 43; Medawar 44, 45 Billingham, Brent, Medawar and Sparrow '54 Steinmuller '61a). Not only are homografts eventually rejected, but this reaction occurs more rapidly in a second homograft which has followed a first graft from the same donor This second-set response has been reported by many workers (Gibson and Medawar 43 Dempster '53b; Billingham, Brent, and Medawar '54 Simonsen '55 Lewis, Murray and Couch '57)

In contrast to the experience that homografts are usually unsuccessful, several investigators in the past few years have been able experimentally to induce animals to tolerate homografts of normal tissues (Billingham, Brent, and Medawar '56a, Medawar and Woodruff '58 Krohn, '58 Billingham and Silvers, '61) as well as to enhance homografts of neoplastic tissues (Snell, Cloudman, Failor and Douglas 46- Kaliss, '55 Snell, Winn, Stimpfling, and Parker '60) What are the mechanism of transplantation immunity or acquired tolerance?

Three major theories, reviewed by Medawar ( 43) have been advanced to explain the mechanism of resistance to homografts (1) the "blood group theory (Davis, '17; Masson '18) (2) the "local cellular" theory (Loeb 45) and (3) the actively acquired immunity theory supported by the work of Schöne ('12) Holman ('24) Stone ( 42) and Gibson and Medawar ('43) Current thinking supports the third theory which holds that homografts, which are genetically different from the host tissue, act as antigens and elicit an immunologic response by the host. The work of Medawar ('44 45) gave conclusive evidence for actively acquired immunity against homografts. Although this theory is generally accepted we still do not know how the immune mechanism operates. As reviewed by Lawrence ('60) homograft rejection could possibly be mediated by serum antibodies by immune factors bound to lymphoid cells by the combined effects of serum antibodies and cell-bound immune factors or by an immune response peculiar to itself Two systems of antigens — those which cause transplantation immunity (T antigens) and those which elicit serum antibodies (H antigens) — have been distinguished (Billingham, Brent, and Medawar '56b) Gorer ('56) has indicated that the type of homograft, whether leucocytic cells, ascites tumor cells, or solid tissue graft, influences the kind of immune mechanism involved. Brent, Brown, and Medawar ('59) have expressed the opinion that homograft reaction against solid tissue grafts is a cell-mediated immune mechanism which is analogous to that operative in delayed-type sensitivity

[1] Based on a dissertation submitted in partial fulfillment of the requirements for the degree of Doctor of Philosophy in The University of Michigan, 1960. The research was aided by a fellowship from the National Medical Fellowships, Inc., through funds appropriated by the National Foundation.
[2] Present address: Department of Anatomy Meharry Medical College, Nashville, Tennessee.

Immunity to orthotopic skin homografts has been adoptively transferred by activiated lymphoid cells (Billingham, Brent, and Medawar '54 '56 Steinmuller '61b Billingham, Silvers and Wilson, '62) and by leucocyte extracts (Lawrence, Rapaport, Converse and Tillett, '60) There is also experimental evidence which demonstrates the presence of humoral antibodies in some experimental animals which have received homografts particularly of tumors (Amos Gorer and Mikulska, '54 Gorer '55) Terasaki, Cannon and Longmire ('60) have evidence that humoral antibody is evoked by solid homografts of normal skin. Successful adoptive transfer of immunity against skin homografts with antisera has been accomplished (Stetson and Demopoulos '58 Chutná, '61) though the reaction seems to be different from the accelerated rejection characteristic of second homografts.

The present investigation was undertaken in order to test the reaction of host against graft and of graft against host after primordia of various organs were implanted either singly or in combinations into adult albino rat hosts. The experiments are an extension of the work of Larkin ('60) who investigated the fate of grafts of testis implanted beneath the kidney capsule of adult male rats. The present investigation has tested the specificity of antigens (?) from different organs by comparing the effects of initial grafts of testis, ovary spleen, or intestine followed by a second graft of any of these four organs. Organs from 4-day-old neonatal donors were selected because they were still differentiating and yet probably incapable of producing antibodies against the host. Woodruff and Simpson ('55) have shown that in the rat the antibody mechanism is not fully established until 14 days after birth. At four days of age however donor tissues could be antigenic to adult host, in which the immunity mechanism is already established. The four organs tested all grow successfully when transplanted singly (Harris and Eakin, 49 Billingham and Parkes '55 Crouse, '56; MacIntyre, '56 Larkin, '60; Kammeraad, 42; Greene, '55) Presumably they differ in antigenicity and in content of immunologically competent cells. The spleen, for example, is both powerfully antigenic and active in producing antibodies (Simonsen, '55 and Castermans '58)

## MATERIALS AND METHODS

Albino rats used in this investigation were secured from the Holtzman Company Madison, Wisconsin. Males approximately one year of age were used as hosts for grafting experiments. To obtain new born rats used as sources of donor organs, adult females were mated with males at times calculated to result in litters on given dates. Inseminations were confirmed by vaginal smears and length of gestation reckoned as 21 days from insemination. Fertility was enhanced by feeding female breeders a special diet of wheat germ cereal, oranges, carrots, and pig liver or pig heart, beginning three or four weeks prior to mating and continuing throughout pregnancy Litters were used for donor organs four days after birth. Spleen, ileum and testis were dissected from male donors. Ovaries were obtained from females in the same litter.

The first procedure was to excise organs from etherized neonatal donors. Different organs were placed in separate sterile Petri dishes containing sterile Ringer's solution. Both testes of male donors were removed and transferred to a dish of Ringer's solution. The epididymis was then removed, and the testis was transferred to a fresh dish of Ringer's where it was bisected. Intestine was prepared by removing a section of the caudal portion of the ileum, placing it in a Petri dish and flushing its lumen by means of a small pipette. It was then transferred to a second dish and cut into segments approximately 2 mm in length. If necessary the segments were flushed again and transferred to a third dish. Spleens were removed and cut into small pieces, approximately $2 \times 2$ mm, which were kept in Ringer's solution until ready for use. Ovaries with surrounding bursa and oviduct were dissected from females and placed in a dish of Ringer's solution. Bursa and oviduct were removed from the ovary under a dissecting microscope, and the ovary was transferred to a dish of fresh solution, where it remained until ready for grafting.

Host animals were then anesthetized with ether shaved in the area where the incision was to be made and placed in a dissecting pan lined with clean towels. After the bare skin was bathed with 70% alcohol, a transverse incision about three-fourths of an inch in length was made through the dorsolateral wall of the abdomen just caudad of the last rib. With a loop improvised from a piece of number 12 copper wire according to the technique used by MacIntyre ('56) and Larkin ('60), the kidney was lifted out of the peritoneal cavity and immediately covered with sterile cotton soaked with Ringer's solution. The desired piece of donor organ was then picked up on one prong of jeweler's forceps modified so that the prong had a blunt end. Tissue was held in a droplet of Ringer's solution on this blunt end. Another pair of jeweler's forceps was used to pick up the kidney capsule and with the pointed prong of the modified forceps the kidney capsule was punctured. The forceps were then turned in the hand so that the clinging tissue could be inserted through the puncture and deposited just beneath the capsule. The muscular layers of the incision were sutured with no. 4-0 surgical thread, the outer skin layer was clamped together with wound clips and the area of the incision was coated with celloidin to protect it.

Control animals received a single graft, always to the left kidney Hosts for two grafts received the first under the left kidney capsule and the second under the right. Single grafts were allowed to grow for periods of two four and six weeks. In hosts for double grafts the first graft was allowed to grow two weeks and then the second graft was implanted. Animals were autopsied and both grafts recovered four weeks after the second operation. Recovered grafts were fixed in Bouin's fixative embedded in paraffin, sectioned at 8 μ, and stained with Heidenhain's azan triple stain.

## RESULTS

### *Histology of donor organs when implanted*

*Testis* The four-day-old testis contained closely packed seminiferous tubules separated by septulae of connective tissue. Sectioned tubules appeared to be solid and made up chiefly of undifferentiated cells in the periphery and fewer large cells scattered mostly toward the interior of the tubule (fig. 1) Hargitt ('26) considered these large cells as possible primordial germ cells. It is believed that they degenerate during normal development and that the maturing sex cells of the adult differentiate from cells contributed by smaller peripheral cells of the young seminiferous tubules.

*Ovary* The four-day-old ovary was less than 1 mm in length. The germinal epithelium appeared to be two or three cells in thickness except at the hilus, where it was reduced to a single layer of cuboidal cells. The secondary cortex and definitive medulla were present, and a delicate irregular tunica albuginea intervened between the germinal epithelium and the cortex. Sections of the cortex revealed distinct cellular cords (Pflüger's tubes) composed of large oogonia and a few undifferentiated cells (fig 2). In some cords the oogonia were devoid of follicle cells. Primary follicles, in which young primary oocytes were surrounded by a single layer of follicle cells, were sometimes present. Occasionally a large oogonium was observed in the layer of germinal epithelium. The definitive medulla, a fibrous vascular stroma, was devoid of oogonia.

*Intestine* The lower intestine at four days was approximately 2 mm in diameter A typical cross section (fig 3) revealed a lumen and villi lined by columnar cells having striated borders, and goblet cells. Low columnar cells lined the glands of Lieberkühn. Many epithelial cells contained mitotic figures. The lamina propria filled the cores of villi and could be seen between the glands. External to the thin vascular submucosa was a thicker layer of smooth muscle which had differentiated into an inner circular layer and an outer longitudinal layer. The longitudinal muscle layer was covered externally by a thin serosa. Lymphocytes were present in both the lamina propria and the submucosa.

*Spleen.* The four-day-old spleen (fig. 4) was surrounded by a relatively thin capsule from which thin trabeculae extended inward. The splenic tissue was still generally myeloid in character although oc

casionally there was an indication of white pulp developing around an artery There was no differentiation of red pulp. Myeloid elements in the rat's spleen reach their maximum development three weeks after birth and then gradually begin to disappear (Maximow and Bloom, 57)

*Fate of single grafts*

*Testis* Single grafts of testis recovered after two weeks had increased in size and differentiated to the extent that most of the seminiferous tubules had lumina or were in the process of forming them. Spermatogonia had proliferated and three to five layers of cells could be counted from the basement membrane of the tubule to the lumen Many cells were fixed in the process of division In some tubules many spermatogonia with pycnotic nuclei were detached from the wall and apparently were being sloughed into the lumen. In several tubules primary spermatocytes some showing signs of degeneration had differentiated. All grafts were well vascularized but there was a variation in the amount of connective tissue present.

Growth and differentiation in grafts of four weeks were more advanced than after two weeks Degeneration and sloughing of cells into seminiferous tubules apparently had continued, but there were still three to five layers of cells. According to Hargitt ('26) degeneration and sloughing of cells seem to be a part of the process of lumen formation Although most primary spermatocytes were massed in the lumen and appeared to be degenerate some appeared normal in tubules with little or no cavitation. Occasionally primary spermatocyes in the first meiotic division (fig 5) were observed No spermatids were observed, whereas they were differentiated in the testis of a normal rat of comparable age. A few Sertoli cells were identified in the peripheral layer of cells next to the basement membrane.

Seminiferous tubules in grafts of six weeks had very large lumina, indicating abundant sloughing Most tubules had no more than two or three irregular layers of cells. Some pycnotic primary spermatocytes were still present. Presumably the peak of differentiation in single grafts was reached by four weeks. After six weeks cell proliferation had decreased and many cells had degenerated and sloughed thereby leaving tubules with wide lumina. Normal testis at a comparable age had seminiferous tubules with complete spermatogenesis.

*Ovary* Single grafts of ovary after two weeks contained many enlarged primary oocytes invested with several layers of follicle cells The cortical stroma in these grafts was more extensive than in the normal ovary and well vascularized connective tissue filled the area between the grafted ovary and the host kidney Germinal epithelium could not easily be distinguished, but recent proliferation of oogonia was evident. Follicles of the grafted ovary were in the same range of size as those of a normal ovary at this age.

In grafts of four weeks (fig. 6) several ovarian follicles with numerous follicular cells, were vesicular Thecal cells had surrounded the follicle but the theca externa was not easily distinguished from the theca interna. Follicular atresia was pronounced and accompanied by extensive interstitial gland formation. These changes occurred in the normal ovary of the same age, but not so frequently Some grafts recovered after four weeks had undergone much degeneration and were hardly recognizable as ovarian. They were essentially a mass of connective tissue heavily infiltrated with lymphocytes.

By six weeks all ovarian grafts had undergone much degeneration. They appeared as large masses of connective tissue in which certain areas were void of lymphocytes and reticular cells apparently had been transformed into fat cells. Several cysts varying from large to small, were observed

*Intestine* Single grafts of intestine at two weeks exhibited epithelial proliferation. Many cells were in the process of dividing and goblet cells were prominent. Villi were pronounced. The lamina propria contained many lymphocytes but apparently not organized into distinct nodules. Some lymphocytes in the epithelium appeared to be fixed in the process of migrating through it into the lumen of the intestine. Submucosa and muscularis were thicker than normal Connective tissue between the graft and host often in-

vaded the kidney cortex, and parts of the uriniferous tubules in this section appeared degenerate.

In some four week single grafts villi were more numerous. Many goblet cells were filled with mucus, and Paneth cells with secretory granules occurred regularly in the bottom of the glands of Lieberkühn (fig. 7) Connective tissue with masses of lymphocytes was concentrated at the junction of the graft and host.

Some grafts were degenerate at two and four weeks, but all were degenerate at six weeks. In cross section such degenerate implants could be identified as a hollow ring of connective tissue with interwoven collagenous fibers. Lymphocytes and plasma cells were present within this ring of connective tissue. Fragments of various layers of the intestinal wall could be identified.

*Spleen.* No two-week single grafts of spleen were recovered. Four-week grafts (fig. 8) were degenerate and surrounded by a zone of connective tissue infiltrated with lymphoid cells neutrophils and macrophages. Sections of splenic tissue within the surrounding connective tissue contained no lymphatic nodules but resembled red pulp interspersed with many neutrophils and macrophages. Throughout the graft and also in the area where proliferating connective tissue had invaded the renal cortex there were numerous macrophages containing golden brown particles of hemosiderin

No grafts were recovered at six weeks but an accumulation of dense connective tissue infiltrated with macrophages indicated the site of implantation in the host kidney

### *Fate of double grafts*

The reaction of host against grafts may vary in severity from complete destruction of graft to no adverse reaction. Histological appearance of the graft and surrounding host tissues were the basis for the analysis of host reactions summarized in tables 1–4

### *Testis as second graft*

*Grafts of testis preceded by testis* All second grafts which had been implanted for four weeks appeared healthy and had grown considerably but differentiation of spermatocytes was retarded (fig 9) when compared with single grafts of testis at four weeks (fig 5) Sections from seven of the ten grafts recovered revealed no primary spermatocyes Three grafts however had a few pycnotic and sloughed spermatocytes in a few of the tubules. There were two to five layers of cells bordering the lumina of seminiferous tubules. Spermatogonia nearest the lumen were often detached and pycnotic, but those nearest the periphery of the tubule were normal and apparently undergoing mitosis. All grafts were well vascularized and only two of the ten showed an excess proliferation of connective tissue at the junction of graft and kidney where the kidney cortex also had been invaded.

First grafts which had grown for six weeks, still had primary spermatocytes although they were degenerate and isolated in the lumina of tubules. These grafts of testis did not appear to be any different from single grafts of the same age.

*Grafts of testis preceded by ovary* All second-set grafts of testis preceded by ovary except the one which had undergone a very severe homograft reaction contained seminiferous tubules with some primary spermatocytes (fig. 10) These cells usually were degenerate and less numerous than in the four-week single grafts (fig. 5)

First-set grafts of ovary varied. Six of the nine grafts showed better growth and differentiation than any single grafts of ovary recovered at six weeks. Some large vesicular follicles were slightly compressed, probably as a result of some pressure by the renal capsule. One multiovulare follicle was observed.

*Grafts of testis preceded by intestine* Six of the nine grafts of testis experienced a very severe homograft reaction. They consisted of a mass of connective tissue highly infiltrated with lymphocytes and were hardly recognizable as testis (fig. 11) Usually most of the tubules had been destroyed. If individual tubules remained, they had no more than one or two irregular layers of cells lining the lumen of the tubule. No primary spermatocytes were observed in any of these six grafts. Both

grafts which had experienced a very mild homograft reaction had seminiferous tubules with primary spermatocytes present. These did not vary greatly from single grafts of a comparable age. The one graft which had undergone a reaction of slightly greater intensity showed evidence of the destruction of interstitial tissue. Tubules were intact but spermatocytes were few. Connective tissue was common at the junction of the graft and host kidney as well as at the outer margin of the graft.

First-set grafts of intestine recovered were severely damaged but they looked about like single grafts after six weeks.

*Grafts of testis preceded by spleen.* No primary spermatocytes were present in second grafts of testis which had undergone a very severe homograft reaction (fig. 12). In grafts where the reaction was less severe retained seminiferous tubules contained some primary spermatocytes. Frequently connective tissue with many lymphocytes had invaded the host kidney cortex.

With one exception, all first-set grafts of spleen were deteriorated. Grafted tissue had been completely replaced by connective tissue that was highly infiltrated with lymphoid cells and macrophages. A slightly less severe reaction only indicated that there remained some recognizable splenic tissue which showed no signs of growth. The graft which experienced a mild host reaction had undergone growth and little differentiation. The splenic tissue had lost its myeloid character and looked more like red pulp with free erythrocytes in the meshes of splenic cords. There were no splenic nodules. Fragments of trabeculae were present and macrophages with engulfed erythrocytes were interspersed throughout the splenic tissue and concentrated at the junction between graft and kidney. Frequently these cells were seen within the kidney cortex in the vicinity of blood vessels.

*Ovary as second graft*

*Grafts of ovary preceded by ovary.* In the seven second-set grafts considered to have experienced no host reaction many large vesicular follicles had differentiated (fig. 13). Follicles were more numerous than in single grafts of comparable age and follicular atresia was less. Proliferation of connective tissue was usually restricted to a band between the kidney and grafted ovary. All grafts were well vascularized. The one second-set graft which had undergone a severe homograft reaction was composed of a large amount of connective tissue interspersed with a few primary and secondary follicles. The graft which experienced a mild reaction had less connective tissue proliferation, but excessive when compared with well established ovarian grafts. Several large atretic, vesicular follicles were present and interstitial gland formation was pronounced.

The one first-set graft of ovary in this series which was severely affected was almost totally replaced by connective tissue. This graft preceded a second graft of ovary which had undergone a severe reaction. When the first graft was well established the second graft was always well established too. Second grafts however generally grew and differentiated better than first grafts.

*Grafts of ovary preceded by testis.* After four weeks differentiation in these second-set grafts of ovary (fig. 14) was better than in single grafts and was similar to the normal ovary of the same age. Hypertrophy of interstitial tissue, however was a little more pronounced in the grafts. Three cases of multiovular follicles were observed in sections from three different grafts.

With the exception of one very severe reaction all first-set grafts of testis looked like typical six week single grafts. Some pycnotic primary spermatocytes were still present.

*Grafts of ovary preceded by intestine.* Five of the nine grafts recovered in this series experienced a homograft reaction classified as severe or very severe (fig. 15). Only two grafts had differentiated comparably to well established grafts of this age. When ovary was preceded by intestine the severity of the reaction was greater than when ovary was preceded by either grafts of ovary (fig. 13) or testis (fig. 14). First grafts of intestine six weeks after implantation looked like single grafts.

*Grafts of ovary preceded by spleen.* These second-set grafts of ovary (fig 16) were much like the ones in the series where ovary was preceded by intestine but the damage was slightly greater (table 2) Each degree of intensity of the homograft reaction has already been described.

Frequently the preceding splenic grafts had sloughed completely or degenerated severely Only two of the ten splenic grafts implanted showed signs of growth with very little differentiation. These were classified as having undergone a mild reaction, previously described.

*Intestine as second graft*

*Grafts of intestine preceded by intestine* No second-set grafts of intestine were recovered after four weeks.

All six first-set intestinal grafts had undergone degenerative changes comparable to those in six-week single grafts. Grafts which had experienced a very severe homograft reaction remained only as a ring of dense connective tissue surrounding the lumen. Occasionally small fragments of epithelial and muscular tissues were still attached to the inner surface of the connective tissue bordering the lumen. Sloughed epithelial cells, muscle cells neutrophils eosinophils, macrophages, and lymphoid cells were present in the lumen, which often contained a non-cellular debris. The host kidney cortex was always invaded by connective tissue. In grafts where the reaction was slightly less severe only certain sections of the intestinal wall, associated with a heavy invasion of lymphoid cells, had sloughed into the lumen. Eosinophils were abundant in the remaining epithelium and lamina propria. In grafts where the reaction was mild practically all of the intestinal wall was intact, but degeneration and sloughing of cells were evident in areas invaded by lymphoid cells. Cell proliferation was still indicated by mitotic figures of many epithelial cells. Connective tissue, highly infiltrated with lymphocytes was concentrated at the junction of graft and host kidney

Seven additional hosts which had received similar grafts were autopsied two weeks after implantation of the second graft rather than after the usual four week period. Only two very severely damaged second grafts were recovered (fig. 17) Six of the seven first grafts of intestine recovered were comparable to four week single grafts.

*Grafts of intestine preceded by testis* Three of the ten second-set intestinal grafts in this series showed extensive growth and differentiation of villi as well as of all layers of the intestinal wall (fig. 18) The epithelium was normal, and many cells were fixed in the process of dividing. Goblet cells were pronounced and Paneth cells with secretory granules were present. Connective tissue invasion was minimal. The remaining grafts were typical of the degenerating intestinal grafts already described.

First-set grafts of testis were apparently affected by the second graft of intestine even though they preceded the latter by two weeks. The general description of a first graft of testis in this series is very similar to the series in which testis was preceded by intestine (fig. 11) When seminiferous tubules were not too severely damaged, primary spermatocytes were present.

*Grafts of intestine preceded by ovary* Second-set grafts of intestine (fig. 19) appeared very much like degenerating single grafts following four weeks of implantation. In general first-set ovarian grafts were not as normal as when ovary was followed by either testis or ovary The host reaction to the ovary was very similar to that in animals where intestine preceded ovary (table 2) One multi-ovular follicle was found in each of two ovarian grafts in this series.

*Grafts of intestine preceded by spleen.* Only six highly degenerate grafts of the ten second-set grafts of intestine were recovered after four weeks (fig 20) Eight of the first grafts of spleen were recovered. Four of these showed signs of growth and little differentiation. All others were severely damaged.

*Spleen as second graft*

*Grafts of spleen preceded by spleen.* No traces of second-set grafts of spleen were found in any hosts after four weeks. First-set grafts following six weeks of implantation in these hosts were severely damaged or not recovered.

Five additional hosts which received similar grafts were autopsied two weeks after placement of the second graft. At this time three highly degenerate second grafts were recovered. In one case connective tissue not only had replaced the graft but this connective tissue apparently had undergone fatty transformation at the free margin of the degenerate implant (fig 21)

*Grafts of spleen preceded by testis* Second grafts of spleen preceded by testis were no more affected than single grafts of spleen after four weeks. The homograft reaction varied from mild (fig 22) to very severe.

First-set grafts of testis after six weeks were far more severely affected than single grafts of a comparable age Most of these grafts highly resembled grafts of testis preceded by spleen (fig 12) Primary spermatocytes were present if seminiferous tubules were not too degenerate.

*Grafts of spleen preceded by ovary* Second grafts of spleen (fig. 23) developed slightly better than single grafts of the same age The number of grafts exhibiting only a mild reaction is greater in this than in any other (table 4)

First-set grafts of ovary varied from no reaction, when compared with single controls to a very severe homograft reaction. Fifty per cent of these grafts were very severely damaged. There was no definite pattern of correlation between the intensities of the reactions of first and second grafts. One well established graft of ovary preceded a graft of spleen which experienced a very severe reaction. One double ovular follicle was observed in a graft very severely damaged while an atretic, triple ovular follicle was observed in a graft very mildly affected.

*Grafts of spleen preceded by intestine* Only four of the ten second-set splenic grafts were recovered. These had undergone a severe or a very severe homograft reaction (fig. 24) The nine recovered first-set intestinal grafts were no different than six week single grafts.

DISCUSSION

*Host reactions against testis*

The results reported in this thesis confirm Larkin's ('60) report that an initial graft of testis inhibits differentiation of primary spermatocytes in a second graft. To explain this result, Larkin postulated that "the host produces antibodies to proteins of differentiating cells of seminiferous tubules but not to the undifferentiated cells." Her theory is difficult to test experimentally but it seems reasonable when one realizes that the differentiating epithelium of seminiferous tubules of the adult (Billingham, '58) forms proteins which elicit the production of autoantibodies (Freund, Lipton and Thompson, '53 Katsh and Bishop '58) Possibly the proteins of seminiferous tubules first become antigenic when primary spermatocytes begin to develop. First grafts of neonatal testis produce numerous primary spermatocytes, but the proteins resulting from this differentiation are possibly antigenic and hence provoke a specific immunity against primary spermatocytes. Second grafts of neonatal testis grew well but differentiation of primary spermatocytes in their seminiferous tubules may have been suppressed by the hypothesized immune reaction

Second grafts of testis preceded by ovary generally grew and differentiated well although primary spermatocytes were less numerous than in single grafts of the same age. Ovary seemed to have elicited only a weak immune response if any Lewis (41) found a relationship among alcohol-soluble antigens of beef corpora lutea testis and brain. Since no corpora lutea were observed in ovarian homografts in these experiments the fact that testicular grafts preceded by ovarian grafts developed relatively few spermatocytes suggests the possibility that even the ovary with relatively young follicles may produce an antigen similar to the testicular antigen hypothesized by Larkin.

First grafts of intestine or spleen preceding testis did not elicit a host immune reaction directed specifically against differentiation of spermatocytes. When testis was preceded by either intestine or spleen testicular tissue in the second graft was severely damaged (table 1) If the remaining tubules were not too severely damaged, however primary spermatocytes were found It appears that the strongly antigenic tissues of spleen or intestine,

TABLE 1
*Host reactions with testis as second graft*

| 1st graft at 6 wks<br>2nd graft at 4 wks | Number grafted | Number recovered | Very severe | Severe | Mild | Very mild | No reaction |
|---|---|---|---|---|---|---|---|
| 1st graft testis | 10 | 10 | 0 | 0 | 0 | 0 | 10 |
| 2nd graft testis | 10 | 10 | 0 | 0 | 0 | 10 | 0 |
| 1st graft ovary | 9 | 9 | 1 | 2 | 2 | 0 | 4 |
| 2nd graft testis | 9 | 9 | 1 | 1 | 4 | 1 | 2 |
| 1st graft intestine | 9 | 6 | 3 | 3 | 0 | 0 | 0 |
| 2nd graft testis | 9 | 9 | 6 | 0 | 1 | 2 | 0 |
| 1st graft spleen | 7 | 6 | 4 | 1 | 1 | 0 | 0 |
| 2nd graft testis | 7 | 6 | 4 | 2 | 0 | 0 | 0 |

Second grafts of testis well established but differentiation of primary spermatocytes inhibited.

TABLE 2
*Host reactions with testis as second graft*

| 1st grafts at 6 wks<br>2nd grafts at 4 wks | Number grafted | Number recovered | Very severe | Severe | Mild | Very mild | N reaction |
|---|---|---|---|---|---|---|---|
| 1st graft ovary | 10 | 9 | 1 | 2 | 2 | 0 | 4 |
| 2nd graft ovary | 10 | 9 | 0 | 1 | 1 | 0 | 7 |
| 1st graft testis | 10 | 10 | 1 | 0 | 0 | 2 | 7 |
| 2nd graft ovary | 10 | 10 | 0 | 1 | 0 | 0 | 9 |
| 1st graft intestine | 9 | 9 | 7 | 1 | 1 | 0 | 0 |
| 2nd graft ovary | 9 | 9 | 3 | 2 | 2 | 0 | 2 |
| 1st graft spleen | 10 | 6 | 3 | 1 | 2 | 0 | 0 |
| 2nd graft ovary | 10 | 9 | 4 | 3 | 1 | 1 | 0 |

both of which contain lymphoid cells, have provoked a non-specific immune reaction in the host. Although a second graft of testis became very degenerate the immune reaction that is hypothesized seemed not to have been directed specifically toward the inhibition of spermatocyte production.

*Host reaction against ovary*

Second grafts of ovary preceded by ovarian grafts generally grew and differentiated well. Primary grafts of ovary in these experiments varied in their reaction. Some grew well and others degenerated (table 2) One wonders whether the apparently better development of second grafts can be explained by the phenomenon of enhancement. Breward and Zuckerman ('49) in their study on the reaction of the body to multiple ovarian grafts in normal adult female rats, found that grafts took better in animals implanted with six than in animals implanted with only two additional ovaries. Parkes ('58) observed that the acceptance and survival of interstrain ovarian grafts were enhanced by pretreatment of the recipient with suspensions of similar ovarian tissue. Although the reaction resembled that of tumor enhancement, Parkes was not certain that the mechanism was the same

Second grafts of ovary preceded by testis grew exceptionally well for four weeks after implantation. The initial grafts of testis in the same hosts usually resembled single grafts grown for six weeks. If there is an antigen in the ovary which might elicit antibodies against spermatocyte differentiation, as discussed above, it appears not to affect differentiation of testis after it has once become established as a first graft.

Intestine or spleen preceding a homograft of ovary resulted in a host reaction which damaged the ovarian graft. Both of these organs elicited such a strong response that even single grafts of them generally degenerated rapidly Their effect on second grafts of ovary as well as testis is

an indication that they elicit a non-specific reaction.

The observation of multiovular follicles in some of the differentiating ovarian grafts was by chance. Serial sections were not made; hence these observations were made on sections of tissue selected at random. Hartman ('26) explained multiovular follicles as due to accidents in development, resulting from variable proportions of germ cells, epithelium, and stroma. Hartman (*op. cit.*) and Harrison ('49) suggested atresia as an explanation, yet Corner ('23), from his observations on pig ovaries, indicated that multiovular follicles may reach maturity and ovulate. Bacsich ('46) suggested that they result from the postnatal withdrawal of the influence of maternal gonadtropin. More recently Kent ('62) has given considerable attention to these atypical ovarian structures and has explained his data on the basis that levels of estrogen and progesterone affect the incidence of polyovular and multinucleate follicles and that both estrogen production and primary and secondary follicular development may be correlated with FSH and LH levels. No conclusive explanation can be made for results obtained from the randomly selected material in this work. Eight multiovular follicles in eight different double grafts were observed in various graft combinations with the exception of ovary preceded by ovary. Grafting experiments now under investigation possibly may provide important clues toward elucidating the causal factors which underlie development of atypical follicles.

### *Host reactions against spleen and intestine*

Both spleen and intestine provoked severe immune reactions even as single grafts. When a graft of intestine was preceded by intestine or when spleen was preceded by spleen, typical immune responses occurred. Second grafts were usually completely destroyed within a period of four weeks or less; first grafts persisted although they were degenerate. It seems likely that the lymphoid cells in the intestine may account for the similarity of reaction to both spleen and intestine. When spleen was grafted antecedent to implantation of intestine, or *vice versa*, both first and second grafts were destroyed by the host antibody response. Second grafts, whether of spleen or of intestine in these combinations, were more rapidly destroyed. The immune reaction appeared to be somewhat more severe when a given type of graft was preceded by one of its own kind (tables 3 and 4). The results indicate that spleen and intestine share some common antigens; yet the slightly more severe immunity reaction against like organs suggests some degree of organ specificity.

As previously mentioned, when testis or ovary preceded either intestine or spleen in double grafting combinations, the gonadal tissues were markedly affected by a host reaction. The fate of either ovary or testis as a first graft was similar to their fates as second grafts when preceded by spleen or intestine. Intestine and spleen evidently are strongly antigenic and probably evoke an immune response which

TABLE 3

*Host reactions with intestine as second graft*

| 1st grafts at 6 wks<br>2nd grafts at 4 wks | Number grafted | Number recovered | Very severe | Severe | Mild | Very mild | No reaction |
|---|---|---|---|---|---|---|---|
| 1st graft intestine | 6 | 6 | 3 | 2 | 1 | 0 | 0 |
| 2nd graft intestine | 6 | 0 | 0 | 0 | 0 | 0 | 0 |
| 1st graft testis | 10 | 10 | 2 | 4 | 1 | 0 | 3 |
| 2nd graft intestine | 10 | 10 | 2 | 5 | 1 | 0 | 2 |
| 1st graft ovary | 10 | 10 | 2 | 3 | 1 | 1 | 3 |
| 2nd graft intestine | 10 | 8 | 5 | 2 | 1 | 0 | 0 |
| 1st graft spleen | 10 | 8 | 2 | 2 | 4 | 0 | 0 |
| 2nd graft intestine | 10 | 6 | 6 | 0 | 0 | 0 | 0 |

TABLE 4
*Host reactions with spleen as second graft*

| 1st graft at 6 wks<br>2nd graft at 4 wks | Number grafted | Number recovered | Very severe | Severe | Mild | Very mild | No reaction |
|---|---|---|---|---|---|---|---|
| 1st graft spleen | 5 | 3 | 1 | 2 | 0 | 0 | 0 |
| 2nd graft spleen | 5 | 0 | 0 | 0 | 0 | 0 | 0 |
| 1st graft testis | 10 | 10 | 6 | 1 | 3 | 0 | 0 |
| 2nd graft spleen | 10 | 6 | 2 | 2 | 2 | 0 | 0 |
| 1st graft ovary | 10 | 10 | 5 | 2 | 1 | 1 | 1 |
| 2nd graft spleen | 10 | 10 | 2 | 3 | 5 | 0 | 0 |
| 1st graft intestine | 10 | 9 | 6 | 0 | 1 | 0 | 0 |
| 2nd graft spleen | 10 | 4 | 2 | 2 | 0 | 0 | 0 |

affects the less antigenic grafts of ovary or testis even after the latter have become well established.

*Influence of graft on host renal cortex*

Connective tissue frequently invaded the host renal cortex adjacent to the graft, resulting in degeneration of uriniferous tubules. This invasion usually was associated with grafts which themselves were degenerating. One explanation for this is a graft-versus-host reaction in the manner reviewed by Billingham ('59). Dempster ('53a) observed that in homotransplanted kidney the reticulo-endothelial system of the graft began to produce plasma cells even before the host developed any against the graft. He envisaged this plasma cell reaction as an indication of possible antibody formation against the host. On the other hand, Porter and Calne ('60) have used an autoradiographic technique in conjunction with tritium-labeled thymidine to trace the origin of infiltrating pyronine-positive cells in skin and kidney homografts. Many of these cells have been clearly shown to be of host origin. In the present experiments grafts were implanted at an age when lymphoid cells either had not reached full competency or had not become numerous enough to elcit a strong immune reaction (Howard and Michie '62). Grafts of organs containing abundant lymphoid cells, e.g. spleen and intestine, underwent extensive regression. It seems likely that an immune response by the host initiated destruction before immunologically compentent cells of the graft could start to produce antibodies inimical to host tissues. Unfortunately tissues of the host other than renal tissue surrounding the graft were not examined. It is possible that graft antibodies against host antigens would affect host tissues far removed from the site of transplantation.

Another explanation is that stroma of the kidney was stimulated to proliferate so extensively that epithelium of renal tubules was crowded out or displaced. Greene ('55) has pointed out that if a graft is to be established successfully it must have stroma inducing properties and the host must be the source of proliferating stromal cells. The host tissue at the site of transplantation must, in turn be responsive to the stroma-inducing stimulus of the graft. Induction of proliferation of stroma in the kidney cortex, rather than production of anti-host antibodies by graft tissues, could explain the apparent invasion of connective tissue which replaced uriniferous tubular components at the site of implantation.

SUMMARY

1. Single homografts of testis, ovary, intestine and spleen from four-day-old newborn rats were implanted beneath the kidney capsule of the adult male albino rat and allowed to grow for periods of two, four and six weeks. Double homografts involving every possible pairing of grafts from the four donor organs were implanted similarly. Second grafts were implanted two weeks after first grafts and hosts were sacrificed after four weeks. The extent of growth and differentiation in single grafts served as a control for determining the differentiation of first and second-set grafts of the four donor organs.

Terasaki, P. L., J. A. Cannon and W. P. Longmire, Jr. 1960 Antibody response to homografts. IV Time of appearance of lymphoagglutinins in partially tolerant animals. Transpl. Bull., 7 (25): 415–518.

Woodruff, M. F. A., and L. O. Simpson 1955 Induction of tolerance to skin homografts in rats by injection of cells from the prospective donor soon after birth. Brit. J. Exp. Path., 36 494–499

## PLATE 1

### EXPLANATION OF FIGURES

Four-day-old neonatal donor organs

1. Section through testis. Solid seminiferous tubules have a peripheral layer of undifferentiated, small cells. Large cells in the interior are primordial germ cells which eventually degenerate. Tunica albuginea can be seen in the upper left corner of photograph. × 410
2. Section through ovary. Secondary cortex is divided into Pflüger' tubes containing oogonia devoid of follicle cells. The definitive medulla in the lower right of photograph is devoid of primordial germ cells. × 410.
3. Portion of cross section through intestine. × 96.
4. Section through spleen. Splenic nodules are not yet pronounced. × 96.




2


3


4

## PLATE 2

EXPLANATION OF FIGURES

Four-week single grafts

5 Section through seminiferous tubules of grafted testis. Arrow points to primary spermatocytes in first meiotic division. × 492.

6 Section through grafted ovary showing developing follicles. Host renal tissue t the left of graft. × 96.

7 Section through graft of intestine showing Paneth cells with secretory granules (arrow) at bottom of glands of Lieberkühn. Host renal tissue is present t the lower border of graft. × 410.

8 Degenerate graft of spleen. Arrow points to necrotic splenic tissue embedded in mass of connective tissue. Host renal tissue is present in lower left corner of photograph. × 96.




6




8

## PLATE 4

### EXPLANATION OF FIGURES

Ovary as second graft

13 Four week, second graft of ovary which was preceded by ovary Tw large follicles show antra. Renal tissue f host is present below graft. × 96.

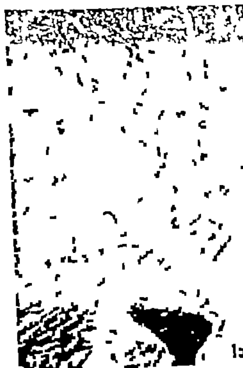
14 Four week, second graft of ovary which wa preceded by testis. Arrow points to double ovular follicl Host renal tissue is below × 96

15 Four week, second graft of ovary which was preceded by intestine. Ovarian tissue has been replaced by connective tissue. T bula tructures in the connective tissue appear to be sections of oviduct which wa probably implanted accidentally along with the ovary Renal tissue of the host below with a large vascular area to the right. Very severe host reaction. × 96.

16 Four-week, second graft of ovary which was preceded by spleen. An ovarian follicl remains in gr fted tissue which has been largely replaced by connective tissue Renal tissue in lower right corner of photograph. Very severe host reaction. × 96.


13


14


15


16

## PLATE 5

### EXPLANATION OF FIGURES

Intestine as second graft

17 Since no second grafts of intestine preceded by intestine persisted for four weeks two-week second graft of intestine preceded by intestine is illustrated. Graft remains only as a thick hollow ring of connective and muscular tissues attached to the host renal tissue. All epithelium has degenerated and sloughed into the lumen. Very severe host reaction. × 96.

18 Four-week, second graft of intestine which was preceded by testis. Graft shows growth and differentiation of glandular epithelium (arrow) as well as all other layers of the intestinal wall. Adjacent renal tissue extends across the lower border and to the right of grafted intestine. Only mild host reaction against graft. × 96.

19 Four-week, second graft of intestine which was preceded by ovary. Epithelium (arrow) bordering the lumen is highly degenerate and most of it has sloughed into the lumen. Connective and muscular tissues comprise most of graft. Very severe host reaction. × 96.

20 Four-week, second graft of intestine which was preceded by spleen. Section of graft shows the most extensive amount of epithelium bordering lumen above. Note adjacent renal tissue below. Very severe host reaction. × 96.




18





# A Mapping of the Distribution of Lactic Dehydrogenase in the Brain of the Rhesus Monkey[1]

REINHARD L. FRIEDE AND LADONA M. FLEMING
*Mental Health Research Institute University of Michigan, Ann Arbor Michigan*

This article provides a quantitative mapping of the distribution of lactic dehydrogenase (LDH) activity in the nuclei and regions of the brain of the rhesus monkey It represents one part of a program of systematic mappings of the distribution of various enzymes in the brain. Previous publications described the distribution of succinic dehydrogenase (SD) in guinea pig brain (Friede '59 a, b '60 a, b) four oxidative enzymes and capillarization in a cat brain brain stem atlas (Friede, '61 a) and DPN-diaphorase in human brain (Friede and Fleming, '62)

These studies were deliberately confined to enzymes involved in different phases of oxidative breakdown of glucose A comparison of the data shows similar distribution of these enzymes in most of the regions of the brain however some exceptional nuclei showed definite differences in gross distribution. In addition, some finer differences in cytological distribution were found throughout the brain. Therefore, the present study emphasizes the comparison and the differences of patterns of LDH and SD with extensive reference made to the articles quoted above.

## MATERIALS AND METHODS

Brains from healthy adult rhesus monkeys were blocked immediately after removal and fixed for one day in 10% neutral formalin at 5 Sectioning and incubation procedures were as those described for fixed tissue in a recent publication (Friede Fleming, and Knoller '63a). Thirty-μ sections were incubated for one hour using the histochemical method for lactic dehydrogenase[2] (Allen and Slater '61) Duplicate series of sections were always prepared, one for histochemical studies and the other for quantitative LDH measurements. The series for histochemical studies was incubated in medium containing Nitro-BT and the sections were mounted in glycerol gel. The other series was incubated in medium containing INT and quantitative measurements of the histochemical reaction were made (Friede and Fleming '62)

Extensive collections of enzyme histochemical series for several other enzymes both in monkey brain and other species were available for comparison

## RESULTS

### *A. Distribution of LDH in the monkey brain*

Measurements of LDH showing the gradations of this enzyme in nuclei and regions of the monkey brain are given in table 1 These measurements represent averages of measurements from three brains they summarize a total of 2,014 measurements. For a better understanding of the cytological distribution of LDH that the measurements represent, the figures should be compared with the plates. For example, the plates demonstrate whether the enzyme was distributed homogenously in the neuropil or in the perikarya of a given region. In other regions, the measurements may represent only a fraction of the true enzyme activity in a given nucleus for example, when there were either perforating fiber bundles or a markedly reticular arrangement of the neuropil

[1] This investigation was supported by U.S. Public Health Grant B-3250.

[2] The composition of the incubation media was as follows: 0.6 M N DL lactate (Sigma), 3 ml 0.01 M DPN 3 ml 1 M phosphate buffer pH 7.2, 13 ml; 1 mg/ml Nitro BT, 7 ml 0.03 M Potassium cyanide, 3 ml pH adjusted to 7.4.

TABLE 1

*Histochemical measurements of lactic dehydrogenase activity in the nuclei and regions of monkey brain*

| | |
|---|---|
| **Medulla spinalis** | |
| Columna ventralis | 52 ± 3 |
| Columna lateralis | 54 ± 2 |
| Lateral tracts | 21 ± 5 |
| Dorsal tracts | 18 ± 1 |
| **Medulla oblongata** | |
| N. cuneatus medialis | 65 ± 6 |
| N. cuneatus lateralis | 58 ± 5 |
| N. tractus desc. n. trigemini (general region) | 44 ± 6 |
| N. nervi hypoglossi | 49 ± 5 |
| N. tractus solitarii | 35 ± 11 |
| N. reticularis | 38 ± 5 |
| N. reticularis lateralis | 52 ± 6 |
| N. vestibularis medialis | 55 ± 6 |
| N. vestibularis lateralis | 46 ± 5 |
| N. prepositus hypoglossi | 47 ± 7 |
| Tractus pyramidalis | 16 ± 1 |
| Corpus restiforme | 20 ± 2 |
| N. nervi facialis | 50 ± 4 |
| N. reticularis gigantocellularis | 41 ± 3 |
| Nervus V | 14 ± 2 |
| **Cerebellum** | |
| Cortex (whole) | 49 ± 11 |
| N. fastigii | 35 ± 9 |
| N. dentatus | 52 ± 7 |
| Substantia alba | 19 ± 3 |
| **Pons** | |
| Nucl. reticularis | 38 ± 3 |
| N. nervi abducentis | 62 ± 4 |
| Griseum centrale | 42 ± 7 |
| N. coeruleus and griseum centrale | 37 ± 4 |
| N. nervi trigemini motorius | 59 ± 6 |
| N. parabrachialis | 40 ± 2 |
| N. parolivaris and n. olivaris superior | 59 ± 4 |
| N. reticularis Bechterew (retic. part) | 44 ± 4 |
| N. pontis (retic. part) | 50 ± 6 |
| Brachia pontis | 17 ± 3 |
| Brachium conjunctivum | 22 ± 2 |
| *N. lemnisci lateralis* | *46 ± 2* |
| **Midbrain (colliculus inf.)** | |
| *Colliculus posterior* (caudal portion) | 74 ± 4 |
| Griseum centrale (ventral portion) | 43 ± 2 |
| Midline n. | 21 ± 1 |
| N. mesencephalicus profundus | 38 ± 4 |
| **Midbrain (colliculus sup.)** | |
| Colliculus superior (laminae profundae) | 43 ± 6 |
| Regio S | 38 ± 3 |
| Griseum centrale (dorsolateral portion) | 44 ± 4 |
| Griseum centrale (ventromedial portion) | 39 ± 3 |
| Pretectal area | 38 ± 5 |
| N. nervi oculomotorii | 64 ± 5 |
| N. ruber | 42 ± 4 |
| N. niger | 38 ± 5 |
| Pedunculi cerebri | 17 ± 2 |
| N. interpeduncularis | 42 ± 3 |
| **Diencephalon (thalamus)** | |
| N. anterior (dorsalis) | 48 ± 9 |
| N. lateralis | 39 ± 6 |
| N. dorsomedialis | 41 ± 5 |
| Anterior midline nuclei | 37 ± 3 |
| Centre median | 32 ± 3 |
| Midline-nuclear group (deep transition into hypothalamus) | 30 ± 3 |
| Pulvinar | 37 ± 4 |
| N. geniculatus medialis | 43 ± 4 |
| N. geniculatus lateralis | 41 ± 6 |
| Capsula interna | 18 ± 2 |
| Tractus opticus | 19 ± 3 |
| N. reticularis thalami | 39 ± 3 |
| **Diencephalon (subthal. centres)** | |
| Tuber cinereum | 44 ± 4 |
| N. subthalamicus | 51 ± 11 |
| Zona incerta | 35 ± 4 |
| Peduncular zone of n. intercalatus | 30 ± 4 |
| Commissura anterior | 21 ± 4 |
| Corpus callosum | 17 ± 2 |
| **Basal telencephalic centres** | |
| N. caudatus (caput) | 49 ± 8 |
| Putamen | 54 ± 6 |
| Pallidum externum | 33 ± 2 |
| Pallidum internum | 36 ± 4 |
| Capsula interna | 18 ± 2 |
| Claustrum | 35 ± 12 |
| Amygdala | 33 ± 5 |
| Septal region | 41 ± 7 |
| **Precentral motor cortex** | |
| Laminae II-IV | 44 ± 5 |
| **Frontal pole** | |
| Laminae II-IV | 40 ± 6 |
| Substantia alba | 20 ± 2 |
| **Parietal cortex** | |
| Laminae II-IV | 54 ± 3 |
| Substantia alba | 17 ± 3 |
| Insular cortex (general) | 43 ± 6 |
| **Occipital cortex** | |
| Area 18, laminae II-IV | 69 ± 9 |
| Area 17, lamina IV | 71 ± 6 |
| Substantia alba | 17 ± 2 |
| **Temporal cortex** | |
| Laminae II-IV | 39 ± 4 |
| Substantia alba | 21 ± 3 |
| **Deep temporal cortex** | |
| Laminae II-IV | 26 ± 3 |
| Substantia alba | 18 ± 2 |
| Cornu ammonis (total) | 45 ± 5 |
| Subiculum | 36 ± 2 |

The measurements indicate μg Formazan/0.131 mm³ tissue 2h/38°C. They represent averages taken from total of 2,014 measurements in the brains of three monkeys (Friede, Fleming and Knoller, '63b).

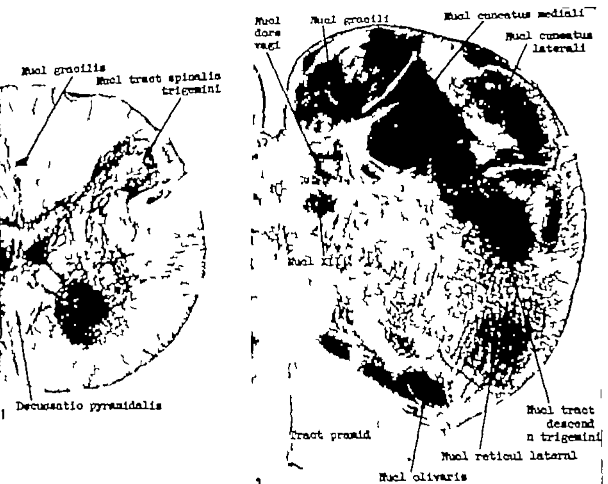



Fig. 1 Cervical cord.

Fig. 2 Medulla oblongata udal portion.

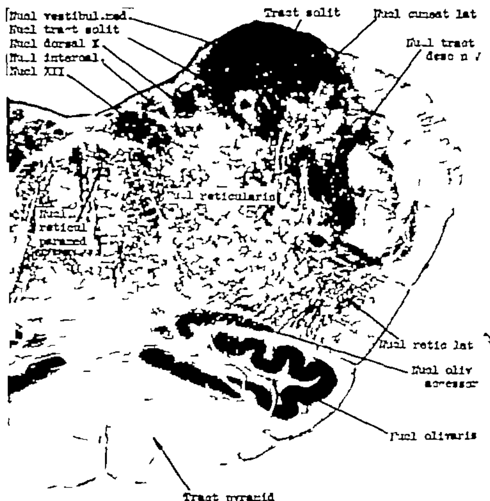



FIG. 3 Medulla oblongata middle portion.

A description of the fine structure of the neuropil in individual nuclei and of the sharpness of the delineation of nuclei from each other was not included in this article because these features were extremely similar to those described in detail for DPN-diaphorase in the human brain (Friede and Fleming, '62)

If one compared the gradation of enzyme activity among the regions of the brain the gradations of SD DPN-diaphorase and LDH among the nuclei of the medulla oblongata of various mammalian species were practically identical (figs 1–6) except for the few particular nuclei listed below Comparison of the measurements of the gradations of DPN-diaphorase in 41 nuclei of the human brain stem with LDH in the same nuclei of the monkeys showed a correlation coefficient of .80

In the mesencephalon (figs. 7–9) there was more variation of enzyme patterns among species while in the thalamus and telencephalon, marked differences were observed between guinea pig, monkey (figs 11 12) and man. This was demonstrated by a comparison of microphotographs published in this article with such in previous publications (Friede '59 a.b. '60 a.b ) it was substantiated by quantitative measurements of the histochemical reaction. The detailed results of this comparison will appear in a forthcoming publication.

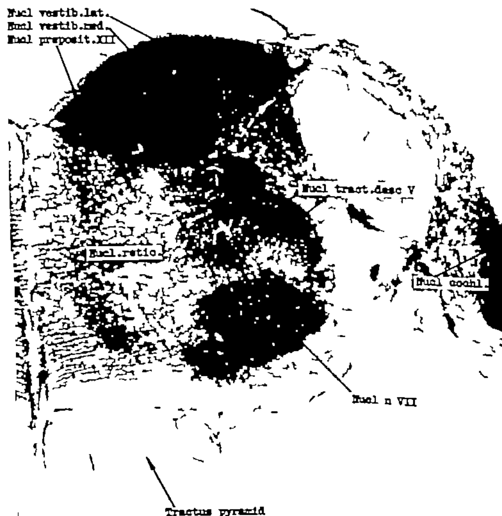



Fig. 4 Medulla oblongata, cranial portion.

The enzyme patterns in the areas of the cerebral cortex resembled those described in a histochemical mapping of the guinea pig cerebral cortex (Friede '60 a) Sensory cortex (postcentral, auditory and visual) showed strongest LDH. The visual cortex showed a striking lamination (fig. 15) similar to that of DPN-diaphorase in human area 17 (Friede and Fleming '62) The strong LDH in the upper laminae terminated sharply at the borders of the area 17 Parietal, frontal (fig. 13) and temporal cortex (fig. 14) in declining order showed weaker activity Betz giant cells (fig. 13) were sharply outlined by strong LDH, while the cell patterns of the temporal cortex (fig. 14) were more diffuse.

### B *Differences in the cytological distribution of SD and LDH*

The cytological distribution of SD and LDH was similar. In some regions the neuropil contained much stronger activity than the perikarya, while in other regions the pattern was vice-versa (fig. 10) However if one compared the distribution of SD and LDH in any given region, some difference of cytological distribution could be observed in that there was always more

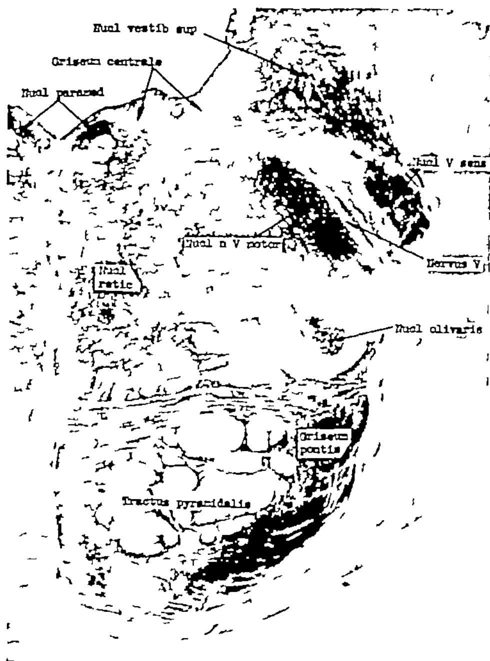



Fig. 5 Pons.

LDH than SD in the perikarya and more SD than LDH in the neuropil A similar but less distinct difference in cytological pattern was observed when comparing SD and DPN-diaphorase (Friede 61 a) A few characteristic regions where this difference in cytological distribution of the enzymes was particularly evident, are described below

The *second or third laminae of the cerebral neocortex* (figs. 13–15) had very little perikaryal SD but the activity was strong in the neuropil where nerve cells were often discernible as optically empty

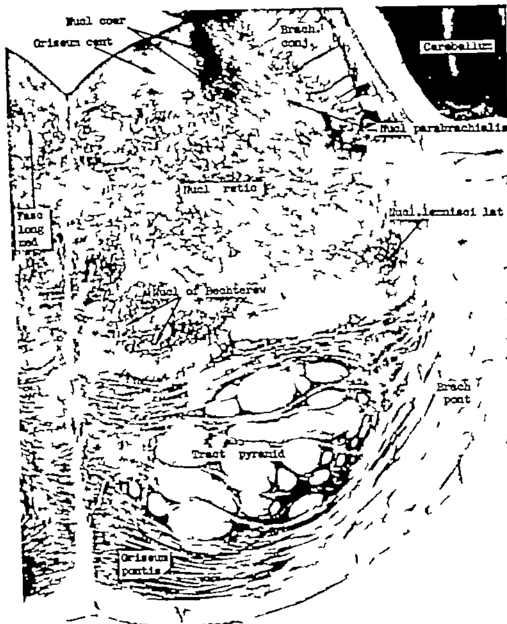



Fig. 6 Pons.

areas. On the other hand LDH permitted one to recognize an abundance of nerve cells with slightly more activity in the perikarya than in the adjacent neuropil (fig. 14)

In the *fascia dentata* the pyramidal cells showed no SD reaction; in the adjacent neuropil of the molecular layer there was a strong reaction that distinctly increased in the distal portion of the layer. In contrast, there was marked LDH activity in the perikarya of the pyramidal cells (fig 18) and the activity appeared to be equal throughout the molecular layer sometimes there was more LDH in the proximal portion of the layer (fig 16)

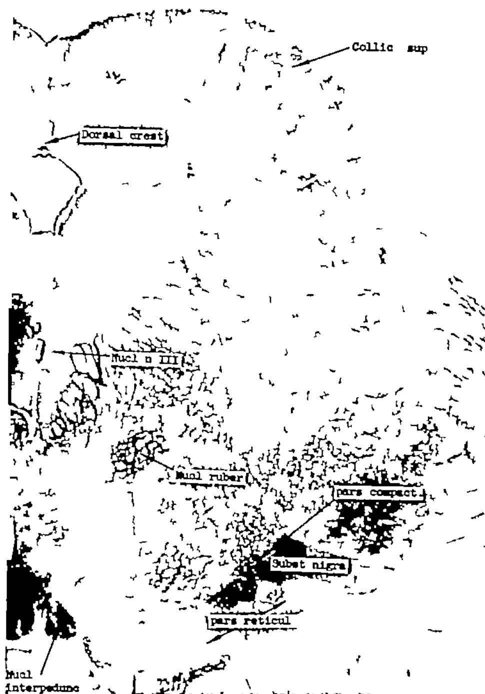



Fig 9 Midbrain at the level of the upper colliculus.

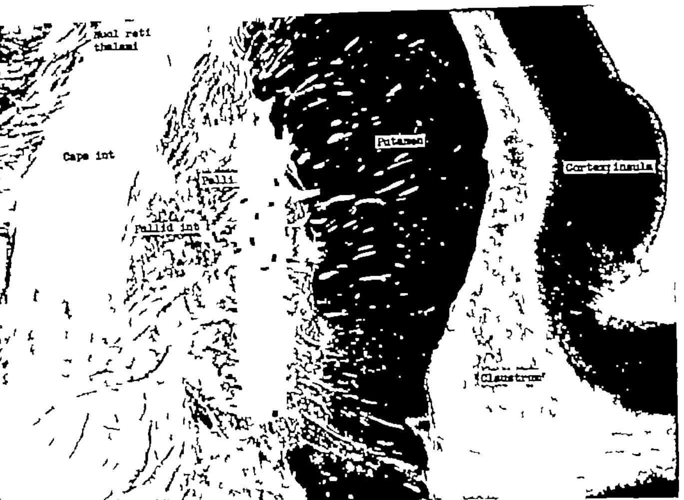



Fig. 10 Basal telencephalic centers.



Fig. 13 Precentral motor cortex.

Fig. 14 Temporal cortex.

Fig. 15 Visual cortex (area 17)




Fig. 16 Corn ammoni and f scia dent ta; survey

but the amount of activity in it apparently was subject to individual variations. The amygdala and part H of the hippocampus (fig 16) likewise had disproportionally more LDH than SD activity but the dif ference was not as marked as in the other exceptional nuclei.

### D Distribution of LDH in white matter

The distribution of LDH in white matter of the monkey brain was quite similar to that of DPN-diaphorase in human brain (Friede, '61b) The white matter in comparison with gray matter had relatively stronger LDH than SD due to the much stronger LDH reaction in the oligodendroglia cells and to some extent, in the capillaries and axons.

Of particular interest were regional dif ferences of the number of oligodendroglia cells and the amount of LDH activity in them Numerous oligodendroglia cells were observed in the white matter of the cerebral and cerebellar hemispheres and in many fibre tracts of the brain stem. These cells were identified as being oligodendroglia by counterstaining their nuclei in enzyme histochemical preparations with chrome alum-gallocyanin. Such cells showed no enzyme reaction in their nuclei and a small margin of cytoplasm with a moderate reaction for LDH (fig. 21) These cells were identified as being Hortega's *oligodendroglia of types III and IV* (Friede '61b)

A different morphology of cells was observed in several tracts containing thick axons with strong LDH In these tracts most of the oligodendroglia cells were larger and had markedly stronger LDH than those in the white matter of the hemispheres (fig. 20) Representative for this pattern were the roots of motor cranial nerves the fasciculus longitudinalis medialis, the pyramidal tract portions of the capsula interna and the portions of the frontal white matter and corpus callosum containing radiations or commissures re spectively of the precentral cortex. In sections cut perpendicular to the course of the fibers one could see the oligoden droglia processes attached to or encircling nerve fibers (fig 20) or else glial peri karya intimately attached to the fibers resembling Schwann cells. The latter was observed particularly frequently in the cranial nerve roots. By these features the cells were identified as Hortega's oligodendroglia types I and II (Friede '61b)

Enzyme histochemical preparations, therefore supported the morphological distinction of types of oligodendroglia cells. These cells were observed in a characteristic distribution among fiber systems in keeping with Hortega's (28) original notes as to where these types of oligodendroglia cells can be found.

Throughout the white matter astrocytes did not show activity of LDH how ever the molecular layer at the surface of the cerebral cortex showed numerous astrocytes with strong activity of LDH

## DISCUSSION

The mapping of LDH marks a new phase of our study of enzyme patterns in mammalian brain because it represents an enzyme involved in the glycolytic break down as compared with SD which represents the citric acid cycle. Certain conclusions as to the relative significance of these two pathways of glucose breakdown can be drawn from the data. The vast majority of nuclei in the brain have amaz ingly similar gradations of LDH SD and capillarization this indicates that these patterns do reflect general gradations of energy metabolism in the nuclei of the *nervous system* The *over-all differential* gradation of these enzymes between perikarya and neuropil suggests the working hypothesis that perikarya depend rela tively more on glycolytic metabolism than the dendrites in the neuropil do dendrites, or neuropil seem to depend relatively more on citric acid cycle.

Even more interesting are the nuclei characterized by marked differences of the distribution of LDH and SD It certainly represents more than a coincidence that the capillarization of these nuclei showed an exceptional disproportion to their SD activity (Friede '61a) Strong LDH ac tivity in itself does not prove that this enzyme is really being utilized up to capacity However the very weak SD activ ity does prove that the nuclei cannot utilize the citric acid cycle to the same extent as other nuclei If these nuclei utilize

glucose at all, it must be assumed that their metabolism is predominantly glycolytic. In addition, current investigations in the same nuclei showed exceptionally strong activity of two enzymes involved in glucose shunt metabolism that is glucose-6-phosphate dehydrogenase and 6-phosphogluconate dehydrogenase.

All the data we have strongly suggests that this group of nuclei with particularly strong LDH is metabolically exceptional as it depends more on glucose shunt and glycolytic metabolism than other regions of the brain do Observations of the resistance to anoxia of the supraoptic and paraventricular nucleus (Grenell and Kabat 47) or on the long survival following circulatory arrest of the dorsal vagal nucleus (Heymans et al. '34 '38 Kalle '33) are well in keeping with this interpretation. Our observations also suggest that oligodendroglia cells depend less on the citric acid cycle than nerve cells do.

This article represents an interim report of a continued effort to map enzyme patterns in the mammalian brain. The detailed mapping of one given enzyme such as SD would seem to be merely of academic interest. If such studies are continued along with parallel studies of other enzymes, similarities and dissimilarities of the patterns become evident and better foundations are obtained for the metabolic interpretation of enzyme patterns. Such information becomes available only through systematic, comparative mappings of most or all the nuclei of the brain.

## SUMMARY

This article reports microphotographically the distribution of lactic dehydrogenase in the monkey brain. Extensive measurements of the histochemical reaction document the characteristic gradations among nuclei. The distribution of this enzyme closely resembles that of succinic dehydrogenase and DPN-diaphorase which had been mapped in preceding investigations. The patterns of these enzymes are almost identical in the medulla oblongata of various species, while differences among species increase in caudo-cranial order

In contrast with these similarities of enzyme patterns, a number of differences could be observed in certain nuclei and also as to the cytological distribution of enzyme activity Lactic dehydrogenase always was somewhat stronger in the cell bodies and somewhat weaker in the neuropil than succinic dehydrogenase. Likewise lactic dehydrogenase was relatively stronger than succinic dehydrogenase in oligodendroglia cells of which several types could be distinguished histochemically

A system of histochemically exceptional nuclei was described they were characterized by very little succinic dehydrogenase but extremely strong lactic dehydrogenase. These nuclei probably depend metabolically more on glycolytic and glucose shunt metabolism than on citric acid cycle

## LITERATURE CITED

Allen, J M., and J J Slater 1961 A cytochemical analysis of the lactic dehydrogenase-diphosphopyridine nucleotide-diaphorase system in the epididymis of the mouse. J Histochem. and Cytochem., 9: 221 233.

Friede, R. L. 1959a Histochemical investigations on succinic dehydrogenase in the central nervous system. II Atlas of the medulla oblongata of the guinea pig. J Neurochem., 4 111–123.

——— 1959b Histochemical investigations of succinic dehydrogenase in the central nervous system. III Atlas of the midbrain of the guinea pig including pons and cerebellum. Ibid., 4 290–303.

——— 1960a Histochemical investigations on succinic dehydrogenase in the central nervous system. IV A histochemical mapping of the cerebral cortex of the guinea pig. Ibid., 5 156–171.

——— 1960b Histochemical investigations on succinic dehydrogenase in the central nervous system. V The diencephalon and basal telencephalic centers of the guinea pig. Ibid., 6 190–199.

——— 1961a A histochemical tlas of tissue oxidation in the brain stem of the cat S. Karger Basel, New York.

——— 1961 A histochemical study of DPN-diaphorase in human white matter with some notes on myelination. J Neurochem., 8 17–30.

Friede, R. L., and L. M. Fleming 1962 A mapping of oxidative enzymes in the human brain Ibid., 9: 179–198.

Friede, R. L., L. M. Fleming and M. Knoller 1963a A quantitative appraisal f enzyme histochemical methods in brain tissue J Histochem. and Cytochem 11 232–245.

Friede R. L., L. M. Fleming and K Knoller 1963b A comparative mapping of enzymes involved in hexosemonophosphate shunt and citric acid cycle in the brain. J Neurochem., 10 263–277

Grenell, R. G., and H. Kabat 1947 Central nervous system resistance. II Lack of correlation between vascularity and resistance to circulating arrest in hypothalamic nuclei. J Neuropath. Exp. Neurol., 6 35–43.

Heymans, C., F Jourdan and S. J G. Novak 1934 Recherches sur la résistance des centres encephalo-bulbaires a l'anémie. C. soc. biol., 117 370–473.

Heymans, C., J J Bouckaert, F Jourdan S. J G Novak and S. Farber 1937 Survival and revival of nerve centers following acute anemia. Arch. Neurol. Psychiatr 38 304–307

Hortega, P Del Rio 1928 Tercera aportación al conocimiento morfológico interpretación functional de la oligodendroglia. Mem. real sociedad espan. de hist. nat. vol. 14 Madrid, Spain.

Kalle, E. 1933 Beobachtungen über den Tod bei Hinrichtung mit dem Strang. Dtsch. Z. gerichtl. Med., 22: 193–203.

# Morphogenetic Studies of the Rabbit

## XXXIV WEIGHTS AND LINEAR MEASUREMENTS OF THE BONES OF SMALL RACE X RABBITS COMPARED WITH LARGE RACE III

HOMER B. LATIMER AND PAUL B SAWIN
*Department of Anatomy University of Kansas Lawrence and Roscoe B Jackson Memorial Laboratory Bar Harbor Maine*

This is the second paper dealing with the skeletons of rabbits of genetically different body size. The first skeletal paper (Latimer and Sawin, '62) presented the weights and linear measurements of the skeleton and most of the individual bones of a race of large body size (approximately 4 kilos) of New Zealand White origin. This paper describes the skeletons of race X of small sized rabbits (approximately 2 kilos) and which transmits one specific dwarf gene as a single Mendelian recessive, lethal at, or shortly after birth when homozygous. Earlier studies have shown that heterozygotes are distinguishable from homozygous normals both by ear length (Crary and Sawin, 49) and by body weight and other dimensions (Latimer and Sawin, '55b '57 '59 and '60)

The present paper compares the rabbits of race X which are non-transmitters of the dwarf gene (thus completely normal) with large size race III. Race X is derived from Castle s small race and has been closely bred for many generations.

### MATERIALS AND METHODS

The race X rabbits were raised under the same conditions as the race III rabbits shipped to Kansas in the same manner sacrificed and studied by the same person (H.B.L.) using the same methods which have been described in detail in the preceding report (Latimer and Sawin '62)

The 65 normal homozygous rabbits of race X will be called simply race X rabbits throughout this report. The skeletons of the heterozygous dwarf rabbits will be described in a later communication. The cleaned and air dried skeletons were weighed on a laboratory balance sensitive to 0 1 gm and the individual bones on an analytical balance sensitive to 0 1 mg, but the weights of most of the bones were recorded only to the nearest milligram. Each of the paired bones was weighed separately and the weights in grams in the following tables are the sums of the weights of right and left bones of the pair The ribs were weighed all together

The linear measurements were likewise made on both bones of each pair and the averages of these are recorded in the following tables. The linear measurements of race X were all made with a sliding straight armed calipers graduated to 0 1 mm. The lengths of the long bones of the extremities are their maximum lengths (Stewart, '52) A few of the irregular bones seemed to require different methods than the standard methods used for human bones and these are described in detail in the earlier report (Latimer and Sawin, '62) This preceding report contains a diagram showing the location of all of the skull measurements.

### *Weights in grams*

Table 1 has the weights of the entire skeleton and 11 of the individual bones or pairs of bones from 35 male and 30 female rabbits of race X All of the weights are greater in the females as expected since the average body weight of the females is 2,480 gm and 1 972 gm for the males (Latimer and Sawin '55b) The clavicle is the only bone not significantly

This investigation was supported (in part) by PHS research grant [illegible] from the National Cancer Institute, Public Health Service, and aided by a grant from the American Cancer Society

heavier in the females. It is also the most variable bone in both sexes. Its marked variability in weight may be due to its vestigial condition in the rabbit. It is merely imbedded in the muscles of the shoulder region and does not articulate with any other part of the skeleton.

The least variable bone is the mandible followed by the radius plus ulna and the calcaneus but not in the same order in both sexes. All of the long bones of both extremities have comparatively low coefficients of variation

In general, the weights of the bones in the females are less variable than in the males for the average of the coefficients of variation in the females is 12.78% and in the males 14.83% The clavicles are not only the most variable but also the lightest in weight, while the femur is the heaviest bone and the ankylosed tibia and fibula is second in weight in both sexes.

### *Weights as percentages of total skeletal weight*

The weights in grams of each bone, or pair of bones, were changed to percentages of the skeletal weight and studied statistically as were the weights in grams but to save space these percentages are not shown The average of the coefficients of variation of these percentages in the males is 5 87% and in the females 5 12% or these averages are less than half the similar averages of the coefficients of variation of the weights in grams in table 1

The "t" values of the sex differences of the percentages are presented in the first column of table 2. While all of the weights in grams are greater in the females only five of the percentage weights are significantly greater Six of the percentages are greater in the males but only three (femur ankylosed tibia and fibula and calcaneus) are significantly greater

Briefly the entire skeleton and all of the individual bones are heavier in the females, but as percentages of skeletal weight the long bones of the extremities are relatively heavier in the males All of the weights and percentage weights are more variable in the males

### *Relative weights in small and large rabbits*

Since the body weight of the larger race III is 170% heavier in the males and 144% heavier in the females one would expect the individual bones to be heavier in race III. Hence the weights of the bones as percentages of the entire skeleton are compared in rabbits of the same sex from the two races. The percentage weights of the race III rabbits are taken from the preceding report (Latimer and Sawin, '62). The "t values of the differences in these percentages are shown in columns two and three of table 2. The race with the larger relative bone weights is indicated.

Five of these bones are relatively heavier in both sexes of each race. The mandible with the largest "t value is relatively heavier in both sexes of small race X. The

TABLE 1

*Weight i grams of the entire skeleton and some of the bones of 35 male and 30 female rabbits of race X. The "t" values of 2.00 and above are significant at 5% and 2.66 and above at 1%*

| | Males | | Females | | "t" |
|---|---|---|---|---|---|
| | A and stand. dev | Coef. of variation | A and stand. dev | Coef of variation | |
| Skeleton | 86.943 ± 11 102 | 12.77 | 101 435 ± 9.186 | 9.06 | ♀ 5.59 |
| Mandible | 6.096 ± 0.715 | 11 73 | 6.952 ± 0.543 | 7 78 | ♀ 5.43 |
| Sacrum | 1.634 ± 0.274 | 16.80 | 2.022 ± 0.262 | 12.96 | ♀ 5.71 |
| Ribs | 4.418 ± 0.680 | 15.40 | 5.610 ± 0.694 | 12.00 | ♀ 7 46 |
| Clavicle | 0.053 ± 0.011 | 21.62 | 0.059 ± 0.022 | 37 71 | ♀ 1.62 |
| Scapula | 2.701 ± 0 413 | 15.29 | 3.311 ± 0.374 | 11.31 | ♀ 6.10 |
| Humerus | 4.890 ± 0.673 | 13.76 | 5.681 ± 0.634 | 11 16 | ♀ 4 78 |
| Radius and ulna | 3.858 ± 0.525 | 13.60 | 4.468 ± 0.368 | 8.21 | ♀ 5.43 |
| Os coxae | 5.958 ± 0.962 | 16.46 | 7.200 ± 1 032 | 14.33 | ♀ 4.89 |
| Femur | 9 769 ± 1.361 | 13.93 | 10.968 ± 1 094 | 9.96 | ♀ 3.80 |
| Tibia and fibula | 8.828 ± 1.249 | 14.15 | 9.934 ± 0.959 | 9.65 | ♀ 3.89 |
| Calcaneus | 1.518 ± 0.189 | 12 46 | 1.663 ± 0.154 | 9.26 | ♀ 3.37 |

relatively heavier mandible in race X is expected since the head of this race is relatively heavier than in race III (Latimer and Sawin, '57). The scapula is the only other bone significantly heavier relatively

TABLE 2

*The "t" values of the differences in the percentages of total skeletal weight in male and female race X rabbits and between races X and III in rabbits of the same sex. The "t" values in columns one and three are; 2.00 and above are significant at 5% and 2.66 and above are significant at 1% and similar values for column two are 1.99 and 2.65, respectively*

| | Sex diff. race X | Racial difference Males | Racial difference Females |
|---|---|---|---|
| Mandible | ♂ 1.55 | X 11.96 | X 10.96 |
| Sacrum | ♀ 3.43 | X 1.76 | X 0.39 |
| Ribs | ♀ 10.59 | — | — |
| Clavicle | ♀ 2.43 | III 4.64 | III 0.64 |
| Scapula | ♀ 4.73 | X 2.13 | X 2.94 |
| Humerus | ♂ 0.57 | III 5.10 | III 6.31 |
| Radius and ulna | ♂ 0.04 | X 0.57 | X 2.78 |
| Os coxae | ♀ 2.06 | III 7.96 | III 6.85 |
| Femur | ♂ 3.76 | III 8.46 | III 10.52 |
| Tibia and fibula | ♂ 3.37 | III 3.78 | III 6.38 |
| Calcaneus | ♂ 4.90 | X 2.67 | X 0.48 |

in both sexes of race X. The two bones of the forearm and the calcaneus are significantly heavier in one sex of race X and heavier though not significantly so in the opposite sex. Likewise the clavicle is significantly heavier in race III males and only slightly heavier in race III females. The humerus, os coxae and the three bones of the hind limb are all significantly heavier in both sexes of large race III.

Thus it is evident that although the larger race has heavier bones, homologous bones in the two races do not always have the same weight relative to the total skeletal weight.

### *Linear measurements*

Linear measurements of these bones are shown in table 3, arranged as in table 1. All of these linear measurements, like the weights in grams, are longer in the females and all except six are significantly longer. The greatest sex difference is in the length of the pubic bone, followed in order by the width of the sacrum and the length of the ilium.

TABLE 3

*Linear measurements in millimeters of race X rabbits. The "t" values are the same as table 1*

| | Males A and stand. dev | Males Coef. of variation | Females A and stand. dev | Females Coef. of variation | "t" |
|---|---|---|---|---|---|
| Atlas, length | 9.91 ± 0.48 | 4.88 | 10.28 ± 0.37 | 3.57 | ♀ 2.37 |
| Atlas, width | 28.50 ± 1.20 | 4.22 | 29.70 ± 1.32 | 4.45 | ♀ 3.77 |
| Axis, length | 16.56 ± 0.82 | 4.94 | 17.36 ± 0.94 | 5.43 | ♀ 3.51 |
| Axis, width | 14.39 ± 1.62 | 11.25 | 14.64 ± 0.83 | 5.65 | ♀ 0.73 |
| Sacrum, length | 38.36 ± 1.92 | 5.01 | 40.16 ± 1.56 | 3.89 | ♀ 4.02 |
| Sacrum, width | 26.10 ± 1.91 | 7.31 | 29.71 ± 1.53 | 5.16 | ♀ 8.04 |
| Manubrium, length | 17.98 ± 2.56 | 14.22 | 19.32 ± 1.37 | 7.10 | ♀ 2.53 |
| Clavicle, length | 18.98 ± 1.61 | 8.53 | 20.90 ± 1.34 | 6.44 | ♀ 5.67 |
| Scapula, length | 55.96 ± 2.54 | 4.54 | 58.90 ± 2.02 | 3.43 | ♀ 5.20 |
| Scapula, width | 32.32 ± 2.26 | 6.98 | 35.52 ± 1.91 | 5.37 | ♀ 6.02 |
| Humerus, length | 67.34 ± 2.66 | 3.94 | 69.15 ± 1.16 | 1.67 | ♀ 3.41 |
| Humerus, width | 13.70 ± 0.65 | 4.73 | 14.10 ± 0.38 | 2.66 | ♀ 2.37 |
| Radius, length | 62.86 ± 2.53 | 4.02 | 64.30 ± 1.12 | 1.74 | ♀ 3.02 |
| Radius, width | 6.88 ± 0.36 | 5.28 | 6.97 ± 0.28 | 4.07 | ♀ 1.06 |
| Ulna, length | 74.96 ± 2.97 | 3.96 | 76.52 ± 1.10 | 1.44 | ♀ 2.68 |
| Ulna, width | 6.76 ± 0.42 | 6.17 | 6.89 ± 0.22 | 3.29 | ♀ 1.50 |
| Os coxae, length | 76.79 ± 4.07 | 5.30 | 81.37 ± 3.10 | 3.81 | ♀ 4.85 |
| Ilium, length | 42.68 ± 2.55 | 5.97 | 46.30 ± 2.12 | 4.56 | ♀ 6.22 |
| Ischium, length | 35.71 ± 1.73 | 4.84 | 36.53 ± 1.22 | 3.33 | ♀ 2.14 |
| Pubis, length | 15.47 ± 1.27 | 8.24 | 19.42 ± 1.57 | 8.11 | ♀ 11.00 |
| Femur, length | 89.70 ± 3.49 | 3.89 | 91.38 ± 2.10 | 2.39 | ♀ 2.34 |
| Femur, width | 16.86 ± 0.75 | 4.47 | 17.67 ± 0.57 | 3.23 | ♀ 4.74 |
| Tibia, length | 96.31 ± 3.54 | 3.62 | 99.64 ± 1.73 | 1.74 | ♀ 1.84 |
| Tibia, width | 15.61 ± 0.83 | 5.30 | 15.98 ± 0.51 | 3.17 | ♀ 2.10 |
| Fibula, length | 37.83 ± 2.08 | 5.49 | 38.58 ± 1.30 | 3.59 | ♀ 1.66 |
| Calcaneus, length | 25.18 ± 1.08 | 4.29 | 25.59 ± 0.63 | 2.48 | ♀ 1.80 |

TABLE 5

*Measurements of the skull in millimeters in male and female rabbits of race X. The "t" values are the same as in table 1*

| | Males | | Females | | "t" |
|---|---|---|---|---|---|
| | A. and stand. dev. | Coef. of variation | A. and stand. dev. | Coef. of variation | |
| Basion-prealv. pt. | 68.48 ± 3.16 | 4.62 | 71.99 ± 1.62 | 2.24 | ♀5.42 |
| Basion-post. n. spine | 34.34 ± 1.49 | 4.34 | 35.94 ± 1.1 | 3.24 | ♀4.71 |
| Post. n. sp.-prealv. pt. | 35.63 ± 2.06 | 5. 4 | 38.04 ± 1.07 | 2.82 | ♀5.21 |
| Palatine bridge | 10.16 ± 0.88 | 8.72 | 11.13 ± 2.20 | 19.75 | ♀2.36 |
| Diastema | 25.51 ± 1.3 | 5.3 | 26.56 ± 0.98 | 3.63 | ♀4.44 |
| Bizygomatic | 40.98 ± 1.36 | 3.31 | 41.24 ± 1.66 | 4.03 | ♀0.68 |
| Bitemporal, a. meatus | 32.45 ± 1.91 | 5.89 | 33.35 ± 1.12 | 3.35 | ♀2.47 |
| Bitemporal, bullae | 29.11 ± 0.73 | 2.52 | 29.51 ± 0.84 | 2.84 | ♀2.33 |
| Bicondylar | 15.63 ± 1.01 | 6.45 | 16.35 ± 0.56 | 3.29 | ♀3.05 |
| W. alveolar process | 25.04 ± 1.83 | 7.31 | 26.10 ± 0.68 | 2.61 | ♀2.95 |
| Basioccipital, length | 11.84 ± 0.57 | 4.82 | 12.38 ± 0.36 | 2.8 | ♀4.42 |
| Basioccipital, width | 9.94 ± 0.21 | 2.12 | 10.22 ± 0.44 | 4.36 | ♀3.26 |
| Basisphenoid, length | 10.93 ± 0.52 | 4.74 | 11.4 ± 0.48 | 4.23 | ♀4.24 |
| Basisphenoid, width | 7.68 ± 0.40 | 5.27 | 7.99 ± 0.36 | 4.56 | ♀3.38 |
| Nasal bones, length | 33.24 ± 3.98 | 11.97 | 35.69 ± 3.60 | 10.09 | ♀2.54 |
| Mandible length | 64.53 ± 2.60 | 4.03 | 68.04 ± 1.20 | 1.76 | ♀6.69 |
| Mandible ramus | 38.84 ± 1.91 | 4.97 | 40.34 ± 1.10 | 2.74 | ♀3.73 |

coefficients of variation in the males. These measurements are the maximum lengths and not the internasal sutures, which are shorter. The internasal sutures were measured by Sawin and Crary ('37).

Briefly, the skulls of this smaller race are larger in the females and more alike in general shape in the two sexes than are the skulls of the larger race III.

### *Measurements of the skull as percentages of body length*

The linear measurements of the skull were likewise changed to percentages of body length and studied in the same manner as the measurements in millimeters. These percentages are not given but the "t" values of the sex differences in these percentages are shown in the first column of table 6. While all of the dimensions of the skull are actually longer in the females as shown in table 5, only two are slightly longer as percentages of body length in the females, and 15 are relatively longer in the males. The three dimensions with the largest sex differences in these percentages are bizygomatic diameter and the two diameters of the temporal bone and they are all larger in the males. These three dimensions are the outstanding transverse measurements of the skull and their greater length in the males suggests a relatively wider male skull. The average

TABLE 6

*The "t" values of the differences in the measurements as percentages of body length in males and females of race X, and between rabbits of the same sex in races X and III. The "t" values are the same as in table 2.*

| | Sex diff. race X | Racial differences | |
|---|---|---|---|
| | | Males | Females |
| Basion-prealv. point | ♂2.61 | X 8.97 | X 4.30 |
| Basion-post. n. spine | ♂2.97 | X 4.19 | X 5.42 |
| Post. n. sp.-prealv. pt. | ♂0.88 | III 0.93 | III 1.57 |
| Palatine bridge | ♀0.58 | III 6.18 | III 3.07 |
| Diastema | ♂1.42 | X 7.03 | X 4.29 |
| Bizygomatic | ♂6.98 | X 11.54 | X 6.43 |
| Bitemporal, a. meatus | ♂3.73 | X 2.57 | X 2.73 |
| Bitemporal, bullae | ♂6.30 | X 8.48 | X 4.59 |
| Bicondylar | ♂1.59 | X 4.34 | X 4.71 |
| W. alveolar process | ♂1.72 | X 2.80 | X 3.00 |
| Basioccipital, length | ♂2.62 | X 8.98 | X 8.31 |
| Basioccipital, width | ♂3.25 | III 5.63 | III 4.85 |
| Basisphenoid, length | ♂2.83 | X 5.24 | X 3.18 |
| Basisphenoid, width | ♂1.73 | X 0.51 | III 0.44 |
| Nasal bones, length | ♀0.11 | III 0.60 | X 1.71 |
| Mandible length | ♂3.06 | X 11.77 | X 8.47 |
| Mandible ramus | ♂3.36 | X 1.17 | X 1.23 |

of the coefficients of variation of these percentage lengths in the males is 4.99% and in the females, 5.66%.

### *Comparison of skull measurements in large and small races*

Columns two and three of table 6 contain the "t" values of the differences between the percentage measurements of the skull in races X and III rabbits of the same sex. The greater length of these dimensions relative to body length in race X is very evident. These relatively longer dimensions of the skull in the smaller race are in agreement with the data reported in an earlier paper (Latimer and Sawin '57) that the head comprises a larger percentage of body weight in race X than in race III.

There are only four measurements in each sex greater in relative length in race III and only two of these are significantly longer. These are the length of the palatine bridge and the width of the basioccipital bone. There are four dimensions in the males and five in the females which are not significantly different in the two races. The three dimensions which show the greatest difference in relative length in both sexes in table 6 but not in the same order are: length of the mandible, length of basioccipital bone and the bizygomatic diameter and all of these are larger in the race X rabbits. The length of the mandible has the largest "t" value in both sexes of race X.

In measuring the skull width at the zygomatic arch in race III, it was noticed that there was a variation in the location of the maximum diameter and so the location of this maximum measurement was recorded on the individual data cards. The maximum diameter in race III rabbits was at the posterior end of the arch in 58% of the males and in 52% of the females. In the others the maximum diameter was near the anterior end or midway of the arch. But in all of the race X rabbits, of both sexes, it was near the posterior end of the zygomatic arch. Thus the location of the maximum width of the skull varies more in race III than in race X rabbits.

An earlier study (Latimer and Sawin, '59) shows that the width of the head or the maximum diameter measured over the zygomatic arch is relatively greater in race X than in race III. These present transverse measurements of the skull confirm the earlier measurements.

There are only two measurements significantly greater in both sexes of race III in table 6. One of these is the length of the palatine bridge which is exceedingly variable (table 5). The second is the width of the basioccipital bone. This measurement suggests a wider posterior part of the skull in race III. A wider basioccipital bone could easily be missed in making the measurements of the external surface of the head.

## DISCUSSION

Measurements of the bones of New Zealand White rabbits have been reported by Sawin and Crary ('57) and Lowrance ('53 and '55) but all of these measurements are much greater than in race X rabbits. These measurements have been compared with race III dimensions in the earlier report (Latimer and Sawin, '62).

Hammar ('32) reports no significant sex differences in the weights of the skeletons and the individual bones in the adult small Swedish rabbit. To better compare race X with his rabbits, the skeletons and the bones in race X have been averaged for the two sexes. The body weight of the Swedish rabbits is 2,514 gm compared to 2,226 gm for race X rabbits. The skeletal weight of the Swedish rabbits averages 91.07 gm. Thus the body weight of the Swedish rabbits is 113% of the average body weight of race X, while the skeletons are only 97% of the weight of race X skeletons. Most of the percentage weights of the individual bones are slightly less in Hammar's rabbits. Only the sacrum, tibia plus fibula and os coxae are relatively heavier in the Swedish rabbits. The relative weights of most of the bones in the Swedish rabbits, vary less than 5% from the similar bones in race X.

Hammar also gives coefficients of variation for the skeleton and the several bones. His adult skeletons have coefficients of variation of 10.1% and race X males 12.77% and race X females 9.06%. All of his coefficients for the individual bones are lower than the corresponding coeffi-

# The Shrew Placenta Evidence that it is Endothelio-endothelial in Type[1]

H. W MOSSMAN AND NOEL OWERS[2]
*Department of Anatomy School of Medicine University of Wisconsin, Madison, Wisconsin*

In '39 when the senior author first examined shrew placentas he was sur prised to find that they were apparently endothelio-endothelial in nature, but he did not publish because certain crucial stages were lacking. In '57 the junior author brought to this laboratory a series of slides of the placenta of the Indian musk shrew *Suncus murinus* Also much more material on the American genera was by this time available to us. Com parison soon convinced us of the close similarity and homology between the placental morphology of the American genera and of *Suncus* It was also obvious that we now had collectively the necessary stages to establish so far as light microscopy is capable of doing the loss of the trophoblast from the chorio-allantoic pla centa, and to indicate therefore the probable endothelio-endothelial nature of the placenta of several Soricidae After preliminary publication of some of these observations (Owers, '58 Mossman, '58 and Mossman and Owers, '60) Owers ('60) presented his evidence for the endothelio-endothelial nature of the placenta of *Suncus*.

This idea of the loss of trophoblast from the placental membrane is, of course contrary to the long established concept of the trophoblast as the primary functional "barrier between maternal and fetal tissue. Specifically with regard to shrews, it is contrary to previous descriptions of shrew placentation. Hubrecht (1894) reported the placenta of *Sorex vulgaris* (now *S araneus*) to be hemo-chorial, and Sansom ('37) described *Crocidura caerulea* (now *Suncus murinus*) as hemo-chorial. Wimsatt and Wislocki (47) interpreted the placentas of *Sorex fumeus* and *Blarina brevicauda* to be endothelio-chorial. Starck ('59a) lists (on his own authority) *Crocidura russula* and *Suncus murinus* as hemo-chorial, but in another publication (Starck '59b) (apparently following Wimsatt and Wislocki's lead) states that the placenta of *Sorex araneus* and of *Crocidura* is endothelio-chorial. He presents no evidence to support either of his conflicting views.

The key to this confusion, is obviously a problem of correct identification of trophoblast during development of the labyrinth. Hubrecht (1894) understandably mistook the unusually enlarged and apparently syncytial maternal endothelium for trophoblast. Wimsatt and Wislocki (47) with good reasons interpreted what we believe to be remnants of maternal epithelium as trophoblast.

The nature and early distribution of the trophoblast in shrews are similar to that of those rodents having incomplete inver sion of the yolk sac (Mossman, '37 and '39) In both implantation is antimesometrial, but in shrews the embryonic disc, and later the placental disc, are also antimesometrial instead of mesometrial as in rodents. There is a persistent bilaminar omphalopleure and a well developed chor io-vitelline placenta. A ring of bilaminar omphalopleure next to the chorio-vitelline placenta possesses a highly specialized trophoblast apparently active in ingestion of maternal erythrocytes which have been extravasated into the uterine lumen. This is a specialization not found in rodents, but an analogous struc ture, the hematome, occurs in carnivores.

The trophoblast persists everywhere in the shrew conceptus through the period

[1] Supported by funds from the Wisconsin Alumni Research Foundation, and from NIH Grant [illegible].
[2] [illegible] Fellow supported by USPHS Training Grant [illegible].

sels (figs 25 26 and 27) In this area the nuclei are also generally pycnotic and the cytoplasm basophilic, often less so however than the maternal endothelial cytoplasm. The basophilia in both areas is chiefly produced by numerous relatively large and characteristic cytoplasmic granules which are not seen in the maternal endothelium. It is this symplasma of *Blarina* which Wimsatt and Wislocki believed to be trophoblast, but which we interpret as modified maternal epithelium, partly because we feel that as in the area shown in figure 25 every transition can be traced back to frank gland epithelium

Additional attention should be paid to the symplasmic degeneration of gland epithelium. The blunt tips of the villi (figs. 13 14 15 17 19 and 20) are in contact with masses of symplasmic degenerating glandular epithelium just as occurs in similar situations in some rodent placentas (Mossman and Weisfeldt, '39) We can see no consistent evidence in *Sorex* of a cap of trophoblast associated with these areas. Rather there is every transition between the symplasmic masses and the more distal column of gland epithelium, while proximally (centrally) as pointed out above, the symplasma frequently is continuous with the interrupted layer of cells lining the crypts (figs 15 and 19); that is with the degenerate gland epithelium (Wimsatt and Wislocki's syntrophoblast ) The similarity between the shrews and the squirrels in the invasion of glands by chorio-allantoic villi and the accompanying symplasmic degeneration of the gland epithelium is striking yet in squirrels syntrophoblast is present and is easily *distinguished from the epithelial symplasma*. The comparative aspects of this phenomenon in the two groups undoubtedly prejudice us in favor of our interpretation. Also there are examples among the genus *Sorex* as well as in *Blarina* for instance the placentas of *S vagrans* and *palustris* at the time of transition from the villous to labyrinthine condition (figs. 15 16 19 and 20) which show a variety of cell sizes and types in the gland tissue at the tips of the villi, some of which cells because of their large size, do resemble trophoblastic giant cells seen in other species; yet they more closely resemble the greatly enlarged gland epithelium cells that are characteristic of similar areas in moles (Prasad, '58)

The epithelial masses on the fetal surface of the placenta in *Blarina* and *Sorex* (figs. 13 17 18 19 and 20) we believe are certainly homologous to the epithelial lobe of *Suncus* (Owers '60) In *Sorex* and *Blarina* these masses are continuous with the epithelial elements lining the crypts discussed above just as the epithelial lobe is continuous with similar elements in *Suncus* Furthermore maternal reticulum of the intercryptal septa extends into the masses. For these reasons as well as from observations on their stage by stage development, we believe these epithelial masses originate from uterine epithelium and are in fact rejuvenated epithelium as Owers maintained in *Suncus* Yet from the position and active growth of these epithelial masses in *Sorex* *Blarina*, and *Suncus* it would be expected that they would be derivatives of the proximal trophoblast, such as that in figure 12, as Wimsatt and Wislocki believed. Complete proof for either interpretation is lacking but we think the evidence favors our view

We agree with Wimsatt and Wislocki on the persistence of the maternal capillary endothelium and for the most part on the modifications it undergoes at the fetal surface and margins of the placental disc (fig 24) We also confirm their observations on the relative scarcity of endometrial stroma.

Regardless of all that has been discussed so far the most important question is whether or not a layer of trophoblastic *cytoplasm separates the maternal endo*thelium from the fetal endothelium in the definitive placental labyrinth. Wimsatt and Wislocki thought that a very attenuated trophoblastic layer persisted and therefore considered the shrew placenta endothelio-chorial in type. Our observations do not agree with this.

In the definitive labyrinth of *Sorex*, light microscopy shows maternal capillaries in direct contact with fetal capillaries With ordinary histological stains the two endothelial layers can be clearly seen (fig 28) With PAS and reticulum stains a slight cleft often appears between the two endo-

thelia. This cleft is bordered on each side by PAS positive material and reticulum which form basement membranes for each endothelium. There is no intervening cytoplasmic layer that can be detected by light microscopy Often the reticular zones of each basement membrane are fused as in figure 30 which is strong evidence that no intervening cytoplasmic layer exists.

If at all places trophoblast cells form an intervening layer between the maternal and fetal capillaries the cytoplasm must be so thin as to be beyond the resolution of the light microscope. We have been unable to see any such cytoplasmic layer neither have we consistently seen any nearby nuclei which would lead us to suspect the presence of such a cytoplasmic layer Electron microscopy can no doubt settle this question.

## DISCUSSION

Completely convincing proof of the presence or absence of trophoblast in the definitive placenta of shrews is lacking. A sex chromatin, or possibly a labeling technique might furnish such proof but this would require collection of very well preserved or experimental material which is impractical for us to undertake at this time. However we believe there is more evidence for the absence of trophoblast than for its presence It we accept this hypothesis, then it is interesting to speculate on the reasons for and consequences of, this deletion

Wekes ('35) "Type I" reptile placenta is so far as light microscopy could determine, partly endothelio-endothelial although it should be pointed out that in the reptiles distinct amounts of trophoblast and uterine epithelium persist beside the adjacent maternal and fetal capillaries and often also as part of the membrane between them. Actually then, this type of reptile placenta is partly epithelio-chorial, partly endothelio-chorial and probably partly endothelio-endothelial. Whatever functions the trophoblast may perform can still be carried out in such a situation In mammals no such condition is known in a chorio-allantoic placenta except possibly in the very early shrew placenta in which the trophoblast may be in the process of disappearing from the villi.

The definitive chorio-allantoic placenta of shrews if it does lack trophoblast must have transferred whatever functions the trophoblast performs to other layers or to other areas such as the chorio-vitelline, chorionic or the inverted yolk sac placenta. The remarkably thickened and basophilic maternal capillary endothelium suggests that this may be a partial functional substitute for trophoblast, although thickened maternal endothelium is also found in many endothelio-chorial placentas.

The fact that the mesoderm of allantoic villi is known to be epitheloid only in shrews indicates that this is possibly an adaptation to the absence of a trophoblastic covering of the villi. Were the mesenchyme to remain in its usual "loose state, one could expect no more secure covering of a villus than a mesothelium. However by being epithelioid, the cells may be more broadly locked together not only on the surface but throughout the villus. This may be a way of sealing off" the interstitial liquids of the villus from the maternal tissue and may also improve the internal liquid dynamics of the villus itself An electron microscope comparison of the mesenchyme of ordinary allantoic villi with that of shrew villi would be worthwhile.

For convenience of the reader the following synopsis of basic data on the morphology of the fetal membranes of Soricidae is appended

Implanation

Orientation (disc) antimesometrial

Orientation (first attachment) bilateral

Depth superficial

Decidua vestigial capsularis no typical decidual cells

Amniogenesis folding

Chorion antimesometrial hemisphere only

Yolk-sac

Bilaminar omphalopleure persists till full term

Chorio-vitelline placenta broad vascular zone up to limb bud period

Vascular splanchnopleure large and inverted as in rodents villous zone facing chorio-allantoic placenta

# PLATE 1

## EXPLAN TION OF FIGURES

1 Amniotic f lds, allantoic bud nd rly ttachment of the trophoblast ( t right) to the endometrium. Notice the dilated subepithelial capillaries, the hypertrophy of the gland epithel m, and the near closure f the gland mouths. The trophoblast ha an intermittently double l yer of nuclei. At the right, where the trophoblast has been slightly separated from the endometrium, note the degenerating epithelial cells linging to it. *S. mf tus* S 932 c (Brambell) × bout 120.

2 Are of contact of horion nd endometrium of stage of *S. raneus* slightly later than that of figure 3. Intact uterine epithelium t the right. There is gre t difficulty in regions such as that shown in the left half of this figure, in distinguishi g between uterine epithelium possible yntrophoblast, and even c pillary endothelium. Notice th t the gland epithelium has hypertrophied to the point of becoming lmost a continuous epithelial mass. *S. raneus* 51 f (H brecht) × 240.

3 The time of initial contact of the ascular llantois with the horion. Notice the modified uterine epithelium with its subjacent dil ted capillaries whose endothelium is beginning to hypertrophy The thin dark layer ttached to the trophoblast t the region of allantoic contact resembles degenerating epithelium, but its location so lose t obviously nearly normal epithelium suggest that it may be syntrophoblast. At the right this darkly stained layer (ep?) appears to continue between the cytotrophoblast and the subepithelial capillaries. It also seems to be invading gland and seems fairly well demarcated from the epithelium of the gland mouth. *S. mf tu* S 959 a (Brambell) × bout 120.

4 The same specimen shown in figure 2, but t the region of allantoic contact and hence showing a more dvanced stage of ttachment of the horion t the endometrium; also it is more advanced than the specimen of *S. mf tus* shown in figure 3. Here trophoblastic invasion of gl nd mouths is learly pparent, but the trophoblast appe rs to be entirely cellular (cy) W belie the dark cell on which the villou tips abut are epithelial symplasma (sy) rather than syntrophoblast; although w must dmit that the latter interpretation is also not reasonable However one cannot see this layer between the capillary endothelium and the cytotrophoblast where it would certainly be expected if it were syntrophoblast. Also these dark cells intergrade through the symplasmic areas to the deeper more normal appearing gland epithelium. *S. araneus* 51 f (H brecht) × 200.

SHREW PLACENTATION
H. W. Mossman and Noel Owers












## PLATE 2

### EXPLANATION OF FIGURES

5 Another specimen from the same uterus as figure 3 showing the very confusing presence of two adjacent dark cellular layers. Centrally in the figure these would normally be interpreted as syntrophoblast and epithelium. However, at the right and left one sees a single layer which appears to be directly continuous with the gland epithelium and has capillary endothelium directly subjacent to it, just as the surface and gland epithelium does elsewhere. We are inclined to believe that both of these dark layers are of epithelial origin. This agrees best with the interpretation we have made of figures 4 and 6. S. minutus × 950 (Brambell) × about 120.

6 Trophoblast (cy) invading gland mouths near the sinus terminalis (st) showing darker degenerating epithelial cells (ep) near the gland mouths, and the transition to deeper hypertrophied gland cells (h). There is little or no symplasma at this area, and the trophoblast appears entirely cellular. S. araneus 125 b (Hubrecht) × 200.

7 S. cinereus showing the chorion of the future chorio-allantoic region penetrating into the antimesometrial endometrial pit characteristic of this species. Note also the open condition of glands at this time in contrast to those of S. minutus and araneus (figs. 1–6). The allantoic bud has not yet made contact with the chorion. The source of the round cells in the chorionic cavity is problematical, but they are probably caused by accidental rupture of vitelline or allantoic capillaries. S. cinereus 1 × 106.

8 Enlargement of the area in the rectangle in figure 7 to show the subepithelial capillaries (c) and the irregular arrangement of the nuclei in the trophoblast (cy). S. cinereus 1 × 273.

9 S. vagrans at the time of allantoic contact with the chorion, showing the shallow antimesometrial pit, homologous to the much deeper one of S. cinereus illustrated in figure 7. Excessive shrinkage during the technical procedures separated the allantoic mesoderm and the chorionic mesoderm (cm) adhering to it, from the trophoblast (cy) which remained attached to the endometrium. S. vagrans 1 × 106.

10 Enlargement of area of figure 9 in rectangle to show the trophoblast (cy), chorionic mesoderm (cm), presumed remnants of uterine epithelium (ep) and hypertrophying endothelium of subepithelial capillaries (en). S. vagrans 1 × 340.






cy
c


st
cy


cy
cm


cm
ep
en
cy

PLATE 2

EXPLANATION O FIGURES

5 Another specimen from the same terus as figure 3 showing the very confusing presence of two adjacent dark cellular layers. Centrally in the figure these would normally be interpreted as syntrophobl st and epithelium. However t the right and left one sees single layer which ppears to be directly continuous with the gland epithelium and has capillary endothelium directly subjacent to it, just as the surface and gland epithelium does lsewhere. W are inclined to believe that both of these dark layers are of epithelial origin. This agrees best with the interpretation we have made of figures 4 and 6. *S min tus* × 950 (Brambell) × about 120.

6 Trophoblast (cy) invading gland mouths near the sin terminalis (st) showing darker degenerating epithelial cells (ep) near the gland mouths, and the transition to deeper hypertrophied gland cells (h) There is little or no symplasma at this area, and the trophoblast appears entirely cellular *S araneus* 125 b (H brecht) × 200.

7 *S cinereus* showing the chorion of the future horio-allantoic region penetrating into the antimesometrial endometrial pit characteristic f this species. Not also the open condition of gland at this time in contrast to those of *S* *araneus* (figs. 1–6) The allantoic bud has not yet made contact with the chorion. The source of the round cells in the horionic avity is problematical but they are probably caused by accidental rupture of vitelline or allantoic capillaries. *S cinereus* 1. × 108.

8 Enlargement of the area in the rectangle in figure 7 to show the subepithelial capillaries ( ) and the irregular arrangement of the nuclei in the trophoblast (cy) *S. cinereus* 1 × 273.

9 *S vagrans* at the time of allantoic contact with the horion, showing the shallow antimesometrial pit, homologou to the much deeper one of *S cinereus* illustrated in figure 7 Excessive shrinkage during the technical procedures separated the allantoic mesoderm and the horionic mesoderm (cm) adhering t it, from the trophoblast (cy) which remained attached to the endometrium. *S vagrans* 1 × 108.

10 Enlargement of area of figure 9 in rectangle to show the trophoblast (cy) chorionic mesoderm (cm) presumed remnants of terine epithelium (ep) and hypertrophying endothelium of subepithelial capillaries (en) *S. vagrans* 1. × 340.






cy
c


st
cy


cy
cm


cm
en
ep
cy

## PLATE 3

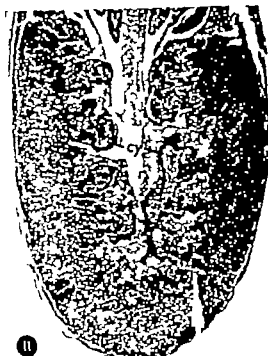
### EXPLANATION OF FIGURES

11 Early chorio-allantoic placenta of *S. cinereus* showing deep pit or core from which allantoic vessels branch out into the broad irregular early villi occupying the dilated central ends or crypts of the glands. Notice the cytotrophoblast (cy) clothing the inner ends of the septa and the gland mouths. *S. cinereus* 2. × 40.

12 Early villus from the placenta shown in figure 11 showing the cytotrophoblast (cy) presumed remnants of surface and gland epithelium (rep) subjacent to it, and especially the apparent absence of trophoblast of any sort from the distal third of the villus. The deeper gland epithelium forms an almost continuous epithelial mass (ep) Little symplasma (sy) has formed at this stage. *S. cinereus* 2. × 150.

13 Early allantoic mesodermal villi (v) occupying gland crypts separated by very narrow vascular septa (s) Hypertrophied capillary endothelium (en) epithelial proliferations (epp) *S. vagrans* 6. × 65.

14 Villus tips and outer endometrium of somewhat older placenta than that of figure 13, showing naked mesodermal villi with their capillaries (f ) and epithelioid mesenchyme (em) Notice the thin septa composed chiefly of maternal endothelium; the small masses of symplasma (sy); and the enlarged basal gland epithelial cells. Study of sections, such as this, shows every transition from symplasma to basal gland epithelium, and, centralward, every transition to scattered degenerate septal epithelial cells (sep) *S. vagrans* 8. × 220.


cy
11


pp


rep
cy
sy
lep


em
sep
fc
sy

PLATE 5

EXPLAN TION O FIGURES

19 Portion of placenta of *S palustris* t time of transition from villous *to labyrinthine phase showing continuity of epithelial proliferation* (epp) at fetal surface with degenerating epithelium (ep) partially lining the crypts and continuou at their bases with the epithelial symplasma (sy) Epithelioid mesoderm of villus (em); maternal capillaries ( ) of intercryptal septa; thick central end of septum (cs) *S palustris* 1 × 160.

20 Placenta from same uterus as figure 19 showing all zones. At the top is the allantoic mesoderm with the epithelial proliferations projecting into it and capping the thick central ends of the interglandular septa which are composed chiefly of maternal capillary endothelium and epithelial remnants. The septa are thin throughout the main body of the placenta consisting of little except the m ternal capillaries with their thick endothelium. At the tips of the villi are masses of symplasma with pycnotic nuclei, and extending to the thin myometrium is thick zone of hypertrophied gland epithelium. *S palustris* 1 × 135.



## PLATE 6

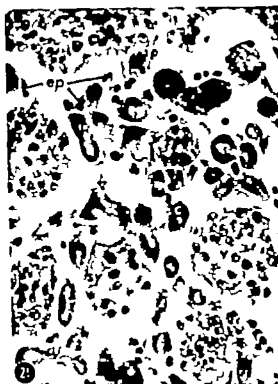
### EXPLANATION OF FIGURES

21 Horizontal section about halfway between the fetal and maternal surfaces of the placenta of *S vagrans* at the period of transition from the villous to the labyrinthine condition; th t is, intermediate in development between the conditions shown in figures 17 and 15. Notice the villi ( ) with their epithelioid mesenchyme; the maternal capillaries (c) with their thick endothelium; the scattered pycnotic nuclei of the degenerating epithelium (ep); and the epithelial symplasma (sy) filling crypt not yet occupied by villus. It is ppar ent that the degeneration of the epithelium results in the breakdown of the intercryptal septa and the change over to the labyrinthine condition. *S vagrans* 20. × 360.

22 Oblique section about halfway between the maternal and fetal surfaces of placenta of *S vagrans* slightly later than shown in figure 21 Almost all of the epithelial symplasma and most of the scattered epithelial nuclei (ep) have disappeared from this area. Fine branches of the villi are numerous, and the maternal capillary net is increasing in amount and complexity *S agrans* 14. × 370.

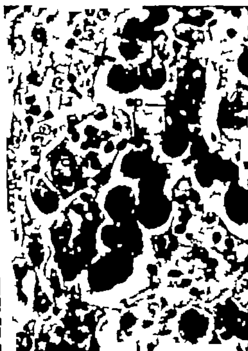
23 Cross section of villi and crypts at about the same stage as figure 21 taken near the fetal surface where the intercryptal septa are thickest. Shrinkage during processing no doubt accounts for most of the space between the villi and the crypt walls. Degenerating crypt epithelium (ep) and maternal apillaries ( ) with their hypertrophied endothelium, together with epithelial symplasma and few stromal cells comprise the septal tissue. *S vagrans* Approx. × 300.

24 Villi (v) and maternal capillaries ( ) near lateral margins f placental disc shown in figures 15 and 16. Note remnants of crypt epithelium (ep) and absence of anything resembling trophoblast on either the surfaces of the villi or that of the maternal capillaries *S agrans* 2. × 375.


ep
21


ep
23


22


24

## PLATE 8

### EXPLANATION OF FIGU ES

26 M ternal rterial channel ( ) entering labyrinth from myometri m. Notice the basal symplasma (sy) (pycnotic nuclei nd basophilic cytoplasmic granules) urrounding the thick arterial endothelium (en) and sending delicate cytoplasmic lamellae (l) between the tips of some f the adjacent terminal allantoic villi. *Blarina brevicauda* 1 × 320.

27 A similar rea t that hown in figure 26 also showing ext sive ramifications f ymplasmic cytoplasm with occasional pyc-notic uclei. Whit dots indicat the pproximate junction f the cytoplasm of the symplasma with that f the endothe-lium. M ternal rterial channel (a); maternal endotheli m (en); epithelial ymplasma ( y) *Blarina brevica da* 1 × 330.


en
a

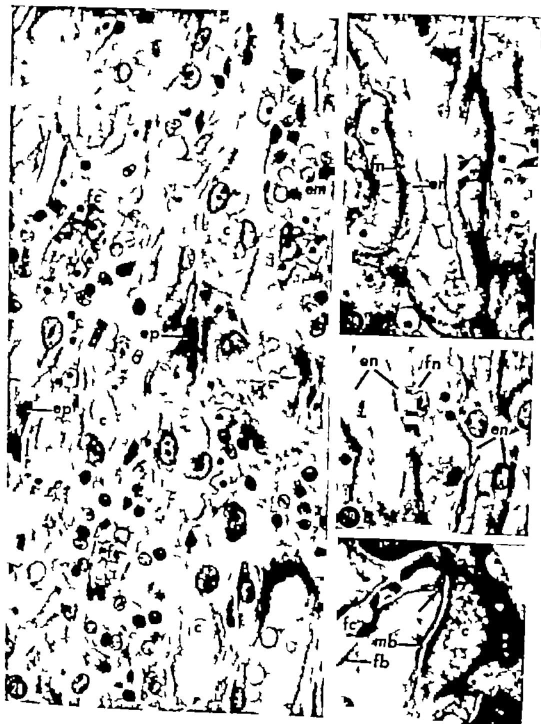
## PLATE 9

### EXPLAN TION OF FIGURES

28 Area of early labyrinth stained with hematoxylin and eosin. Maternal capillaries with their endothelium ( ); fetal capillaries (f ); epithelioid mesenchyme (em) remnants of crypt epithelium (ep) with basophilic cytoplasmic granules. S egrams 2. × 465.

29 A and B Early placental labyrinth stained with hematoxylin, eosin, and orange G. Basophilic material of unknown nature at the outer margins of the endothelial cytoplasm clearly outlines the maternal and f tal capillaries and demonstrates their contiguity. Maternal endothelium (en) fetal endothelium (fn) S egram 5 (A) and 2 (B) × 780.

30 Silver reticulum stain of early l byrinth showing reticulum layer of fetal capillary (f ) its basement membrane (fb) fused (arrow) with the basement membrane (mb) of the maternal capillary (c) This seems to negate the possibility of the existence of layer of trophoblastic cytoplasm between the two endothelia in such regions. S grams 9. × 280.


fc
em
fb
c
ep
ep
c
fc
c
21
fn
en
en
fn
en
fc
mb
fb
c

and the cartilage plate toward the distal edge of the ear The donor tissue was then eased into the base of the pocket near the distal edge of the ear Gentle pressure with the side of the forceps was applied to the ear in an effort to remove any trapped air The auricular artery at the base of the ear was deliberately cut in an attempt to provide a clot to seal off the opening of the pocket, as well as to provide a potential source of nutrition to the graft until vascularization occurred. Healing of the pocket incision occurred after a short period of inflammation and usually within 10 to 14 days pulsatile activity of the transplant could be observed Figure 1 illustrates the gross appearance of a whole heart graft in the ear

Observations of the grafts were made utilizing transilluminated light every two–three days during the first three weeks post transplantation to study the gross appearance of the graft, the patterns of vascular supply to the graft area, as well as the pulsatile activity Follow-up monthly observations were made for a period up to two to two and one-half years.

Electrocardiograms of the grafts as well as the animal s intact heart were recorded using the Physiograph. Animals were anesthetized with 500 mg% sodium pentobarbital at a dosage of 75 μg/gm body weight or by ether inhalation technique Pick-up electrodes for the grafts were made from size 000 insect pins. The impulses were transmitted through a preamplifier having a gain of 5 000 The time constant was 0 05 seconds The preamplifier output was led to a two stage direct coupled power amplifier which in turn drove the recording stylus. A recording sensitivity range of 20–670 mv/cm was employed Pick-up electrodes for recording the electrocardiogram of the heart *in situ* were made from bare sewing

E & M Instrument Co., Inc., Houston, T as.




Fig. 1 Gross appearance of a whole heart graft. (AA = tria V = ventricles)

needles (0 03 mm in diameter) A smaller preamplifier with an input sensitivity > 1 mv and a 2 second time constant was used with a similar direct coupled amplifier and pen recorder Figure 2 illustrates a recording layout.

Histologic preparations of 111 of the grafts were also studied. The ears containing the grafts were fixed in 10% neutral buffered formalin, paraffin embedded, cut at 5 μ, and stained with hematoxylin and eosin. All slides were studied and then classified plus or minus with no previous knowledge of the history of the graft. "Plus indicated the slide contained "*microscopically viable* tissue which should have pulsated or been electrically active (a successful graft) A minus indicated that the morphology was such that the graft should not have pulsated (an "unsuccessful" graft) The morphological classification was then correlated with the functional" record of the graft.

## RESULTS

*Viability* One hundred twent five of 234 transplants were observed grossly or recorded electronically to have pulsatile activity This represented 53 4% success using pulsatile or electrical activity of the graft as the criterion of success. However the viability of a graft was initially based solely on observable pulsatile activity and it was approximately eight months following transplantation before all of the grafts were tested for electrical activity There fore, this percentage of success represents the composite result of both observations extending over a long period of time. As seen in table 1 the percentage of successful transplants did not vary significantly according to the type of cardiac tissue transplanted, that is, atrial, ventricular or whole heart. The earliest pulsations were observed seven days after transplantation. The longest survival time of a graft with continuous pulsatile activity was 910 days

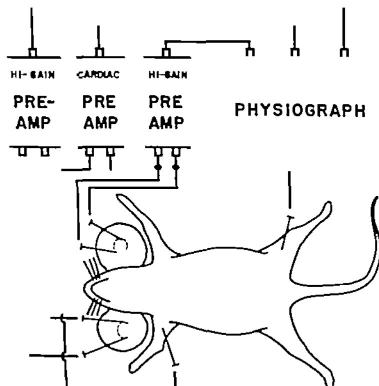



Fig. 2 Physiograph recording layout schema.

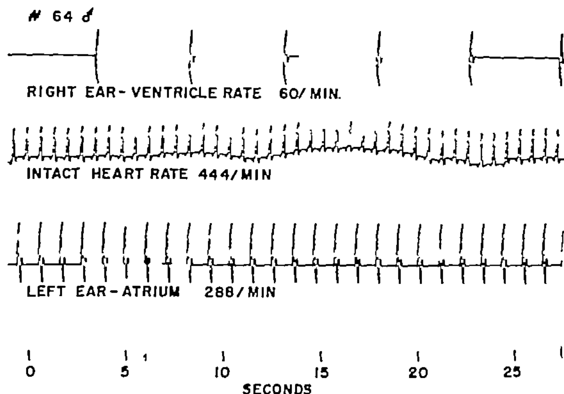



Fig. 3 Record of simultaneous recordings of both ear grafts and the intact heart demonstrating the difference in intrinsic rates of atrial and ventricular grafts, as well as the rate of the intact heart.

The significant morphological characteristics of the cardiac tissue were (1) the presence of a deeper quality of the eosin stain in the muscle cells with respect to the general staining characteristics of the whole section (fig 4) (2) the presence of striations within the muscle cells (fig. 6) similar to the findings of Rumery et al. ('61) in tissue culture studies; (3) a sinusoidal pattern of the capillary bed which became established between units of cardiac muscle cells (Browning, 49) cf figures 8 9 10 and 11 and (4) fatty change or metamorphosis completely replacing large areas of the grafted tissue (fig 7) associated with brown atrophy of the muscle cells (Robbins '62) Also noted were fatty infiltration into the central cavity of the graft (figs. 4 5 and 8) and areas of coagulative necrosis located both on the periphery of the graft (fig 5) and also in the central region of many of the grafts leaving pale translucent areas within the transplanted tissue.

The relationship of the graft to the surrounding tissue was generally of two types either the borders of the graft were fused" to the surrounding subcutaneous tissue (figs. 4 5 and 8); or the borders were "intact and the graft was within a sac or pericardial cavity (figs. 7 and 10) The fused" borders of the graft with the surrounding tissue often demonstrated areas of cartilage formation and calcification (figs. 4 5 and 8) Also noted in the area surrounding the grafts was an increase of fat cells (figs. 4 8 and 10) connective tissue or scar formation as well as cartilage and calcium deposits (fig. 8) Several grafts were found to have pieces of lung tissue that were transplanted along with the cardiac tissue (probably attached to the pulmonary vessels) Fibrinoid degeneration of the larger vessels (aorta, etc.) united with the cardiac tissue transplant was present in ten grafts.

*B Correlation with function.* Fifty-seven of 111 grafts were graded as "plus ;

that is, using the first three microscopic morphological characteristics of grafted cardiac tissue — (1) the deeper quality of eosin stain, (2) the presence of striations and (3) the sinusoidal pattern of the capillary bed — as criterion of *microscopic viability* or rather a *potentially viable* graft as defined by pulsatile and/or electrical activity. Thus 57 grafts had morphological characteristics such that the tissue should have pulsated or been electrically active. Fifty-four grafts were graded as "minus" indicating that the morphological characteristics were such that the graft should not have pulsated. Comparison of the microscopic grade with the functional record resulted in a positive correlation in 79 of the 111 grafts (71.2%); i.e., 39 grafts (35.1%) were graded as "plus" and had pulsated or had been electrically active and 40 grafts (36.1%) were graded as "minus" and were non-functional. The remaining 32 grafts (28.8%) did not correlate when compared with their functional records. Eighteen (16.2%) of these were graded as "plus" and had been non-functional grafts, and the remaining 14 (12.6%) were graded as "minus" and had been functionally active. It was noted that the sinusoid pattern of the capillary bed was maintained in 34 of the 58 non-functional grafts as demonstrated in figures 8 and 9 and therefore was used only as a guide for defining microscopic viability in the above correlations.

Twenty-three of the 32 grafts that did not correlate with their functional record were serially sectioned so the entire graft could be studied. Of these 23 grafts 17 revealed morphological characteristics that correlated with their functional record — seven were structurally and functionally negative and ten were positive. Therefore, the overall results of this study to correlate morphological characteristics with functional activity revealed that 96 of the 111 grafts (86.5%) showed a positive correlation and 15 (13.5%) did not. (Ten were graded as "plus" and had been non-functional grafts, and five were graded as "minus" and had been functionally active.)

## DISCUSSION AND CONCLUSIONS

This study demonstrates a relatively simple technique to study transplanted cardiac tissue *in vivo*. The end point of a successful "take" is readily demonstrated by either direct observation of pulsations or more definitively by recording electrical activity. The fact that only 53.4% of the grafts were classified as "successful" on the basis of grossly observed pulsations or electrical activity raises the question concerning the reasons for the "failures." Certainly the technique of transplantation must be suspected in those cases when pulsatile activity was not observed or recorded within a short period of time after transplantation. However, it should be emphasized that numerous grafts which did not demonstrate gross pulsatile activity shortly after grafting were not studied with the electronic equipment until approximately eight months post-transplantation because initially the former observation was being used exclusively to determine viability of the graft. In some recent unpublished studies in which electrical activity was the sole criterion for designating a "successful graft" it was found that approximately 95% of whole heart grafts were electrically active from 60 to 90 days post-transplantation. Thus host and donor factors deserve a more thorough study including the duration of time the graft was in the host.

Of the parameters studied it would appear that the age of the host was not a critical factor from 32 days to an age of approximately 150 days, but in hosts older than this age a decrease in the percentage of successful grafts was apparent. However, successful grafts were obtained in hosts ranging from 32 to 425 days of age at the time of transplantation. Portions of heart as well as whole hearts from donors of newborn to 11 days of age were grafted successfully suggesting the absence of a donor factor during this age period that would influence transplantation. However, 14 day old whole heart grafts were uniformly unsuccessful; but these were of a size which necessitated being "forced" with some difficulty into the prepared "pockets." Thus this raised the possibility of pressure atrophy of these grafts. This aspect of the study must be extended to include older donors with grafts composed of only a given size of the

## PLATE 1

### EXPLANATION OF FIGURES

4 Cross section of seven month old graft illustrating the deeper" staining characteristic of viable graft which has a "fused" border continuous with surrounding subcutaneous adipose tissue. × 30.

5 Same section as figure 4 showing "fused" border with coagulative necrosis of cardiac cells in upper left portion of graft, infiltration of fat cells in the center of the graft and an area of cartilage near the upper right border of the graft. × 130.

6 Same section as in figure 4 demonstrating striations (S) in cardiac muscle fibers which have syncytial pattern separated by inter calated discs (ID) × 600.

7 Cross section of 15 month old non-functional graft with an "intact" border contained within "pericardial" cavity or sac. The graft has been completely replaced by fat cells. × 30.


4
9
ID
g
ID
6
7

## PLATE 2

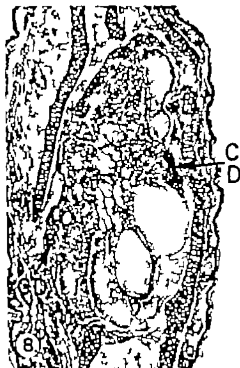
### EXPLAN TION OF FIGURES

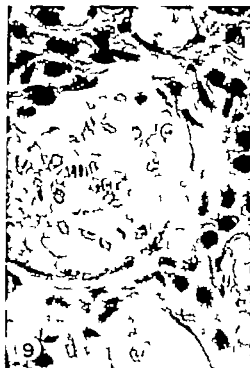
8 Cross section of an 11 month old non-functional graft demonstrating central fatty change numerou blood sinuses throughout the graft, and the presence of cartilage and calcium deposits (CD) along the fused" border of the graft. × 39.

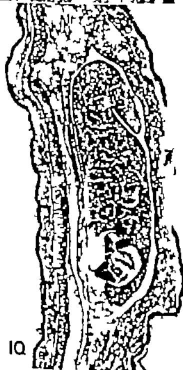
9 Same section as in figure 8 demonstrating units of cardiac cells" between the blood sinuses or capillaries of the graft. × 600.

10 Cross section of an eight month old functional graft which ppears t be completely replaced by blood sinuses and has maintained an intact border within a pericardial" cavity or sac. × 39

11 Same section as in figure 10, illustrating the complete absence of unit of myocardial cells between the blood sinuses or capillary bed of this electrically active graft. × 600.


C
D
8


9


10


11

# Innervation of the Tensor Tympani Muscle of the Cat[1]

CHARLES E. BLEVINS
*Department of Anatomy University of Washington, Seattle Washington*

In recent years the middle ear muscles have been the subject of numerous investigations. Although considerable neurophysiological data have accumulated on both the tensor tympani and stapedius muscles, much less is known of the neuromuscular substrate on which their behavior depends. A variety of animals have been used for studies of middle ear function, but the literature affords few accounts of the pattern of fine innervation of the tympanic muscles in any of them. Calibers of nerve fibers and sizes of motor units have been reported for both muscles in the rabbit (Berlendis, '55 Berlendis and DeCaro '55; Malmfors and Wersäll, '60a, b) and a single work has appeared on the motor unit size of the human tensor tympani (Torre '53) There are no complete studies for the cat despite its wide use in otological research. The current study was undertaken to add to our knowledge of the neurological basis for the activity of the tensor tympani muscle in this species Attention has been directed toward the diameters of nerve fibers, nature and distribution of nerve endings and innervation ratios.

## MATERIALS AND METHODS

Ten adult cats were used in this study Under nembutal anesthesia each specimen was fixed by perfusion The cannula was placed in the aortic arch the thoracic aorta was clamped above the diaphragm, and the perfusate was drained from the right atrium. The circulatory system of the head neck and upper extremities was flushed free of blood with isotonic heparinized saline and then followed immediately by 10% neutral formol Perfusion pressures were maintained below normal blood pressure levels by means of a mercury manometer attached to the perfusion system.

The tympanic portion (auditory bulla) of the temporal bone was exposed from the ventral aspect. After removal of the bony wall of the bulla, dissection was carried out under the stereoscopic microscope. Illustrations and photographs were made directly from the specimen at various stages during the exposure For histologic purposes tensor tympani muscles were removed with their nerve supply intact. The nerves were dissected forward to the foramen ovale to permit removal of a short segment of the mandibular nerve and the otic ganglion.

To reduce hardening of the tendinous portion of the muscle dehydration times in higher alcohols were minimized and oil of cedarwood was used as the clearing agent. Tissues were doubly imbedded with nitrocellulose and paraffin or subjected to four changes of paraffin under vacuum.

Serial sections were cut at 10 to 30 μ for study of nerve endings and at 5 μ for counts of nerve and muscle fibers. Specimens for histochemical studies were prepared by freezing the muscle in acetone and dry ice followed by section at 25 to 30 μ.

For analysis of nerve fibers two techniques were used, the Alzheimer-Mann-Häggqvist method (Rexed, 48) and the silver protargol method of Bodian ('36) counterstained with aniline blue Iron hematoxylin and aniline blue were utilized for counts of muscle fibers and for tracing intramuscular nerves. Bodian's silver method proved most successful for studying nerve endings. Silver protein (Chroma Gesellschaft, Schmidt & Co ) and Protargol S (Winthrop Stearns Inc.) were employed with equal results. For histo-

[1] Supported by the John C. and Edward Coleman Memorial Fund.
Work done while in the Division of Otolaryngology and Department of Anatomy, University of California, San Francisco Medical Center, San Francisco, California.

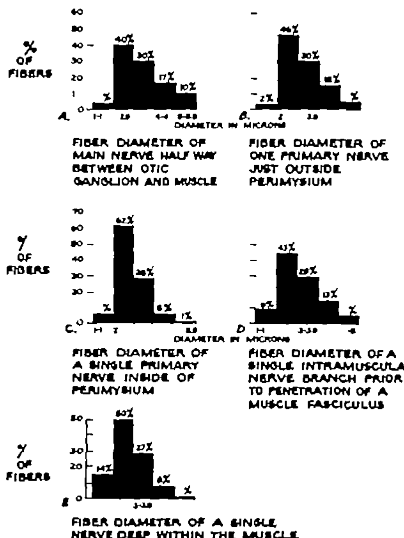



Fig. 1 Caliber spectrum of nerve fibers in the nerve to the tensor tympani muscle of the cat.

chemical studies the Gomori ('52) modification of the thiocholine technique of Koelle was used.

Calibers of nerve fibers were measured from photomicrographs at a magnification of 750 according to the methods of Hägg qvist ('36) and Rexed ('44). A modification of the method of Davenport and Barnes ('35) was utilized for the enumeration of nerve and muscle fibers.

## OBSERVATIONS AND RESULTS

### *Gross nerve-muscle relations*

The auditory bulla of the cat is divided by an osseus partition into a small lateral chamber and a larger medial cavity (Stromsten '52). The lateral or true tympanic chamber contains the auditory ossicles and the tensor tympani muscle. Its walls are marked by four apertures: the

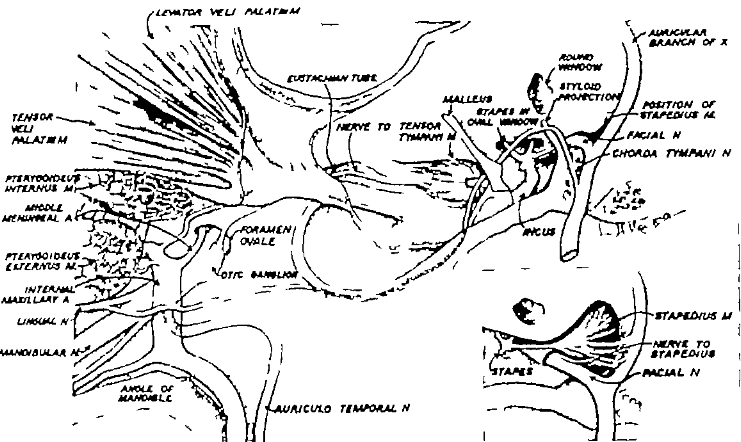



Fig. 2 Gross nerve-muscle relations of the middle ear f the cat from the ventral aspect. The bony partition separating the medial and lateral chambers of the auditory bulla the lateral wall of the l teral tympani chamber and the tympani membrane have been removed. The left of the field is anterior and the lower margin is lateral. (Drawing by Mrs. Lynn H. Young.)

oval and round windows on the medial wall the tympanic membrane on the lateral wall and the auditory (Eustachian) tube on its anterior wall. The posterior wall of the lateral chamber opens into the medial chamber of the bulla near the round window

Removal of the bony partition brings the ventral surface of the tensor tympani immediately into view (fig 2) It has the shape of an eccentric teardrop and rests in a fossa shaped to its contour Its average dimensions are 3 to 4 mm long, 1.5 to 2 mm wide, and 2 to 2.5 mm deep. The longitudinal axis is approximately 90 to the plane of the manubrium of the malleus. The belly of the muscle is not therefore in the plane of the auditory tube.

The epimysium is continuous with the periosteum of the middle ear cavity Near the anteroventral surface of the muscle it is continuous with the perichondrium and connective tissue of the auditory tube. The tendon merges from a broad base within the muscle and gradually tapers to its point of insertion on the manubrium of the malleus. The tip of the tendon is approximately one millimeter ventral to the plane of the auditory tube

The muscle fits into the circumpennate classification described by Grant ('52) The majority of muscle fibers run meridionally from the fibrous epimysium to the tendon which extends into their substance A few fibers originate on the auditory tube and merge tangentially with the others (figs. 2 5)

The nerve to the tensor tympani issues from the mandibular nerve in close relation to the proximal border of the otic ganglion (fig 2) After receiving fibers from the ganglion it passes underneath the cartilaginous wall of the auditory tube It runs for a distance of 4 to 5 mm to enter the muscle at nearly right angles (figs. 4 7) The nerve may branch just before or shortly after penetrating the epimysium.

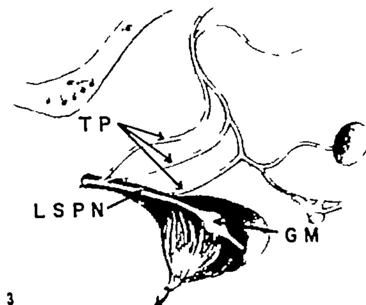
Relations of the tensor tympani to the tympanic plexus are shown in figure 3. The lesser superficial petrosal nerve lies closely adherent to the epimysial capsule of the muscle. Its course is interrupted by an autonomic ganglion identified by Morat ('11) and further described by Pollcard ('13) Posterior to the ganglion, the nerve follows the contour of the muscle and descends to join the tympanic nerve of Jacobson (IX) Just rostral to the fossa of the muscle, the lesser superficial petrosal nerve lies in a narrow fissure on the medial wall of the auditory tube. While in this cleft (fig 3) it receives branches from the tympanic plexus. Two branches can be followed over the promontory to the oval and round windows A third branch supplies the mucous membrane lining the bony wall of the bulla. Anterior to the points of anastomosis the nerve continues through a separate canal to join the otic ganglion and mandibular nerve.

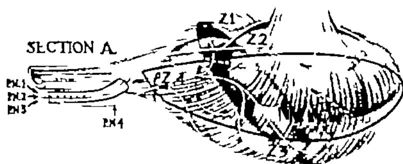
### *Neuromuscular histology*

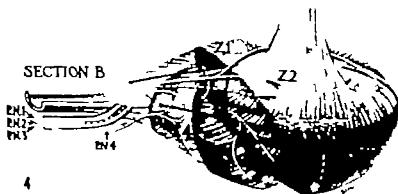
In a sagittal section the tensor tympani is shaped like an eccentric teardrop with one flattened edge (fig 5) From its apex, the tendon fans out broadly within the muscle. Collagenous fibers of the tendon separate in a radial fashion and are then directed to different regions in the base of the muscle Near their termination they form spiral tendrils which wrap around the muscle fibers Muscle fibers envelop the base and sides of the tendon. A small group of muscle fibers are oriented in the plane of the auditory tube. These fibers correspond to those of the tubal portion of the muscle in other species (e.g. rabbit) but constitute only a

Fig. 3 Relations of the tensor tympani muscle to the tympani plexus. The muscle has been reflected ventrolaterally to expose the fossa. LSPN lesser superficial petrosal nerve; GM ganglion of Morat TP branches of tympanic plexus. (Drawing by Mrs. Lynn H. Young.)

Fig. 4 Diagram of the nerve supply to the tensor tympani. The muscle has been pulled out of the fossa and rotated medially along its longitudinal axis. The lateral surface faces the viewer The main nerve divides into four primary nerves (PN 1–4) each of which supplies one distinct zone (Z 1–4) in the muscle; (PN 1 supplies Zone 1 etc.) Primary nerves 1–3 enter the muscle at the same level. Primary nerve 4 leaves the main nerve outside the muscle and enters the muscle at lower level. Section A indicates the level of section for figure 6 and Section B the level for figure 7 (Drawings by Mary D Brown.)




Figures 3–4

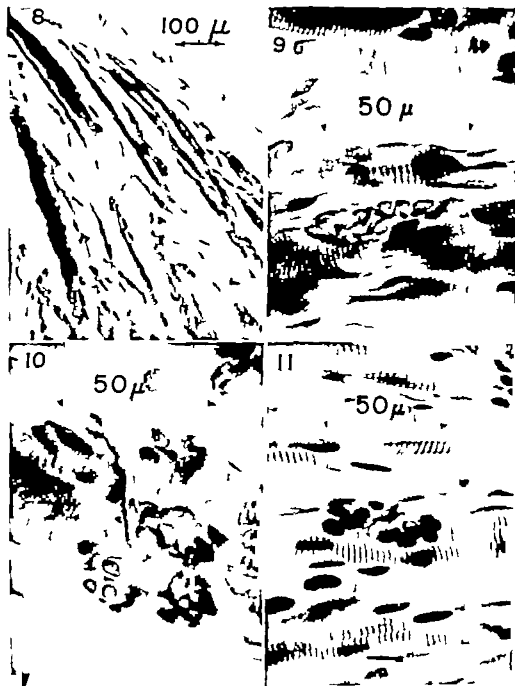



Fig. 8 Small diameter muscle fibers on the periphery of the tensor tympani. A few large diameter fibers are also visible in this section. Bodian stain.

Fig. 9 Single elongated motor end plate. Bodian stain.

Fig. 10 Short, compact motor end plates. Bodian stain.

Fig. 11 Bifurcated, elongated motor end plates. Bodian stain.

*Nerve endings*

The Bodian silver protargol method permitted the identification of many well-developed motor end plates in the tensor tympani. Such endings were highly concentrated in the innervation zone and were not found in other areas. The length of the sole plates varied from 14 to 40 μ. Each end plate was supplied by a single axon approaching the muscle fiber at right or oblique angles. The axon reached the end plate either at its mid-point or its periphery. Endings were of the "terminasion en placque" type which were classified in the following manner:

1. Single elongated endings (fig. 9). The axon enters one pole of an elongated end plate which exhibits large oval sole plate nuclei. Nuclei are densely packed along the entire length of the end plate. Slender axon arborizations terminate among the nuclei. These endings generally appear singly along individual muscle fibers.

2. Short compact endings (fig. 10). The terminal axon approaches the edge or center of the sole plate where it forms short thick terminal arborizations that end among large nuclei of various shapes. This type of ending is usually found where several motor end plates are packed in groups on adjacent muscle fibers.

3. Bifurcated, elongated endings (fig. 11): The main axon forms two branches each of which supplies separate groups of sole plate nuclei on the same muscle fiber.

Although elaborate motor innervation is clearly evident, the nature of sensory innervation is more difficult to establish. Scant data are present in the literature on this point. Ota ('58) found one typical muscle spindle in 25 muscles of the cat. Malmfors and Wersäll ('60a) reported fine free endings in the rabbit tensor tympani which they assumed to be sensory. Portmann ('49) was unable to find muscle spindles in the guinea pig but described simple free endings and sensory corpuscles. Physiological evidence of the proprioceptive function of these structures is not yet available.

The silver techniques employed in the current investigation revealed structures which resembled sensory formations but did not withstand critical analysis as such. Small nerve branches were observed to form arcades about muscle fibers (fig. 12) but in serial sections their fiber components were traced to end plates. Near the periphery of the muscle argyrophilic spiral tendrils suggestive of annulospiral formations, enclosed muscle fibers (fig. 13). However such formations stained intensely with aniline blue and were identified as connective tissue fibers of tendinous or epimysial origin.

It is well established that stretch or pressure receptors exhibit cholinesterase activity (Coërs '54, Gerebetzoff '55, Abraham, '56, Coupland and Holmes '57). To investigate the possibility that sensory endings escaped detection in our silver preparations the thiocholine method was utilized. A high degree of cholinesterase activity was found in the middle third of the muscle fibers (fig. 14) closely coincident with the innervation zone observed with the Bodian technique. Localized activity was not observed at other points in the muscle or tendon although cholinesterase cuffs were occasionally found at the junction of muscle fibers and tendon. Individual sites of cholinesterase activity were limited to the subneural apparatus of extrafusal motor end plates (figs. 15, 16). Both compact and elongate endings were observed but spindles, free nerve fibers, or encapsulated endings were not detected in the muscle or its tendon.

*Motor units and innervation ratios*

Data for ratios of nerve fibers to muscle fibers are shown in table 1. Nerve fibers were counted in the main nerve trunk in advance of axon branching. The number of nerve fibers in each specimen is shown in column 2 with two subdivisions, one indicating one-half and the other two-thirds of each count. These fractional values estimate the number of efferent fibers if one believes, as Sherrington (1894) did, that the number of afferent fibers in nerves to skeletal muscles range from one-half to one-third. Counts of muscle fibers represent composite enumerations at different levels. The sizes of motor units are shown in column 5. The upper figure for each specimen represents values for nerves with a 50% motor fiber population and the lower figure indicates values

## DISCUSSION

The gross features of the tensor tympani of the cat observed in this study essentially resemble those described by Malan ('34a) and Kobayashi ('56) The muscle is neither spindle-shaped as in the rabbit nor cylindrical as in man. It has the shape of a teardrop and thus more closely resembles the tensor tympani of the dog Unlike the rabbit (Malmfors and Wersäll '60a) only a very few of its fibers originate from the auditory tube. Slight species differences may be noted in the relations of the muscle to the tympanic plexus In the cat the tympanic plexus lies anterior and inferior to the fossa of the muscle while in the rabbit numerous branches are deeply recessed within the fossa. In man, the plexus is found below the posterior third of the muscle. The lesser superficial petrosal nerve of the cat is enclosed in the epimysium

The tensor tympani muscle is richly supplied with nerves. Numerous nerves of variable sizes are readily found within the perimysial septae Each primary nerve supplies a major zone within the muscle and all nerves derived from them are confined to an innervation network in the middle third of the muscle The short length of terminal axons and the low innervation ratios indicate that each axon supplies adjacent muscle fibers or those within close proximity

Feindel et al ('52) have shown that terminal axons overlap and intermingle to a great degree in some muscles In the intrinsic plantar muscles they found axon collaterals supplying different regions of the muscle and conversely end plates in a given zone of muscle were derived from different parent axons. These same investigators observed single nerve fibers terminating in multiple end plates on the same muscle fiber in the extrinsic ocular muscles. Thoughout the course of the present study axons did not appear to overlap terminally nor did they lead to multiple end plates.

Differences in composition of the tensor tympani have been described by other investigators. Muscle fibers of both small and large diameters have been observed in the dog (Policard '13 Wohlfart, '37) and cat (Malan, '34b) Spiral myofibrils or "Ringbinden have been found which wrap around and intermingle with the muscle fibers Malan ('34b) reported such formations in association with muscle fibers of both small and large diameters in the cat and dog Wohlfart ('37) observed "Ringbinden in association with large muscle fibers in the human tensor tympani. The small muscle fibers encountered in the present investigation are similar to "Ringbinden" in some respects. Their small diameter striations and tendency to intermingle with one another near their terminations resemble the pattern of "Ringbinden However they contain peripheral nuclei (fig. 8) and their constituent myofibrils do not appear to anastomose

Some workers have attempted to assign different functional capacities for large and small muscle fibers in the tensor tympani Okamoto et al. ('54) concluded that motor units of two types were present in the cat, each demonstrating differences in thresholds action potentials and adaptation. Wersäll ('58) found that some motor units of the rabbit tensor were weaker than others He suggested that this was due to the small diameter of muscle fibers in these units. Erulkar et al ('62) have recently reported that fibers of small diameter in the cat show both resting and action potentials different from those of large muscle fibers The present study has uncovered no other morphological features that could account for such physiological differences

The diameter of nerve fibers in the tensor tympani nerve of the cat is in close agreement with those found in the rabbit by Malmfors and Wersäll ('60a) In both species the peak of fiber population is within the 2 to 2.9 μ range and no fibers are observed above 6 μ. Such unimodality is characteristic of cranial nerve branches to skeletal muscles in the monkey (Fernand and Young '51) rabbit and newborn human (Rexed 44). Some authors (Fernand and Young '51; Fulton, 49) have associated unimodality with non-weight bearing muscles in which spindles had not yet been found. Since neuromuscular spindles have not been observed in the tensor tympani in this study it might be tempting to employ the same logic. However Kadanoff

('58) and Bowden and Mahran ('56) have subsequently found spindles in facial muscles and Lucas-Keene ('61) has observed spindles in muscles of the larynx.

Nerve fibers of 1 to 6 μ fit into the group III classification of Lloyd (Ruch and Fulton, '60) This would allow for somatic efferent and preganglionic autonomic fibers but would not provide for either 1A (annulospiral fibers) or 1B fibers to Golgi tendon organs. The latter are considerably larger than any fibers found in this study Although the observed fiber diameter is consistent with the absence of spindles it may be possible that fiber composition of the tensor tympani nerve of the cat does not fit into existing caliber classifications.

The most striking feature of innervation of the tensor tympani is the rich pattern of motor innervation in contrast to the apparent absence of sensory endings. Silver and thiocholine techniques consistently demonstrate a network of motor endings within the middle third of the muscle fibers. A central position of end plates is characteristic of the majority of human muscles although scattered innervation is present in the sartorius and gracilis (Coërs and Durand, '57) The crescentic disposition of end plates in the tensor tympani might provide evenly balanced tension from all directions whether motor units are firing simultaneously or in synchronous rotation. The en placque endings are not significantly different from those of other skeletal muscle and specific functional differences are not attributed to them. End plates of small diameter muscle fibers do not appear to differ from those of large muscle fibers. The rapidity and refined nature of contractions of the tensor tympani muscle provide adequate testimony of the physiological efficiency of the motor endings observed.

Although structures have been observed in this study which might be mistaken for annulospiral fibers or single nerve endings, they have been identified subsequently as collagenous fibers or small nerve branches. The capricious nature of silver stains may account for some of the earlier interpretations of these formations as sensory endings. Cholinesterase techniques failed to detect intramuscular or intratendinous proprioceptor endings If such endings are present they would presumably have been stained in the same sections in which the subneural apparatus of motor end plates were evident. A brief report by Erulkar et al. ('62) indicates that some muscle fibers of small diameter exhibit cholinesterase activity similar to intrafusal muscle fibers but the presence of proprioceptive nerve endings in association with such fibers is not mentioned. On the basis of existing evidence, it is difficult to conclude that endings subserving sensory function are present in the tensor tympani muscle of the cat.

The innervation ratios observed in this study are consistent with the views of Sherrington (1894) and Clark ('31). They believed that skeletal muscles associated with organs of special sense exhibited a finer degree of motor innervation than other skeletal muscles. Additional evidence supporting this concept is available in the work of others (Tergast, 1873; Bors '25 Berlendis '55) Except for the current study all data have been calculated on the assumption that afferent fiber populations for muscle nerves of cranial origin are of the same proportion as nerves of spinal origin. There are no studies to verify such an interpretation. It is difficult to measure either afferent or efferent components of cranial nerves. Instead of severing a dorsal or ventral root, lesions must be placed at the brain stem level or along the course of the appropriate nerves. Until more quantitative data are available on the functional components of cranial nerves calculations of motor unit values will remain approximations.

The absence of histological confirmation of spindles or other proprioceptive endings in this study leads one to believe that afferent fiber populations in the nerve to the tensor tympani of the cat are either absent or present in negligible proportions. It, therefore seems that the more accurate evaluation of the ratio of nerve fibers to muscle fibers in this case should make no allowances for afferent fibers.

The motor unit of the tensor tympani of the cat is almost identical with that in the rabbit, in which Malmfors and Wersäll ('60a) estimated that each motor neuron supplied seven or less muscle fibers. The

innervation ratio is one-half of this value or 1:3 5 Regardless of which value one accepts, it would seem safe to say that swiftness and fine gradation of contraction could be accomplished by either ratio The critical factor would seem to be the size of the total unit rather than a matter of seven or four muscle fibers being supplied by each neuron. Both ratios would provide finer gradation of movement than ratios of 1:120 or 1 165 for such muscles as the soleus and extensor digitorum longus (Clark, '31) If a maximum allowance of 50% were not made for afferent fibers in ratios this large then the innervation ratio would be 1 240 and 1:330 Such ratios presumably would enhance strength but reduce swiftness, coordination and gradation of contraction.


SUMMARY

A review of gross nerve-muscle relations and a study of the pattern of fine innervation have been reported for the tensor tympani muscle of the cat.

1 As in other species the motor nerve supply to the tensor tympani is derived from the mandibular nerve Species differences were noted in the relations of the muscle to the tympanic plexus and the lesser superficial petrosal nerve

2. The muscle structure has been described Muscle fibers of both large and small diameter were found but were otherwise morphologically similar "Ringbinden" were not observed but muscle fibers of small diameter appeared to simulate them in some respects.

3 The muscle was supplied by three to four primary nerves which branched profusely but supplied distinct zones within the muscle with little or no overlapping. Intramuscular nerve branches were confined to a narrow network in the middle third of the muscle. Terminal axons were short and did not appear to supply more than one motor end plate

4 Nerve fibers exhibited a unimodal spectrum, for the majority of fibers were within 2 to 2.9 μ in diameter No fibers were observed above 6 μ

5 Numerous motor end plates of three basic types were found within the clearly defined innervation network. Sensory endings were not detected by either silver or histochemical techniques.

6 The size of the motor unit was estimated at seven or less. The innervation ratio was established at four or less While the question of afferent innervation was not resolved the absence of detectable sensory endings suggests that coordination and limitation of activity of the tensor tympani muscle are accomplished by other than proprioceptive means


LITERATURE CITED


Abraham A. 1956 Über die Strucktur und die Endigungen der Aorticusfasern im Aortenbogen des Menschen mit Berücksichtigung der cholinesterase-Aktivität der Pressorezeptoren. Z. mikr -anat. Forsch., 62: 194-228.

Berlendis, P A. 1955 L'unità motoria del muscolo tensore del timpano. Boll. Soc. med-chir P via, 69 37–39

Berlendis, P A., and L. G. DeCaro 1955 L'unità motoria del muscolo stapedio. Ibid., 69 33–36.

Bodian D 1936 A new method for staining nerve fibers and nerve endings in mounted paraffin sections. Anat. Rec 65 89–97

Bors, E. 1925 Über Zahlenverhältnis zwischen Nerven und Muskelfasern. Anat. Anz., 60 415.

Bowden R. E. M., and Z. Y Mahran 1956 The functional significance of the pattern of innervation of the muscle quadratus labii superioris of the rabbit, at, and rat. J Anat Lond. 90 217–227

Clark, D A. 1931 Muscle counts of motor unit ; a study in innervation ratios. Am. J Physiol., 96 296–331

Coërs, C. 1954 La localisation histochimique de la cholinestérase dans les fuseaux neuromusculaires. Bull. Acad. Roy Belg. Cl. Sci 40 1000–1002.

Coërs, C., and J Durand 1957 La repartition des appareils cholinesterasiques en cupule dans divers muscle striés. Arch. Biol., Paris. 68 209–215.

Coupland, R. E., and R. L. Holmes 1957 The use of cholinesterase techniques for the demonstration f peripheral nervous structures. Quar J micr Sci., 98 327–330.

Davenport, H. A., and J R. Barnes 1935 The strip method for counting nerve fibers or other microscopic units. Stain Techn 10: 139.

Erulkar S. D M. L. Shelanski, B. L. Whitsel and C. N Gessey 1962 A dual fiber system in the tensor tympani of the cat. Fed. Proc., 21 357 (abstract)

Feindel, W H. J R. Hinshaw and G. Weddell 1952 The pattern of motor innervation in mammalian striated muscle. J Anat., Lond 86 35–48.

Fernand, V S. V and J Z. Young 1951 The size of the nerve fibers of muscle nerves. Proc. Roy Soc. Ser B 139 38–57

Fulton, J F 1946 Howell's Textbook of Physiology 15th ed., W B. Saunders Co., Philadelphia p. 190.

Gerebtzoff, M. A. 1955 Les quatre localisations de l'acétylcholinestérase dans les muscles striés des mammifères et des oiseaux, C. R. Soc. Biol., 149 823–826.

Gomori, G. 1952 Microscopic Histochemistry Principles and Practices U of Chicago Press, Chicago, p. 210.

Grant, J C. B. 1952 A Method of Anatomy William & Wilkins, Baltimore, Chap. 1 p 77

Häggqvist, G 1936 Analyse der Faserverteilung in einem Rückenmarkquerschnitt. Z. mikr.-anat. Forsch., 39 1

Kadanoff, D. 1956 Die Sensiblen Nervendigungen in der mimischen Muskulatur des Menschen. Z. mikr.-anat. Forsch., 62: 1–15.

Kobayashi, M. 1956 Comparative anatomical studies of the morphology of the tensor tympanic muscles of various mammals. Hiroshima. J Med. Sci., 5 85–108.

Lucas-Keene, M. F 1961 Muscle spindles in human laryngeal muscles. J Anat., 95 25–29

Malan, E. 1934a Morphologica comparata de musculo "tensor tympani. Z. ges. Anat., 103 407–437

——— 1934b Etude d'histologie comparée sur quelques modifications particulières des fibres du Tensor Tympani dues a la senescence. Arch. Biol., Paris, 45 355–381.

Malmfors, T and R. Wersäll 1960a Innervation of the middle ear muscles in the rabbit with special reference to nerve calibres and motor units I. Acta neerl. morphol., 3 167–182.

——— 1960b Innervation of the middle ear muscles in the rabbit with special reference to nerve calibres and motor units II. Ibid., 3: 183–189

Morat, R. 1911 Revue de Medicine. (Cited by Policard, '13.) See also Le Chat, cited by Bonnier L oreille III, p. 139.

Okamoto, M., M. Sato and I. Kirikae 1954 Studies of the acoustic reflex Part II. Experimental studies on the function of the tensor tympani muscle. Ann. Otol. Rhinol. & Laryngol., 63 950–959

Ota, N 1958 Studies on nerve endings of the middle ear muscles of the cat (in Japanese) J Otol. Rhino-Laryng. Soc., Japan, 61 1614–1630.

Policard, M. A. 1913 Quelques points sur la structure du muscle du marteau chez le chien. J Anat., Paris, 49 304–321

Portmann, M. 1949 Le muscle de marteau son innervation. Rev Laryng., Paris, 76 534–546.

Rexed, B. 1944 Contributions to the knowledge of postnatal development of the peripheral nervous system in man. Acta psychiat., Kbh., Suppl., 33 1–205.

——— 1948 A modified myelin staining method for paraffin sections. J Neuropath., 7 463–466.

Ruch, T C., and J F Fulton 1960 Medical Physiology and Biophysics. W B. Saunders Co., Philadelphia, 91–92.

Sherrington, C. S. 1894 On the anatomical constitution of nerves of skeletal muscles. J Physiol., 17 211–258.

Stromsten, F A. 1953 Davison Mammalian Anatomy Revised 7th ed., The Blakiston Company New York, Chap. 3, p. 80.

Tergast, T 1873 Ueber das Verhältniss von Nerven und Muskeln. Arch. mikr. Anat., 9: 36–46.

Torre, M. 1953 Nombres et dimensions des unités motrices dans les muscles extrinsèques de l'oeil et en général dans les muscles squelettiques reliés à des organes de sens. Schweiz. Arch. Neurol Psychiat., 72: 362–376.

Wersäll, R. 1958 The tympanic muscles and their reflexes. Acta otolaryng., Suppl., 139 1–106.

Wohlfart, G. 1937 Über das Vorkommen verschiedener Arten von Muskelfasern in der Skelettmuskulatur des Menschen und einiger Säugetiere. Acta psychiat., Kbh., Suppl., XII, 1–19

# Denudation of the Rabbit Egg Time-sequence and Mechanism

Z. DICKMANN
*A.R.C Unit of Reproductive Physiology and Biochemistry*
*University of Cambridge England*

The newly ovulated rabbit egg enters the oviduct surrounded by a mass of cells which consists of two parts: the *corona radiata* ( corona") four to eight cells in thickness, which immediately surrounds the *zona pellucida*, and the *cumulus oophorus* ( cumulus") which surrounds the corona. The cumulus can be readily distinguished from the corona, since the cells of the latter are much more densely packed; furthermore hyaluronidase has no effect on the corona, but it liquefies the matrix of the cumulus, causing its cells to fall away from the egg.

With time both the corona and the cumulus become removed from the egg which is then said to be denuded. No conclusive evidence is available as to whether or not the corona and the cumulus contribute to the maintenance of the tubal egg. It was shown that loss of fertilizability of the rabbit egg coincides with complete denudation (Chang, '51a, '52) but whether or not the two phenomena are correlated has not been established. Therefore experiments were done to find out whether the corona and the cumulus contribute to the welfare of the tubal egg The present paper which is the first of a series, describes the chronology of egg denudation in non-mated and mated does, and affords some insight into the mechanism involved in denudation.

## MATERIALS AND METHODS

### *Animals and treatments*

Cross-bred domestic rabbits (*Oryctolagus cuniculus*) were used. The females were sexually mature virgins, 6–12 months old, weighing 3–4 kg. They were placed in individual cages at least 21 days before they were used in an experiment.

In the studies on non-mated rabbits does were injected intravenously with 25 i.u. chorionic gonadotrophin (Pregnyl Organon Laboratories) to induce ovulation. In studies on mated rabbits does were mated with two fertile bucks (cross-bred) in rapid succession and immediately given an ovulatory injection of gonadotrophin; the latter procedure ensures a higher proportion of does ovulating (C E. Adams personal communication, '62) Twelve to twenty-four hours after the ovulatory injection the does were killed, their oviducts removed and flushed with physiological saline (0.9% NaCl) in order to recover the eggs. To describe the degree of denudation, the eggs were examined in the fresh state, first under a dissecting microscope and then mounted in a hanging drop and examined with a compound microscope.

### *Criteria for changes in the corona and the cumulus*

With time changes take place in the corona and the cumulus. Those occurring in the corona will be described in terms of its thickness when three or more cells thick it is referred to as "thick corona, and when reduced to one to two cells in thickness it is referred to as "thin corona. Regarding the cumulus, whenever appropriate a distinction is made between "egg-containing cumuli" and additional-cumuli" which do not contain eggs; when no distinction is made, the words cumulus mass, or simply cumulus whichever is more applicable are used. The cumulus will be described in terms of its *size elasticity* and *cell density* these

Present address: Department of Obstetrics and Gynecology Vanderbilt University Nashville, Tennessee.

three characteristics being associated with the ageing of the cumulus. As regards the size only those cumuli which had dimensions of 0.5 mm or more were recorded, measurements being rounded off to the nearest 0 5 mm. A measurement such as 2 × 1 × 1 mm for example (see tables 1–7) gives a rough indication of the size but not necessarily the shape of a particular piece of cumulus, which usually was quite irregular Elasticity was determined by stretching the cumulus with two fine glass needles under a dissecting microscope a procedure which was repeated two to three times for each piece of cumulus. The elasticity was graded from 4 to 0 4 being the most elastic and 0 designating lack of elasticity The cell density in the cumulus of newly ovulated eggs is desig nated as standard. With time the cell density may change in either of two ways: cells may become removed from the cumulus matrix which results in reduced cell density or cells may draw closer to one another which results in "increased" cell density The difference between the three grades of cell density was great enough to be readily seen under the dissecting microscope.

*Timing of the experiments*

In our colony does ovulate at nine and one-half to thirteen hours after an ovulatory injection (Harper '61) the majority of ovulations occurring between ten and twelve hours. Because of the spread of ovulation time intervals of four hours were considered sufficiently short for recording progress in denudation. The earliest time at which eggs were examined was 12 hours after the ovulatory injection.

## OBSERVATIONS

*Denudation of eggs in non mated rabbits at 12 16 20 and 24 hours after the ovulatory injection —*

*Denudation at 12 hours*

A cumulus mass recovered from an oviduct 12 hours after an ovulatory injec tion is shown in figure 1 A higher magnification of approximately the central area of this cumulus in which four eggs are recognizable is shown in figure 2.

TABLE 1

*The size f cumuli and the number of eggs they contained, recovered from oviducts at 12 hours after the ovulatory injection*

| Rabbit no. | Left oviduct: Size of cumulus | Left oviduct: No. of eggs | Right oviduct: Size of cumulus | Right oviduct: No. of eggs |
|---|---|---|---|---|
| | mm | | mm | |
| 1 | 3 × 2 × 2 | 6 | 3 × 2 × 2 | 3 |
| 2 | 5 × 1 × 1 | 3 | 6 × 1.5 × 1.5 | 5 |
| 3 | 5 × 0.5 × 0.5 | 3 | 2 × 0.5 × 0.5 | 2 |
| | | | 1 × 0.5 × 0.5 | 1 |
| 4 | 3 × 1 × 1 | 4 | 3 × 2 × 2 | 5 |
| 5 | 3 × 2 × 2 | 5 | 3 × 1 × 1 | 2 |
| 6 | 3 × 2 × 2 | 5 | 5 × 1 × 1 | 4 |
| 7 | 2 × 0.5 × 0.5 | 2 | 2 × 2 × 2 | 4 |
| 8 | 6 × 0.5 × 0.5 | 1 | 3 × 2 × 2 | 6 |
| | 1 × 0.5 × 0 5 | 1 | | |
| 9 | 1 × 1 × 1 | 1 | 5 × 2 × 2 | 8 |
| | 1 5 × 1 × 1 | 1 | | |
| 10 | None | none | 1.5 × 0.5 × 0.5 | 3 |
| | | | 1.5 × 0.5 × 0.5 | 1 |
| 11 | 2 × 0.5 × 0.5 | 1 | 4 × 1 × 1 | 8 |
| | 2 × 0.5 × 0.5 | 1 | | |
| | | 1 | | |
| 12 | 2 × 2 × 2 | 3 | 5 × 1.5 × 1.5 | 6 |
| 13 | 3 × 0.5 × 0.5 | 2 | 1 × 1 × 1 | 2 |
| 14 | 5 × 1.5 × 1.5 | 9 | 1.5 × 1 × 1 | 2 |
| 15 | 4 × 1 × 1 | 4 | 2 × 1.5 × 1.5 | 4 |
| 16 | 6 × 1.5 × 1.5 | 7 | 1 × 1 × 1 | 1 |

Reduced cell density which is very unusual for 12-hour cumulus.
This egg was in corona, but devoid of cumulus.

Sixteen does were used in this experiment. The sizes of the cumuli recovered and the number of eggs they contained are recorded in table 1 In general, the figures show a good correlation between the size of the cumulus and the number of eggs it contains; however cumuli of different sizes may contain the same number of eggs, a fact which indicates variability in the amount of cumulus extruded by the individual follicle

Thirty-one out of 32 oviducts yielded cumuli, all containing eggs. In each of 26 oviducts all the eggs were in one cumulus mass, whereas in each of five oviducts the eggs were divided between two pieces of cumulus, at least one of which contained one egg only When two cumuli are recovered from the same oviduct, it cannot be stated with certainty whether a one-piece cumulus had already been broken up, or whether the two pieces had not yet fused. The latter alternative is somewhat more likely because of the close proximity of the recovery of the eggs to the time of ovulation. On four occasions the discrete cumuli of the individual eggs, within a cumulus mass, could still be discerned in other words, the cumuli of the individual eggs had united, but had not yet "blended" into each other As these were the only instances in which this was seen, the "blending" of cumuli must be rapid, and probably occurs within an hour of ovulation.

The elasticity of all the cumuli was 4 and the cell density standard. Two unusual observations were made in rabbit no. 11 In the left oviduct one egg was in corona but without cumulus, and the cumulus from the right oviduct had a somewhat reduced cell density

A slight hemorrhage into the follicle shortly before ovulation or while the follicle ruptures may result in the cumulus being tinged with variable amounts of blood. Thus of the 36 cumuli recovered, 14 had blood spots in several areas of the cumulus in seven, practically the whole cumulus was stained with blood except for the areas immediately around the eggs (i.e the corona layers) eight had very little blood and seven did not have any blood.

Painstaking manipulations of the cumulus, with a pair of fine glass needles, are necessary to remove an egg from a cumulus mass. When this is done, the eggs usually emerge with their coronae and a variable amount of cumulus (fig 3) The difficulty in removing an egg is due to the elasticity and stickiness of the cumulus and perhaps also due to filaments which connect the corona and the cumulus cells.

There were no "additional-cumuli" (i.e. cumuli which do not contain eggs) in the flushings of any of the oviducts.

*Denudation at 16 hours*

Six does provided material for this study The data on the cumuli and the eggs which were recovered are recorded in table 2. All 12 oviducts yielded eggs, the number of which corresponded with the number of ovulation points (i.e. 100% egg recovery) An egg in cumulus is shown in figure 4 The fact that in size, cell density and elasticity the cumuli which contained eggs were indistinguishable from 12-hour cumuli (compare figs. 1 and 2 with fig 5) might have led one to deduce that denudation had not yet started. Nevertheless, additional observations indicated that denudation had started. Four oviducts contained one egg each and one oviduct contained two eggs which were in corona, but devoid of cumulus. Six oviducts contained one or more additional-cumuli, showing that the cumulus had started to break up. Also noteworthy was the fact that in some of the additional-cumuli the elasticity had decreased to three.

Another change observed was that the number of corona cell layers around the majority of eggs was reduced, although the eggs were still in the thickness of the cumulus. Furthermore the eggs could be removed from the cumulus mass by means of a pair of fine glass needles, with much greater ease than at 12 hours, emerging in the majority of cases with only their coronae It is emphasized that the cumulus was manipulated in such a way that the removal of an egg was a separation, rather than a tearing of the egg and its corona from the cumulus, and that in the process very few if any corona cells were brushed off. Eggs with the smallest, the average, and the largest amount of

TABLE 2

*Characteri tics of egg-containing cumuli nd dditional cumuli, nd the number of eggs devoid of cumulus 18 hours fter the ovulatory injection*

| Rabbit no. | Egg-containing cumuli: Size | Egg-containing cumuli: Cell density | Egg-containing cumuli: El sticity | No. of eggs | No. of eggs out of cumulus | Additional cumuli: Size | Additional cumuli: Cell density | Additional cumuli: El sticity |
|---|---|---|---|---|---|---|---|---|
| | mm | | | | | mm | | |
| 17 L | 7 1.5×1.5 | standard | 4 | 3 | 1 | 10* 1×1×1 | standard | 3 |
| R | 3×2×2 | tand rd | 4 | 5 | 0 | none | — | – |
| 18 L | 7×1.5 1.5 | stand rd | 4 | 8 | 0 | 5 1×1×1 | standard | 3 |
| R | 1×1×1 | st ndard | 4 | 2 | 0 | none | — | – |
| 19 L | 4×1.5×1.5 | t dard | 4 | 5 | 0 | 1 1×0.5×0.5 | standard | 3 |
| R | 3×1.5×1.5 | st dard | 4 | 2 | 0 | 1 0.5×0.5×0.5 | standard | 3 |
| 20 L | 3×1.5×1 | tandard | 4 | 3 | 0 | none | — | – |
| R | 5×3×3 | standard | 4 | 10 | 0 | none | — | – |
| 21 L | 6×1.5×1.5 | stand rd | 4 | 3 | 1 | none | — | – |
| R | 6×1.5×1.5 | standard | 4 | 2 | 2 | 1 1×1×1 | standard | 4 |
| 22 L | none | — | – | — | 1 | 1 2×1×1 | standard | 4 |
| R | 6×2×2 | stand rd | 4 | 6 | 1 | none | — | – |
| Total | | | | 49 | 6 | | | |

L — Contents of left oviduct.
R — Contents of right oviduct.
* Indicates the number of cumuli having the ize indicated.

TABLE 3

*Characteristics of egg-containing cumuli and additional-cumuli, and the number of eggs devoid of cumulus recovered from oviducts 20 hours after the ovulatory injection*

| Rabbit no. | Egg-containing cumuli: Size | Cell density | Elasticity | No. of eggs | Eggs out of cumulus: Total no. | No. coated with mucin | Additional-cumuli: Size | Cell density | Elasticity |
|---|---|---|---|---|---|---|---|---|---|
| | mm | | | | | | mm | | |
| 23 L | none | — | | — | 2 | 2 | 1 3×1×1 | reduced | 4 |
| R | none | — | – | — | 4 | 2 | 1 3×1.5×1.5 | reduced | 4 |
| | | | | | | | 1 1.5×1.5×1.5 | reduced | 4 |
| 24 L | none | — | – | — | 5 | 5 | 1 4×1×1 | reduced | 4 |
| | | | | | | | 1 1.5×1.5×1.5 | reduced | 4 |
| R | none | — | – | — | 4 | 4 | none | — | – |
| 25 L | 2×1×0.5 | reduced | 4 | 2 | 5 | 1 | none | — | – |
| | 2×2×1 | reduced | 4 | 2 | | | | | |
| R | none | — | – | — | 4 | 0 | 1 3×0.5×0.5 | reduced | 2 |
| 26 L | none | — | – | — | 3 | 3 | 1 2×1×1 | reduced | 4 |
| R | none | — | – | — | 6 | 6 | 1 4×1×1 | reduced | 4 |
| | | | | | | | 1 1×1×1 | reduced | 4 |
| 27 L | 1×1×1 | standard | 2 | 1 | 0 | — | 1 1×1×1 | standard | 2 |
| | 1×1×1 | standard | 2 | 1 | | | | | |
| | 1×1×1 | standard | 2 | 2 | | | | | |
| R | 6×1.5×1.5 | standard | 3 | 1 | 2 | 0 | 1 4×2×2 | standard | 3 |
| | 1×1×1 | standard | 3 | 1 | | | 1 1.5×1.5×1.5 | standard | 3 |
| | 1×0.5×0.5 | standard | 3 | 1 | | | 6 1×1×1 | standard | 3 |
| Total | | | | 11 | 35 | 23 | | | |

*Denudation of eggs in mated rabbits at 12 16 and 20 hours post coitum (p.c.)* —

*Denudation at 12 hours p.c.*

Seven does provided material for this study The data on the cumuli and the eggs recovered are recorded in table 5 Fifty-eight ovulation points were counted but only 55 eggs were recovered; two eggs were still in their follicles although the follicles had ruptured and one egg could not be accounted for

The data presented in table 5 reveal that at 12 hours p.c. denudation is well under way With four exceptions (from tubes 33L, R 34R 35R) all cumuli had started to disintegrate as evidenced by the presence of additional-cumuli. No changes (as compared with 12-hour cumuli from non-mated does) were observed in the egg-containing cumuli; thus in all instances, the cell density was standard" and the elasticity was four In the majority of the additional-cumuli on the other hand, changes which did not seem to follow a consistent pattern were observed. Thus the cell density was either standard" or reduced, and the elasticity ranged from four to one.

Of the 55 eggs recovered, 28 (51%) were still in cumulus (one of which is shown in fig. 18) 19 of these were in thick and nine in thin coronae. The manual removal of eggs from the cumulus was as difficult as with cumuli obtained from unmated does at 12 hours and the eggs emerged with their coronae and with variable amounts of adhering cumulus. An egg in a thick corona which had been removed from the cumulus is shown in figure 19

Of the 27 eggs which at recovery time were already out of cumulus, six were in thick and 21 in thin coronae One of these eggs in a thin corona is shown in figure 20

The total number of spermatozoa within the eggs including those in the vitellus perivitelline space and zona pellucida, was recorded in order to assess whether or not there is a relationship between the degree of denudation and the number of spermatozoa The data as a whole show that the number of spermatozoa in eggs devoid of cumulus was considerably higher than in those with the cumulus intact. It should be noted however that in those animals (32L, 34L, 35R) in which it was possible to make intratubal comparisons the difference was not appreciable Intratubal (32L 35L) comparisons between eggs with thick versus thin coronae did not show a significant difference in the number of spermatozoa.

*Denudation at 16 hours p.c.*

Five does provided material for this study The data on the cumuli and eggs which were recovered are recorded in table 6 Of the 51 eggs (corresponding with the number of ovulation points) which were recovered, four were enveloped in thick and four in thin coronae (fig 21) 28 had variable amounts of corona ranging from a few cells scattered on the surface of the zona (fig. 22) to a few clumps of corona cells interspersed with denuded areas (fig 23) and 15 were completely denuded (fig 24) one of which had a thin layer of mucin.

There were no egg-containing cumuli. The additional-cumuli had been broken up into smaller pieces in all of which the cell density was reduced and the elasticity ranged from two to zero.

*Denudation at 20 hours p.c*

Five does provided material for this study The data on eggs and additional-cumuli which were recovered are recorded in table 7 Forty five of the 49 eggs ovulated were recovered. All were denuded; 38 (84%) were coated with mucin ranging in thickness from 2 to 20 μ, and seven had no detectable mucin. One of the eggs with a thin layer of mucin is shown in figure 25.

Only two of the ten oviducts yielded additional-cumuli in these the cell density was either standard" or reduced and the elasticity was one or zero.

*Additional observations on cumuli obtained from mated and non-mated does*

In the section "Materials and Methods it was pointed out that only cumuli 0.5 mm or longer were recorded. It is therefore emphasized here that at 16 20 and 24 hours after the ovulatory injection, and at 12 16 and 20 hours p.c. small pieces of cumulus were identified in the flushings.

TABLE 6

*Characteristics of additional-cumuli and number of eggs recovered from oviducts 16 hours post coitum*

| Rabbit no. | No. of eggs recovered | Additional-cumuli | | |
|---|---|---|---|---|
| | | Size | Cell density | Elasticity |
| | | mm | | |
| 38 L | 3 | 2 0.5×0.5×0.5 | reduced | 2 |
| R | 6 | 1 5×0.5×0.5 | reduced | 2 |
| | | 1 1.5×1×1 | reduced | 2 |
| | | 2 1×1×1 | reduced | 2 |
| | | 2 0.5×0.5×0.5 | reduced | 2 |
| 39 L | 6 | 2 1×1×1 | reduced | 2 |
| R | 4 | none | — | – |
| 40 L | 7 | none | — | – |
| R | 4 | none | — | – |
| 41 L | 5 | none | — | – |
| R | 5 | none | — | – |
| 42 L | 2 | 2 2.5×1×1 | reduced | 0 |
| | | 5 1×1×1 | reduced | 0 |
| R | 6 | 6 1×0.5×0.5 | reduced | 1 |

TABLE 7

*Characteristics of additional-cumuli and the number of eggs recovered from oviducts 20 hours post coitum*

| Rabbit no. | Eggs recovered | | Additional-cumuli | | |
|---|---|---|---|---|---|
| | Total no. | No. coated with mucin | Size | Cell density | Elasticity |
| | | | mm | | |
| 43 L | 7 | 7 | none | — | – |
| R | 5 | 5 | none | — | – |
| 44 L | 1 | 1 | 4 1×1×1 | reduced | 1 |
| | | | 10 0.5×0.5×0.5 | reduced | 1 |
| R | 6 | 5 | none | — | – |
| 45 L | 2 | 2 | none | — | – |
| R | 7 | 7 | none | — | – |
| 46 L | 6 | 0 | 1 1.5×0.5×0.5 | standard | 0 |
| | | | 6 0.5×0.5×0.5 | standard | 0 |
| R | 5 | 5 | none | — | – |
| 47 L | 4 | 4 | none | — | – |
| | 2 | 2 | none | — | – |
| Total | 45 | 38 | | | |

It is notable that the cell density of the larger cumuli was reduced but never increased, whereas in the small pieces of cumulus, reduced and increased cell density occurred with roughly the same frequency The elasticity was zero in most of the pieces of cumulus which had increased cell density In pieces with reduced cell density some elasticity was retained; however due to their small size it was difficult to stretch them hence the degree of elasticity could not be ascertained accurately

At 16 hours after the ovulatory injection, from one to several clumps of cumulus cells, referred to as "aggregates, were observed in all the egg-containing cumuli (figs. 26 27) The photographs show that the cell density in such an aggregate is considerably increased. The occurrence of aggregates was recorded only sporadically for periods other than 16 hours after the ovulatory injection, since the significance of these cell formations was not appreciated. When additional experiments were completed, it was realized that the for-

mation of aggregates is correlated with ageing of the cumulus.

On several occasions clumps were observed in the cumulus which were thought to be aggregates when examined with the dissecting microscope. However when removed from the cumulus and examined under the compound microscope they were identified as acellular bodies surrounded by cumulus cells (fig 28) These bodies varied in size, the one shown in figure 28 was among the largest observed others were up to one quarter this size. Since they were not bodies of Call and Exner as was ascertained by comparing them with the photomicrographs shown by Brambell ('56) it is believed that these bodies have not hitherto been described. As these bodies were not systematically studied no further mention of them will be made in this study

When examining an egg which is still invested by a corona, such as the one shown in figure 19 one gains the impression that the corona cell processes extend through the zona pellucida. However it is easier to demonstrate these processes when the majority of corona cells have been denuded (figs. 29 30) Occasionally when a corona cell is removed (presumably *in vitro*) from the zona its process (or processes) is not removed with it (fig 31)

## DISCUSSION

### *Denudation of eggs in non-mated does*

The time required for denudation of the rabbit egg has been studied by Pincus ('30) and by Chang ('52) In Pincus's study does were mated to vasectomized bucks in order to induce ovulation At 17 hours after sterile mating, most of the eggs were still in cumulus and by 20 hours the vast majority were denuded and coated with a thin layer of mucin. Chang obtained material from does which were *superovulated by means of gonadotrophin* injections. He found that at 12 hours after the ovulatory injection all the eggs were in compact cumulus at 14 hours in loose cumulus at 16 hours two thirds of the eggs were in cumulus the rest in corona only and by 19 hours most of the eggs were denuded.

According to both Pincus and Chang, denudation is virtually completed by 20 hours. In the present study at 20 hours denudation had occurred in just over 50% of the eggs and had reached 100% between 20 and 24 hours. However the difference between the results of the present study and those of Pincus and Chang is not considered to be significant.

The mechanism causing denudation is unknown; Swyer (47) suggests that it is mechanical, with both cilia and muscular contractions of the oviduct playing a part. A rational assumption would be that due to tubal action the cumulus is gradually removed followed by removal of the corona. However the present study by showing that changes in the corona precede changes in the cumulus disproves this supposition. Thus, it was found that, although at 16 hours the cumuli which contained eggs looked very similar to 12-hour *cumuli, the thickness of the corona had* been reduced and in several eggs parts of the zonae were already free from corona cells (see fig 6) This could not have been merely due to physical action of the tube since the corona was still enveloped in the cumulus. The change in the corona could have been initiated by a chemical action of the tube or the egg, or alternatively it could be an inherent property of the corona cells. Evidence in support of a chemical action of the tube can be adduced from *experiments* of Smith (49) who when incubating eggs in cumulus frequently noted detachment of corona cells from the zona when the preparation contained scrapings of tubal mucosa however detachment of corona cells did not occur in the absence of the mucosal scrapings.

What happens to the corona cells during the process of denudation *in vivo* is quite obscure. It is possible that the corona cells migrate away from the egg, and that they do so under the influence of some *chemical secreted by the tubal* mucosa, which diffuses through the matrix of the cumulus so that a concentration gradient is formed which is lowest near the egg and rises towards the periphery of the cumulus. This would mean that the corona cells respond to chemotaxis viz. they migrate from regions of low to regions of

high concentration of the substance. It is emphasized that the suggestion concerning corona cell migration and their chemotaxis is pure speculation. While changes in the corona began to appear between 12 and 16 hours, changes in the cumulus started between 16 and 20 hours although a slight decrease in elasticity was already noted in some of the additional cumuli at 16 hours. The changes in the cumulus were: breakdown into smaller pieces, either reduction or increase in cell density and a gradual loss of elasticity

The breakdown of the cumulus is undoubtedly influenced by muscular contractions of the oviduct, although a chemical action by the tubal secretions is probably also involved. At 20 hours the cell density was reduced in about half the cumuli recorded (see table 3) The fact that the cell density in all the cumuli at 24 hours was "standard" does not necessarily mean a deviation from the trend towards a change in cell density probably the cumuli in which a change occurred had been broken up into small pieces which were not recorded. Regardless of the period at which they were recovered, most of the small pieces of cumulus exhibited either reduced or increased cell density indicating that both changes are correlated with ageing of the cumulus. Increased cell density was not recorded in the larger pieces of cumulus except when the cumuli contained aggregates (see figs. 26 27) It is suggested that the changes in cell density occur as a result of migration of the cumulus cells. No ready explanation can be offered as to why in some cases the cells migrate out of the matrix and in other cases towards each other to form aggregates. That cumulus cells have the ability to migrate was indicated by Blandau ('59) who had observed *in vitro* such migrations in freshly ovulated rat cumuli.

The results indicated that during the period of 12 to 24 hours after the ovulatory injection, a very gradual reduction in the elasticity of the cumulus occurred. On the other hand, in most of the small pieces of cumulus with an increased cell density the elasticity had fallen to 0 suggesting that, at least in a certain proportion of the cumuli, ageing is associated with loss of elasticity

*Denudation of eggs in mated does*

The schedule of denudation in does which had been mated to fertile bucks according to Pincus ('30) was as follows at eleven and one-half hours p.c. most of the eggs were devoid of cumulus but in thick corona; at 13 hours p.c. most eggs were in thin corona, by 15 hours p.c. all the eggs were denuded and a very thin layer of mucin could already be detected on their zonae. Chang ('51a) using superovulated does, found that most eggs were denuded by 16 hours p.c. The rate of denudation in the present study was somewhat slower although the difference was not considerable. Thus at 12 hours p.c. 28 (51%) of the 55 eggs recovered were still in cumulus, 19 of them in thick and nine in thin corona, of the remaining 27 eggs already out of cumulus six were in thick and 21 in thin corona. By 16 hours p.c. denudation was not yet completed of the 51 eggs recovered eight (16%) were invested in corona (four in thick and four in thin corona) 28 had variable amounts of corona interspersed with denuded areas, whereas 15 (29%) eggs were completely denuded, one of which had a thin layer of mucin. Denudation reached completion between 16 and 20 hours p.c. all the 45 eggs recovered were denuded 38 (84%) being coated with mucin

At 12 hours p.c. differences were observed between egg-containing cumuli and additional-cumuli whereas no changes were detected in the egg-containing cumuli (as compared with cumulus recovered at 12 hours after an ovulatory injection) in most of the additional-cumuli either the cell density or the elasticity or both were altered (see table 5) At 16 hours p.c. the cell density was reduced and the elasticity ranged from two to one in all the additional-cumuli. At 20 hours p.c. only two of the ten oviducts yielded additional-cumuli with elasticity ranging from 1 to 0 the cell density in the cumuli from one oviduct was standard, and from the other oviduct, reduced. The absence of additional-cumuli in eight out of the ten oviducts examined, shows that by 20 hours

p.c. most of the cumuli had disintegrated into small pieces.

It is evident that the changes in the cumulus (i.e. in size, cell density and elasticity) as well as those in the corona appear several hours earlier in mated than in non-mated does. Thus in mated animals at 12 hours p.c. denudation was in a somewhat more advanced stage than at 16 hours in the non-mated animals. During subsequent periods too denudation in the mated animals was more than four hours ahead of that in non-mated animals. Why is denudation faster in the mated animals? The mating act and the presence of seminal plasma in the female reproductive tract can be ruled out as factors contributing to denudation, since in Pincus's ('30) experiments in which does were mated with vasectomized bucks to induce ovulation, the schedule of denudation was similar to that observed with non-mated animals in the present study. Therefore, the only remaining factor which differentiates the mated from the non-mated is the presence of spermatozoa in the female reproductive tract, or more specifically at the site of denudation (i.e. in the oviduct).

There was some indication that denudation was more advanced in eggs containing a larger number of spermatozoa (see table 5). This is supporting evidence that spermatozoa are responsible for the accelerated rate of denudation in mated animals. It is generally accepted that this is due to the hyaluronidase carried by the spermatozoa (Chang, '51a; Chang and Pincus '51; Austin '61). Hyaluronidase depolymerizes hyaluronic acid which is contained in the cumulus matrix, thereby liquefying it; as a result the cumulus cells fall away from the egg. In the discussion that follows the validity of the hyaluronidase theory is examined and challenged.

*The hyaluronidase theory*

Until '46 the prevalent theory had been that the fertilizing spermatozoon cannot reach the egg unless the egg's cumulus is dispersed. It was assumed that the site of fertilization is reached by a large number of spermatozoa, which provide a sufficient concentration of hyaluronidase for the dispersion of the cumulus. This assumption was based on the fact that a concentration of 20 000 spermatozoa per cubic millimeter was needed for the dispersal of rabbit cumulus *in vitro* (Pincus and Enzmann '36).

This theory was invalidated on two grounds. (1) It was shown that the rat egg is penetrated by the spermatozoon before any visible dispersal of the cumulus cells occurs (Leonard, Perlman and Kurzrok, '47; Austin '48a; Austin and Smiles, '48; Blandau and Odor '49; Bowman, '51). In the rabbit also, it was shown that denudation was not a prerequisite for sperm penetration into the egg (Chang, '51a). (2) It was established that not millions, but only very few spermatozoa reach the site of fertilization: in the mouse a mean of 17 spermatozoa (Braden and Austin, '54); in the rat, less than 50 spermatozoa (Austin, '48b; Blandau and Odor '49) and in the rabbit, less than 1,000 spermatozoa (Austin, '48b; Chang, '51b; Braden, '53).

Consequently the idea that substantial quantities of hyaluronidase reach the site of fertilization was abandoned. Instead, the hypothesis was advanced that the individual spermatozoon is able to traverse the matrix of the cumulus owing to the hyaluronidase it carries (Leonard, Perlman and Kurzrok, '47; Austin '48a; Blandau and Odor '49; Chang '51a). However this hypothesis too is open to criticism: (1) Blandau ('59) discredited it on the grounds that the speed at which spermatozoa swim through the cumulus, as observed *in vitro* was too rapid to allow depolymerization of the cumulus matrix ahead of the spermatozoon. (2) Rabbit semen was treated with a hyaluronidase inhibitor before insemination yet spermatozoa made their way into the perivitelline space of the eggs (Parkes, Rogers and Spenseley '54). This indicates that although the sperm hyaluronidase was inhibited spermatozoa were still capable of transversing the cumulus.

*Alternatives to the hyaluronidase theory*

In view of the foregoing account, it is doubtful whether a spermatozoon's ability to make its way through the cumulus is due to the hyaluronidase it carries. It is

also doubtful whether the small number of spermatozoa at the site of fertilization, carrying minute amounts of hyaluronidase, could accelerate the rate of denudation by acting directly on the cumulus matrix.

Substances other than hyaluronidase have been shown to disperse cumulus cells *in vitro* pancreatin (Yamane '30) trypsin (Pincus and Enzmann '36) and ascorbic acid alone or in combination with hydrogen peroxide (Rodel and Karg, '55) but there is no evidence that any of these substances are involved in denudation *in vivo*

Apparently then, the accelerated denudation of eggs *in vivo* in the presence of spermatozoa, cannot be adequately explained in the light of the available facts. As the hyaluronidase theory is not acceptable two new hypotheses are proposed. A substance (or substances) secreted by the oviduct initiates denudation, affecting first the corona and, a little later the cumulus. Muscular contractions and perhaps also ciliary action, supplement the denudation process after it has been initiated chemically This sequence is similar in both mated and non-mated animals. In the mated animals, however the spermatozoa carry a certain agent, probably an enzyme, which does not act directly on the cumulus but acts as a catalyst accelerating the chemical reaction involved in denudation. A second possibility is that the spermatozoa affect the eggs rather than the tubal secretion. Thus, following sperm penetration, the egg releases a substance which accelerates denudation.

## SUMMARY

The newly ovulated egg is enclosed in the corona — a four to eight cell thick investment, which in turn is surrounded by the cumulus. With time both the corona and the cumulus become removed from the egg which is then said to be denuded In the present study the successive stages of denudation are described and illustrated pictorially in the mated and non-mated doe. Hitherto the denudation of eggs has been attributed to the physical action of the oviduct therefore it might be assumed that the outer covering — the cumulus — is removed first, followed by removal of the corona. However this assumption is invalidated by the present observations which show that a reduction in the number of corona cell layers precedes changes that take place in the cumulus. The reduction in the thickness of the corona is attributed to a chemical action, possibly exerted by the tubal secretions. It is postulated that both physical and chemical action by the oviduct may be involved in inducing changes in the cumulus. These changes are break up into smaller pieces, either reduction or increase in cell density and gradual loss of elasticity

The progress of denudation is described at four hour intervals at 12 16 20 and 24 hours after the ovulatory injection in non-mated does and at 12, 16 and 20 hours p c. in mated does. Denudation is faster by about four hours in the mated does. It is generally accepted that the more rapid denudation in mated does is due to the hyaluronidase carried by spermatozoa which acts by liquefying the cumulus matrix. The evidence for this explanation is examined. It is concluded that spermatozoa are unlikely to accelerate the rate of denudation by acting directly on the cumulus matrix, since only very minute quantities of hyaluronidase are carried by an individual spermatozoon, and since only a small number of spermatozoa reaches the site of fertilization. Therefore two alternative hypotheses are proposed. (1) That spermatozoa carry a certain agent probably an enzyme which acts as a catalyst, accelerating the chemical reaction involved in denudation. (2) That following sperm penetration into the egg the egg releases a substance which accelerates denudation.

## ACKNOWLEDGMENTS

I wish to thank Dr T R. R. Mann, F.R.S for reading the manuscript. Financial support from the Population Council (U.S.A.) and from the Agricultural Research Council (U.K.) is gratefully acknowledged.

## LITERATURE CITED

Austin, C. R. 1948a Function of hyaluronidase in fertilization. Nature, 162. 63–64.

——— 1949b Number of sperms required for fertilization. Ibid., *162* 534–535.

——— 1961 The Mammalian Egg. Blackwell Scientific Publications, Oxford.

Austin, C. R., and J Smiles 1948 Phase-contrast microscopy in the study of fertilization and early development of the rat egg J R. micr Soc., 68 13–19

Blandau, R. J 1959 In Physiological Mechanisms Concerned with Conception. Ed. W O. Nelson. Pergamon Press, New York. (In press.)

Blanda R. J and D. L. Odor 1949 The total number of spermatozoa reaching various segments of the reproductive tract in the female albino rat at intervals after insemination. Anat. Rec 103: 93–110.

Bowman, R. H. 1951 Fertilization of undenuded rat ova. Proc. Soc. exp. Biol. & Med 76 129–130.

Braden, A. W H 1953 Distribution of sperms in the genital tract of the female rabbit after coitus. Aust. J biol. Sci., 6 693–705.

*Braden A W H., and C. R. Austin 1954 The* number of sperms about the eggs in mammals and its significance for normal fertilization Aust. J biol. Sci 7 543–551

Brambell, F W R. 1956 In Marshall' Physiology of Reproduction chap. 5. Ed. A. S. Parkes. Longmans Green & Co., London.

Chang, M C. 1951 Fertility and sterility as revealed in the study of fertilization and development of rabbit eggs. Fertil. & Steril., 2: 205–222.

——— 1951b Fertilization in relation to number of spermatozoa in the Fallopian tubes of rabbits. Ann. ostet. ginecol. Milano, 73 918–925.

——— 1952 Fertilizability of rabbit ova and the effects of temperature *in vitro* on their subsequent fertilization and activation *i vivo*. J Exp. Zool., *121* 351–381

Chang, M C., and G. Pincu 1951 Physiology of fertilization in mammals. Physiol. Rev 31 1–26.

Harper M. J K. 1961 The time of ovulation in the rabbit following the injection of luteinizing hormone. J Endocrin 22 147 152.

Leonard, S. L., P L. Perlman and R. Kurzrok 1947 Relations between time of fertilization and follicle cell dispersal in rat ova. Proc. Soc. exp. Biol. & Med., 66 517–518

Parkes, A. S., H. J Rogers and P C. Spensley 1954 Biological and biochemical aspects of the prevention of fertilization by enzyme inhibitors. Proc. Soc. Study Fertility *6* 65–80.

Pincus, G. 1930 Observations on the living eggs of the rabbit. Proc. roy Soc., *107* 132–167

Pincus, G and E. V Enzmann 1936 The comparative behaviour of mammalian eggs *i vivo* and *i vitro*. II. The activation of tubal eggs of the rabbit. J Exp. Zool., 73 195–208.

Rodel L., and H. Karg 1956 Beitrag zum Mechanismus des Befruchtungsvorganges bei Saugetieren. Dtsch. tierarztl. Wschr 62 25–28.

Smith, A. V 1949 Cultivation of rabbit eggs and cumuli for phase-contrast microscopy Nature *164* 1136–1137

Swyer G I. M. 1947 A tubal factor concerned in the denudation of rabbit ova. Ibid., *159*, 873–874

Yamane J 1930 The proteolytic action of mammalian spermatozoa and its bearing upon the second maturation division of ova. Cytologia *1* 394–403.

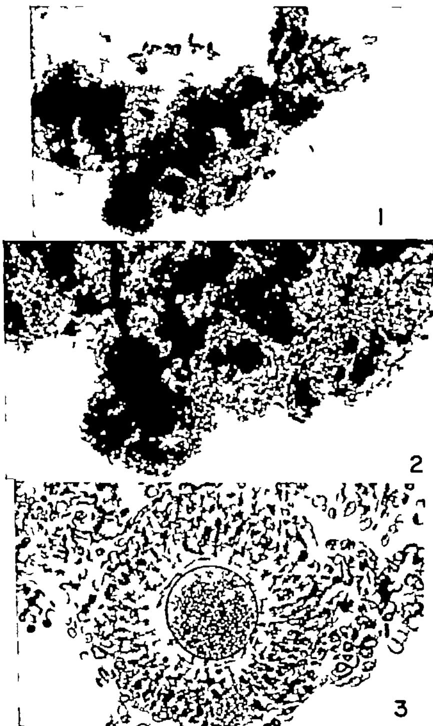
## PLATE 1

### EXPLANATION OF FIGURES

1 Cumulus mass recovered 12 hours after the ovulatory injection. × 14

2 The central area of the cumulus shown in figure 1 Four eggs are recognizable. × 33.

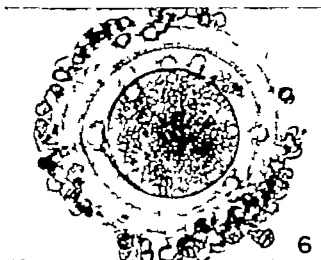
3 Egg removed from cumulus recovered 12 hours after the ovulatory injection. Note thick corona partly surrounded by cumulus. × 224.


1
2
3

## PLATE 3

### EXPLANATION OF FIGURES

6–8 Eggs removed from cumuli recovered 16 hours after the ovulatory injection, showing smallest, verage, and largest amount of corona respectively × 358. × 358 × 221


6

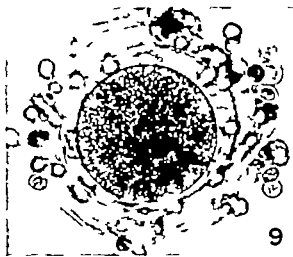

7


8

## PLATE 4

EXPLANATION OF FIGURES

9–11 Eggs recovered 16 hours after the ovulatory injection, showing smallest, average and largest amount of corona respectively. All × 358.


9

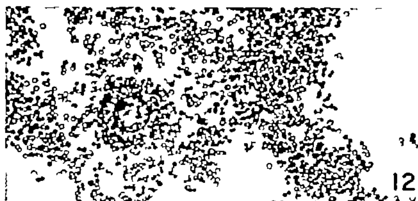

10

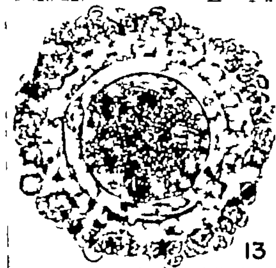

11

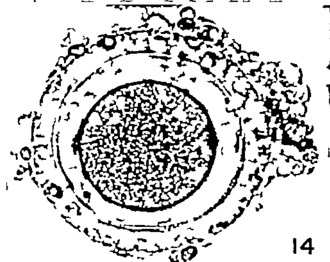
## PLATE 5

### EXPLANATION OF FIGURES

12–14 Eggs recovered 20 hours after the ovulatory injection. Figure 12 In cumulus. × 88. Figure 13 In thin corona. × 358 Figure 14 Almost denuded. × 358.


12


13


14

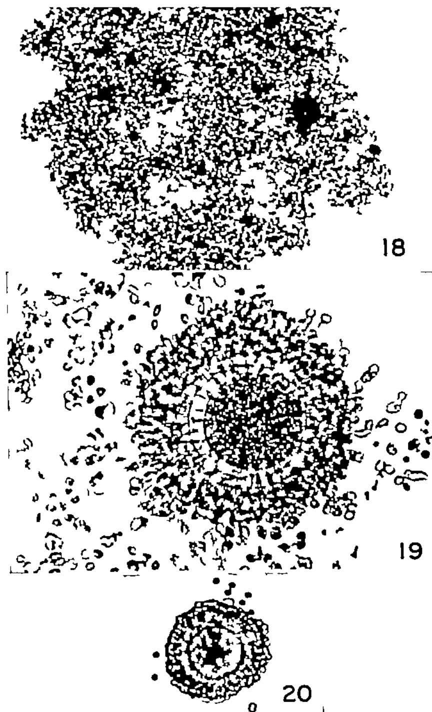
## PLATE 7

EXPLANATION OF FIGURES

18 Egg in cumulus recovered 12 hours p.c × 35.

19 Egg removed from cumulus, recovered 12 hours p.c. × 224.

20 Egg in thin corona recovered 12 hours p.c. × 140.

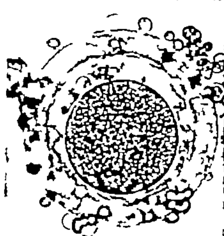

18
19
20

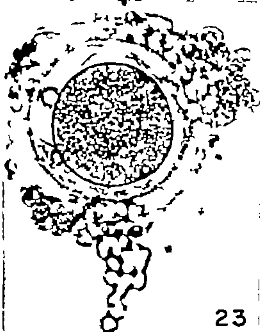
## PLATE 8

### EXPLANATION OF FIGURES

21–24 Eggs recovered 16 hours p.c. Figure 21 In thin corona. × 358. Figure 22 With few corona cells attached to the zona pellucida × 286. Figure 23 With few clumps of corona. × 358. Figure 24 Denuded. × 358.


21


22


23


24

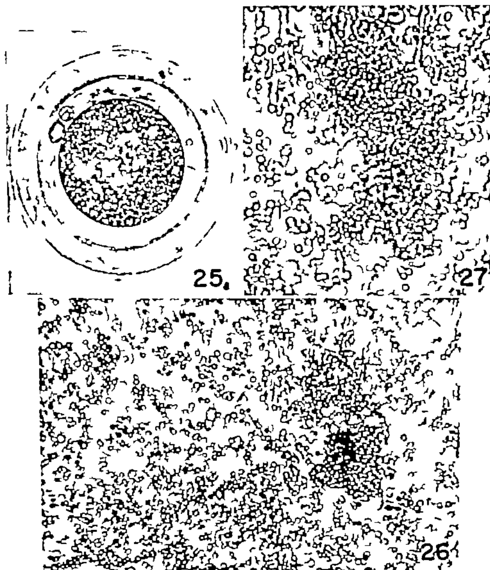
## PLATE 9

### EXPLANATION OF FIGURES

25 Denuded egg coated with mucin recovered 20 hours p.c. × 358

26 A aggregate in a cumulus mass recovered 10 hours fter the ovulatory injection. × 88

27 A higher magnification of the aggregate shown in figure 26. × 140.


25
27
26

## PLATE 10

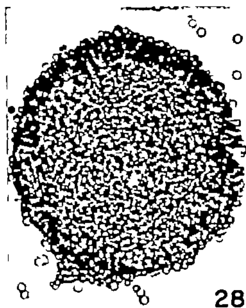
### EXPLANATION OF FIGURES

28 Spherical body of unknown nature removed from a cumulus mass × 170

29 Three corona cells on the surface of the zona pellucida. Not process projecting from each of two corona cells and extending through the zona pellucida. Phase contrast. × 1 400.

30 A corona cell with its process extending through the zona pellucida × 898.

31 Coron cell processes extending through the zona pellucida. Note bsence of corona cells. Phase contrast. × 898.


28


29


30


31

# A Histochemical Study of Hypophysectomy induced Changes in Rat Submandibular and Sublingual Glands

JOSEPH H. KRONMAN
*Tufts University School of Dental Medicine Boston, Mass.*

There are extensive references in the literature concerning the interrelationship of the salivary glands and the endocrine system. Bixler Webster and Muhler ('57) noted marked histologic changes in the rat submandibular gland following hypophysectomy These changes were characterized by atrophy in the duct system, particularly the granular tubules. In hypophysectomized mice Lacassagne and Chamorro ( 40) found repair in the tubular structure of the submandibular gland after androgen administration. Utilizing submandibular gland homogenates Sreebny ('60) noted drastic reductions in the protease levels of hypophysectomized rats. Shafer Clark and Muhler ('56) and Shafer and Muhler ('56) found that in the submandibular gland of the rat, a combination of thyroxine and testosterone completely prevented the decrease in proteolytic activity and the tubular atrophy which follows hypophysectomy In one of the few studies of histochemical changes in rodent submandibular glands following hypophysectomy Bixler Muhler et al. ('57) reported reduction in acinar RNA.

The purposes of the current investigation were to characterize histochemically the changes in the submandibular gland following hypophysectomy and to ascertain whether hypophysectomy-induced changes were manifest in the acinar cells as well as in the ductal and tubular segments. This investigation was extended to include the sublingual gland because of sparse information relating this gland to endocrine influences

## MATERIALS AND METHODS

Seven hypophysectomized and five untreated female Wistar strain rats were used. The rats were hypophysectomized at 22 days of age, and all the animals were killed by decapitation at 12 weeks. Animals were fed an unsupplemented Chow diet *ad libitum*. Histologic examination confirmed the success of the hypophysectomy At death, the submandibular-sublingual gland complex was immediately removed and placed in neutral buffered formalin (NBF) cold acetone or Susa fixative After routine paraffin embedding the tissues were sectioned at 7 µ, stained dehydrated, and mounted in Permount. Those sections to be utilized for the demonstration of acid and alkaline phosphatase, however were mounted directly in glycerine jelly after staining.

Morphology was studied on NBF-fixed tissues stained with hematoxylin and eosin Azan staining of Susa-fixed material as recommended by Jacoby and Leeson ('59) was also employed for morphologic examination, particularly of the granular tubules. Tryptophan and tyrosine (NBF-fixed tissues) were demonstrated with the techniques of Glenner and Lillie ('57 '59) Sulfhydryl groups (NBF) were stained by means of the DDD (2,2'-dihydroxy-6 6'-dinaphthyl disulfide) procedure described by Barrnett and Seligman ('52)

Aqueous toluidine blue (0 05% pH 4.5) was used for the demonstration of RNA and metachromasia after NBF Susa and acetone fixation. Parallel control sections were incubated for one hour at 37°C in an unbuffered ribonuclease solution (1 mg ml) prepared with glass-distilled water The Alcian blue (pH 1 8) and Feulgen reactions were combined for the demonstration of acid mucopolysaccharides and DNA respectively In order to release ld hyde groups from the deoxypentose

faintly reactive and the duct system was negative. In the hypophysectomized animals fewer acinar cells were strongly reactive and in these, the response was not as intense as in the controls (fig. 11). The reaction in the majority of these cells was only faint. The duct system was again negative. Malt diastase and distilled water treatment did not alter the PAS response in the submandibular gland of normal (figs. 12 and 13) or hypophysectomized animals.

Strong alkaline phosphatase activity was localized in the connective tissue and probably the capillaries as well as at the basal end of the acinar cells of untreated animals. The remainder of the acinar cells as well as the entire duct system, showed no alkaline phosphatase activity histochemically (fig. 5). In the hypophysectomized rats alkaline phosphatase was not detectable in any area of the parenchyma (fig. 6). In all instances, the parallel control slides (incubated in buffer without substrate) were negative.

A faint, uniform acid phosphatase reaction was observed throughout the parenchyma of the submandibular gland in both treated and untreated animals. No differences were observed between the groups. The parallel control sections (incubated in buffer solution without substrate) were negative.

*Sublingual gland*

Histologic examination of hematoxylin and eosin as well as Azan-stained tissues revealed no morphologic variations between the sublingual glands of the untreated and hypophysectomized animals. The structure consisted of mucous alveoli, serous demilunes and intercalated ducts, which, in turn, emptied into secretory ducts. Granular tubules were not present.

The histochemical demonstration of tryptophan, tyrosine and sulfhydryl groups revealed faint staining in the basement membranes, demilunes and duct system of the sublingual gland. The mucous alveoli were negative. No variations were observed in the treated and control animals.

After NBF and Susa fixation the toluidine blue procedure revealed an orthochromatic alveolar response of moderate intensity the duct system was negative. No variations between the treated and untreated groups were noted. Following acetone fixation, the moderate alveolar reaction in the control animals was again orthochromatic. In the hypophysectomized rats, however a strong metachromatic response was observed in the alveolar cells. In all instances the duct system was negative.

The Alcian blue and Feulgen reactions were identical in both treated and untreated animals. An intense uniform, Alcian blue response was noted throughout the alveolar portion of the sublingual gland. The duct system was negative. The nuclei were DNA positive throughout all glandular components.

No variations in the PAS reaction were observed between the untreated and hypophysectomized animals. The alveolar cells were intensely PAS-positive the duct system was negative. Prior water incubation produced no changes but diastase of malt treatment resulted in a diminished PAS response (figs. 14 and 15). Although the alveolar cell reaction became faint, the basement membranes remained strongly reactive.

Histochemical study of enzymes revealed no alkaline phosphatase activity in the sublingual glands of treated or untreated animals. Acid phosphatase activity however was faint and restricted to demilune cells and the duct system. The response was comparable in the untreated and hypophysectomized rats. All control slides (incubated in buffer without substrate) were negative.

DISCUSSION

Morphologic changes in the rat submandibular gland following hypophysectomy were in accord with the findings of Eartley and Leblond ('54) and others. The major morphologic alterations were atrophic changes in the granular tubules. It was not surprising therefore to observe concomitant histochemical alterations in this component of the submandibular gland. Hypophysectomy-induced morphologic changes in the sublingual gland were not observed.

In the submandibular gland of the normal female rat, protein reactions were pri-

marily localized in the ductal components. The localization of tryptophan and tyrosine was comparable to that reported in the hamster (Kronman '63) The localization of tyrosine was similar to that reported in the rat by Junqueira ( 49) and in the mouse by Junqueira et al ( 49) Distribution of the sulfhydryl reaction agreed with the reported investigation of Kensaku Deguchi, and Ryuichi ('62) Following hypophysectomy reactivity of all protein constituents was diminished The reduction of protein reactivity in the treated animals therefore was undoubtedly related to the atrophic changes in the ductal components. This theory is further substantiated by the lack of concomitant acinar changes Protein histochemistry within the sublingual gland was unchanged by hypophysectomy The insensitivity of this gland to alteration in pituitary function agreed with the findings of Baker and Abrams ( 55) These investigators reported changes of only minor importance in mucus-secreting glands following hypophysectomy It may be concluded therefore that protein metabolism within the sublingual gland is relatively unaffected by removal of the pituitary

The toluidine blue reaction in the submandibular gland of the untreated rat was uniform and orthochromatic throughout the acinar cells. This was in accord with the findings of Quintarelli and Chauncey ('60) The ductal basophilia observed in acetone and NBF fixed control animals was comparable to the findings in normal hamsters (Kronman '62) The acinar cells of the hypophysectomized animals were unchanged In the duct system however basophilia was no longer present These findings were not in accord with those reported by Bixler et al ('57) These workers reported decreased acinar RNA in the rat submandibular gland following hypophysectomy In addition they observed no ductal cytoplasmic basophilia in the untreated animals. Since RNA is intimately related to the synthesis of secretory protein the ductal findings observed in this study are consistent wi h the decreased reaction of protein constituents described above

In the sublingual gland the toluidine blue reaction was the same in both groups after NBF and Susa fixation Following acetone fixation however the strong, metachromatic reaction in the alveolar cells of hypophysectomized animals contrasted with the orthochromatic response observed in the controls The exact significance of metachromasia is still not clearly defined Pearse ('60) stated

> from the theoretical point of view metachromasia signifies only the presence of free electronegative surface charges of a certain minimum density The older theory of specific groups cannot be sustained "

Although the mechanism of metachromasia may be uncertain, it can be stated that some difference does exist in the alveolar cells of the sublingual gland following hypophysectomy

The description of Alcian blue and Feulgen reactions in the submandibular and sublingual glands of the untreated rats agreed with the findings of Shackelford and Klapper ('62) Since no changes occurred after hypophysectomy it must be assumed that salivary gland acid mucopolysaccharides and DNA are not affected histochemically by this alteration in endocrine function

Changes were observed in the acinar cells (NBF) when the submandibular glands of treated and untreated animals were subjected to the PAS procedure Since no changes were apparent after diastase or distilled water incubation. water soluble glycoprotein and glycogen were not the observed PAS-positive material The chemical nature of this material will have to be established in subsequent biochemical studies. The faint reaction after acetone fixation may be related to diffusion of this NBF-stable PAS-positive material In the sublingual gland the alveolar cells of hypophysectomized and control rats were strongly PAS-positive Diastase treatment diminished the PAS reaction, but water incubation did not. It may be assumed therefore that glycogen was one of the major constituents in this glandular component

A review of the literature concerning alkaline phosphatase activity in normal rat submandibular glands is rather confusing Gomori ( 41) reported that the capillaries were the only active compo-

nents. Noback and Montagna ('57) found strong alkaline phosphatase activity in the parenchyma. Leeson ('56) stated that the myo-epithelial basket cells were the only active elements. The findings of the current study are in agreement with those of Gomori. In addition, this investigation established a reduction of alkaline phosphatase activity in the submandibular glands after hypophysectomy In the sublingual glands, alkaline phosphatase activity was negative. Acid phosphatase activity however was faint and restricted to the demilunes and the duct system. These findings in the sublingual gland agreed with those of Noback and Montagna ('57)

Although endocrine-salivary gland interrelationship is well documented further studies will have to be initiated in order to clarify its nature Sreebny ('60) stated that those salivary gland reactions induced by alteration of endocrine function were a result of non-specific metabolic effects Shafer Clark, and Muhler ('56) reported that the combination of thyroxine and growth hormone was completely effective in preventing hypophysectomy induced salivary gland changes. Yoshimura ('56) reported that the administration of somatotropin following hypophysectomy partially restored ductal cytology Sreebny Meyer Bachem and Weinmann ('57) reported that simultaneous administration of thyroxine and testosterone restored the submandibular gland to a nearly normal morphologic appearance Baker and Abrams ('55) and Volker ('58) included the possible role of the adrenal cortex in salivary gland regulation

The concept of non-specific versus specific hormonal influence on the salivary glands should be further clarified The controversy may be resolved when subsequent histochemical studies are employed Such studies must determine which hormone(s) restore normal morphologic appearance and histochemical reactions in rodent salivary glands after alteration of endocrine function

## SUMMARY

In addition to morphologic changes in rat salivary gland following hypophysectomy differences in tryptophan, tyrosine, sulfhydryl groups RNA metachromasia, 1 2 glycol linkage groups and alkaline phosphatase were demonstrated histochemically in this study In the duct system of the submandibular gland, RNA, tryptophan tyrosine and SH groups were less reactive in the hypophysectomized animals than in the controls. The PAS reaction was diminished in the acinar cells of the treated animals acid phosphatase activity was also decreased in hypophysectomized rats. The only hypophysectomy induced histochemical change observed in the sublingual gland was a metachromatic reaction in the alveoli of the hypophysectomized rats in contrast with an orthochromatic reaction in untreated animals.

## LITERATURE CITED

Baker B. L., and G D Abrams 1955 Growth hormone (somatotropin) and the glands of the digestive system. In The Hypophyseal Growth Hormone, Nature and Actions, (Edit. by R. W Smith Jr O. H. Gaebler and C. N H. Long) Chap. 6, pp. 107–122. The Blakiston Div McGraw-Hill Book Co., Inc.

Barrnett, R. J and A. M. Seligman 1952 Demonstration of protein bound sulfhydryl and disulfide groups by two new histochemical methods. J Nat. Cancer Inst., *13* 215–216.

Bixler D J C. Muhler R. C. Webster and W G Shafer 1957 Changes in submaxillary gland ribonucleic acid following hypophysectomy thyroidectomy and various hormone treatments. Proc. Soc. Exp. Biol. and Med., *94* 521–524

Bixler D R. C. Webster and J C. Muhler 1957 The effect of testosterone thyroxine and cortisone on the salivary glands of the hypophysectomized rat. J Dent. Res., *36* 566–570

Burstone M. S. 1953 A histochemical study of normal and irradiated salivary gland tissue in the mouse. Anat. Rec., *115* 543–55

Eartley H., and C. P Leblond 1954 Identification of the effects of thyroxine mediated by the hypophysis. Endocrin., *54* 249–271

Glenner G. G., and R. D Lillie 1957 The histochemical demonstration of indole derivatives by the post-coupled p-dimethylamino-benzylidene reaction. J Histochem. Cytochem., *5* 279–296

——— 1959 Observations on the diazotization-coupling reaction for the histochemical demonstration of tyrosine Metal chelation and formazan variants Ibid *7* 416–422.

Gomori G. 1941 The distribution of phosphatase in normal organs and tissues. J Cell. and Comp Physiol *17* 71–83

Hill C R., and G. H Bourne 1954 The histochemistry and cytology of the salivary gland duct cells Acta Anat., *20*: 116–128

Hot[illegible] s, R. D. 1948 A microchemical re[illegible] resulting in the staining of polysac

harkic structures in fixed tissue preparations. Arch. Biochem., 16 131–141
Jacoby F and C. R. Leeson 1959 The post natal development of the rat submaxillary gland. J Anat., Lond., 93 201–216.
Junqueira L. C. 1949 Estudo histológico, histoquimico, bioquimico experimental da glândula submaxilar do camondongo (*Mus. musculus L.*)
Junqueira, L. C., A. F fer M. Rabinovitch and L. Frankenthal 1949 Biochemical and histochemical observations on sexual dimorphism of mice J Cell. and Comp. Physiol., 34. 129–158.
Kensaku K., Y Deguchi and O Ryuichi 1962 Histochemical study of protein-bound sulfhydryl and disulfide groups in normal salivary glands. J Dent. Res., 41 104–111
Kronman, J H. 1962 A morphological and histochemical study of hamster salivary gland development. Ph.D dissertation, Medical College of Virginia, Richmond.
——— 1963 Hamster salivary gland sexual dimorphism. I. A protein histochemical study J Dent. Res., 42: 123–127
Lacassagne, A., and A. Chamorro 1940 Réaction la testostérone de la glande sous-maxillaire trophiée consécutivement a l'hypophysectomie chez la souris. Compt. Rend. Soc. de Biol., 134 223–224
Leeson C. R. 1956 Localization of alkaline phosphatase in the submaxillary gland of rat. Nature 178 858–859
Lillie R. D and J Greco 1947 Malt diastase nd ptyalin in place of saliva in the identifi cation of glycogen. Stain Tech., 22 67–70
McManus, J F 1948 Histological and histochemical uses of periodic acid. Ibid., 23 99–108.
Noback, C. R., and W Montagna 1947 Histochemical studies of basophilia, lipase and phosphatases in mammalian pancreas and salivary glands. Am. J Anat., 81 343–367
Pearse A. G. E. 1960 Histochemistry Theoretical and Applied. Little Brown and Co., Boston.
Quintarelli, G., and H H. Chauncey 1960 Metachromatic reactivity of mammalian submaxillary glands. Arch. Oral Biol., 2 169–168
Rutenburg A. M., and A. M. Seligman 1955 The histochemical demonstration of acid phosphatase by a post-incubation coupling technique. J Histochem. Cytochem. 3: 455–470.
Shackelford, J M and C. E. Klapper 1962 Structure and carbohydrate histochemistry of mammalian salivary glands. Am. J Anat., 111 25–47
Shafer W G., P G Clark and J C. Muhler 1956 The inhibition of hypophysectomy induced changes in the rat submaxillary glands. Endocrin., 59 516–521.
Shafer W G and J C. Muhler 1956 Some observations on the relationship between the salivary glands and endocrine system. J Am Coll. Dent., 23 193.
Sreebny L. M. 1960 Study of salivary gland proteases. Ann. N Y Acad. Sc., 85 182 188
Sreebny L. M J Meyer E. Bachem and J. P Weinmann 1957 Restoration of enzymatic activity in the submaxillary gl nd of the hypophysectomized albino rat. Endocrin 60 200–204
Volker J F 1938 Relation of salivary glands to certain endocrine glands. J Dent. Med 13 125–129
Yoshimura F 1956 Cytological changes in rat salivary glands following hypophysectomy and somatrophic hormone administration. Okaj Folia Anat. Jap 28 195–205.

## PLATE 1

### EXPLAN TION OF FIGURES

1 Granular tubule in submandibular gland of untreated rat. Azan-stained, Susa-fixed, × 400.

2 S bmandibular gland of hypophysectomized rat. Not marked reduc tion in t bular dimension Azan-stained Susa-fixed × 400.

3 Tryptophan reaction in normal rat submandibular gland. NBF-fixed 400.

4 Tryptophan reaction in hypophysectomized rat. Compare reaction in granular tubule (GT) with that in figure 3 NBF-fixed, × 400.

5 Alkaline phosph tase reaction in normal submandibular gland. Re action localized t basal end of acinar cells. Cold acetone-fixed × 400.

6 Alkaline phosph tase submandibular gland reaction in hypophysectomized rat Cold acetone-fixed × 400


GT

PLATE 2

EXPLANATION FIGURES

7 Submandibul gland of normal rat. Toluidine blue stain observe tubular cytoplasmic basophilia. NBF-fixed × 400.

8 Same figure 7 after prior ribonuclease digestion. Cytoplasmic basophilia removed.

9 Toluidine blue reaction in hypophysectomized rat submandibula gland. Acinar reaction comparable to figure 7 NBF-fixed × 400

10 PAS reaction in normal rat submandibular gland. NBF-fixed, × 400

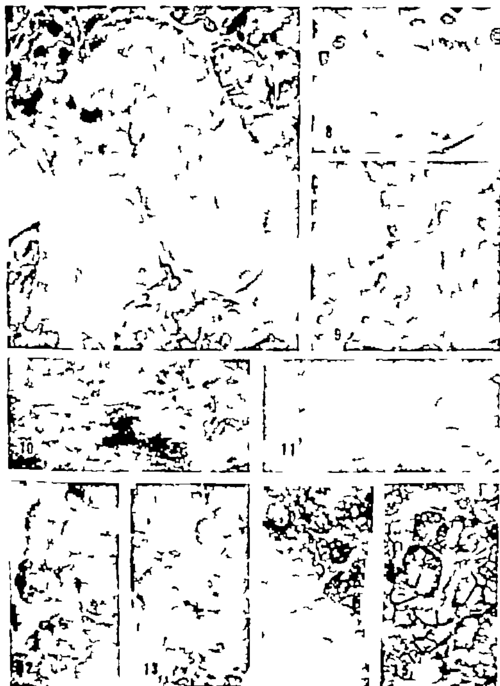
11 Same as figure 10 hypophysectomized rat.

12 Normal submandibular gland, PAS reaction NBF-fixed × 200.

13 Same as figure 12 after prior water incubation.

14 PAS reaction in normal rat sublingual gland. NBF-fixed, × 200.

15 Same as figure 14 after prior diastase treatment.


8
9
10
11
12
13
15

# Two Kinds of Extrafusal Muscle Fibers and Their Nerve Endings in the Garter Snake

ARTHUR HESS
*Department of Physiology University of Utah College of Medicine Salt Lake City Utah*

Ordinary extrafusal muscle fibers respond to nerve stimulation with a relatively rapid twitch. Such twitch fibers have a distinctive morphological appearance and innervation. Their fibrils are regularly separated from each other and cross sections of such muscle fibers have a punctate appearance (Fibrillenstruktur) Twitch fibers are usually innervated by a single motor end-plate. However other extrafusal muscle fibers, called slow fibers and found in the frog (Kuffler and Vaughan Williams, '53) chick (Ginsborg '60) and cat extraocular muscles (Hess and Pilar '63) respond to nerve stimulation with a prolonged contracture. In all the places where such slow fibers have been found, muscle fibers with a different morphological appearance and innervation from those of twitch fibers have been found. In these fibers, the fibrils in cross section appear to be larger less in number and irregularly separated from each other (Felderstruktur) (Krüger 49 Hess, '60 '61a '61b) These fibers have multiple motor endings, usually of the en grappe type, ending on a single muscle fiber That the physiologically slow fiber and the fiber with the more irregular distribution of fibrils (Felderstruktur) and multiple motor terminals are the same, can be best illustrated perhaps by referring to the anterior part of the latissimus dorsi of the chick where all the fibers are physiologically slow (Ginsborg '60) and all have the irregular distribution of fibrils (Felderstruktur) and multiple nerve endings (Hess, '61a) Confirmation of this view at least for frog muscle, has recently been provided by Peachey and Huxley ('62) Hence since there is a strong correlation between the physiological reaction and the morphological appearance and innervation of the muscle fiber it is apparent that extrafusal muscle fibers can be classified using either morphological or physiological standards as twitch type or slow type.

As discussed above slow type fibers have been found in amphibia birds and mammals. It was decided to see if such fibers occur also in reptiles.

## MATERIAL AND METHODS

The garter snake was used For study of muscle structure pieces of the dorsal longitudinal muscles and the muscles arising on the ribs and inserting into the skin were used As far as I can determine by referring to the studies of Auffenberg ('58 '61) on snakes other than the garter snake, the dorsal longitudinal muscles were the semispinalis et spinalis inter articularis superior and the longissimus The muscles were fixed in Dalton's or Susa fluid. The tissue was dehydrated and embedded in epon (Luft '61) Thin and thick sections were cut on Porter Blum or LKB microtomes. The thick sections of Dalton-fixed material were studied in the phase contrast microscope The thin sections of Dalton-fixed material were picked up on uncoated copper mesh grids stained with lead (Karnovsky '61; Millonig '61) and studied in an RCA EMU 3F electron microscope or in the Akashi Bendix Tronscope The thick Susa fixed sections were stained with a mixture of equal parts of 1% methylene blue in 1% borax and 1% azure II (Richardson Jarett and Finke '60) and studied in the light microscope

For study of the nerve endings pieces of muscle were fixed outstretched in 10% glyoxal in tap water treated with calcium carbonate. They were then teased and stained for cholinesterase by a modified

koelle procedure They were incubated in acetylthiocholine iodide or butyrylthiocholine iodide at a pH of 5 or 5 6 The higher pH yielded the more intense generally satisfactory preparations, although the more delicate staining at the lower pH was also instructive. Some teased preparations were treated with 5 × 10 diisopropylfluorophosphate before incubation After staining the teased preparations were mounted in glycerine.

The technique for studying fibers with known type of nerve endings in the light and electron microscopes will be described in the appropriate place below

## RESULTS

*Muscle fiber structure* Cross sections of stained Susa fixed muscle fibers reveal two kinds of muscle fibers. In one (figs. 10A 12) the fibrils are relatively small, regularly separated from each other and a punctate appearance is readily apparent. This type of muscle fiber is similar in structure to the twitch fiber in other animals. The other kind of muscle fiber (figs. 10B 12) has relatively larger fibrils which are separated from each other by irregular spaces This kind of muscle fiber is frequently smaller in diameter and stains more darkly This latter type of fiber is similar to the slow fibers previously described in other species

Cross sections of muscle in the electron microscope also demonstrate the differences between these two kinds of muscle fibers In one kind the twitch type muscle fiber (figs. 1 2A 3A) each fibril is more or less surrounded by sarcoplasmic reticulum and separated from its neighbor; hence this type would yield a punctate appearance in the light microscope In the other kind of muscle the slow type fiber (figs. 1 2B 3B) the fibrils are not separated from each other but adjacent fibrils frequently appear to join each other Sarcoplasmic reticulum is present especially at the level of the lighter I band but is much scantier in amount than in twitch type fibers.

Longitudinal sections also reveal these differences although in general not as obviously as in cross sections. Longitudinal sections of some muscle fibers show muscle fibrils with sarcoplasmic reticulum extending between the fibrils and separating adjacent fibrils from each other (fig. 4A) These are easily identified as twitch type fibers. In a like manner muscle fibers can be seen which are easily identified as slow type fibers (fig. 4B) In these the sarcoplasmic reticulum is present only in relatively small amounts at the level of the Z line and the I band, while essentially no sarcoplasmic reticulum can be seen separating neighboring fibrils in the level of the A band. However other muscle fibers are found which it is difficult in longitudinal sections to classify as fast or slow type. For instance a muscle fiber has been seen which has sarcoplasmic reticulum on either side of the H zone bisecting the A band with essentially none along the remaining portions of the A band (fig. 5) Nevertheless, it is my opinion that the muscle fibers of the snake do indeed fall into slow or fast type categories, even in longitudinal sections. And it is my impression that the distribution of sarcoplasmic reticulum in longitudinal sections is not always the best way to classify muscle fibers because the disposition of this material can differ depending on the level of the muscle fiber through which the section passes. In a longitudinal section of a muscle fiber which is not completely relaxed and whose fibrils are not necessarily stretched to the same length, it might be expected that the section would pass through at least slightly different levels of adjacent fibrils and hence yield pictures of the sarcoplasmic reticulum of slightly differing disposition, different enough at times to make it difficult in some sections of some fibers to classify the fibers.

*The nerve endings* The nerve endings seen on teased muscle fibers after cholinesterase staining are obviously of two kinds In one (figs. 6 9) the endings are darkly stained The whole ending most frequently tends to be circular in shape and always appears compact on the muscle fiber The units of the ending itself are composed of very closely approximated circles with intensely stained outer borders This more intensely stained part is probably the subneural aparatus. Sometimes the circles are not complete and two or more anastomose with each other to form short channels

The other ending presents a different [illegible]ce from this (figs. 7 8) It stains [illegible]her than be- [illegible]ds to spread [illegible] of the mus- [illegible]ng a greater [illegible]not as much [illegible]f consists of [illegible]l units with [illegible]erconnected [illegible]ly gives the [illegible]d along the [illegible]

[illegible]cribed is the [illegible]muscle. The [illegible]valent to the [illegible]er animals. [illegible] en grappe [illegible]have a cer [illegible]n the end- [illegible]red as hav [illegible] of grapes. [illegible]ween these [illegible]ore evident [illegible] individual [illegible]

[illegible]me on each [illegible]stretches of [illegible]l and two [illegible]seen on a [illegible]in one end- [illegible]r the dis- [illegible] extremely [illegible]n one en [illegible]ys seen on [illegible] The end- [illegible]y close to- [illegible]one ending [illegible]r For ex [illegible] 7A and B [illegible]n a teased [illegible]00 μ long [illegible]nd of the [illegible]is 1,300 μ, [illegible]nd ending [illegible]he third is [illegible] fourth is [illegible]e fifth is [illegible]ling to the [illegible]r is 600 μ. [illegible]ll the illus- [illegible]nations on [illegible]ld also be mentioned that an end-plate and an en grappe ending are never found on the same muscle fiber

All the muscles examined have fibers with multiple en grappe terminations. These fibers are by far in the minority in all instances and much less than half of the fibers in the muscles examined have multiple nerve terminations. Quantitative studies were not performed. However the muscle slips from the ribs to the skin appear to have the largest percentage of fibers with multiple endings while the muscle identified as the interarticularis superior has the least number of such fibers with the other muscles having an intermediate number

Both end-plate and en grappe endings are revealed after incubation in acetylthiocholine iodide with diisopropylfluorophosphate treatment (which reveals only true cholinesterase) and after incubation in butyrylthiocholine iodide (which reveals only pseudocholinesterase) Hence, all types of endings have both true and pseudocholinesterase which is true for all nerve endings thus far investigated in other animals. As a control, treatment with diisopropylfluorophosphate and subsequent incubation in butyrylthiocholine iodide results in no staining.

*Correlation of kind of muscle fiber and kind of nerve ending* Although two different kinds of nerve termination have been found on two different kinds of muscle fiber it is still necessary to determine if a certain type of nerve ending is restricted to one kind of muscle fiber Hence muscle fibers with known type of ending were viewed in the microscope both light and electron to determine the type of muscle fiber

Muscle fibers previously fixed in glyoxal, stained for cholinesterase and mounted in glycerine were rinsed in water refixed in Susa or Dalton, dehydrated, and embedded in epon. Thicker sections of Susa fixed material were stained and studied in the light microscope Thin sections of Dalton-fixed fibers were studied in the electron microscope

Cross sections of muscle fibers with known end-plate endings, refixed in Susa (fig. 13A) reveal a punctate distribution of the fibrils The fibrils are separated from each other by rather regular dis-

Hess, A. 1960 The structure of extrafusal muscle fibers in the frog and their innervation studied by the cholinesterase technique. Am. J Anat., *107* 129–152.

——— 1961a Structural differences of fast and slow extrafusal muscle fibers and their nerve endings in chickens. J Physiol., London 157 221 231

——— 1961b The structure of slow and fast extrafusal muscle fibers in the extraocular muscles and their nerve endings in guinea pigs. J Cell. and Comp. Physiol., 58 63–80

Hess, A., and G. Pilar 1963 Slow muscle fibers in the extraocular muscles of the cat. J Physiol., London. In press.

Hines, M. 1932 Studies in the innervation of skeletal muscle. IV Of certain muscles of the boa constrictor. J Comp. Neur., *56*: 105–133.

Karnovsky M. J 1961 Simple methods for staining with lead" at high pH in electron microscopy J Biophysic. Biochem. Cytol., *11*: 729–732.

Krüger P 1949 Die Innervation der tetanischen und tonischen Fasern der quergestreiften Skeletmuskulatur der Wirbeltiere. Anat. Anz., 97 169–175.

Kuffler S. W and E. M. Vaughan Williams 1953 Small-nerve junctional potentials. The distribution of small motor nerves to frog skeletal muscle, and the membrane characteristics of the fibers they innervate. J Physiol., London, *121* 289–317

Kulchitsky N 1924 Nerve endings in muscle. J Anat., London, *58* 152–169.

Luft, J H. 1961 Improvements in epoxy resin embedding methods. J Biophysic. Biochem. Cytol., *9* 409–414

Millonig, G., 1961 A modified procedure for lead staining of thin sections. Ibid., *11*: 736–739

Peachey L. D and A. F Huxley 1962 Structural identification of twitch and slow striated muscle fibers of the frog. J Cell. Biol., *13* 177–180.

Richardson, K. C., L. Jarett and E. H. Finke 1960 Embedding in epoxy resins for ultrathin sectioning in electron microscopy Stain Tech., 35 313–323.

Smith, G. E. 1926 Discussion on the sympathetic innervation of striated muscle. Proc. Roy Soc. Med., *19*: 16–23. (Section of Neurology )

Tiegs, O W 1932 The innervation of the striated musculature in python. Austral. J exp. Biol. and Med. Sci., *9* 191–201

——— 1953 Innervation of voluntary muscle. Physiol. Rev 33: 90–144.

## PLATE 1

### EXPLANATION OF FIGURES

Electron micrographs of cross sections (slightly oblique) of snake muscle fibers. The line on each photograph indicates 1 μ.

1A Slow type muscle fiber on the top twitch type muscle fiber on the bottom. × 8,800.

1B Twitch type muscle fiber on the top slow type muscle fiber on the bottom. × 22,000.


1A
1B

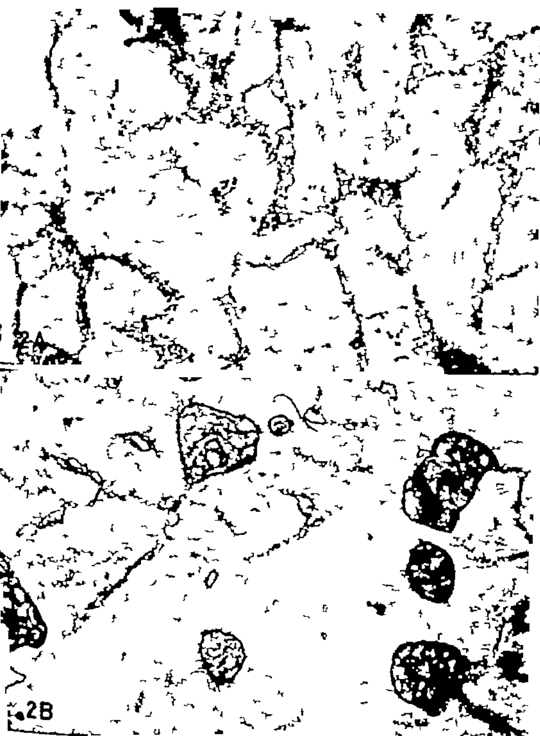
## PLATE 2

### EXPLANATION OF FIGURES

Electron micrographs of cross sections (slightly oblique) of snake muscle fibers. The line on each photograph indicates 1 μ. × 33,000

2A Twitch type muscle fiber

2B Slow type muscle fiber


2A
2B

## PLATE 3

EXPLANATION OF FIGURES

Electron micrographs of cross sections (slightly oblique) of snake muscle fibers. The line on each photograph indicates 1 μ. × 32,000

3A Twitch type muscle fiber

3B Slow type muscle fiber


3A
3B

## PLATE 4

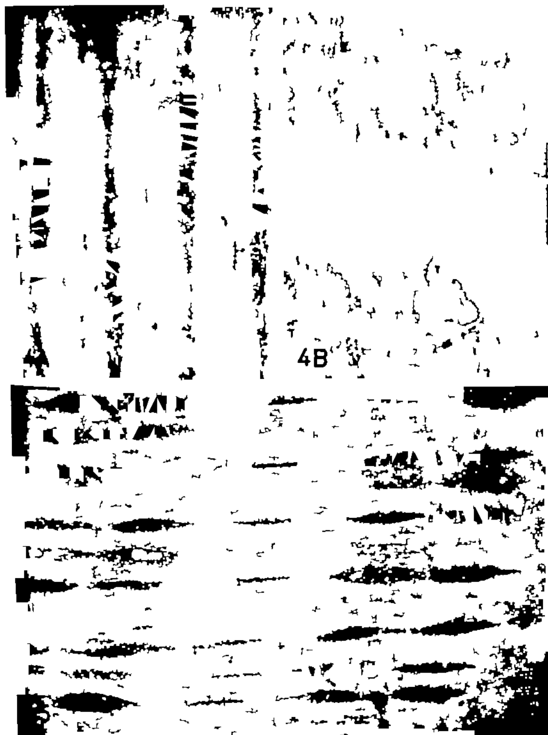
### EXPLANATION OF FIGURES

Electron micrographs of longitudinal sections of snake muscle fibers. The line on each photograph indicates 1 $\mu$. $\times$ 32,000.

4A Twitch type muscle fiber

4B Slow type muscle fiber

5 Muscle fiber with sarcoplasmic reticulum at the level of the H zone bisecting the dark A band as well as at the level of the light I band and Z line


4B

## PLATE 5

### EXPLANATION OF FIGURES

Figures 6, 7 8 9 Photomicrographs of teased snake muscle fibers stained with the cholinesterase technique

6 A–E End-plates. The line on figure 6C indicates 100 $\mu$. × 150.

7 A–C "En grappe" endings. Two endings are seen on each fiber The arrows in figures A and B point to the endings. Figures 7 A and B are different parts of the same muscle fiber The line on figure 7A indicates 100 $\mu$. × 150.

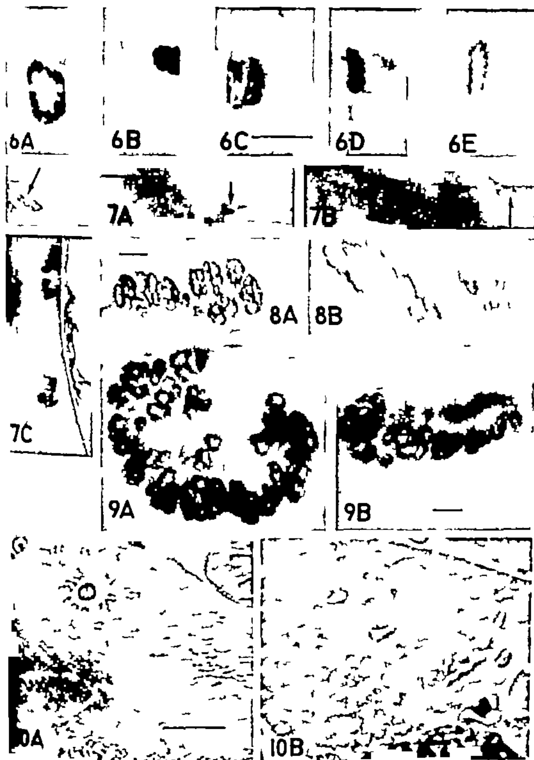
8 A, B "En grappe" endings. The line on figure 8A indicates 10 $\mu$. × 650.

9 A, B End-plates. The line on figure 9B indicates 10 $\mu$. × 650

10 Photomicrographs of Susa-fixed stained epon cross sections of snake muscle fibers. The line on figure 10A indicates 10 $\mu$. × 1,500.

A Twitch type muscle fiber

B Slow type muscle fiber


6A
6B
6C
6D
6E
7A
7B
7C
8A
8B
9A
9B
0A
10B

# Morphogenetic Studies of the Rabbit

## XXXIII. CARTILAGES AND MUSCLES OF THE EXTERNAL EAR AS AFFECTED BY THE DACHS GENE (*Da*)[1]

NEVEN P LAMB AND P B. SAWIN
*Roscoe B Jackson Memorial Laboratory Bar Harbor Maine*

The dachs rabbit is a chondrodystrophic, disproportionate dwarf induced by a single incompletely dominant gene which has been described with respect to over-all adult characteristics by Crary and Sawin ('52) Sawin and Crary ('57) as to prenatal ossification by Sawin, Crary and Atkinson ('56) Sawin, Crary and Webster ('59); and with respect to the spheno-occipital synchondrosis by Sawin, Ranlett, and Crary ('59) It induces a general bed retardation of growth which is accentuated in the skeleton particularly the proximal limbs posterior skull atlas and axis. All of the pleiotropic retardation effects of the gene studied thus far have involved tissues considered to be derived from embryonic mesenchyme (Arey '54) One of the most conspicuous characteristics of the dachs rabbit however has been the peculiar carriage and relative immobility of the ears, which is particularly striking in a species whose ears are normally carried erect and are capable of vast and subtle degrees of motion. Thus this gene not only affects skeletal tissues (cartilage and bone) but could also involve muscles, considered to be of mesenchymal origin, and nerves which are not. In view of the fact that derivation of the cartilage which envelops the membranous labyrinth is also considered to be of mesenchymal origin, at least in man a study of the morphology and function of this region was initiated to learn the precise extent of malfunction of the region and the tissues specifically involved The material has also afforded an opportunity to determine simultaneously the origin and nature of the peculiar cartilaginous papilla-like projection rising from the bottom of the intertragic notch and has revealed other chondrodystrophic abnormalities The papilla has been discussed and portrayed photographically by Sawin and Crary ('57) and has been extremely useful in identification of the homozygous and heterozygous genotypes even in fetal development.

### MATERIALS AND METHODS

The study involved examination and dissection of 16 normal unrelated animals of several different genetic stocks, ranging from age 8 to 11 months and 14 segregated dachs (*DaDa*) rabbits of 1 to 11½ months segregated from the race of origin (DA) and from outcross experimental matings Three (one normal and two dachs) had died of natural causes The rest were killed by a lethal dose of nembutal and of these seven normal and eight dachs were embalmed to facilitate dissection.

Histological examination was made of (1) the ear cartilages to determine the existing types of cartilage and the degree of dystrophic involvement and (2) the muscles to determine the presence of possible extent of atrophy or other abnormality All specimens were fixed in Vandegrift's modification of Bouin's solution for 24 hours, washed in 70% alcohol sectioned and stained with H and E Functional response of muscle and nerve was tested by a light stimulus of ten volts (5 or 10 pulses per second) applied to the nerve as close to its foramen as possible Deafness was tested by Preyer's ear reflex (Denes and Kocher '61) placing the animal in a bell-box used for testing audio-

[1] Supported (in part) by PHS research grant C3010 from the National Cancer Institute, National Institutes of Health, Public Health Service and in part grant E-40 from the American Cancer Society
Present address Department of Anthropology University of Arizona, Tucson

genic seizures as described by Antonitis Crary Sawin and Cohen ('54) This equipment subjects the animal to approximately 95 decibels in all parts of the box.

## OBSERVATIONS

### *Morphology*

The habitual ear carriage of dachs and normal rabbits are illustrated in figure 1 Almost without exception the ears of the dachs rabbit project divergingly backward over the shoulders back and sides and the greatest movement is a scarcely noticeable opening of the ear and a lateral motion that only slightly increases the angle of divergence All other movement is a function solely of movements of the head with the positional relations to the head remaining constant. Normal rabbits may occasionally be seen bearing their ears in a similar position, but never are the ears immobile Previous studies have shown this relatively prone position of the ears to be associated with abnormal positioning of the external auditory meatus arising from the relative disproportionate growth of the basal bones of the skull. However this would not account for the relative immobility of the ears and leads to questions about the normality of function as well as of form of all the associated tissues concerned in normal carriage of the ear some of which notably nerves, are not derived from mesenchyme.

The ear papilla in the intertragic notch is clearly manifest in all homozygous *DaDa* dachs animals It is also manifest, as has been shown by Sawin and Crary ('59) in a very high percentage of heterozygous (*DaDa*) animals. Expression in heterozygotes, however is variable and penetrance often incomplete apparently depending in considerable measure upon the genome in which the gene resides as determined by outcrossing into races X and III of smaller and larger body size Usually the variation in heterozygotes is in the degree of projection of the papilla nil to one half that of *DaDa* and in its point of origin from either anterior bottom or lateral margins of the notch

### *Anatomy*

The external ear of the rabbit as described by Gerhardt ('09) and more completely and clearly by Meinertz ('35) is a complex organ consisting of three distinct cartilages and over 20 muscles and their associated nerves and vessels Since understanding of the changes induced by the

*Except otherwise indicated, the normal rabbit is hown i the figures to the left nd the dach to the right*



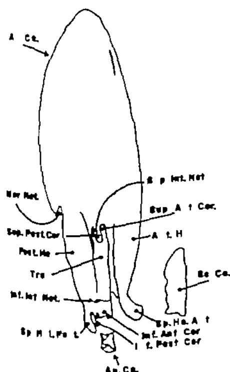
Fig. 1 Heads of normal and dachs rabbit showing typical ear carriage Among the pleiotropic effect of the dachs mutation i a virtual immobility of the ars, which are arried in the position shown (see text)

*Abbreviations for cartilages of ear*

An.Ca., Auricular cartilage
Ant.He., Anterior helix
Post.He., Posterior helix
Tra. *Tragus*
Sup.Int.Not., Superior Intertragic notch
Inf.Int.Not. Inferior intertragic notch
Sup.Ant.Cor., Superior anterior cornu
Sup.Post.Cor., Superior posterior cornu
Inf.Ant.Cor. Inferior anterior cornu
Inf.Post.Cor. Inferior posterior corn
Mar.Not., Marginal notch
Sp.He.Ant., Spina helicis anterior
Sp.He.Post., Spina helicis posterior
Sc.Ca., Scutular cartilage
An.Ca., Annular cartilage

*Abbreviations for muscles of ear*

Sp.Co.Supf., Sphincter colli superficialis
Sp.Co.Pro. Sphincter colli profundus
Pl.My. Platysma myoides
Man.Aur. Mandibulo-auricularis
St.Aur. Sterno-auricularis
Pl.Cer. Platysma cervicale
Fr., Frontalis
Intsc. Interscutularis
Cer.Sc.Post., Cervico-scutularis posterior
Cer.Sc.Ant., Cervico-scutularis anterior
Oc.Sc., Occipito-scutularis
Sc.Aur.Ant. Scutulo-auricularis anterior
Sc.Aur.Post., Scutulo-auricularis posterior
Aur.Ant.Inf., Auricularis anterior inferior
Cer.Aur.Supf., Cervico-auricularis superficialis
Cer.Aur.Sup., Cervico-auricularis superior
Cer.Aur.Inf., Cervico-auricularis inferior
Cer.Aur.Pro., Cervico-auricularis profundus
Tem.Aur. Temporo-auricularis
Zy.Aur. Zygomatico-auricularis
Su.Aur. Subscutulo-auricularis
Aur.Ant.Pro., Auricularis anterior profundus
Tra., Tragicus
Antitra., Antitragicus
Tra.He., Trago-helicinus
He., Helicis
Con.He., Concho-helicinus
Tran.Obl., Tranversi obliqui
Orb.Or., Orbicularis oris
Sp.Med., Splenius medius
Tem., Temporalis



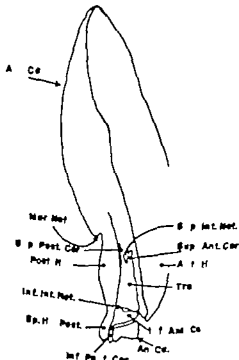




Fig. 2 The right  ar cartilages of the normal and dachs rabbit. The three distinct cartilages of the normal are shown out of context. In the normal animal the annular cartilage lies snugly against the inferior cornu and the scutular cartilage lies on the skull medial to the ear. Ligaments join the annular and scutular cartilages to the auricular cartilage. Only two cartilages are found in the dachs; the scutular cartilage is not developed. The spina helicis anterior of the auricular cartilage is also missing. The   nnular cartilage is shown in its proper relation to the inferior cornua. Note the broadening of the ear  t the base.

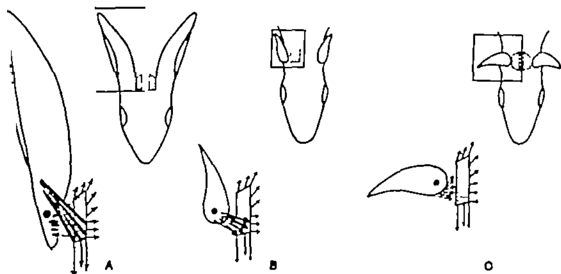



Fig. 5 Schematic drawing of the right ear and its auricular and scutular cartil ges illustrating the function of the scutular cartilage. The black dot represents the pivot point of the ear on the external uditory meatus. Muscle fibers are represented by lines, and the state of contraction and direction of pull by arrows. The only fibers shown that are not in the horizontal plane are those represented by double lines (scutulo-auricularis) Dotted lines (subscutulo-auricularis) represent fibers lying beneath the scutular cartilage. In (A) the auricle is prone and contracting fibers have moved the scutular cartilage into the most advantageous position for the functioning of the levators and are holding it there. Meanwhile the deep posterior rotators (not shown) antagonists of the subscutulo-auricularis (dotted lines) are preventing the latter from rotating the ear forward. In (B) the scutular cartilage is now a fixed, rigid platform and the scutulo-auricularis fibers acting from the ventral surface of the cartilage have contracted to raise the ear (subscutulo-auricularis not shown) (C) The scutulo-auricularis here is exerting lateral (as well as upward) pull on the scutular cartilage freeing the subscutulo-auricularis of this function. When the posterior rotators relax, the direction of pull of the subscutulo-auricularis fibers i changed and the ear is rotated forward (scutulo-auricularis not shown)

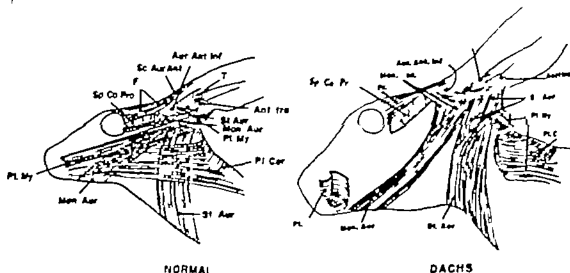



Fig. 6 Superficial ar muscles, lateral view In the normal the sphincter colli superficialis has been removed along with all of the sphincter colli profundus except that portion which inserts into the frontalis. The platysma myoides of the dachs has been cut and all sphincter colli superficialis fibers removed. Note the splitting of both the sterno-auricularis and mandibulo-auricularis and the fragmentary nature of the tragicus Especially note the bnormal insertion of the frontalis.

*II Musculature*

To facilitate description, the muscles have been divided into seven regional groups. The first five groups contain extrinsic muscles (i.e., muscles having at least one attachment free of the auricular cartilage) and the last two the "intrinsic muscles (i.e. having all attachments to parts within the auricular cartilage) All of the normal muscles are listed in table 1 together with origins and insertions of each, and the effect of the dachs gene when homozygous. In the case of eight of the extrinsic and five of the intrinsic muscles, no effect was noted these are described in greater detail by Meinertz ('35)

*Group 1* These are the extrinsic muscles which lie over the neck and the sides of the face. They are broad, extensive and paper thin. The sphincter colli superficialis sphincter colli profundus, and the platysma cervicale are only indirectly associated with the ear Nevertheless their description is included since they are closely related to the ear muscles

*A. Normal*

*Sphincter colli superficialis* This muscle the more superficial of the two sphincters in this region covers the back, sides and front of the neck. From the mid-lines on the ventral and dorsal aspects of the neck, the posterior half of the muscle sweeps around the lower part of the neck and the forward part of the shoulders. The anterior half sweeps upward and forward from the ventral mid-line and downward and forward from the dorsal midline to converge over the angle of the mandible in an insertion into a sheet of muscle of deeper origin Scattered fibers from the ventral origin may occasionally be found in the area between the eye and the ear Similarly some from the dorsal origin may be found over the musculature medial to the ears.

*Sphincter colli profundus* This is the deeper muscle into which the above sphincter inserts. That part of this muscle originating from the sternum is treated here as a separate muscle the sterno-auricularis. The rest of this sphincter covers the ventral surface of the neck and mandible and runs laterally upward from beneath the mandible to insert into the skin and fascia over the side of the face A muscle closely related to the most posterior of these fibers (but not separately named in this paper) continues upward between the eye and the base of the ear inserting into the lateral side of the frontalis (figs. 6 and 7) (These fibers are overlain by the sphincter colli superficialis except between the eye and the ear ) A small slip of this muscle takes its origin from the zygomatic process of the temporal bone.

*Platysma myoides* Unlike the previous two muscles, this runs anteroposteriorly It originates from the tissue around the mouth and travels posteriorly over the side of the face, spreading to make a very broad insertion over the side of the neck with a slip inserting upon the auricular cartilage (fig. 6) The former insertion consists of an intermingling with the sphincter colli superficialis over the back and sides of the neck. The latter fibers pass over the lateral surface and wrap around the posterior border of the ear to insert on the medial surface of the auricular cartilage a few millimeters below the marginal notch (figs. 8 9 and 10)

*Platysma cervicale* Originating from the ligamentum nuchae over the anterior part of the neck, this broad sheet of muscle passes over the trapezius to the mid-point on the side of the neck and inserts into the platysma myoides (figs. 6 7 8 and 9) The sphincter colli superficialis covers it on the side of the neck and the cervico-auricularis superficialis covers it partially at the ligamentum nuchae.

*Mandibulo-auricularis (intermedio-mandibularis).* This and the following muscle are thin straps (1 to 2 cm wide) lying beneath the platysma muscles (figs. 6 7 and 10) It originates from a small area at the side of the mandible just behind the mental foramen. Lying under the platysma myoides for most of its length it inserts over the lower third of the tragus into the fascia and fibers of the auricularis anterior inferior The posterior border of this muscle and the anterior of the sterno-auricularis converge lying adjacently and *often intermingling they continue to their*

TABLE 1

*Ea muscle of normal rabbit nd as ffected by the dachs gene*

| Group | Muscle See fig. in ( ) | Origin | Insertion | Effects of Da gene |
|---|---|---|---|---|
| I | Sphincter colli superficialis | Midlines of ventral and dorsal aspects of neck | Broad lower neck, upper shoulders; angle of mandible into sphincter colli profundus; between eye and ear | Some increase in size |
| | Sphincter colli profundus (6,7) | Ventral urface of neck | Into skin and fascia over side of face; and into lateral margin of frontalis | None |
| | Platysma myoides (6,8,9,10) | Angle of mouth | Broadly over side of neck; medial surface (posterior border) of auricular cartilage | None |
| | Platysma cervicale (6,7,8,9) | Ligamentum nuchae | Platysma myoides at side of neck | None |
| | Mandibulo oricularis (6,7 10) | Mandible t mental foramen | Lower ½ f tragus | Insertion displaced |
| | Sterno uricularis (6,10) | Man brium sterni | Lower ⅓ of tragus | Insertion displaced |
| II | Frontalis (6,7,9 10 11) | Posterior supraorbital process of frontal bone | Anterior border of scutular cartilage; anterior helix | Extreme displacement of inser tion |
| | Interscutularis (7,8,9 11) | Lateral borders of scutular cartilages | | Extreme ttenuation |
| | Cervicoscutularis posterior (7,9) | Ligamentum nuchae | Posterior corners of scutular cartilage | Slight fragmentation |
| | Cervicoscutularis anterior (9) | Ligamentum nuchae | Medial borders of scutular cartilage | None |
| III | Scutulo uriculari anterior (6 7,9,10 11) | Anteromedial corner and anterior border of scutular artilage | Anterior surface of anterior helix with frontalis | Extreme displacement nd fragmentation |
| | Scutular uricularis posterior (7) | Medial border and dorsal aspect of scutular cartilage | Anterior helix | Poor differentiation nd displacement |
| IV | Cervico uriculari superficiali (7,8,9) | Anterior part of ligamentum nocha | Medial urface of uricular artilage | Slight diminution |
| | Cervico auricularis superior (8,9) | Ligamentum nuchae | Medial urface of uricular cartilage | Very poor differentiation |
| | Cervico uriculari inferior (8,9,10) | Ligamentum nuchae | Medial urface of uricular cartilage | Very poor differentiation |
| | Cervico uricularis profundus (8,9 10) | Ligamentum nuchae | Spina helicis posterior | None |
| V | Subscutulo uricularis (9 10,11) | Medial border ventral surface of scutula rtilage | ( ) ½ on entral urface di tal end of *spina helicis* nterior (b) ½ on anterior helix | None |

TABLE 1 (Continued)

| Group | Muscle See fig. no. ( ) | Origin | Insertion | Effects of Da gene |
|---|---|---|---|---|
| | Auricularis anterior profundus (9,13) | Ventral surface of spina helicis anterior | Base of anterior helix, medial surface | Origin displaced |
| | Tempora auricularis (9,10) | Temporal bone and annular cartilage medial to external auditory meatus | Posterior aspect of anterior helix | Insertion substantially displaced and attenuated |
| | Zygomatico auricularis (9,10,12,13) | Temporo-mandibular joint | Base of anterior helix, medial surface | Origin displaced extremely[a] |
| VI | Transversi and Obliqui (9,10) | Medial surface of auricular cartilage | | None |
| | Auricularis anterior inferior (6,7,10) | Dorsal aspect of spina helicis anterior | Lateral aspect of posterior helix | None |
| | Tragicus (6,7,10) | Tragus | Anterior helix | Slight fragmentation |
| | Antitragicus (6,7,10) | Antitragus | Posterior helix | None |
| VII | Tragohelicinus (10) | Anterior surface of tragus | Tragus and anterior helix | Insertion displaced slightly |
| | Helicis (10) | Base of anterior helix (concave side) | Free margin of anterior helix | None |
| | Concho-helicinus (9,10) | Anterior border of spina helicis posterior | Base of anterior helix | None |

[a] One case.

frequently common insertions on the lateral side of the ear

*Sterno-auricularis (pars auris des sphincter colli profundus)* This muscle (figs. 8 and 10) considered by Meinertz to be the most posterior section of the sphincter colli profundus originates from the manubrium sternum and passes from there over the parotid region and the angle of the mandible to the lateral surface of the posterior helix. There the fibers insert, usually in common with the previous muscle on a line *running upward and slightly posteriorly* nearly to the level of the intertragic notch.

## B Dachs

Although the dachs ear muscles are generally small and thin with fascial planes frequently indistinct and rendering identification of specific muscles difficult in some areas this group tends to be exceptional in several respects.

*Sphincter colli superficialis* It is important to note that the sphincter colli superficialis is the only muscle that is more extensive about the ears in the dachs than in the normal. In those places on the normal animal where the muscle is thinned to scattered fibers (that is between the eye and ear and over the musculature medial to the ear) the dachs animal exhibits fibers so reduced as to form only thin discontinuous sheets. In particular the fibers from the ventral origin not only cover and obscure the frontalis muscles, but they also cover the ears at the base (fig

Meinertz found that this muscle inserted partly into the underside of the platysma myoides and partly into the sterno-auricularis (pars auris des sphincter colli profundus) muscle, with only a few fibers inserting commonly with the latter. The findings of the present dissections were quite the contrary for only occasionally were fibers inserted into the platysma myoides.

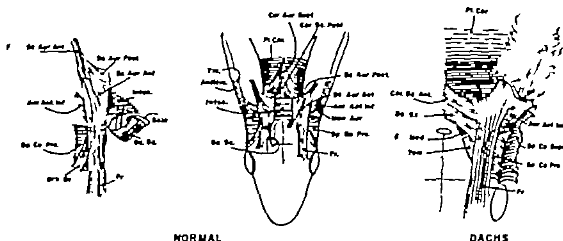



Fig. 7 Superficialis ear muscles, dorsal view In the normal the anterior portion of the occipitoscutularis (homologous with the epicranius of the cat) is transected. Detail of relationships of the interscutularis, frontalis, and sphincter colli profund is on the left. In the dachs, the sphincter colli superficialis is reflected and shown far heavier and more distinct than it actually is. All remnants of the extremely thin interscutularis have been removed. The frontalis approaches the ear somewhat laterally and spreads flatly against the lower part of the anterior helix and into the muscle mass medial to it. The anterior portion of the occipitoscutularis is not shown.

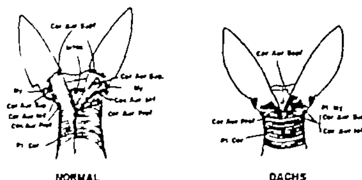



Fig. 8 Posterior uricular muscles. In the normal the cervicoscutularis posterior hs been removed to show the relations of the cervico-auricularis muscles more learly On the left the superficialis covers all but the insertions of the remaining muscles. On the right the superficialis has been cut t it insertion and removed at its origin. Note that profundus underlies all these muscles t the origin and that inferioris only partially underlies superioris. In the dachs, these muscles, with the exception of the cervico-auricularis profundus, are small, thin, and poorly differentiated. The cervico-auricularis superficiali has less extensive insertion than normal (see the right side) It has been removed on the left side to show the lack of distinction between the cervico- uricularis superior and the cervico-auricularis inferior

7) and being continuous across the head cover the interscutularis The precise extent of these fibers was impossible to determine

*Mandibulo-auricularis (intermedio-mandibularis).* In no case does this muscle insert as it normally does into the fascia over the auricularis anterior inferior Running upward and backward beneath the platysma myoides it inserts into the area immediately above and lateral to the anterior inferior cornu of the tragus. Figure 6 illustrates an unusually high insertion Generally the insertion i lower In several the insertion also invol ed the lower border of the auricularis ant rior inferior In others fibers from the nterior margin split off before the insertion at

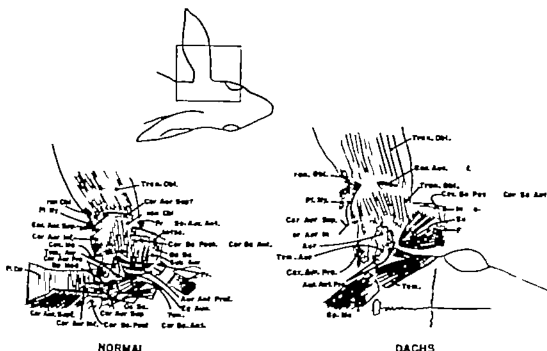



Fig. 9 Deep ear muscles, medial side. The superficial muscles lying medial to the ear have been cut, together with the frontalis and the ear reflected to the side, exposing both those muscles which are medial to the meatus and those which are ventral to the scutular cartilage. In the dachs, the stumps of these muscles are not shown. Note the origin of the auricularis anterior profundus from the squamosal process posterior to the ear, the arrangement of fibers of the subscutularis auricularis, and the small area of insertion of the cervico-auricularis superficialis.

taching to connective tissues between the tragus and anterior helix below the lower border of the auricularis anterior inferior The posterior fibers are frequently overlapped by the insertion of the sterno-auricularis and the fibers of the two muscles may mingle. A few fibers may also insert into the underside of the platysma myoides a centimeter or two anterior to the base of the ear.

*Sterno-auricularis (pars auris des sphincter colli profundus)* This muscle, like the mandibulo-auricularis has a lower insertion than normal, but also one that is more posterior It frequently overlaps the mandibulo-auricularis above the inferior intertragic notch and inserts on a line running posteriorly upward from there with fibers clearly inserting onto the posterior border of the helix and wrapping around somewhat onto the medial surface. On one animal these extremes of insertion are separated by a longitudinal splitting of the muscle with a slip from the anterior border inserting into the underside of the platysma myoides (fig. 6)

*Group 2.* This group consists of the frontalis and extrinsic muscles which lie medial and posteromedial to the scutular cartilage.

### *A Normal*

*Frontalis* This muscle originates anterior to the scutular cartilage from the posterior supraorbital process of the frontal bone (figs. 6 7 9 10) Less than a centimeter wide in adult animals, it presents a flat oval in cross-section, inserting on the anterior border of the scutular cartilage and on the ligaments between it and the spina helicis anterior Joining the scutulo-auricularis anterior it continues upward with it to a tendonous insertion on the anterior helix at the level of the superior intertragic notch. A small portion of its deep fibers extends over the anterior part of the ventral surface of the scutular cartilage (fig 11) Fibers from the sphinc

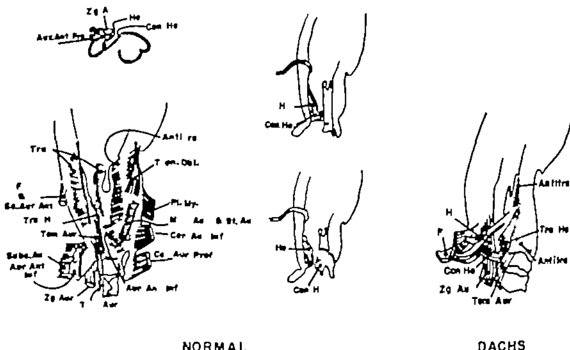



Fig. 10 Deep ear muscles lateral ide The tragicus and uricularis anterior i ferior have been severed, exposing the deep-lying temporo-auricularis and trago-helicis muscles, which completely fill the space between the anterior helix nd the tragus. In the dachs, the superficial muscles have been removed. The temporo-auricularis is shown typically inserting ont the tragus rather tha onto the nterior helix Not the extraneous fibers attaching t the ventral surface of the frontalis; whether they were parts of the trago-helicinus, the scutulo-auricularis, the uricularis anterior profundus, or some other muscle could not be determined. The smaller figures umbered counter-clockwise show the ttachments of the normal muscles that lie within the folds of ricular cartilage The dachs animals displayed no bnormalities with respect t these muscles.

ter colli profundus muscle insert into the lateral edge of this muscle from the scutu lar cartilage to the orbit. At the antero-medial corner of the scutular cartilage the most medial fibers of the frontalis curve medially to mingle with the fibers on the anterior border of the interscutularis muscle In this same place as it emerges from beneath the interscutularis the occipito-scutularis sends several fibers into the frontalis The frontalis is commonly joined on its lateral side by a band of fibers from the orbicularis oris

*Interscutularis* The interscutularis stretches between the entire length of the medial borders of scutular cartilages (figs. 7 8 9 and 11) It is a flat sheet of fibers with no attachments other than those on the scutular cartilage

*Cervicoscutularis posterior* This forms a small triangle directly behind the inter scutularis (figs. 7 and 9) Originating from the ligamentum nuchae its posterior fibers run obliquely forward its anterior fibers more transversely to converge on the posterior corners of the scutular car tilage It is closely applied to the more

Fig. 11 Comp rison of scutul regions. (A) Coronal section through the anterior part of the right scutular rtilage (7) of ormal rabbit (compare with fig. 3, mag. 20 ×) (B) Coronal section f the dachs rabbit through an area medial t the right ar where the scutula cartilage is normally found (mag. 20 ×) It is however noticeably bsent with the fron alis fibers lying adjacent t the subcutularis-auricularis. Not the extremely poor development of the interscutularis compared to the normal It could not be determined whether the fibers overlying the frontalis are from the scutulo- ricularis or from the sphincter colli superficial or both (1) Frontalis; (2) Interscutularis; (3) Cervico-sc tularis terior; (4) Subscutulo-a ricularis; (5) Scutulo-auriculari anterior (on normal); Scutulo-a ricularis or Sphincter colli superficialis or both on the dachs; (6) Temporalis (7) Scutu la rtilage.

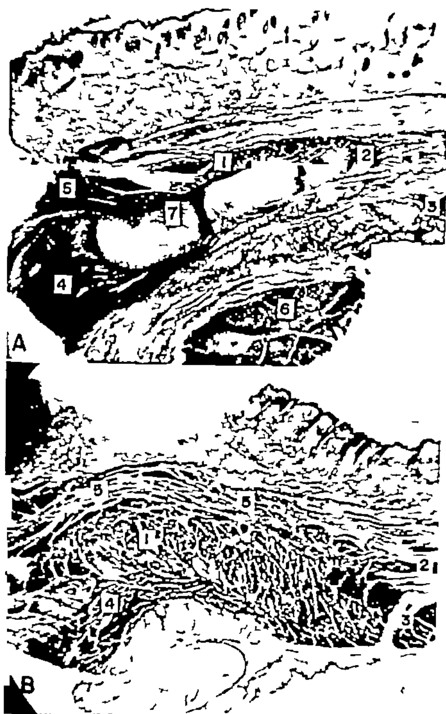



Figure 11

posterior cervicoauricularis superficialis, which it partly overlies. Its anterior extension is not distinguishable from the cervicoscutularis anterior On two animals a small group of its fibers continue upward to insert in the medial surface of the auricular cartilage posterior to the common insertion of the frontalis and scutulo-auricularis anterior muscles.

*Cervicoscutularis anterior* This muscle (fig 9) distinguishable from the cervicoscutularis posterior only by the transverse direction of its fibers originates from the anterior 3 or 4 mm of the ligamentum nuchae above the origin of the splenius medius and inserts into the posterior one-third to one-half of the medial border of the scutular cartilage It appears as a cylindrical bundle of fibers when the ligamentum nuchae is forward but it flattens into the same plane as the posterior section when the ligament is pulled back.

*Occipito-scutularis (occipito-scutularis anterior and posterior)* The occipito-scutularis springs from the occipital crest beneath the cervicoscutularis anterior and the splenius medius and in approximately one-half the animals examined from the occipital ridge as well Its insertion is also extensive the fibers sweeping forward and laterally to attach to the anterior two-thirds to one-half of the medial border of the scutular cartilage to the frontalis just anterior to its insertion on the scutular cartilage and, overlying the frontalis into the skin at a point above and medial to the supraorbital process of the frontal bones (figs 7 and 9)

### B Dachs

Although the DA gene effects no remarkable differences from the normal with either the cervicoscutularis anterior or the occipito-scutularis it has pronounced effects on the other muscles of this group

*Frontalis* Removal of the fibers of the sphincter colli superficialis anteriorly reveals a muscular displacement of major importance The absence of the thick bundle of converging fibers normally inserting by a heavy tendon onto the anterior helix is striking in all dachs animals Instead the frontalis fibers of the dachs directed somewhat laterally approach the medial side of the base of the ear and spread flatly into the muscle mass medial to it. The anterior helix itself accepts only thinly scattered fibers on its lower portion (figs. 6 7 9 and 10) The scutulo-auricularis muscles (see normal description, Group 3) cannot be distinguished among these fibers. Within the muscle mass the greatest contribution is made by the frontalis fibers which extend posteriorly throughout most of its length rather than merely over the anterior part (fig. 11)

*Interscutularis* In the dachs this normally thin muscle is attenuated almost to the point of invisibility It is extremely difficult to dissect and is identified with certainty only by sectioning where it appears covered by scattered fibers of the sphincter colli superficialis Sectioning also reveals that the location of the dachs interscutularis is normal at least in the anterior portions but that its attachments are necessarily to the connective tissue which occupies the site of the scutular cartilage (fig. 11)

*Cervicoscutularis posterior* The cervicoscutularis posterior in the dachs could not be distinguished as a separate muscle Normally it is immediately recognizable as a small triangle lying on top of the larger triangle formed by the cervico-auricularis superficialis. The smaller triangle is not present in the dachs possibly because the fibers of this part of the muscle take a less extensive origin from the ligamentum nuchae and run parallel to the anterior muscle

*Group 3* This group contains two muscles the only muscles orginating from the dorsal aspect of the scutular cartilage

### A Normal

*Scutulo-auricularis anterior (scutulo-auricularis superior anterior).* This muscle with the frontalis is the major levator muscle of the ear It originates from the anteromedial corner and the anterior border of the scutular cartilage on the dorsal side (figs. 6 7 9 10 and 11) Its fibers and those of the frontalis converge to insert commonly at a point high (at the level of the intertragic notch) on the anterior surface of the anterior helix This portion comprises the thickest and heaviest section of the ear musculature and inserts by a relatively heavy tendon

*Scutulo-auricularis posterior (scutulo-auricularis superior posterior).* This muscle originates from the medial border and the dorsal aspect of the scutular cartilage (fig. 7) and converges to an insertion on the anterior helix beneath and somewhat proximal to the scutulo-auricularis anterior. It is smaller and shorter than that muscle.

*B Dachs*

The effect of the DA gene on both muscles is one of such poor differentiation that dissection could distinguish neither muscle as a discrete unit from the fibers of the frontalis (see dachs *frontalis*, Group 2 above) The failure to find fibers in the area of normal insertion however indicates medial displacement.

Group 4 includes four muscles all springing from the ligamentum nuchae and inserting at various points on the medial and posterior aspects of the auricular cartilage.

*A Normal*

*Cervico-auricularis superficialis (cervico-scutulo-auricularis)* This, the most superficial muscle of the group, is also the largest (figs 7 8 and 9) It originates from the anterior 3 or 4 cm of the ligamentum nuchae and forms a broad triangular sheet, its fibers running obliquely forward to insert onto the medial surface of the auricular cartilage This insertion, which occurs at the level of the intertragic notch, extends from the common insertion of the frontalis and scutulo-auricularis anterior in front to that of the platysma myoides behind. Attachment is made to the posterior border of the scutular cartilage by the anteriormost fibers. The anterior half of the muscle is covered by the triangular posterior part of the cervico-scutularis

*Cervico auricularis superior (cervico-scutulo auricularis medius).* This muscle originates from the first centimeter of the ligament (figs. 8 and 9) It is a wide band that runs laterally upward, its fibers spreading slightly to insert onto the medial surface of the auricular cartilage beneath the cervico-auricularis superficialis muscle. Again a passing attachment is made to the posterior border of the scutular cartilage

*Cervico auricularis inferior (cervico-auricularis medius)* This is the third deepest muscle (figs. 8, 9 and 10) The anterior three-fourths of the origin, from the ligamentum nuchae lie beneath the cervico-auricularis superior but its anterior extension is not as great as the previous muscles. It is very similar to the cervico-auricularis superior in its flatness, size, and direction. For much of its length it lies partly beneath that muscle, emerging at its insertion onto the posterior border and posterior third of the medial surface of the auricular cartilage.

*Cervico auricularis profundus (cervico-auricularis posterior profundus)* This is the deepest muscle of the group the origin being from the anterior centimeter of the ligamentum nuchae (figs. 8 9 and 10) It runs directly laterally to insert on the spina helicis posterior

*B Dachs*

The effects of the DA gene on these muscles are difficult to describe. The muscles themselves are not only small and poorly differentiated, but their facial planes are indistinct and their origins from the ligamentum nuchae and their insertions are less extensive than normal. Of the four the cervico-auricularis profundus shows the least abnormality

*Cervico auricularis superficialis (cervico-scutulo-auricularis).* The extent of the origin of this muscle from the ligamentum nuchae is reduced in most cases to approximately one-quarter that of the normal (fig. 8) Its area of insertion on the medial surface of the auricular cartilage is smaller and lower than normal and it is never found as high as the intertragic notch. Those fibers normally attaching to the scutular cartilage instead attach to the subscutulo-auricularis.

*Cervico auricularis superior and inferior (cervico-scutulo-auricularis medius and cervico auricularis medius).* These muscles cannot be distinguished from one another in the dachs (figs. 8 and 9) and presumably intermingle to form a single muscle having the same breadth of origin from the ligamentum nuchae as is involved by both muscles in the normal. The insertion also is broader than one would expect if this muscle represented

only one or the other of the normal muscles. It is low close to or onto the proximal border and its fibers frequently are mixed with those of the muscles above and below. On one animal some stray fibers of the platysma cervicale (which has an origin immediately posterior to these muscles in the same plane) originate from the anterior end of the ligamentum nuchae and cross over and through this band of muscle to join the balance of the platysma passing around the neck. Likewise the attachments normally made to the scutular cartilage are made to the subscutulo-auricularis.

Group 5, the last group of extrinsic muscles, contains four deep muscles. While their origins are varied — the *ventral surfaces of the scutular cartilage and* spina helicis anterior, the annular ring, and or the region of the temporo-mandibular joint — all but one insert into a small area at the base of the anterior helix. The auricularis anterior profundus is strictly an intrinsic not extrinsic muscle but because it is closely related to these muscles and because on the dachs it actually is an extrinsic muscle it is included here.

*A. Normal*

*Subscutulo-auricularis (subscutulo-auricularis intermedia)*. This is the only muscle originating from the ventral surface of the scutular cartilage and it does so for the entire length of the medial border (figs. 9, 10 and 11). The fibers have two distinct insertions. The anterior third run laterally to insert on the ventral surface of the distal end of the spina helicis anterior. The posterior fibers also run *laterally* but converge slightly and insert into a small area on the anteromedial surface of the base of the anterior helix (anterior to the

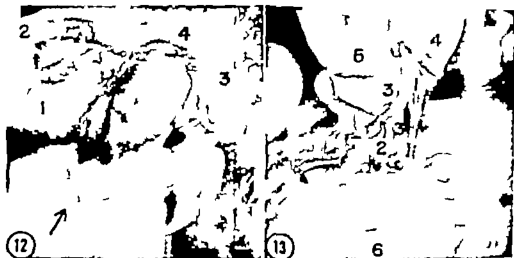



Fig. 12 Abnormal zygomatico-auricularis. This was the only dachs animal with abnormal zygomatico-auricularis. The photograph is of the left temporal area. The ear has been pulled down and the area cleared of superfluous tissues to show clearly the abnormal zygomatico-auricularis. The muscle arises normally from the end of the zygomatic arch but instead of taking its normal insertion at the base of the auricular cartilage it avoids the ear altogether and attaches instead to the squamosal process of the temporal bone posterior to the meatus. Compare with figure 8. (1) Zygomatic arch, posterior end. (2) Zygomatic process of temporal bone. (3) Squamosal process of temporal bone. (4) Zygomatico-auricularis.

Fig. 13 Auricularis anterior profundus. The dachs animal consistently displays a muscle that arises from the squamosal process of the temporal bone and inserts at the base of the anterior helix anterior to the zygomatico-auricularis. The muscle appears to be the auricularis anterior profundus. In this photograph the dachs ear has been rotated, exposing the lateral surface and revealing the relationships of the auricularis anterior profundus, the zygomatico-auricularis, and the temporo-auricularis. Note that the latter is closely applied to the annular cartilage and inserts onto the tragus. (1) Auricularis anterior profundus. (2) Zygomatico-auricularis. (3) Temporo-auricularis. (4) Anterior helix. (5) Tragus.

insertion of the auricularis anterior profundus) and partly upon the proximal end of the spina helicis anterior

*Auricularis anterior profundus (subscutulo-auricularis frontalis).* This muscle (fig. 9) runs in an anteroposterior direction at right angles to the fibers of the subscutulo-auricularis. It originates from the ventral surface of the spina helicis anterior both from the lateral border and the distal end, which it shares with the anterior insertion of the subscutulo-auricularis. It passes back under the spina helicis anterior under the posterior insertion of the previous muscle then moves upward medial to the zygomatico-auricularis and inserts just anterior to it on the medial surface of the base of the anterior helix. (Note the ventral surface of the spina helicis anterior actually faces medioventrally on the intact rabbit, just as the dorsal surface faces laterodorsally )

*Temporo auricularis (trago tubo helicinus).* This is a long and narrow but sturdy muscle that originates from the bony groove medial to the external auditory meatus and from the medial surface of the annular cartilage (figs. 9 and 10) With the trago-helicinus it entirely fills the deep cleft between the tragus and the anterior helix. The muscle enters the cleft from below and, running upward adheres to the anterior face of the tragus inserting onto the posterior face of the anterior helix (that is the anterior wall of the cleft) at a level midway up the tragus. It never emerges from the cleft. Some of its fibers continue upward with those of the trago-helicinus.

*Zygomatico auricularis (mandibulo-auricularis)* Originating from the end of the zygomatic arch with occasional fibers from the tissues covering the temporomandibular joint (figs. 9 and 10) this thick bundle runs backward then upward crosses over the temporo-auricularis medially and inserts onto the medial surface of the base of the anterior helix, partially covering the insertion of the auricularis anterior profundus. In a few animals the origin of this muscle may be more extensive including fibers attached to the temporal bone in a small area medial to the origin of the temporo-auricularis.

*B Dachs*

Only two of these muscles were consistently affected by the *Da* gene the temporo-auricularis and the auricularis anterior profundus. In one animal however the zygomatico-auricularis was affected in a noteworthy way

*Auricularis anterior profundus (subscutulo-auricularis frontalis)* The *D* gene consistently causes an extraordinary posterior displacement of this muscle On all the dachs animals examined a very sturdy flat band of muscle arises from the squamosal process of the temporal bone and, running upward and forward, crosses the zygomatico-auricularis medially to insert just anterior to it (figs. 9 and 13 No muscle whatever assumes this position on the normal rabbit. This muscle has been interpreted as the auricularis anterior profundus for the following reasons (1) There is no muscle which clearly occupies the normal position of the auricularis anterior profundus. In some animals its complete absence is obvious, as the only fibers that are present ventral to the normal location of the scutular cartilage are situated mediolaterally in the manner of the normal subscutulo-auricularis. In others anteroposteriorly arranged fibers are also present however they cannot be distinguished from the mediolateral fibers and are probably a part of the subscutulo-auricularis (2) regardless of the arrangement of these ventral fibers they all insert wholly into the area in which normally the posterior part of the subscutulo-auricularis inserts and nowhere else. That is, all of the fibers which may occur in the area where the auricularis anterior profundus is normally found insert like subscutulo-auricularis, not auricularis anterior profundus fibers and (3) the place of insertion of the muscle arising from the squamosal process is precisely that of the auricularis anterior profundus. With the exception of the single zygomatico-auricularis muscle described below this is the only instance of a displacement of muscle fibers from cartilage to bone

*Temporo auricularis (trago tubo helicinus).* Although normal both in its origin and in its position in the cleft between the tragus and the anterior helix in the dachs this muscle is displaced posteriorly in-

variably inserting onto the tragus rather *than onto the anterior helix (figs 9 and* 10) (The closely related trago-helicinus of Group 7 is also displaced posteriorly ) It is furthermore a considerably thinner muscle scarcely resembling the thick bundle found in the normal. In some dachs it is nearly transparent (fig. 13)

*Zygomatico auricularis (mandibulo-auricularis).* The zygomatico-auricularis in every case but one was essentially normal The exception however is remarkable In this animal the muscle a cylindrical bundle of fibers, arises normally from the end of the zygomatic arch. But instead of inserting normally at the base of the auricular cartilage (see figs. 9 and 13) it avoids the ear altogether and attaches instead to the squamosal process of the temporal bone posterior to the meatus (fig. 12)

The muscles of the last two groups (6 and 7) are all intrinsic to the auricular *cartilage; that is they both originate from* it and insert into it. There are eight such muscles four being superficial four deep One of the deep muscles the auricularis anterior profundus has already been described.

*Group 6* This group contains the superficial intrinsic muscles including the transversi and obliqui, auricularis anterior inferior and antitragicus none of which are affected by the dachs gene and the tragicus. The auricularis anterior inferior which in normal rabbits attaches to the spina helicis anterior in the dachs attaches instead to the connective tissue and muscle fiber that occupies the area. It is not, however displaced or otherwise affected.

*A Normal*

*Tragicus (trago helicinus retro auricularis)* The tragicus consists of short fibers running transversely from the tragus to the anterior helix (figs 6 7 and 10) Distally they run from the anterior superior cornu of the tragus obliquely upward to the anterior helix the fibers become less oblique proximally and end near the base of the anterior helix. These fibers bridge the cleft in which the temporo-auricularis and the trago-helicinus lie

*Transversi and obliqui.* Running between the anterior and posterior borders on the medial surface of the auricular *cartilage are two rows one more proximal* than the other of short fibers directed along the length of the ear (fig 9) Both muscles lie flat against the cartilage and have long tendonous insertions applied over the proximal half of this surface The lower row lies well down on the eminentia conchae the fibers running upward and somewhat anteriorly Its insertion ends under that of the cervico-auricularis superficialis. The distal row lies on an oblique line higher posteriorly than anteriorly somewhat below the level of the marginal notch Its fibers are very short A specialized portion of these muscles lies over the posterior border and is evident on both the lateral and medial sides (figs 9 and 10) The origin is slightly more than a centimeter below the marginal notch and the fibers run directly upward to bridge the notch and insert on the cartilage above.

*Auricularis anterior inferior* Beneath the scutulo-auricularis anterior a small sheet of fibers arises from the dorsal aspect of the spina helicis anterior and from the ligaments and connective tissues between it and the scutular cartilage (figs. 6, 7 and 10) These fibers run obliquely over the lateral side of the auricular cartilage to insert on a line running from a point midway up the tragus to another on the posterior helix near the base It is a flat thin muscle covering the lower half of the tragus

*Antitragicus (antitrago-tubo-helicinus).* Posteriorly a similar muscle runs from the tragus to the posterior helix (figs. 6, 7 and 10) The distal fibers especially those originating from the posterior superior cornu run obliquely upward. Those at the proximal end are less obliquely situated and are distinctly longer They accept parts of the insertions of the auricularis anterior inferior and sterno-auricularis muscles.

*B Dachs*

Only the tragicus is affected by the *Da* gene the others being essentially normal.

*Tragicus (trago helicinus retro auricularis).* This muscle tends to be fragmentary in bridging the cleft which separates the tragus from the anterior helix (fig 6) Distally the fibers which nor

mally attach to the anterior superior cornu attach instead to the intervening skin.

*Group 7* This last group is comprised of the three deep intrinsic muscles with origins and insertions as shown in table 1 Of these muscles only the trago-helicinus is affected by the *Da* gene.

### A. Normal

*Trago-helicinus* This is a thin band of fibers originating in the cleft from the anterior surface of the tragus just above the anterior inferior cornu. It runs upward in the cleft, inserting on both the anterior helix and the tragus (fig 10) The insertions face each other at a level just below the base of the intertragic notch. Below the muscle is hidden by the larger temporo-auricularis muscle above, it is covered by the tragicus

*Helicis* The helicis (fig. 10) is a small flat, somewhat triangular muscle lying in the anterior concavity at the base of the auricular cartilage. It arises medially within the concavity of the ear at the base of the anterior helix, and runs upward to insert into the free margin of the anterior helix from the proximal end to a level somewhat below the base of the inter tragic notch. Since at this point the margin faces the medial wall of the cartilage the muscle is oriented in a mediolateral direction. It cannot be seen from the medial side and only from the lateral side by pulling the anterior helix open. The proximal fibers are covered by the concho-helicinus.

*Concho-helicinus* This is a smaller thinner muscle than the helicis, but like the latter it also runs in the concavity of the auricular cartilage (figs. 9 and 10) It arises from the anterior border of the spina helicis posterior and crosses the concavity in a horizontal plane to insert lateral to the helicis muscle at the very base of the anterior helix. As it has a more posterior origin than the helicis its orientation is somewhat more anterior

### B Dachs

*Trago-helicinus* The insertion of this muscle is displaced posteriorly It originates from the tragus more laterally than normal, and instead of running upward in the cleft to insert on both the tragus and anterior helix, the muscle long flat, and tendonous, runs obliquely upward and backward over the tragus. It inserts on the lateral side of the tragus just below the intertragic notch and, covering the antitragicus, onto the posterior helix (fig 10)

Finally in many dachs animals small slips of muscle are found crossing from the helix upward to attach to the tragus They have a variable origin from the base of the anterior helix (fig. 10) Whether these muscle fibers represent parts of the trago-helicinus the scutulo-auricularis the auricularis anterior profundus or some other muscle could not be determined.

### Histology

Samples of muscle and cartilage for histological examination were taken from ten normal and eight dachs animals varying from newly born to ten months of age The scutular cartilage the distal end of the auricle the spina helicis anterior and both the anterior and posterior superior cornua of the tragus were studied. The scutular cartilage was discovered to be fibrocartilage in the normal rabbit (fig 3) and the auricular cartilage to be hyaline cartilage In the dachs rabbit the scutular cartilage was absent (fig. 11) and the spina helicis either absent or very greatly reduced The comparable parts of the auricular cartilage were hyaline cartilage showing no abnormalities. (In the dachs the base of the anterior helix was studied in the absence of the spina helicis anterior )

The muscles examined were posterior auricularis, sphincter colli superficialis and profundus, cervicoscutularis and occipitoscutularis frontalis interscutularis, scutulo-auricularis anterior subscutulo-auricularis, zygomatico auricularis and temporo-auricularis. In the dachs only one case of atrophy of muscle fiber was evident. It occurred in a section of an interscutularis muscle and was highly localized, evidently the result of a vascular infection.

### Further observations

In addition to investigating the hypothesis of muscular displacement as the cause of ear immobility three alternate but not

mutually exclusive hypotheses were considered.

The first deafness was suggested by the extreme deformity and reduction of the tympanic bulla occurring in all dachs rabbits. It was thought that if the dachs animals were deaf there would be little attempt at ear movement. To test this hypothesis, rabbits were observed for Preyers ear reflex, a twitch of the pinna in response to sound stimulation. The apparatus consisted of a cubic wooden sound box measuring 20 inches on a side lined with padded plastic and fitted with an Edwards 4 inch bell type 55 and a one way glass window for observation. The decibel output, measured in all corners and the center ranged from 90 to 97 The animal was allowed to become completely quiescent before the bell was sounded and any reaction noted A startle response manifested usually by very slight ear movement but in some cases by movement of the animal, was interpreted as evidence that the animal had heard the bell. By this procedure 22 dachs and 10 unrelated normal animals ranging from two to four months of age were tested All non-dachs and eleven dachs animals responded positively This was not a test of hearing acuity but demonstrated that at least some of the dachs animals do hear although some may not.

It was also considered possible that the compression of the external auditory meatus along with the abnormally close zygomatic arch might prevent the ear from moving Dissection of the tissues around the base of the ear however made it apparent that these elements do not interfere with the movements of the cartilaginous joints

An attempt was made also to eliminate (as a cause of ear immobility) any neurological interruption that might have occurred in the branches of the facial nerve This was considered a possibility not only because such a malfunctioning could produce an immobile ear but also because it was noted in two efforts to trace the branches of a facial nerve that the upper division of this nerve was fragmented and split into several branches immediately after leaving the lower division Normally the upper branch is a single common trunk several millimeters long which splits into the temporal and zygomatic branches before proceeding to further divisions. Of course splitting similar to this is what would be expected in muscle dysplasia (the facial nerve itself is an excellent example of how far and in how many directions a nerve will pursue muscles to which it had become attached in early embryology) but the dysplasias occurring here are subtle certainly not requiring such exuberant division. An effort was made therefore to test the functioning of the nerve

Should the facial nerve be functioning properly an electrical stimulus applied to the nerve where it emerges from the stylomastoid foramen should produce twitching in all ear and facial muscles. Three animals were anesthetized with nembutal and the lower division of the facial nerve exposed anterior to the parotid gland. This approach allowed us to trace the nerve to the stylomastoid foramen with minimum danger of severing either the cervical or posterior auricularis branches or the upper division The muscles were exposed and a light stimulus of 10 volts (8 or 10 pulses per second) was applied to the nerve as close to the foramen as possible The animals were killed afterwards. Definite twitching was noticed in the frontalis intermittent twitching among the posterior auricularis muscles (despite the fact that the platysma cervicale innervated by the same branch twitched incessantly) and slight twitching along the lateral side of the ear

This method was not considered satisfactory however for no attempts could be made to observe the deep muscles since in exposing them their innervation might be severed Furthermore while there was no doubt of the response of the frontalis muscle it was difficult to determine if other movements noticed were independent of the motion produced by the frontalis.

Although the failure to find the musculature atrophy which would result from neurological malfunction indicates that there is no neurological difficulty it is felt that this question is not adequately answered.

The possibility of a deficient blood supply to these muscles was not considered

as a cause of the immobility since neither dissection nor histological examination indicated any vascular abnormalities specific to the dachs rabbit.

DISCUSSION

The lack of atrophy and the obvious dysplasia of cartilage and muscle strongly indicates that the ear carriage and immobility of the ear of the dachs rabbit is a developmental fault. Retardation demonstrated by the diminution in size of the proximal external ear cartilages and certain of the muscles is obviously the primary effect, as it was with the abnormalities of the spheno-occipital and occipitovertebral junctures and the generalized malformation of the posterior skull. In this location, however the hypoplasia secondarily affects both cartilage and muscle so as to seriously interfere with the normal functions of these parts.

The effects which can arise from similar abnormal interrelations between connective tissue cartilage and bone have been recognized for some time for example, in the work of Weiss ('29) Glücksmann ('32 42) Weiss and Amprino ('40) Bryson ('45) and Chin ('52, '53) They are also illustrated by the changes in the occipitovertebral articulation of the dachs rabbit (Sawin, Ranlett, and Crary '62) If tension and compression forces are prime factors in establishment, differentiation and shaping of mesodermal tissues inducing such abnormal units as traction epiphyses (described by Barnett and Lewis, '58) and irregularities in pattern of ossification of the sternum as described by Bryson, the irregularities in these muscles of the ear are not surprising since they are so dependent for optimum development upon the physical forces which they generate.

Precise details of how the individual muscle derangements come about can be supplied only by study of fetuses Nevertheless, it is apparent that the ear immobility itself is caused by the *Da* gene both indirectly through dwarfing and malforming of the skull and, less obliquely by preventing the formation of two small but essential pieces of ear cartilage.

At the meati, the basioccipital of the adult dachs is significantly narrower (94%) than normal, although a similar reduction across the vault is not demonstrable (Sawin and Crary '57) This condition has the effect of pulling the entire ear mechanism down and displacing it laterally in such a manner that the frontalis and the scutulo-auricularis anterior muscles fail to make their normal insertions on the anterior helix, instead attaching medial to it. Since such an event could only have taken place early in fetal life, it is interesting to note that Crary Sawin, and Atkinson ('58) found the basioccipital reduced as much as 18% in width and 26% in length in 22-day dachs fetuses. The effects of this on the ear mobility should not be underestimated. These two muscles are the major levators of the ear and, despite their size, are at a considerable disadvantage by being deprived of the leverage given them by their normal insertion

Of particular interest with respect to the total immobility of the ear is the direct effect of the *Da* gene on the scutular cartilage and the spina helicis anterior As mentioned previously the scutular cartilage provides a platform from which certain muscles act on the ear Figure 12B illustrates clearly that the *Da* gene in preventing the formation of cartilage has reduced this platform to a loose-hinged frame of connective tissue filled mostly with frontalis fibers Normally when the ear is to be lifted all the muscles attaching to the scutular cartilage act in concert some to steady this platform, others to raise the ear In the dachs, these muscles merely stretch, distort, elongate and twist the frame of connective tissue to which they are attached without moving the ear Almost all the muscles inserting into this frame are thus made quite useless including the small slips from the posterior auricularis muscles, all of the occipitoscutularis (except the anterior fibers which normally insert elsewhere) the entirety of the interscutularis and cervicoscutularis muscles and the frontalis. The muscles originating from the frame are similarly made inactive the levating scutulo-auricularis muscles and the rotator the subscutulo-auricularis. The unemployment spreads for unless raised the ears cannot be depressed (by the mandibulo-auricularis and sterno-auricularis) pointed (by the

zygomatico-auricularis and the temporo-auricularis) nor rotated (by the posterior auricularis muscles) (cf., fig 5) Furthermore by prohibiting the formation of the spina helicis anterior the *Da* gene reduces the action of the auricularis anterior inferior solely to moving connective tissue The only muscles not obviously affected are the majority of the intrinsic muscles which are undoubtedly responsible only for the small amount of ear opening and closing which is observed occasionally The slight lateral motion of the ears in the horizontal plane is undoubtedly caused by the platysma myoides.

With respect to the muscle dysplasias, the fragmentation of tragicus muscles and the failures of the temporo-auricularis and tragohelicinus muscles to insert on the anterior helix may well be caused by the widening of the cleft between the anterior helix and the tragus. This separation of parts held closely together in normal rabbits is related to the retardation of the *Da* gene on the basicranium for in addition to being narrower the dachs basicranium in 21 and 22-day-old fetuses is also significantly shorter than in normals. This shortening brings the zygomatic arch abnormally close to the meatus which thereby causes the lateral compression so characteristic of the dachs meatus. The annular cartilage and the auricular cartilage adapting themselves to this elliptically-shaped meatus become broad and flat with the anterior helix spread well away from the tragus. If this excessive widening of the cleft occurred at a critical time with respect to the attachment of the muscles bridging it, displacement and fragmentation of those muscles would be expected as well as the exposure of the anterior superior cornu

The causes of the muscle dysplasias involving the auricular anterior profundus seem less apparent. The failure of the spina helicis anterior to develop is probably contributory but it is hardly a cause in itself since the muscles attaching normally to the scutular cartilage are not displaced in its absence The problem of the single zygomatico-auricularis that inserted onto the squamosal process of the temporal bone may not be quite so obscure since the normal point of insertion of this muscle during fetal development is actually adjacent to the process.

Although the primary cause of the ear immobility resides in the retardation of muscle and cartilage elements of the ear it is of further significance to note that one of the muscles (the sphincter colli profundus) is not retarded. In fact, this muscle presented some difficulty in dissection of underlying muscles of the dachs animals due to an apparent sheet of fibrous material which appeared as an extension of it. Although this sheet could have arisen as a secondary compensatory adjustment to the primary hypoplasias of the other units of the system specific adjustments are difficult to define Summary table 1 shows that all muscles tend to be present in some degree and furthermore that the dysplasia thus affects only certain members of both extrinsic and intrinsic groups in varied degrees. Some such as tragicus have lost only the unit to which they normally attach. However all seem to have made the nearest possible attachment. Still others have themselves been reduced or fragmented. All but one (auricularis anterior profundus) retain their normal origins.

A similar situation was found by Carter ('51) in the limbs of the luxate mouse Kadam ('62) has called attention to the fact that several investigators of such specific gene induced skeletal anomalies as polydactylism (in cats and mice) syndactylism, hemimelia, and undulated in mice have shown a tendency for muscular anomalies of the "localized" type in the limbs to appear as a direct consequence of skeletal anomalies with which they coexist.

In comparison, the case of oligodactylism (*Os*) where the relationship is less close the muscular anomalies are present on the postaxial side of the limb whereas the skeletal deficiencies are preaxial This situation is interpreted by Danforth ('47) and Grüneberg ('61) as due to the early localization of the defect in the limb bud. In this case essentially a demonstrable deficiency of material on the preaxial side. Whether this deficiency can bring about the entire complex of muscular anomalies is still not clear Kadam notes the unusual insertions of some of the muscles

which, he believes, contravene the well-founded concepts of homologies and render dubious their value for identification of structures concerned. Kadam's conclusion may not necessarily follow when more is known about the early development of related parts. In each of the above cases the most important feature seems to be the disturbance in the relationship between neighboring units of tissue particularly with respect to their individual capacities for growth and differentiation. All the abnormalities seem to stem primarily from localized disturbance of growth, first of some one specific tissue such as mesenchyme, or of one or more individual units derived from it. Deficiency can apparently be compensated in one of two ways (1) from the growth potentialities of adjacent tissue units which at the time happen to possess a relatively greater reserve growth capacity or (2) from the division of a primordial growth center into more than one unit. In the dachs the retardation at the occipitovertebral border is compensated in both ways (Sawin, Ranlett, and Crary '62) However, the retardations in cartilage and muscle of the ear for some reason are not as easily compensated. The so-called fragmentation of muscles (above) would seem to indicate a division of the muscle subsequent to its attachment or insertion possibly the result of delayed growth of the cartilage. Failure or displacement of insertion indicates an inability to make proper contact. Here the very nature of muscle function is such that delay in establishing normal contacts is critical and relatively in some cases at least, nonadjustable. Thus in contrast to the compensatory adjustments of cartilage and bone made at the occipitovertebral border the enlargement of the sphincter colli profundus (the only unit at all enlarged) seems a relatively feeble adjustment. In view of its normally broad origin and insertion the real significance of this muscle is at present in doubt.

Although no observations have been made on the morphology of the middle ear the apparent response of some of the dachs to auditory stimulation, coupled with no external evidences of semicircular canal involvement, would indicate that the units are probably normal and that the relative immobility of the ear is not due to deafness.

The fact that, as shown by Sawin Ranlett, and Crary ('59) fusion at the spheno-occipital border is accompanied by minimal fusion at the more posterior occipital sutures together with the cartilage and muscle deficiencies of the ear and the induction of accessory centers at the occipitovertebral border suggests not only a retardation effect common to all parts but also some overall adjustment in the distribution of the peak capacity for growth. In relation to successive segmental units of the skull this peak appears to be centered more posteriorly and in such a way that anterodorsally the ear muscles and cartilages are deficient.

## SUMMARY AND CONCLUSIONS

Gross dissection and histological examination of the cartilage and muscle of the ears of 14 dachs rabbits and 16 normal controls segregating from heterozygous parents reveals that the horizontal carriage the appearance of the superior anterior cornu of the tragus and the immobility of the ears are essentially the result of developmental retardation involving the occipital, otic, and atlanto-axial regions. The immobility is due to dysplasia of cartilage and muscle which disturbs the normal relations and attachments of these parts and thus the mechanism for normal effective elevation, depression, and rotation. The spina helicis anterior at the base of the auricular cartilage is absent in most individuals and very much reduced in others. The scutular cartilage, which normally provides a moveable platform from which levator and forward rotator muscles can function to best advantage in terms of leverage, is absent. These skeletal and cartilaginous effects lead to diminution, attentuation, fragmentation, and displacement of the ear muscles, thereby preventing the erection of the large auricle Hypotheses that neurological, vascular and auditory disorders might be the cause of the immobility were examined and discarded as remote.

The papilla-like structure of the dachs ear proves to be the superior anterior cornu of the tragus which in normal rab-

bits develops in contact with the anterior belix and like the posterior cornu is not apparent beneath the skin.

Similarities between these skeletal and muscle anomalies and those found in syndactylism and oligodactylism in mice are discussed.

## LITERATURE CITED


Antonitis, J J Dorcas D. Crary P B Sawin and Carl Cohen 1954 Sound induced seizures in rabbits. J Heredity 45 279–284.

Arey L. B 1954 Developmental Anatomy 6th ed. W B. Saunders, Philadelphia.

Barnett, C. H., and O J Lewis 1958 The evolution of some traction epiphyses in birds and mammals. J Anat., 92 593–600.

Bryson, V 1945 Development of the sternum in screwtail mice Anat. Rec., 91 119–148

Carter T C. 1951 The genetics of luxate mice. I. Morphological abnormalities of heterozygotes and homozygotes. J Genet., 50: 277–299

Chen, J M. 1952 Studies on the morphogenesis of the mouse sternum. II. Experiments on the origin of the sternum and its capacity for self-differentiation in vitro. J Anat., 86 387–401.

——— 1953 Studies on the morphogenesis of the mouse sternum. III. Experiments on the closure and segmentation of the sternal bands. Ibid., 87 130–149

Crary D D and P B. Sawin 1952 A second recessive achondroplasia in the domestic rabbit. J Heredity 43 254–259

Danforth, C. H. 1947 Morphology of the feet in polydactyl cats. Am. J Anat., 80 143–172.

Denes, P and W Kocher 1961 The reliability of Preyer ar reflex in the mouse (mus musculus) Die N turwissenschaften, 48 82–83.

Gerhardt, U 1909 Das Kaninchen. Werner Klinkhardt, Leipzig.

Glücksman A. 1939 Studies on bone mechanics in vitro II. The role of tension and pressure on chondrogenesis. Anat. Rec., 73 39–55.

Grüneberg, H. 1961 Genetical studies on the skeleton of the mouse. XXVII. The development of oligodactylism. Genet. Res., 2. 33–42.

Kadam, K. M. 1962 Genetical studies of the skeleton of the mouse. XXXI. The muscular anatomy of syndactylism and oligodactylism. Ibid., 3 139–156.

Meinertz, T 1935 Die Hautmuskulatur der Saugetiere. Yahrb. Morph. u Mikrosk. Anat. Abt. I, Gegenbaurs Morph. Yahrb., 76: 1–51

Sawin P B., and Dorcas D Crary 1957 Morphogenetic studies of the rabbit. XVII. Disproportionate adult size induced by the Da gene. Genetics 42: 72–91.

Sawin, P B D. D Crary and Nancy Atkinson 1958 Morphogenetic studies of the rabbit. XXI. The nature of disproportionate dwarfism induced by the Da gene revealed by the early fetal ossification pattern. Am. J Anat., 103. 69–97

Sawin, P B Dorcas D Crary and Judith Webster 1959 Morphogenetic studies of the rabbit. XXIII. The effects of the dachs gene Da (chondrodystrophy) upon linear and lateral growth of the skeleton as influenced by time. Genetics, 44: 609–624

Sawin, P B., Mary Ranlett and D. D Crary 1959 Morphogenetic studies on the rabbit. XXV The spheno-occipital synchondrosis of the dachs (chondrodystrophy) rabbit. Am. J Anat., 105 257–280.

——— 1962 Morphogenetic studies of the rabbit. XXIX. Accessory ossification centers at the occipitovertebral border in the dachs rabbit. Ibid., 111 239–257

Weiss P 1929 Erzwingung elementarer strukturverschiedenheiten am in vitro wachsenden Gewebe. Roux. Arch., 116 438.

Weiss, P and R. Amprino 1940 The effect of mechanical tress in the differentiation of scleral cartilage in vitro and in the embryo. Growth, 4 245–258.

# Morphogenesis of the Down Feather in the Presence of Pyrimidines a Riboside and Related Compounds[1]

CHARLES WILLIAM GIBLEY JR.
*Department of Zoology and Entomology Iowa State University Ames, Iowa*

Antimetabolites and structural analogues of normal cell components were used as tools in the study of development by Brachet (45 46 47) who studied the effects of acriflavine barbituric acid and benzimidazole on gastrulation and neurulation in the the frog embryo Hisaoka and Hopper ('57) explored the effects of barbituric acid and one of its derivatives on the development of the zebra fish, *Brachydanio rerio* Derivatives of nucleic acids have also been employed in the study of the embryology of higher animals. For example, Frair and Woodside ('56) and Waddington and Perry ('58) used 8-azaguanine in studies of the growth and development of early chick embryos. The same analogue produced abnormalities of the skeletal system in developing mice (Kelton and Woodside '55 Nishimura and Nimura, '58)

In a previous study (Gibley and Hamilton, '63) the developing down feather was grown in the presence of certain compounds structurally related to the purine and pyrimidine bases of nucleic acids. These experiments tested the effects of the growth- promoting substance orotic acid, and the purine and pyrimidine analogues, isoguanine sulfate 8-azaguanine thiouracil, and 2 amino-4-hydroxy-6-methylpyrimidine on organogenesis and differentiation. Briefly orotic acid and the guanine derivatives inhibited the development of feathers at concentrations of 333 and 166 $\mu g$/ml. They also disturbed the pattern of alkaline phosphatase and the reaction for ribonucleic acid. Alkaline phosphatase was either not present, or diffused throughout the tissue with no localization in feather loci. Thiouracil increased the reaction for alkaline phosphatase particularly in the outlying fibroblasts.

A striking effect of the analogues was noted in the nucleoli. These were enlarged or vacuolated, irregular in size and shape, or even linked in chains. The principal effect seemed to be upon nucleolar RNA, although there was good correlation between the activity of phosphatase and growth of feathers

The present investigation was an outgrowth of the earlier one, with the aim of employing additional compounds related to components of nucleic acids to see how they would affect development of the feather The substances selected included such relatives of uracil as 5-bromouracil 5-nitrouracil, and barbituric acid the pyrimidine analogues dithiopyrimidine isoorotic acid, and 2,4 6-triaminopyrimidine inhibitors of the synthesis of ribonucleic acid, diethylbarbituric acid and 4,5,6-(or 5 6 7) trichloro-1-(β-D-ribofuranosyl)-benzimidazole and, an inhibitor of protein synthesis puromycin. Specifically the effects of these compounds on alkaline phosphatase and ribonucleic acid were noted, since the latter two substances always seem to be active during the development of the down feather (Koning and Hamilton 54 Hamilton and Koning, '56

This investigation was supported in part by research grant, RG-3612 (C5), from the Division of Research Grants and Fellowships, National Institutes of Health, U S. Public Health Service, and by the Industrial Science Research Institute of Iowa State University of Science and Technology
This paper is based on a dissertation submitted to the Graduate Faculty of Iowa State University in partial fulfillment of the requirements for the degree, Doctor of Philosophy in May 1961 The author expresses sincere gratitude to his major professor Dr. Howard L. Hamilton, for suggesting the problem and for the advice and constructive criticism he has so graciously offered during the course of the investigation.

Present address Department of Biology Villanova University Villanova, Pennsylvania.

This compound, hereafter abbreviated to TRB, was provided through the courtesy of Dr Karl Folkers of Merck and Company

Puromycin was supplied through the courtesy of Dr. B L. Hutchings of the American Cyanamid Company

Fabiny '59) Where applicable tests were also made for protein. In addition, the total growth of treated cultures was measured and compared with controls. Because of previous interest in the nucleolus (Gibley and Hamilton, '59 '63) this structure was examined closely in an effort to determine what role it might play in the morphogenesis and differentiation of the down feather

## MATERIALS AND METHODS

The procedures used in preparing solutions incorporating them with paired explants of chick skin and processing the tissues for study were identical with those given in a previous paper (Gibley and Hamilton, '63) The one additional technique used was that of staining sectioned cultures for total protein with mercuric bromphenol blue (Mazia, Brewer and Alfert '53). Some sections were pre-treated with ribonuclease to remove nucleic acids that might bind basic groups and interfere with the interpretation of the protein stain Other sections were stained in bromphenol blue without mercury in the solution in an attempt to identify the kind of protein.

## RESULTS

The concentration of chemical in the cultures was varied between 1666 and 1 6 μg/ml to determine the least amount which would affect development of the feathers Cultures were incubated for two to four days and examined microscopically The results obtained from the living cultures are summarized in table 1 2 4 6-Triaminopyrimidine produced no significant effect except at high concentrations (1666 and 833 μg ml) At such levels it was probably toxic 5-Bromouracil 5-nitrouracil diethylbarbituric acid and isoorotic acid had no substantial effect at any of the concentrations tested. Barbituric acid dithiopyrimidine puromycin and 4,5 6-(or 5 6 7 ) trichloro-1 (β-D-ribofuranosyl)-benzimidazole all produced various degrees of feather inhibition depending on the concentrations used

*Barbituric acid* (BA) This close relative of uracil was inhibitory only at high concentrations (833 and 333 μg ml) and then not consistently (see table 1) The most striking effects were produced at 833 μg/ml. Feathers were prevented from forming in about 35% of the explants. In another 27% of the cases the feathers in the treated cultures were less numerous and smaller than in controls. Alkaline phosphatase was active but splotchy in the centers of affected loci. Histologically phosphatase-positive granules were found between cells. The nuclei were also phosphatase-positive. Dotlike deposits of the enzyme reaction appeared where there should have been a build-up of alkaline phosphatase in a feather locus. Peripherally each feather locus seemed to be broken into smaller centers of phosphatase activity as though the morphogenetic field had lost control over the outlying zones (figs. 5–7)

Serial sections of cultures treated with barbituric acid showed just the beginnings of feathers. There was some outgrowth, but there seemed to be a lack of organization. The distribution of ribonucleic acid was comparable to that of the control. The most striking effect was found in the nucleoli. Normally there are two per nucleus small and spherical or ovoid in a control feather (fig. 1) In treated cultures the nucleoli of the epidermis were very prominent typically single (fig. 2) The same situation was seen in the nucleoli of the pulp but not as often Multiple nucleoli were also observed (fig 3) They were smaller and not as prominent as the single type

*Dithiopyrimidine* (DTP) arrested growth of feathers at a concentration of 333 μg/ml. Lower levels had no significant effect. Treated cultures showed a variety of conditions: (1) some positive reaction for alkaline phopshatase in the fibroblasts (2) localization of the phosphatase within a few feather loci and, (3) the explant completely negative for alkaline phosphatase The most prevalent condition was an inhibition of feathers with a corresponding diminution in the amount of alkaline phosphatase (figs. 9–10)

In contrast to barbituric acid sectioned material of cultures treated with DTP showed no effect on the nucleoli. The amount of ribonucleic acid was also comparable to the control. There was consid-

Toxicity — no growth of cultures explant were nothing more than cellular debris

erable necrotic material localized in the pulp. The organization of the prospective feather germ was poor Even though the epidermis had begun to protrude to form a feather, cells were arranged haphazardly The destructive effect seemed to be concentrated in the pulp with a concomitant lack of organization in the epidermis (fig. 4)

*4,5 6-(or 5 6 7) Trichloro-1-(β-D-ribofuranosyl)-benzimidazole* (TRB). Concentrations of 83.3 and 41 6 μg/ml completely stopped growth and differentiation of feathers. Alkaline phosphatase was present but not localized in feather loci (figs. 8 and 11) Lower levels (20 μg/ml) permitted growth but totally suppressed the development of feathers. Phosphatase was diffuse throughout the original explant. A few feather areas were present, but they were splotchy in appearance. The feather appeared broken up into little centers within a larger one (figs. 12–14) as though there had been some weakening and subdivision of the original field Concentrations of 10 μg/ml still produced some inhibition but feather growth and the appearance of phosphatase approached the conditions in the control. Some feathers were nearly normal in morphology and histology Others had definite centers surrounded by an encampment of little centers much as occurred at 20 μg/ml. Levels below 10 μg/ml produced no significant effect.

Sections of cultures treated with TRB (20 μg/ml) showed a much-thickened epidermis above the pulp. The only sign of an epidermal response to the underlying pulp was a nodular aggregation of cells above the dermis (figs. 15–16) Sections stained with toluidine blue contained basophilic material in both the epidermis and the pulp (compare with the control fig 15)

The nuclei were elongated and boat shaped, not characteristically oval. The epidermal nuclei contained single large and many smaller nucleoli which were not as prominent as those seen in the cultures treated with barbituric acid (figs 30–32) The majority of the nuclei of the epidermis and pulp contained 4–6 nucleoli they were small and sometimes lined up in chains.

The use of ribonuclease in conjunction with toluidine blue revealed a striking difference between control cultures and those treated with TRB Controls treated with toluidine blue alone showed the typical picture described by Koning and Hamilton ('54) in which the epidermal cytoplasm was heavily basophilic especially where it bordered the pulp (fig. 17) The cytoplasm of the pulp cells was lightly stained. Nuclear (and nucleolar) basophilia was about as intense in the epidermis as in the pulp. In a control feather treated with ribonuclease and then toluidine blue (fig 18) all of the cytoplasmic basophilia next to the basement membrane had disappeared, indicating that this material was ribonucleic acid (cf Koning and Hamilton '54) Some basophilia remained in the nuclei and nucleoli of both the epidermis and the pulp after treatment with the enzyme with stronger reaction in the epidermis. In a culture treated with TRB and stained with toluidine blue there was basophilia in the nuclei, including the nucleoli but less than in the control (fig. 19) The amount of basophilia found in the cytoplasm was far less than in the control, and there was no comparable accumulation of basophilic material next to the basement membrane (compare figs. 17 and 19) Treatment of TRB sections with ribonuclease removed almost all of the basophilia The cytoplasm was completely negative (fig 20) Nuclear basophilia was absent except in the nucleoli, and even these were not as prominent as before treatment with ribonuclease

In general, the amount, distribution, and localization of protein in a TRB-treated culture were comparable to a control. Treatment of sections with ribonuclease prior to application of the protein stain did not result in a significant difference between these and the normally-stained sections. If anything the sections treated with ribonuclease were a little darker Sections stained with bromphenol blue without mercury were equal in color to those stained with mercuric bromphenol blue.

*Puromycin* stopped growth at concentrations of 333 166 83.3 41 6 20.8 10 4 5.2 and 1 7 μg/ml (see table 1) Such levels were probably toxic At 1 μg/ml

TABLE I

*Effect of analogues on the growth nd development f feathers*

| Chemical | Conc. | Total no. | | Average diameter of cultures | | Average no. of feathers | | ND | S | C | Stim. | Per cent inhibition of feathers |
|---|---|---|---|---|---|---|---|---|---|---|---|---|
| | | Embryos | Cultures | Control | Treated | Control | Treated | | | | | |
| | μg/ml | | | mm | mm | | | | | | | |
| BA | 833 | 16 | 104 | 3 16 | 2 88 | 4 0 | 2.3 | 10 | 29 | 37 | 19 | 63.5 |
| BA | 333 | 5 | 21 | 4 47 | 3.96 | 4.9 | 3.5 | 2 | 14 | 2 | 6 | 66.6 |
| BA | 166 | 7 | 35 | 3.82 | 3.46 | 3.94 | 2 83 | 6 | 9 | 10 | 10 | 54.2 |
| BA | 33 | 12 | 74 | 3.90 | 3.81 | 4.26 | 4 04 | 21 | 22 | 3 | 28 | 33.7 |
| TRB | 83.3 | 2 | 9 | 3.01 | 1.00 | 3.77 | 0.00 | 0 | 0 | 9 | 0 | 100 |
| TRB | 41.6 | 2 | 9 | 3.85 | 1.00 | 4.00 | 0.00 | 0 | 0 | 9 | 0 | 100 |
| TRB | 20 8 | 16 | 74 | 3.41 | 2.16 | 4 41 | 0.12 | 0 | 4 | 70 | 0 | 100 |
| TRB | 10.4 | 5 | 31 | 3.08 | 2.69 | 5.25 | 2.38 | 4 | 13 | 11 | 3 | 77.3 |
| TRB | 5 2 | 2 | 15 | 2.83 | 2.70 | 5.26 | 5.06 | 0 | 9 | 0 | 6 | 60 |
| DTP | 333 | 9 | 57 | 4 42 | 3.77 | 4 71 | 0.43 | 1 | 7 | 48 | 1 | 96.5 |
| DTP | 166 | 8 | 55 | 4.53 | 4 49 | 4.56 | 2.60 | 9 | 25 | 14 | 7 | 71.0 |
| DTP | 83.3 | 7 | 51 | 4 46 | 4 44 | 5.27 | 4.25 | 15 | 26 | 2 | 8 | 54.9 |
| DTP | 41.6 | 2 | 15 | 3.96 | 3.84 | 4.26 | 3.80 | 3 | 8 | 0 | 4 | 53.3 |
| DTP | 20.8 | 2 | 14 | 3.64 | 4.30 | 5.65 | 5.65 | 6 | 5 | 0 | 3 | 35.7 |
| T | 1666 | 2 | 12 | 5.45 | 1.00 | 3.91 | 0 00 | 0 | 0 | 12 | 0 | 100 |
| T | 833 | 3 | 15 | 4.52 | 2.60 | 3.33 | 0.00 | 0 | 0 | 15 | 0 | 100 |
| T | 333 | 8 | 50 | 4 46 | 3.72 | 4.54 | 1.94 | 6 | 25 | 17 | 2 | 84 |
| T | 166 | 6 | 31 | 4 63 | 4.26 | 4.63 | 2.61 | 5 | 16 | 7 | 3 | 74.2 |
| T | 83.3 | 5 | 34 | 4.47 | 4.53 | 4 71 | 4.38 | 12 | 12 | 3 | 7 | 44.2 |
| T | 33.3 | 11 | 66 | 4 42 | 4 65 | 4.51 | 3.42 | 19 | 28 | 5 | 16 | 47 |
| T | 16.6 | 7 | 46 | 4.94 | 5.29 | 5.15 | 4.59 | 7 | 21 | 2 | 16 | 50 |
| [illegible] | 500 | 2 | 15 | 2.77 | 2 59 | 4.53 | 3.60 | 4 | 6 | 0 | 3 | 83.3 |
| [illegible] | 333 | 2 | 9 | 3 06 | 3.04 | 5.77 | 5 08 | 1 | 5 | 0 | 3 | 85 |
| [illegible] | 166 | 3 | 16 | 3 42 | 3.56 | 6 06 | 5.53 | 1 | 6 | 2 | 7 | 50 |
| [illegible] | 83.3 | 2 | 12 | 2 80 | 3.17 | 5.41 | 5 75 | 2 | 4 | 0 | 5 | 33 |
| [illegible] | 41 6 | 2 | 16 | 3 62 | 2.70 | 06 | 6.21 | 6 | 4 | 0 | 6 | 25 |
| | | | | | | | == | | – | | | 73 |

| | | | | | | | | | | | | |
|---|---|---|---|---|---|---|---|---|---|---|---|---|
| [illegible] | [illegible] | | | [illegible] | | [illegible] | [illegible] | | | | | [illegible] |
| NU | [illegible] | | [illegible] | 04 | [illegible] | | | | | | | [illegible] |
| NU | [illegible] | | [illegible] | 40 | 4.87 | 3. | .84 | | | | | [illegible] |
| NU | [illegible] | | | 00 | 3.08 | .00 | .00 | | 0 | | [illegible] | 0 |
| NU | 83.3 | [illegible] | 18 | 3.36 | 3.43 | 3.85 | 2.33 | [illegible] | [illegible] | [illegible] | [illegible] | 17 |
| IO | 500 | 3 | 22 | 3.09 | 2.83 | 3.80 | 3.09 | 4 | 10 | 4 | 4 | 63.6 |
| IO | 333 | 3 | 21 | 2.99 | 2.90 | 3.14 | 3.38 | 5 | 7 | 1 | 8 | 36.1 |
| IO | 166 | 3 | 20 | 2.85 | 2.55 | 3.05 | 2.20 | 7 | 10 | 3 | 0 | 60 |
| IO | 83.3 | 1 | 8 | 3.25 | 3.10 | 2.50 | 2.12 | 4 | 2 | 1 | 1 | 37.5 |
| P | 333 | 1 | 7 | 3.41 | 1.0 | 3.58 | 0.00 | 0 | 0 | 7 | 0 | 100 |
| P | 166 | 1 | 7 | 3.27 | 1.0 | 2.14 | 0.00 | 0 | 0 | 7 | 0 | 100 |
| P | 83.3 | 1 | 7 | 2.78 | 1.0 | 3.86 | 0.00 | 0 | 0 | 7 | 0 | 100 |
| P | 41.6 | 1 | 10 | 3.49 | 1.0 | 3.80 | 0.00 | 0 | 0 | 10 | 0 | 100 |
| P | 20.8 | 2 | 13 | 3.15 | 1.0 | 3.15 | 0.00 | 0 | 0 | 13 | 0 | 100 |
| P | 10.41 | 1 | 7 | 2.92 | 1.0 | 3.00 | 0.00 | 0 | 0 | 7 | 0 | 100 |
| P | 5.20 | 2 | 11 | 3.23 | 1.0 | 3.64 | 0.00 | 0 | 0 | 11 | 0 | 100 |
| P | 1.7 | 3 | 13 | 2.83 | 1.0 | 3.22 | 0.00 | 0 | 0 | 13 | 0 | 100 |
| P | 1.06 | 13 | 60 | 2.90 | 1.01 | 3.67 | 0.00 | 0 | 0 | 60 | 0 | 100 |
| P | 0.53 | 2 | 15 | 3.16 | 2.66 | 5.80 | 3.67 | 0 | 11 | 1 | 3 | 80 |
| P | 1/3 | 2 | 9 | 2.58 | 1.66 | 2.67 | 1.33 | 1 | 2 | 4 | 2 | 66 |
| P | 1/6 | 1 | 6 | 2.20 | 2.40 | 2.50 | 1.87 | 1 | 2 | 1 | 2 | 50 |
| DB | 1666 | 3 | 19 | 2.78 | 2.82 | 4.38 | 4.26 | 5 | 8 | 0 | 6 | 42.1 |
| DB | 833 | 3 | 15 | 3.26 | 3.12 | 4.73 | 4.60 | 7 | 4 | 1 | 3 | 33 |
| DB | 500 | 3 | 16 | 2.53 | 2.56 | 2.74 | 2.56 | 8 | 4 | 1 | 3 | 31.2 |
| DB | 333 | 3 | 14 | 2.75 | 2.74 | 2.28 | 2.64 | 5 | 3 | 0 | 6 | 21.4 |
| DB | 166 | 2 | 9 | 2.78 | 2.75 | 3.22 | 2.78 | 3 | 2 | 1 | 3 | 33 |
| DB | 83.3 | 2 | 11 | 2.96 | 2.93 | 3.64 | 2.92 | 1 | 5 | 1 | 4 | 54 |

ND no difference; R reduction in size and number; O complete absence of feathers; Stim. better growth of feathers; BA barbituric acid; TRB 4,5,6-(or 5,6,7-) trichloro-1-(β-D-ribofuranosyl)benzimidazole; DTP dithiopyrimidine; T 2,4,6-triaminopyrimidine; B bromouracil; NU nitrouracil; IO isoorotic acid; P puromycin; DB diethylbarbituric acid.

Per cent inhibition of feathers — the sum of columns "R" and "C" divided by the total number of cultures.

the observation that halogenated derivatives of benzimidazole interfere with the metabolism of RNA (Tamm Folkers and Shunk, '56) a complete inhibition was not noted in our experiments. RNA did not accumulate in the cytoplasm next to the basement membrane as in the control (compare figs. 17 and 19) Nevertheless some RNA was present, principally in nuclei because a considerable amount of basophilic material was removed from TRB cultures treated with ribonuclease (compare figs. 19 and 20) Evidently there had been some synthesis of RNA in the nucleus and either no movement of it to the cytoplasm or no independent synthesis of RNA in the cytoplasm.

In amount and distribution, proteins were comparable in controls and TRB-treated cultures. Possibly TRB had no effect on the synthesis of protein and the protein stained in the treated cultures was already present before the addition of the chemical. Addition of TRB could have prevented the formation of new proteins destined for the construction of feathers

The suggestion was made above that TRB interfered with the appearance of RNA in the cytoplasm either by preventing the release of RNA from the nucleus or by stopping the formation of RNA directly in the cytoplasm itself It was also suggested that the synthesis of new protein was inhibited How might these possibilities be explained?

DRB and TRB are structurally related to adenosine the normal nucleoside derivative of RNA. Adenosine has been found to block the action of DRB (Tamm '57) indicating the DRB and adenosine are antagonists. In the present experiments there was some indication that adenosine could prevent the effects of TRB because additions of adenosine permitted growth in the TRB-treated cultures (see table 2) Being an antagonist of the naturally occurring nucleoside TRB could have been incorporated into RNA forming an aberrant molecule incapable of performing the usual metabolic functions of RNA. Such an abnormal RNA could have stopped the transfer of materials from the nucleus to the cytoplasm and prevented the accumulation of RNA normally seen along the basement membrane in a control feather

If on the other hand there were an independent synthesis of RNA in the cytoplasm, and no transfer from the nucleus, TRB could still affect the synthesis of RNA by directly interfering with the incorporation of various components of nucleic acid within the molecule Either mechanism of limiting the functioning of RNA in the cytoplasm would restrict the production of new proteins and stop morphogenesis.

*Puromycin.* Nakamura and Jonsson ('57) found that puromycin inhibited the growth of *Endamoeba histolytica.* This inhibition was reversed completely with adenylic acid partially with adenine not at all with guanine. It was suggested that puromycin blocked the synthesis of nucleic acids in the amoeba. The inhibition of the growth of *Tetrahymena* by puromycin (Bortle and Oleson '55) was reversed by guanylic acid. It would thus appear that the metabolic block is a competitive action in the direct pathway of synthesis of nucleic acid by this protozoan Additional investigations (Agosin and von Brand '54 Hewitt et al. '54; Hutchings, '57) have provided further evidence for the hypothesis that puromycin interferes with purine metabolism.

In this investigation there was a reduction of basophilia (RNA) in the epidermis of treated cultures when compared with controls of the same stage of development (figs. 23–24) Coincident with this decrease in the amount of RNA were abnormalities of the nucleoli (figs. 27–29). Once again there seems to be a parallel relationship between an upset in the RNA content and changes in nucleolar structure.

In *Pseudomonas fluorescens* strain A..., puromycin did not inhibit the synthesis of RNA, whereas it completely abolished the formation of protein (Takeda Hayashi, Nakagawa and Suzuki '60) The incorporation of $P^{32}$-orthophosphate into RNA was not affected significantly The RNA formed in the presence of puromycin was stable in growing and resting cells. Contrary to expectation there did not appear to be less protein in our treated cultures than in the controls Apparently initial induction had taken place for the epidermis was thickened and showed some feather outgrowth Consequently there

had to be some formation of protein (probably from RNA that was present before the chemical was added to the system) The addition of puromycin might have stopped the synthesis of protein after the initial stock of RNA was exhausted. This would in turn, affect further growth and morphogenesis.

Attempts to counteract the effects of puromycin with adenylic acid were only partially successful. There was a definite indication of better growth, and some signs of better differentiation, when adenylic acid was added simultaneously with puromycin (see table 2) Thus it appeared that the antibiotic was antagonistic to adenylic acid. Such antagonism might have inhibited the formation of new RNA and secondarily limited the further synthesis of proteins.

*The nucleolus growth and differentiation.* Probably the most striking effect of the analogues used in this and a previous investigation (Gibley and Hamilton, '59 '63) was the change in the structure of the nucleolus. Most of the compounds tested (orotic acid, 8-azaguanine isoguanine sulfate, barbituric acid, TRB and puromycin) changed the shape size or number of the nucleoli in the cells of the treated cultures. Some of these chemicals decreased the amount of ribonucleic acid in the cells others may have produced an aberrant RNA. Similar results have been obtained by other investigators. β-2-Thienylalanine (an analogue of phenylalanine) produced large swollen nucleoli in the epidermal cells of inhibited feathers (Fabiny '59) Kischer and Hamilton, ('60 '63) observed large nucleoli in feather cultures treated with sodium cyanide.

In viral studies, the nucleoli of infected cells treated with 5-fluorouracil were enlarged (Pollard, Starr Tanami, and Elliott '60) It was suggested that fluorouracil caused accumulations of abnormal RNA-staining material which inhibited multiplication of the virus. The incorporation of fluorouracil into RNA to form an unnatural nucleotide has also been proposed by Grey ('60) Actinomycin decreased the RNA in non-malignant and malignant cells, with a corresponding reduction in the size of the nucleoli (Rounds Nakanishi and Pomerat, '60) An enlarged nucleolus has been considered a major criterion of a rapidly growing tumor (Mac Carty '36) Inhibition of cellular growth by ribonuclease also produced modifications of the nucleolus while repressing or completely preventing nucleolar and cytoplasmic basophilia (Chèvremont, Chèvremont-Comhaire and Firket, '58) Variations in metabolism have produced changes in the size and number of nucleoli (Swift, '59) These results indicate that modifications of the nucleolus accompany changes in RNA and in the growth and differentiation of the cell. The close relationship between RNA and the nucleolus in these processes is not surprising in view of increasing evidence that some synthesis of RNA takes place in the nucleolus.

How could modifications in the metabolism of RNA manifest themselves in structural abnormalities of the nucleolus? Antimetabolites and analogues of naturally-occurring metabolites could cause an accumulation of aberrant RNA in the nucleolus which might lead to its enlargement. Similar suggestions have been made by Fabiny ('59) and Pollard et al. ('60) In addition to the change in size other abnormalities of the nucleolus found in our experiments included a change in shape and vacuolization (*cf* Gibley and Hamilton, '63) Of the two types of RNA found in the nucleolus one is bound to the structural framework (Pollister and Leuchtenberger 49) and the other is soluble in acid solutions. An abnormal RNA could form in either type and produce structural changes in the nucleolus. If an abnormal soluble type passed into the cytoplasm it could interfere with normal growth and differentiation. It is apparent from the literature that the nucleolus has a high synthetic activity and rapid turn over of metabolites. For example the nucleolus incorporated glycine about a hundred times more rapidly than the cytoplasm in starfish oocytes (Ficq '53) With such a rate of turnover it is easy to visualize the incorporation of analogues into both types of nucleolar RNA.

In conclusion the results of the present study indicate that the nucleolus (acting through RNA) is important in the growth and differentiation of the down feather

## PLATE 1

### EXPLANATION OF FIGURES

1 Part of cross section of feather from control culture of skin from an embryo of stage 31 Sectioned at 7 µ and tained with toluidine blue. The nucleoli, which usually number two per nucleus, are small and ovoid. × 1,512.

2 Part of a cross section of feather from the corresponding bilateral half of the piece of skin shown in figure 1 grown in the presence of *barbituric acid (833 µg/ml) Note the single nucleolus in each* nucleus. × 1,512.

3 Part of a cross section of the same piece of tissue shown in figure 2. Note the numerou nucleoli within the nucleus. × 1,512.

4 Sagittal section of piece of tissue from an embryo of stage 32 grown in the presence of dithiopyrimidine (333 µg/ml) The pulp directly beneath the heavily stained epidermis, is necrotic. × 216.

5 Control explant of skin from the back of an embryo of stage 31. Note the strong reaction for alkaline phosphatase in the pulp of each feather immediately below the growing epidermal tip. × 56.

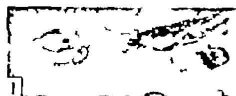
6 The corresponding bilateral half of the piece of tissue shown in figure 5 grown in the presence of barbituric acid (833 µg/ml) Peripherally each feather locus ppears broken into smaller centers of phosphatase activity × 56.

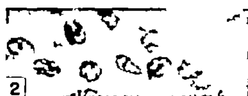
7 A higher magnification of the large feather locus shown in the center of figure 6. × 216.

8 Control explant of skin from the back of an embryo of stage 30 showing normal feathers and strong phosphatase reaction within the feather germs. × 56.

9 The corresponding bilateral half of the piece of tissue shown in figure 10 grown in the presence of dithiopyrimidine (333 µg/ml) There is an inhibition of f thers and diminution in the activity of alkaline phosphatase. × 56.

10 Control explant of skin from an embryo of stage 31 showing normal feathers and phosphatase reaction. × 56.


1

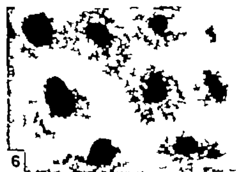

2


3


4


5


8


6


9


7


10

## PLATE 2

### EXPLANATION OF FIGURES

11 The corresponding bilateral half of the piece of skin shown in figure 8, grown in the presence of TRB (41.6 µg/ml) Alkaline phosphatase is present, but not localized within feather loci. × 56.

12 Control explant from the back of an embryo of t ge 32 showing the strong reaction for phosphatase within the feathers. × 56.

13 The corresponding bilateral half of the piece of tissue shown in figure 12, grown in the presence of TRB (20 µg/ml) The phosphatase is localized within feather loci. × 56.

14 A higher magnification of one of the f ther loci shown in figure 13. Note the subdivision of the area into smaller centers of phosphatase activity × 216.

15 Sagittal section of a control feather from skin explanted from an embryo of stage 31. Sectioned t 7 µ and stained with toluidine blue Note the heavy concentration of basophilia (RNA) in the epidermi especially in the cells which lie adjacent to the pulp. × 216.

16 Sagittal section of culture from the corresponding bilateral half of the piece of skin shown in figure 15, grown in the presence of TRB (20 µg/ml) Note the nodular aggregation of epidermal cells bove the pulp. × 216.

17 Sagittal section of control feather from an embryo of stage 32 Sectioned at 7 µ and stained with toluidine blue. The epidermis is heavily stained. × 216.

18 Sagittal section of a control feather from the same piece of skin shown in figure 17 Sectioned at 7 µ and stained with toluidine blue after prior treatment with ribonuclease. Note the removal of the intense basophilia in the epidermis shown in figure 17 especially that next to the basement membrane. × 216.

19 Sagittal section of a piece of tissue from the corresponding bilateral half of the explant shown in figure 17 grown in the presence of TRB (20 µg/ml) Sectioned t 7 µ and tained with toluidine blue Note the absence of the intense basophilia normally seen in the epidermis. There is little basophilia in the cytoplasm. × 216.

20 Sagittal section of piece of tissue from the same explant shown in figure 19 Stained with toluidine blue after treatment with ribonuclease. There is no basophilic material in the epidermis and the pulp. × 216.


11


12


13

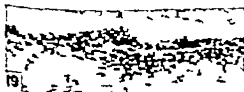

14


15


16


17


18


19

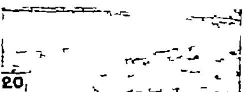

20

PLATE 3

EXPLAN TION O FIGURES

21 Sagittal section of control f ther from embryo of stage 32. Sectioned t 7 µ and stained with toluidine blue Note the large amount f basophilia (RNA) in the epidermis, especially in the cell bordering the basement membrane. × 480.

22 Sagittal section of piece f kin from the back f an embry f tage 33 grown in the presence of puromycin (1 µg/ml) The epiderml is thickened, but there is no outgrowth f f ther. Compare with control, figure 21 × 480.

23 Sagittal section of you g f ather from an embryo of stage 32 The epidermis, which is thickened and has begun t leval from the skin, is strongly basophilic × 480

I Sagittal section of piece f kin from n embryo f stage 32, grow in the presence of puromycin (1 µg/ml) There is slight protrusion of the epidermis, but a lack of the st ng basophilia seen in figure 23. × 480.

-5 Control explant f skin from the back of an embry of st ge 32, showing a normal reaction for phosphatase and normal f ther growth. × 56.

°6 The corresponding bilateral half of the piece of skin shown in figure 25, grown in the presence of puromycin (1 µg/ml) The reaction for alkaline phosphatase is diffuse. × 56.

27 Part of cross section of the feather shown in figure 21 The nucleoli are small and u ually double. × 1,312.

28 A higher magnification of figure 22, showing a single nucleolus in each nucleus. × 1,512.

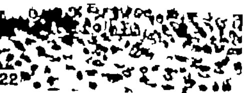
29 Part of cross section f skin from the corresponding bil teral half of the explant shown in figure 21 grown in th presence of puromycin (1 µg/ml) The nucleoli are multiple × 1,512.

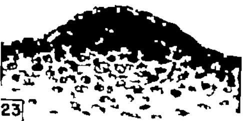
30 Part of cross section of the feather shown in figure 15, showing two nucleoli. × 1,512.

31 A higher magnific tion of figure 16 showing single nucleolus in one nucleus (see nucleus in top left hand corner) × 1,312.

32 A higher magnific tion of figure 19 showing multiple nucleoli w thin the nucleus. × 1,512.


21


22

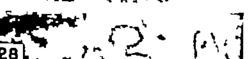

23


24

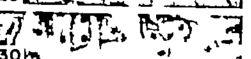

25


26

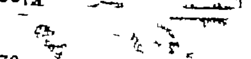

27


28


29


30


31


32

# Anatomy of the Normal Human Atrioventricular Conduction System[1,2]

JACK L. TITUS, GUY W. DAUGHERTY AND JESSE E. EDWARDS
*Section of Pathologic Anatomy and Section of Medicine, Mayo Cl... Mayo Foundation, Rochester, Minnesota*

The major morphologic features of the atrioventricular (AV) conduction system of the human heart have been discussed for several years — from time to time even the anatomic existence of the system has been questioned. In order to familiarize ourselves with the morphologic features of this system and to assess points of disputation before investigating it in relation to congenital ventricular septal defects, we reviewed the literature relevant to the human heart and carried out the studies reported herein of essentially normal human hearts. Attention was focused on the major divisions of the AV conduction tissue. As this was a morphologic study, we made no attempt to demonstrate the physiologic significance of the structures collectively called the atrioventricular conduction system.

## HISTORICAL REVIEW

Anatomic studies related to the problems of origin and conduction of stimuli for contraction of the heart may be regarded as beginning with the work of Purkinje (1845), as mentioned by Willius and Dry (48). Purkinje described fibers[a] in hearts of the sheep, cow, pig, and horse, which were probably muscular and related to a specific function. Ludwig's observation of ganglion cells in the interauricular septum of the frog, as was mentioned by Garrison ('29) and by Willius and Dry (48) and Bidder's discovery of ganglion cells at the AV junction in the frog (Willius and Dry, 48) seemed to support the neurogenic theories of cardiac contraction.

However, major anatomic discoveries in support of the theory that the conducting tissue is muscular also were made. His in 1893 discovered a muscle bundle connecting the auricular and ventricular septal walls and Kent (1893) described a[...]ssory muscular connections between [th]e right auricle and ventricle. Keith a[n]d Flack ('06) confirmed and extended the descriptions of the AV bundle and the branches from it to the right and left ventricles. Tawara ('06) traced out the bundle described by His (41), noted its apparent origin from a node in the floor of the right atrium, and showed the connection of the fibers described by Purkinje to those described by His. Retzer ('07) and Keith and Flack ('07) confirmed these findings, and Keith and Flack found the sino-auricular node in the right auricle which they believed to be the site of origin of the cardiac impulse.

Thus an anatomic basis for myogenic conduction of the impulse for cardiac contraction was established. Subsequent investigations reviewed by Lev ('60) have confirmed, with few exceptions (Van der Stricht and Todd, '20; Todd, '32; Glomset and Glomset, '40a,b; Glomset, Glomset and Birge, '44; Glomset and Birge, '45, '48; Glomset and Cross, '52), the presence of these structures and have extended knowledge of their gross and histologic features. Demonstration of the atrioventricular conduction system by the use of histochemical

---

[1] Abridgment of portion of thesis submitted by Dr. Titus to the Faculty of the Graduate School of the University of Minnesota in partial fulfillment of the requirements for the degree of Doctor of Philosophy in Pathology.

[2] This study was supported in part by Research Grant No. H-4014 from the National Heart Institute, United States Public Health Service.

[3] Presently Director, Department of Pathology and Clinical Laboratories, Charles T. Miller Hospital; Clinical Professor of Pathology, Medical School, and Professor of Pathology, Graduate School, University of Minnesota, St. Paul, Minnesota.

[a] The use of the term "Purkinje fiber" requires at least brief definition by the user to avoid mainly semantic arguments such as have filled the literature in the past regarding the existence of Purkinje fibers in the human heart. Tawara ('06) neatly handled the problem when he used the term "Purkinje fibers or their equivalents."

technics has been reported (Carbonell, '56, '58; Uhley and Rivkin, '59; Allen, Lederman and Pearl, '59; Bittencourt et al. '59; Wennemark, Benvenuto and Lewis, '60; Iwa et al., '61). Recently James ('61) has correlated the morphologic features of the AV node and the fibers surrounding it with electrophysiologic observations.

From these studies was derived the usual description (Barry and Patten, '60) of the AV conduction system in the normal human heart. *The AV node is located in the floor of the right atrium near the coronary sinus ostium, and the AV bundle extends anteriorly and inferiorly from this node to pass through the membranous septum to the ventricular septal musculature wherein it divides into left and right branches.*

## MATERIALS AND METHODS

The major parts of the AV conduction system of human hearts, which were free of any (or any significant) congenital anomaly and which had given no clinical evidence of arrhythmia, were examined both grossly and histologically. The identification and location of (1) the AV node (node of Tawara), (2) the AV bundle (bundle of His, common bundle) and (3) the right bundle branch were specifically sought. When possible the location and course of the left bundle branch (or branches) were noted; this usually was done but no special search was made for this structure. These normal control specimens were taken at random. Included were hearts from eight adults (ages 21, 32, 35, 56, 60, 67, 69 and 72) and one child (age 6). Fresh specimens and specimens fixed in formalin for a few days to several weeks were examined.

### *Gross examinations*

The dissections were carried out without magnification. Methods were in general those recommended by many authors, especially Mistin ('49) and Widran and Lev ('51). Minor variations of personal choice were made. The usual dissection made in this study was performed according to the following technics.

In the conventionally opened heart, the attachments of the chordae tendineae of the septal leaflet and of the adjacent portion of the posterior leaflet of the tricuspid valve were cut and these structures were reflected atrialward or removed. The endocardium of the right atrium above and contiguous with these structures (in the area bounded roughly by the coronary sinus ostium posteriorly, the fossa ovalis superiorly, and the central fibrous body anteriorly) was dissected free and reflected cephalad or removed. Usually a thin band of atrial muscle oblique or at right angles to the tricuspid valve margin was encountered. This was carefully teased away.

*The AV node was then seen lying in the base of the atrium just above the margin of the tricuspid valve.* After the central fibrous body and the adjacent membranous portion of the intraventricular septum were identified, either the common bundle was followed as a slender muscle fascicle extending anteriorly from the node and passing through these structures or the membranous septum was split longitudinally and the slender muscle fascicle (representing either the common bundle or the right bundle branch) was followed back though the central fibrous body to its junction with the AV node. While these methods differ only slightly, different specimens seemed to be handled more easily by one method than the other. The origin of the left bundle branch (or branches) from the common bundle was sometimes noted as the dissections were carried out.

### *Histologic examinations*

Serial histologic sections of eight human hearts were examined. Six of these specimens were those in which the AV conduction system had been grossly studied and two were specimens in which gross dissection of the conduction system had not been done. One purpose of studying both specimens grossly dissected and those not was to ascertain what if any artifacts and distortions were introduced by gross dissection.

*Sites sectioned and planes of section employed.* To obtain material for histologic examination blocks of tissue were cut in about the same manner as had been reported in the literature (Lev and associates, '51). The approximate region removed for sectioning is outlined in figure 1. One to four blocks were made depending on the size of the heart, the object

being simply to include the area under study in blocks of a size easily handled in the tissue laboratory. The posterior limit of the blocks for section was approximately level with the margin of the coronary sinus ostium; the anterior limit was approximately level with the posterior aspect of the crista supraventricularis. Superiorly the blocks included approximately 1 cm of atrial septal tissue; inferiorly they included approximately 2 cm of ventricular septal tissue. The blocks were thick enough to include essentially all of the ventricular septum and all (or nearly all) of the atrial septum.



Fig. 1. Closeup of opened tricuspid valve of normal adult heart with right atrium above and right ventricle below. Area of gross dissection and block removed for histologic study is indicated by rectangle. Dotted lines indicate cuts made to prepare blocks of tissue for serial histologic sectioning. Plane of sectioning employed was parallel to dotted lines. Left upper corner of rectangle is at coronary sinus ostium.

Each block was serially sectioned in its entirety. The thickness of individual sections was approximately seven microns.

In seven instances the plane of section was parallel to the vertical plane of section used to obtain the original block (or blocks) of tissue (fig. 1). In one case the gross block was obtained as described, but the plane of section for the preparation of serial histologic sections was roughly horizontal, the first cuts being made at the uppermost level of the block (that is, on the atrial side) and the final cuts in the ventricular septum. This second method of sectioning (1) failed to show the elements under study in some sections because of irregularities in the pathway of the system, (2) made preparation of large sections difficult, and (3) increased the difficulty of comparing our findings with those reported in the literature, since most reported studies have been on sections cut by the method first given. Therefore this second method of sectioning the tissue blocks was not used again.

Every histologic section from the first three specimens was stained and examined (3 000–4 000 sections). However, this was found to be unnecessarily laborious for determination of architectural features of the conduction system (as opposed to cytologic details); selection of every tenth or twentieth section of the serially cut block proved adequate. Whether every tenth or every twentieth section was stained and examined depended on the size of the specimen — every twentieth section of large specimens was selected and every tenth section of small specimens. After we studied these selected serial sections, intervening sections were stained when we thought they would demonstrate more adequately the pathway in a given area. Thus 200 to 300 sections were finally examined from the last six specimens.

Attempts to circumvent the rather lengthy procedure involved in studying the serial sections were unsuccessful.

*Staining of histologic sections.* A variety of stains were tried. These included hematoxylin and eosin (H & E), Mallory-Heidenhain (M–H) stain, iron-hematoxylin method, Verhoeff's stain for elastic tissue, van Gieson's stain for connective tissue, and Masson's trichrome stain. In the initial studies various combinations of these stains, often all of them, were employed on different sections. In the majority of instances, the selected sections were stained with H & E and adjoining sections were stained with the M–H stain. H & E was employed because of its general use as a standard in histologic studies. M–H stain was used for its sharp differentiation of muscle or musclelike tissue and mature connective tissue.

In regard to the problem of selective differential staining of the conduction system it was found that none of the stains mentioned imparted a reliably specific tinctorial quality to any of the elements of the conduction system The use of enzymatic histochemical technics has been shown to impart specific differential staining of the conduction system because of the presence of certain enzymes in higher concentrations in conduction tissue than in surrounding myocardial tissue (Carbonell, '56 '58) Most reported studies of this type have been done in laboratory animals. Preliminary attempts were made to use these technics in fresh human tissue, but were not pursued because of the requirement for fresh material and the relative complexity of the methods compared to more routinely used technics.

The orders of magnification used in the study were 10 35 100 400 and occasionally 1,000 After initial assessment of finer structural details, magnifications of 35 and 100 were found to be adequate in general with occasional use of greater magnification to better define some particular feature of the system

## RESULTS

### Gross dissections

The AV node common bundle, and right bundle branch were identified in seven of the eight specimens examined. In the eighth specimen, the AV node and common bundle were found but the right bundle could not be demonstrated satisfactorily As mentioned before the left bundle branch was not especially sought; however it was conclusively demonstrated in two of the eight dissections The gross anatomic features of the proximal portions of the AV conduction system of the nor-

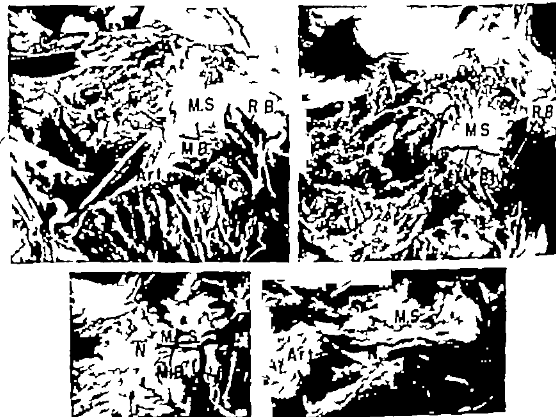



Fig 2 Gross dissections of AV conduction system of four "normal" human hearts. N = AV node M B = main (common) bundle M S = region of membranous septum and central fibrous body R.B = right bundle branch Art = artery to node

mal"* heart (fig. 2) were found to be as follows:

*The atrioventricular node* The AV node was found to be roughly oval or fan-shaped. It resembled muscle in texture and appearance, except that it was somewhat paler or more yellow in color than the surrounding myocardium, in both the fresh and formalin-fixed states. It lay in the AV canal (sulcus) of the posterior portion of the right atrium, under the endocardium and a thin layer of atrial muscle, on a level slightly inferior to the coronary sinus ostium. It was anterior to the coronary sinus ostium, and nearly directly inferior to the lower limit of the fossa ovalis. Thus, it was found just above, often partially overriding, the base (attachment) of the commissure between the posterior and the septal leaflet of the tricuspid valve and adjacent or slightly posterior to the central fibrous body Apparent posterior and anterosuperior connections of the node to the atrial muscle were noted. Usually a moderate-sized artery was found to be related to the node It usually originated from the right coronary artery on the posterior aspect of the heart and extended anteriorly through atrial fat to the node. The AV node measured in the adult specimens an average of 3.7 mm wide 7.5 mm long, and 1 mm thick. It thus formed a flattened, racket-shaped structure with its flattened surface in the plane of the atrial septum.

*Common bundle* The proximal extremity of the common AV bundle (bundle of His) was somewhat difficult to delineate from the AV node so that rather arbitrary definitions of its extent had to be made. In agreement with most previous investigators we defined the common bundle as extending from the point where the AV node narrowed, apparently to a single muscle fascicle, to a point where it appeared to contain only fibers destined for one side of the heart. Thus it commenced at the anterior extent of the AV node (a junctional zone not a sharp boundary) ran through the central fibrous body (the junction of the posterior extent of the membranous septum and the annuli fibrosae of the mitral and tricuspid valves), and entered the lower part of the membranous septum. Emerging from the membranous septum above the muscular part of the ventricular septum the bundle lay just over the center or slightly to one side of the center of the muscular septum. Since branches to the left ventricular myocardium usually arise from this bundle near its nodal end and continuously throughout most of its length the portion of the AV conduction system designated common bundle is often a combination of right bundle-branch fibers and only some of the left bundle-branch fibers the number of left bundle-branch fibers decreases usually as the distance from the AV node increases. In general, it appeared grossly that the muscle fascicle emerging from the inferior edge of the membranous septum contained only right bundle-branch fibers Because of the variations in left bundle branching, the length of the common bundle varied widely from 6.5 to 20 mm. In diameter the common bundle measured 1 5 to 2.0 mm.

*Left bundle branch.* The left bundle branch as indicated in the foregoing arose from the common bundle as either a single, broad, flat, delicate structure or as several delicate, discrete fascicles. When viewed from the left side of the heart, the left bundle-branch tissue was indicated by a ridge or ridges in the endocardium which fanned out over the upper part of the interventricular septum from the region of the junction of the left and posterior cusps of the aortic valve. Because of their delicacy and intimate association with the left ventricular endocardium gross dissection was usually not possible However in two cases, the origin of the left bundle branch from the common bundle was seen and followed for 1 to 2 mm. This was confirmed histologically It appeared that left bundle branching occurred anywhere along the course of the common bundle (this problem was better elucidated by histologic studies)

*Right bundle branch.* The right bundle branch was found to be grossly a larger more discrete, and more readily identifiable muscle fascicle than the left branch. As mentioned, precisely where to establish its origin by gross examination was difficult because of the problem of determining the site of origin of the left-branch

*"Normal" here means free of any significant congenital anomaly or any disease of the conduction system.

elements Often the problem was resolved only after histologic examination At any rate a structure (whether truly right bundle branch or partly common bundle) could be readily traced within the posterior inferior part of the membranous septum and for a distance of 2 to 10 mm after its emergence from the inferior margin of the membranous septum. Occasionally it could be followed anteriorly and apexward to the region just posterior to the septal part of the crista supraventricularis where it was associated with the moderator band if that structure was identifiable However as only the upper part of the right bundle (that is, the part near the AV node) pertained to this study specific attempts to follow it beyond its departure from the area adjacent to the membranous septum were not made The length of the dissected portion averaged 15 mm the average diameter was approximately 1 mm

### *Histologic examinations*

The AV node common bundle and right and left bundle branches were identifiable on histologic examination (fig. 3) The microscopic appearances of the component parts of the conduction system will be described individually

*Atrioventricular node* The AV node could be identified by its location and structure In histologic section it was seen lying on the AV fibrous ring just above the attachment of the posterior or the septal leaflet of the tricuspid valve A thin layer of atrial muscle lay over the node in those cases not grossly dissected (that is toward

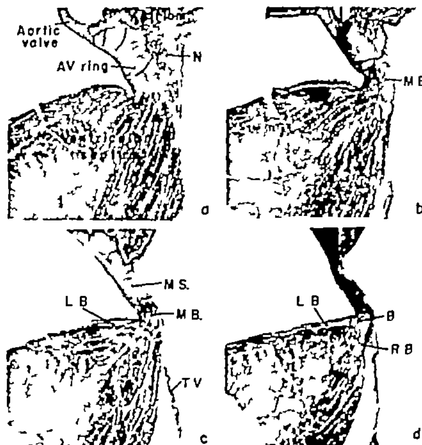



Fig 3 Histologic appearance of proximal portions of AV conduction system ( normal adult heart in selected serial sections from block of tissue outlined ( figure 1 ) L B = left bundle branch T V tric pid alve B = branching part of mal bundle other l bel in figure 2 (Mallory Heidenhain × 7)

the right endocardial surface) The histologic structure of the node was distinct: it consisted of musclelike fibers that were smaller than either atrial or ventricular fibers and that were arranged in a peculiar, loose, grouping of irregularly whorled interlacing bundles. Nuclei seemed to be more numerous per given microscopic field than in other areas of the atrium (Lev and co-workers ('51) stated that this appearance is due to the presence of an endothelial-lined sheath about the conduction tissue) With the Mallory-Heidenhain stain, these fibers seemed somewhat paler red than other myocardial fibers (Kistin ('49) noted a similar paleness of these fibers when stained with the Masson trichrome stain) In some preparations stained with H & E, the nodal fibers appeared somewhat less eosinophilic than other fibers. Striations were readily seen. While nerves and ganglion cells were noted in the area, their appearance and concentration did not seem especially remarkable compared to other areas of the adjacent myocardium; however no detailed study was made in this regard.

*Common bundle* The junction of the AV node and common bundle was not a sharp boundary (This was also noted grossly) At the anterior end of the AV node some nodal fibers became less tortuous and gathered into a more compact bundle. In some sections when the plane of sectioning was slightly oblique these fibers appeared in longitudinal view so that continuity of the AV node and the structure regarded as common bundle could be definitely established The common bundle was usually seen in cross section but sometimes in an oblique view It was found to be usually a rather compact structure composed of cross-striated fibers that were of smaller diameter than either ventricular or atrial fibers. These fibers proceeded anteriorly (that is toward the anterior aspect of the intact heart) from their origin at the anterior aspect of the AV node they passed through the central fibrous body and the membranous interventricular septum usually in a compact bundle but sometimes as closely related multiple fascicles separated by connective tissue. D ermination of the exact extent of the common bundle was difficult and variable as noted in the gross dissections, because of vagaries of origin of the right and left bundle branches especially the left In their course from the AV node to the level of the membranous septum fibers of the conduction system in more or less of a bundle were found to be either on top of the center of the muscular interventricular septum or situated more to either the right or left side of the apex of the muscular septum.

*Left bundle branch.* The left bundle branch was found to originate either as multiple discrete branches or as a single broad band from the common bundle Regardless of the manner in which it arose the fibers comprising it ran subendocardially at almost a right angle from the common bundle toward the left side of the heart. The fibers then appeared to fan out over the endocardial surface of the left ventricle. Within 1 to 2 mm of their origin, these fibers developed a fairly distinctive structure that made them appear different from myocardial fibers adjacent to them they were larger in diameter, seemed to possess fewer cross striations and appeared to have a perinuclear clear zone. While they did not coincide exactly with Purkinje's original descriptions of certain peculiar myocardial fibers found in animals the term "Purkinje fiber (or "Purkinjelike fiber") was used to designate them.

*Right bundle branch.* As indicated in the gross description the right bundle branch usually appeared to be a continuation of the common bundle Rarely it was given off before the left bundle branch Histologically no remarkable characteristics were observed The fibers gradually became larger so that their distinction from the surrounding ventricular myocardial fibers on the basis of size was lost. Usually a fine connective-tissue sheath separated the group of conduction fibers from adjacent fibers. We concluded that the fibers of the right bundle branch could be best (or only) definitely identified by tracing them in serial sections from their origin in the AV node (or common bundle) The direction of the right bundle-b nch fibers in the basal portions of the mc l r sept m was different from the rect n of mo of the septal fibers; that

is in the plane of sectioning employed in this study the bundle fibers appeared to lie oblique to most of the fibers which had a more longitudinal direction This was of some aid in following the bundle.

The course of the right bundle when followed in serial histologic sections was found to be the same as indicated by the gross dissections. It branched from the common bundle at or in the membranous septum ran through the posterior-inferior portion of the membranous septum and then was buried within the septal muscle a variable distance from the right endocardial surface It was not followed beyond a distance of approximately 1 cm below the level of the inferior border of the membranous septum since the blocks of tissue removed only included this much of the ventricular septum.

*Mahaim fibers* In some of the preparations fibers were seen of the type described by Mahaim and Benatt ('37) and Mahaim and Winston ( 41) which run from the common bundle directly into the subjacent septal myocardium. As suggested in the past, these were referred to as Mahaim s paraspecific fibers, or "Mahaim fibers or paraspecific fibers.

## SUMMARY

The atrioventricular (AV) conduction system was examined by means of gross dissections and serial histologic sections in nine normal hearts from eight adults and one child Previous descriptions of a demonstrable morphologically distinct, continuous system were confirmed The major components of the system were found to be (a) the AV node (node of Tawara) situated in the floor of the right atrium on the fibrous AV ring just anterior to the coronary sinus ostium (b) the AV bundle (common bundle or bundle of His) extending anteriorly and inferiorly from the AV node through the fibrous ring into the inferior part of the membranous septum; (c) the left bundle branches given off as discrete fascicles over a broad portion of the common bundle usually from a point just distal to the fibrous valvular ring and to a point at the posterior-inferior angle of the membranous septum and (d) the right bundle branch forming a continuation of the common bundle and passing obliquely anteriorly and inferiorly through the upper part of the ventricular septum toward the crista supraventricularis

## LITERATURE CITED

Allen Peter J J Lederman and G. J Pearl 1959 Prevention of surgical heart block by the use of supravital stain. J Thoracic Surg., 38 57–61

Barry Alexander and B. M Patten 1900 The structure of the adult heart. In Gould, S. E. Pathology of the Heart, Thomas, Springfield, Illinois ed. 2., pp. 123–128.

Bittencourt, Delmonte D M. Long Y K Lee and C. W Lillehei 1959 I travital staining of the trioventricular bundle with iodine compounds during cardiopulmonary bypass. Circulation Res., 7 753–758.

Carbonell L. M. 1956 Esterases of the conductive system of the heart. J Histochem. and Cytochem., 4 87–95.

——— 1958 El sistema de conduccion cardiaca desde l punto de vista histologico histoquimico. Rev lat.-amer Anat. patol., 2: 109–116.

Garrison F H 1929 An Introduction to the History of Medicine With Medical Chronology Suggestions for Study and Bibliographic Data. Saunders, Philadelphia, ed. 4 pp. 555–557

Glomset D J and R. F Birge 1945 A morphologic study of the cardiac conduction system. Part IV The anatomy of th upper part of the ventricular septum in man Am Heart J 29 526–538

——— 1948 A morphologic study of the cardiac conduction system. Part V The Pathogenesis of heart block and bundle branch block. Arch. Path., 45 135–170.

Glomset, D. J and K. R. Cross 1952 Morphologic study of the cardiac conduction system. Part VI. The intrinsic nervous system of the heart. A.M.A. Arch. Int. Med 89 923–930

Glomset, D. J and Anna T A. Glomset 1940a A morphologic study of the cardiac conduction system in ungulates dog and ma Part I. The sinoatrial node Am. Heart J 20 389–398.

——— 1940b A morphologic study f the cardiac conduction system in ungulates dog, and man. Part II. The Purkinje system Ibid 20 677–701

Glomset D J Anna T A Glomset nd R. F Birge 1944 Morphologic tudy of he cardiac conduction system. P rt III. Bundle branch block. Ibid., 28 348–369

His, Wilhelm, J 1941 Quoted by Willius, F A., and T E. Keys. Cardiac Cla ics, Mosby St. Louis, p. 695.

Iwa, Takashi, Zwi Steiger Milton Weinberg and E. H. Fell 1961 Vital staining of the conduction tissue of the heart. Arch Surg 83 833–838

James, T N 1961 Morphology of the human atrioventricular node with remark pertinent to its lectrophysiology Am H art J 62 756–771

Keith, Arthur, and M. W Flack 1906 The auriculo-ventricular bundle of the human heart. Lancet, 2: 359–364.

—— 1907 The form and nature of the muscular connections between the primary divisions of the vertebrate heart. J Anat. and Physiol., 41 172.

Kent, A. F S 1893 Researches on the structure and function of the mammalian heart. J Physiol., 14 233–254

Kistin, A. D 1949 Observations on the anatomy of the atrioventricular bundle (bundle of His) and the question of other muscular atrioventricular connections in normal human hearts. Am. Heart J 37 849–867

Lev Maurice 1960 The conduction system. In Gould, S. E. Pathology of the Heart, Thomas, Springfield, Illinois, ed. 2, pp. 132–165.

Lev Maurice, Jerrold Widran and Ethel E. Erickson 1951 A method for the histopathologic study of the atrioventricular node, bundle and branches. A.M.A. Arch. Path., 52: 73–83.

Mahaim, Ivan, and Alfred Benatt 1937 Nouvelles recherches sur les connexions supérieures de la branche gauche du faisceau de His-Tawara avec la cloison interventriculaire Cardiologia, 1 61–73.

Mahaim, Ivan, and M. R. Winston 1941 Recherches d'anatomie comparée et de pathologie expérimentale sur les connexions hautes du faisceau de His Tawara. Cardiologia, 5 189–260.

Purkinje Professor 1845 Mikroskopisch-neurologische Beobachtungen. Arch. f. Anat. Physiol. u. wissensch. Med., pp 281 295.

Retzer, Robert 1907 The atrio-ventricular bundle and Purkinje's fibers. Anat. Rec., 1 41

Tawara, S. 1906 Das Reizleitungssystem des Säugetierherzens. Eine anatomisch-Histologische Studie über das Atrioventrikularbündel und die Purkinjeschen Fäden Gustav Fischer Jena.

Todd, T W 1932 The specialized systems of the heart. In Cowdry E. V Special Cytology The Form and Functions of the Cell in Health and Disease Hoeber, New York, ed. 2, pp. 1175–1210

Uhley H. N and L. M. Rivkin 1959 Visualization of the left branch of the human atrioventricular bundle. Circulation, 20 419–421.

Van der Stricht, O and T W Todd 1920 The structure of normal fibers of Purkinje in the adult human heart and their pathological alterations in syphilitic myocarditis. Johns Hopkins Hosp Rep., 19 1–60.

Winnemark, J R., R. Benvenuto and F J Lewis 1960 Destruction of the specialized conduction tissue in the live canine heart with iodine J Thoracic Surg., 39 137–143

Widran, Jerrold, and Maurice Lev 1951 The dissection of the atrioventricular node, bundle and bundle branches in the human heart. Circulation, 4: 863–867

Willius, F A., and T J Dry 1948 A History of the Heart and Circulation, Saunders, Philadelphia, pp. 129 130, 370.

# Development of the Raccoon Placenta

R. F. S. CREED AND J. D. BIGGERS
*King Ranch Laboratory of Reproductive Physiology School of Veterinary Medicine University of Pennsylvania, Philadelphia, Pa.*

Despite the widespread distribution of the raccoon (*Procyon lotor* L.) throughout the American continent, relatively little investigation has been made into its reproductive activity The chief recent contributions in this respect have been those of Hamilton ('35) Bissonette and Csech ('37 '38 '39) Steuwer ( 43) Pope ( 44) Rinker ( 44) Sanderson ('50 '51) George and Stitt ('51) Llewellyn ('53) Llewellyn and Enders ('54a, '54b) and McKeever ('58) None of these authors, however have reported on placentation in the raccoon. In fact, knowledge of the raccoon placenta has for 80 years been based primarily upon the observations of Watson (1881) who had at his disposal a single gravid uterus, fixed in spirit, presented to him by the proprietors of the Belle Vue Zoological Gardens Manchester England. This uterus which possessed but one conceptus was according to Watson that of an individual which had reached an advanced stage of pregnancy Thus Watson s findings suffered from the strict limitations of his material and the methods of study available to him at the time.

It is of interest therefore, when specimens of placentae of such an animal become available and particularly when a developmental series is presented. Indeed, it is surprisingly difficult to obtain wild animal placental material of sufficient quantity and quality upon which to use modern methods of study and thus we were fortunate to obtain the present raccoon material. The fact that the raccoon is a member of a particular family of carnivores — the Procyonidae — of somewhat uncertain canoid affinities, is of additional interest. In the literature the coati presumably *Nasua narica* L. seems to be the only other procyonid mentioned briefly with respect to the placenta (Amoroso '5_a)

Preliminary observations on our material have been made elsewhere (Biggers and Creed, '62) and the present paper is the result of a more detailed study with the light microscope of the placental region only

## MATERIAL AND METHODS

The material consists of four pregnant uteri removed from raccoons (*Procyon lotor lotor* L.) numbered 97 142, 148 209 These animals were obtained in the spring of '61 during the course of an extensive program of live trapping of a range of wild animal species in the environs of New Bolton Center — the field station of the University of Pennsylvania — situated in Chester County Pennsylvania and some 35 miles from Philadelphia.

The animals were brought to the laboratory killed by use of carbon monoxide gas and after weighing were dissected. In each instance the reproductive tract was removed and incisions were made in the uterus between the conceptuses and at their anterior and posterior poles. This was done to allow for quicker and more complete penetration of fixative without causing damage to the placentae and fetal membranes. In a few cases the conceptus was opened by a deep incision into the lateral wall. Each tract was then fixed in its entirety by complete immersion in Bouin s solution. Subsequently each specimen was studied by further dissection and observations were made on its gross anatomy Measurements of embryos were taken and owing to the fact that embryo tails were tucked well between the hind legs the greatest length is defined as the distance between the anterior pole of the head and the base of the tail. Ap-

Present address: Division of Histology and Embryology Royal Veterinary College Royal College Street, London, England

propriate pieces of the placenta were removed, processed sectioned and stained for histological and histochemical investigation Sections were stained by means of either hematoxylin and eosin, Masson's trichrome stains or Lillie's periodic acid — Schiff (PAS) procedure

## OBSERVATIONS

### *Gross anatomy and measurements*

*Animal no 97* This animal was killed on April 5 1961 The bicornuate uterus contained two locular enlargements in the left horn and three in the right horn, these being approximately evenly spaced in their respective cornua Dissection of these conceptuses revealed that each contained a developing fetus surrounded by its amnion lying in the allantoic cavity Figure 1 shows a conceptus from which a piece of the uterine wall together with a part of the placenta has been removed, exposing the embryo within its membranes, lying in the allantoic cavity In each case the embryo lies with its ventral side apposed to the mesometrial region of the uterus and is attached by means of its umbilical cord to the placenta.

The chorio-allantoic placenta is zonary as in many other carnivores and the annulus extends completely around the midsection of the conceptus. It is widest at its anti mesometrial region and narrowest at the mesometrial side This variation in width is well shown in figure 1 and further revealed by the measurements in table 1

The umbilical vessels emerging from the umbilical cord of the embryo form four main branches one branch running along each margin of the annulus in each direction from the mesometrial to the anti-mesometrial region. As they run towards the anti-mesometrial region they give off further branches to the body of the annulus and eventually break up to form numerous smaller branches running towards the mid-antimesometrial zonary region. It is at the central area of this anti-mesometrial position in the annulus that the most outstanding feature of the raccoon placenta can be seen. It is a large and conspicuous placental structure recently named the *hemophagous organ* (Biggers and Creed '62) (fig. 1) This organ is highly vascular and is saclike in its general configuration. As will be seen subsequently however it is by no means a mere blood-containing sac. Its base which is narrower than its distal extremity emerges from this central anti-mesometrial position of the annulus and the structure hangs into the allantoic cavity the free distal region tending to be disposed towards the anterior region of the embryo. There is no evidence of the presence of so-called marginal hematomata as found in the dog, fox, and coyote Measurements of the embryos, the annuli, and the hemophagous organs are given in table 1

*Animal no 148* The conceptuses of this animal which was killed on May 1 1961 proved to be of a later developmental stage then those of no. 97 Their over-all measurements are larger and it was adjudged that two-thirds to three-fourths of the gestation period had elapsed The four conceptuses were equally distributed in the cornua and again were more or less evenly spaced. The zonary placenta (fig 2) is notably larger than that of no 97 and although the main umbilical vessels are distributed in a similar manner they are larger and their smaller branches are more extensive and complex in their peregrinations as they converge upon the hemophagous organ. This organ in each conceptus is of considerable magnitude and takes up a large proportion of the allantoic cavity

Figure 2 is a photograph of one of the conceptuses of this animal. A lateral window of tissue has been removed to reveal the lay-out of the placenta with its hemophagous organ. It can be seen that the latter organ has at this stage developed a considerable tubular proximal portion, which also emerges from the central anti-mesometrial region of the annulus and runs forward along the dorsal side of the embryo in an anterior direction. This ultimately bends to the right over the embryo's head region, then to the left, and finally leads into an expanded bulbous region which hangs down on the left side of the anterior part of the embryo, reaching right down to the mesometrial side of the allantoic cavity It must be remembered however that this may not be the

TABLE 1

| | Embryos | Placenta | | |
|---|---|---|---|---|
| | | Annulus | | |
| | Greatest length (Head-tail base) | Mesometrial width | Anti-mesometrial width | Hemophagous organ length |
| *No. 97* | mm | mm | mm | mm |
| Left horn | | | | |
| Conceptus 1 | 19.0 | 9.0 | 16.0 | 12.0 |
| Conceptus 2 | 18.0 | 8.0 | 16.0 | 9.0 |
| Right horn | | | | |
| Conceptus 1 | 16.0 | 9.0 | 14.0 | 8.0 |
| Conceptus 2 | 19.0 | 10.0 | 17.0 | 8.0 |
| Conceptus 3 | 17.0 | 8.0 | 16.0 | 9.5 |
| Mean | 17.8 | 8.8 | 15.8 | 9.3 |
| *No. 148* | | | | |
| Left horn | | | | |
| Conceptus 1 | 69.0 | 25 | 46 | 62 |
| Conceptus 2 | 75.0 | 28 | 45 | 58 |
| Right horn | | | | |
| Conceptus 1 | 72.0 | 23 | 36 | 56 |
| Conceptus 2 | 72.0 | 25 | 40 | 40 |
| Mean | 72.0 | 25.3 | 41.8 | 54.0 |
| *No. 142* | | | | |
| Left horn | | | | |
| Conceptus 1 | 79 | 20 | 31 | 36 |
| Conceptus 2 | 77 | 19 | 30 | 40 |
| Right horn | | | | |
| Conceptus 1 | 72 | 19 | 28 | 40 |
| Conceptus 2 | 71 | 22 | 29 | 45 |
| Mean | 74.8 | 20.0 | 29.5 | 40.3 |
| *No. 209* | | | | |
| Left horn | | | | |
| Conceptus 1 | 96 | 15 | 21 | 19 |
| Conceptus 2 | 104 | 18 | 27 | 34 |
| Right horn | | | | |
| Conceptus 1 | 99 | 21 | 29 | 12 |
| Conceptus 2 | 94 | 21 | 31 | 0 |
| Mean | 98.3 | 18.8 | 27.0 | 16.3 |

precise position of the hemophagous organ in the living unfixed conceptus. There is every indication, however that these organs are arranged in the allantoic cavity so that they run forward and occupy an antero-dorso-lateral position with respect to the embryo Table 1 shows the relative developmental stages of the conceptuses in this animal.

*Animal no. 142* This animal was killed on April 28 1961 and like no. 148 possessed a gravid uterus with two conceptuses evenly spaced in each horn. The gross anatomical differences between the conceptuses of this animal and that of no. 148 were not well marked. An examination of table 1 shows the mean greatest length of the embryos of this animal to be a little in excess of that of animal no 148 It also reveals however that both the annuli and the hemophagous organs are of smaller size. Based on embryo size this could mean that pregnancy in animal no. 142 has proceeded a little further than in animal no. 148 and the reduction in size of the annuli and hemophagous organs which becomes quite evident in the near full term condition (animal no. 209) may have already started at this stage. As with animal no. 148 this animal too is assessed to have completed approximately two-thirds to three-fourths of the gestation period.

*Animal no. 209* This animal killed on May 19 1961 proved to be at a later stage of gestation than any of the other

three. As in animals no. 148 and no. 142 four conceptuses were present and were again equally distributed between the two cornua. The embryos are larger than those hitherto encountered, possess a body-covering of fine lanugo hair (fig. 3) and have well defined vibrissae. It seems clear that this animal was approaching the end of the gestation period and nearing parturition. The measurements shown in table 1, however, indicate a reduction in the size of the annuli and the hemophagous organs relative to those of nos. 148 and 142. Considerable variation in the degree of regression of the hemophagous organs occurs, and in one conceptus this is represented by a mere oval plaque of tissue in the anti-mesometrial position, where at one time it is assumed the active organ was present (figs. 3 and 4).

Thus on gross anatomical observation the material represents a developmental series and it seems from the limited material we have described that both the annulus and the hemophagous organ of the raccoon placenta increase in size until approximately two-thirds of the way through pregnancy after which time a regression occurs. This regression is particularly striking in the hemophagous organ. It may be noted that in each of the 17 conceptuses examined, the placental annulus was complete. This finding is contrary to reports in the literature (Watson, 1881; Rau, '25; Mossman, '37; Amoroso, '52b). Watson (1881) first reported a gap in the placenta, this gap being disc-shaped and in a central and anti-mesometrial position in the annulus. It seems clear that this was in fact created accidentally at the base of the hemophagous organ by partial destruction of the organ itself and removal of tissues of the fetal side of the placenta from the maternal side. Rau ('25), misinterpreting Watson's report, figured a continuous gap across the whole width of the annulus. In this manner the erroneous impression that the raccoon zonary placenta is an incomplete one has crept into the literature.

## Microscopical anatomy

Since the difference between the microscopical anatomy of the placentae of animals no. 142 and no. 148 are only slight, it will be convenient to treat the material as representative of three stages of development, the remarks concerning animal no. 142 being appropriate to no. 148. Thus the three stages to be discussed will be (1) the early placenta (17–18 mm embryos), (2) the two-thirds to three-quarter-term placenta (72-75 mm embryos), (3) the near full-term placenta (98 mm embryos). It must not be overlooked, however, that these stages in the absence of a timed sequence can only be relative.

Customarily four regions are recognized in the carnivore placenta (Amoroso, '52b). These are, (1) the region of the placental labyrinth, (2) the transition, penetration or junctional zone, (3) the deep glandular or spongy zone and (4) the central and marginal hematomata. Because of the nature of the raccoon placenta and for ease of its description in the present material, the following four regions will be recognized: (a) the placental labyrinth, (b) the junctional and deep glandular or spongy zone, which will be confined to that region below the placental labyrinth, (c) the hemophagous organ, and (d) the subhemophagous region.

### The early placenta

*(a) The placental labyrinth.* It can be seen in vertical sections that this part of the placenta occupies slightly over one-half of the placental depth (fig. 5). It consists of a series of lamellae which branch and run tortuously. Each lamella is bounded by trophoblast cells which surround and enclose maternal capillaries. Between these lamellae are varying amounts of allanto-chorionic mesenchyme, sometimes forming conspicuous light staining areas.

The maternal capillaries have two outstanding characteristics. Firstly, they are much larger than ordinary capillaries and may be sinusoidal in appearance, and secondly, their endothelial lining is morphologically unlike that of true capillaries in that the endothelial cells forming it are of a cuboidal nature and are surrounded by a relatively thick basement membrane.

Dr. H. W. Mossman has reported to us privately that he has one record of a raccoon placenta which had an incomplete band at the mesometrial side but the ends were in contact.

(figs. 7 8 9) This membrane, although difficult to observe in sections stained with hematoxylin and eosin is readily demonstrated by the periodic acid — Schiff stain. Thus, with respect to these maternal sinusoidal capillaries the raccoon is similar to the ferret (Strahl and Ballman, 15) the zorille (Rau, '25) the wolverine (Wislocki and Amoroso '56) and certain Pinnepedia (Harrison and Young '61) and unlike the dog the cat (Amoroso '52b) and the bear (Rau, '25) which possess more flattened endothelial cells.

The trophoblast cells which surround the maternal capillaries are present as a relatively thick syncytium with haphazardly disposed nuclei. At this stage the syncytium may be confluent with that of a neighboring lamella (fig. 8) be adjacent to fetal allanto-chorionic mesenchyme or more generally be bounded by a layer of cellular trophoblast (fig. 9) In those places where cellular trophoblast is present, this intervenes between the syncytial trophoblast and the fetal mesenchyme. The nuclei of the syncytial trophoblast are large and the cytoplasm is somewhat basophilic while the cellular trophoblast consists of a single layer of cells with smaller more heavily staining nuclei and more lightly staining cytoplasm, and in which mitotic figures can sometimes be observed. There is no evidence of giant decidual cells being present between the trophoblast surrounding neighboring maternal capillaries as is the case in the cat (Duval 1895 Wislocki and Dempsey 46) and the hyena (Matthews '54 Morton, '57 Amoroso '59)

The fetal capillaries, carried in the allanto-chorionic mesenchyme are thin walled and of various sizes. In certain places they invade the cellular trophoblast where it is present but even at their most advanced invasive points they are well separated by syncytial trophoblast from the maternal capillaries (fig. 8) Therefore at this stage of development of the placental labyrinth even at points of closest proximity maternal capillary endothelium, a PAS positive basement membrane a layer of syncytiotrophoblast and fetal capillary endothelium intervene between the fetal and maternal blood.

*(b) The junctional and deep glandular or spongy zone* This zone below the placental labyrinth takes up rather less than one-half of the depth of the placenta. Essentially it consists of a region of endometrial glands which are greatly expanded at this level, and into which the tips of invading fetal villi project (figs. 5 6 10) These parts of the glands are spacious and their cavities contain varying amounts of histotrophic material. They possess lateral walls which are considerably folded and a floor which is generally smooth but which may exhibit an occasional fold (fig. 11) Their distal regions are blocked by fetal villi. Owing to the degree of expansion and proliferation of these glands their lateral walls form septa with the lateral walls of neighboring glands These septa consist, therefore of a core of maternal connective tissue bounded on either side by glandular epithelium. Maternal blood vessels of different sizes run in this connective tissue and these vessels are the means of ingress to and egress from the placental labyrinth of the maternal blood. There is also a rich supply of maternal capillaries immediately below the glandular epithelium. The appearance of this epithelium varies according to its position. That in the floor of the glands is of a simple low columnar type formed of cells with oval centrally placed nuclei whereas that in the proximal regions of the septa may be pseudostratified columnar epithelium. More distally it becomes mainly cuboidal, and in this region the cells are larger stain more deeply and many seem to undergo cytolysis and often fusion. This gives rise to a region of disintegration which appears to add to the histotrophic material found in the cavities of the glands.

The invading fetal villi which project into the gland lumina consist of a core of fetal mesenchyme covered by a columnar epithelium. It can be seen (fig. 10) that this columnar cytotrophoblast is tallest at the villous tip and gradually decreases in height towards the labyrinth, eventually becoming cuboidal. The columnar cells have basally disposed nuclei and their cytoplasm in the neighborhood of the nuclei is somewhat basophilic in character whereas the rest of the cytoplasm stains

more lightly. The role of these cells appears to be the uptake of the histotrophic material present in the gland cavities. Fetal capillaries present in the fetal mesenchyme in many instances have a subepithelial position.

Below the expanded parts of the endometrial glands there is a region containing their unmodified segments (figs. 6, 11). These are lined by cuboidal or low columnar epithelium and are active in the secretion of histotrophe which accumulates within their lumina. They form a narrow region in the stroma which abuts on the underlying uterine muscle layers.

*(c) The hemophagous organ.* In vertical section the length of this organ can be seen to be approximately four times the depth of the labyrinthine part of the placenta (fig. 5). At this stage its distal half consists of an expanded region containing maternal blood. The walls of this sac are formed by the allanto-chorionic membrane whose epithelium is columnar and is bathed by maternal blood. The proximal half of the organ consists of a complex series of branching lamellae formed of allanto-chorion (fig. 12). Each lamella consists of a thin core of fetal mesenchyme lined on either side by fetal columnar epithelium. Here too this columnar epithelium is bathed by maternal blood and it seems that this blood from the subhemophagous region gains access to the expanded distal portion of the hemophagous organ by passing through the channels between the lamellae.

The fetal epithelium both of the wall of the expanded sac-like portion and of the lamellae consists of simple high columnar cells with basally disposed nuclei and with cytoplasm which is more basophilic near the nuclear end of the cell (fig. 13). The free edges of the cells have cytoplasmic processes and the supra-nuclear cytoplasm is noteworthy for such inclusions as blood cells, vesicular bodies, granules and yellow-orange pigment granules. In fact these fetal epithelial cells give every sign of considerable phagocytic activity. Although a certain amount of histotrophic debris is present in the sac and the interlamellar spaces, they are filled mainly with maternal blood and thus it seems that the predominant function of the fetal epithelium of the hemophagous organ is hemophagocytosis. The maternal blood present in the organ seems to contain a mixture of effete and fresh blood corpuscles. At the base of the fetal epithelial cells, both in the sacular part and in the lamellar region, fetal allanto-chorionic mesenchyme supports numerous thin-walled fetal capillaries. Many of these capillaries are immediately adjacent to the bases of the fetal epithelial cells (fig. 13) or in some cases are intra-epithelial in position.

*(d) The sub-hemophagous region.* This zone lies immediately below the hemophagous organ and extends over a circular region whose diameter is approximately equal to the diameter of its distal sac-like portion (fig. 5). As this zone exhibits a number of differences from the junctional and glandular zone it deserves separate description. Like the junctional and glandular zone, however, it consists essentially of a series of glandular compartments formed by the expansion of the endometrial glands. In this case the expansion involves the whole of each endometrial gland since the unmodified basal segments which are present below the junctional and glandular zone are absent or extremely rare. Thus these glandular compartments are more capacious than those below the labyrinthine part of the placenta. Furthermore, both their floors and lateral walls are considerably folded and the inter-compartment septa formed by adjacent lateral walls appear to be branched at their distal ends (fig. 6). The epithelium of the floor of each gland and that of the proximal part of their lateral walls is simple columnar. The height of the columnar epithelial cells decreases towards the more distal parts of these walls and at the most distal regions the epithelium appears to have undergone considerable proliferation, cellular change and disintegration. Thus there is a well marked region at the level of the distal ends of the septa where large heavily staining cuboidal cells and symplasma indicate the formation of histotrophic material (figs. 5, 6). A certain amount of cellular disintegration, confined to the tips of the glandular folds, also occurs in the more proximal regions of the lateral walls and in the floors of the glands

The more distal parts of the septa, unlike those of the junctional and glandular zone beneath the labyrinthine placenta, are not attached to invading fetal villi. Indeed in this region tongues of invading fetal tissue are absent. An outstanding difference between this zone and that of the junctional and glandular zone is the presence of maternal blood filling up the cavities of the glands. This blood gains access to the overlying hemophagous organ through channels between the distal ends of the glandular septa forming first a supraglandular reservoir of blood (figs. 5 6)

*The two-thirds to three-quarter term placenta*

(a) *The placental labyrinth* At this stage, in vertical section, the placental labyrinth can be seen to occupy rather more than three-quarters of the depth of the placenta (fig. 14) Thus during development, not only is there an overall increase in size of the annulus but also a change in relative proportions. A comparison of the labyrinth at this stage with that of the early placenta shows its increase in dimensions to be due primarily to an expansion of the maternal sinusoidal capillaries, together with a less obvious increase in the amount of trophoblastic tissue. The maternal sinusoidal capillaries still retain their cuboidal epithelium the cells of which are similar to those of the early labyrinth and their size increase is presumably due to the proliferation of their cuboidal cells. The basement membrane of these capillaries is still PAS positive (fig. 16) but it can now be more readily demonstrated by the use of the hematoxylin and eosin staining technique and it appears as a band of homogeneous ground substance. The surrounding trophoblastic tissue is essentially syncytial and very rarely can cytotrophoblast be observed at this stage. The syncytial trophoblast layer is slightly thinner than in the early placenta, but its nuclei are still disposed in depth. The large lacunae of fetal allanto-chorionic mesenchyme present in the early placenta are now absent except in the invading fetal villi, presumably because of the encroachment of the expanded maternal sinusoidal capillaries. The fetal mesenchyme between the lamellae is heavily infiltrated with fetal capillaries and in many places these lie between the syncytial trophoblast and the maternal capillary endothelium. They can also be seen, in some instances, to have invaded even further and to have assumed an intra-endothelial position (fig 17) Thus the fetal blood in the labyrinth at this stage is in closer proximity to the maternal blood than it is in the early placenta, and may be separated from it only by fetal capillary endothelium and maternal cuboidal cell cytoplasm, an endothelio-endothelial condition.

(b) *The junctional and deep glandular zone* Relative to the placental labyrinth this zone is smaller at this stage than in the early placenta, being less than one-quarter of the placental depth (fig. 14) It appears that although the labyrinth undergoes an increase in size, the dimensions of the junctional and deep glandular zone change very little. Other changes, however do occur in this region. The lateral walls of the glandular compartments have lost their folds and they like the compartment floors, are relatively smooth (fig 18) The epithelium of the floor is of a low columnar nature, while that of the proximal region of the septa is low cuboidal. At the more distal parts of the septa there are signs of proliferation of large cuboidal cells and various disintegrative processes seem to be occurring. These are less marked, however than in the early placenta.

A large proportion of each gland compartment is taken up by a fetal villus and these fetal villi by this time have invaded almost to the floors of the gland cavities (fig 18) In many instances, too they have become broad tongues of tissue and the cytotrophoblast covering them varies. It may be of tall columnar cells at the villous tips of some and of low columnar or cuboidal cells at the tips of others. In those cases where tall columnar cytotrophoblast is present, the cells appear to phagocytose the histotrophic material which is present in small quantities in the reduced spaces between the villous tongues and the compartment walls. In all cases the epithelium of the villi becomes cuboidal in their more distal regions.

Below this site of expanded glands the region of so-called unmodified basal glandular segments is much more marked than in the early placenta and it seems that considerable extension and coiling of these segments has occurred. The epithelia lining them may be low cuboidal and quite flattened cuboidal or high cuboidal and these portions of the glands appear to be partaking in active apocrine secretion. Such activity would account for the considerable variation in the lining epithelium. The products of this secretion can be seen in quantity in the lumina of these basal glandular segments (fig. 18) The histotrophic material phagocytosed by the cytotrophoblast of the fetal villi therefore seems to consist predominantly of the secretion of these basal segments and cytolytic material from the region of cell disintegration seems of lesser importance.

*(c) The hemophagous organ.* The large size which the hemophagous organ has attained by this stage is due to a considerable increase in extent and complexity of its lamellae The blood filled interlamellar channels are also larger than in the early placenta although the saccular cavity at the distal end of the organ is relative to the amount of lamellar tissue smaller than in the earlier stage The epithelium of the lamellae has seemingly undergone extensive proliferation and has become variously folded in contributing to the increased complexity of the organ. This tall columnar fetal epithelium is similar to that of the hemophagous organ of the early placenta. The nuclei of its cells however are not so regularly basal in position and many are disposed in a central position. Perhaps the most outstanding feature of these cells is the large accumulation of orange colored granules and crystals of pigment in the cell cytoplasm (figs. 19 20) It seems therefore that during the course of development these particular cells gradually accumulate more and more pigment material which presumably is formed as breakdown products of hemoglobin. Occasional discrete masses of pigment in the maternal blood suggest that the fetal epithelial cells may disgorge their accumulations of pigment after a certain time. Fetal mesenchyme forms the core of the lamellae but large lacunae of fetal mesenchyme are no longer present as in the early hemophagous organ. This mesenchyme is well supplied with fetal capillaries many of which are sub- or intra-epithelial in position (fig. 20)

*(d) The sub-hemophagous region* The differences between this region and the junctional and glandular zone at this stage are even more marked than those in the early placenta. Proliferation of the glandular epithelium has proceeded to such a degree that the foldings and extensions of the wall and floor have almost obliterated the compartment cavities (fig. 14) Thus this whole region appears as a complex branching system of glandular mucosa between whose inter-epithelial spaces maternal blood passes towards the hemophagous organ. The epithelium may be low columnar cuboidal or stratified cuboidal and some of the cells of the most distal region appear to be undergoing disintegration. Below this proliferating glandular region a few unmodified basal segments of the glands may be seen. These lie immediately below this region, and are neither as large nor as extensive as those below the labyrinth They possess low columnar cuboidal or flattened cuboidal epithelium and are actively concerned in the production of histotrophic secretion which can be seen in their lumina.

### *The near full-term placenta*

*(a) The placental labyrinth.* A further increase in the size of the maternal sinusoidal capillaries appears to have been undergone in development from the earlier labyrinth. Thus at this stage they appear as large sinusoidal spaces bounded by the capillary endothelium. This endothelium is low cuboidal and considerably more flattened than in the earlier stages (fig 22) The endothelial cell nuclei are often more elongated and lie in a plane parallel to the basement membrane (fig 23) The latter is still readily demonstrated by the PAS technique The trophoblast surrounding the maternal sinusoidal vessels is now in most places a single attenuated layer of syncytium broken by fine strands of fetal mesenchyme and infiltrated by a profusion of fetal capillaries containing fetal blood corpuscles.

instances of intra-endothelial fetal capillaries (fig. 23) are more numerous than in either of the earlier stages. Thus in the labyrinth at this stage both maternal and fetal blood appear to be present in great amounts and in the closest proximity in many places.

(*b*) *Junctional and deep glandular zone* This zone resembles generally that of the two-thirds — three-quarter term placenta. Both the floor and the lateral walls of the glandular compartments are devoid of folds and only the tops of the septa are slightly branched and form folds. In this region, as in the case of the earlier placentae, a certain amount of cell disintegration seems to be occurring This is not well marked at this stage and little histotrophe is being formed in this position. The broad tongues of the fetal villi fill up most of the glandular cavities. These tongues consist mainly of fetal mesenchyme covered by a layer of cytotrophoblast. Rarely does this cytotrophoblast consist of the tall columnar cells as seen in the early placenta. It consists instead of low columnar cells at the villous tips and cuboidal cells elsewhere. Nevertheless there are signs that these low columnar cells carry out a certain amount of phagocytic activity and fetal capillaries can be found in sub-epithelial positions in the mesenchymal cores of the villi A well marked region of basal glandular segments is present and the epithelium lining their lumina continues to secrete histotrophe at this stage.

(*c*) *The hemophagous organ.* In many respects the hemophagous organ is similar to that of the preceding stage, although owing to its vast reduction in size the lamellae are greatly reduced and the area of phagocytosing fetal epithelium is considerably less The cells of this tall columnar fetal epithelium show one striking difference from those of both the earlier placentae Whereas in the earliest stage these cells possessed basally disposed nuclei, and in the next stage they were either basal or central in position, in this late stage the nuclei are to be found in most cases near the free ends of the cells (fig. 24) Some have the nucleus in a mid-cell position but rarely can basally disposed nuclei be found The cells still appear to be phagocytosing maternal blood corpuscles and considerable accumulations of orange brown pigment granules and crystals can be seen in many of them. Other cells however seem to have disgorged their pigment, and variously-sized masses of pigment crystals can be seen in the interlamellar maternal blood. Owing to the decrease in size of the organ there is a great reduction in the amount of maternal blood present. The distal blood sac is variously reduced and in one conceptus contained only a pigment mass (fig. 21) Fetal capillaries can still be seen in sub- and intra-epithelial positions with respect to the phagocytosing fetal epithelium.

(*d*) *The sub-hemophagous region.* A considerable decrease in the extent of this region has occurred by this time and all evidence of the glandular compartments as seen in the earlier placentae has been lost (fig 21) The degree of branching and folding of the glandular mucosa is greatly reduced. The intact cells of the glandular epithelium are cuboidal and are particularly large at the distal edges of the gland. In this distal region symplasma is also present and disintegrative processes appear still to produce a certain amount of histotrophic material. It seems that the over-all reduction in the sub-hemophagous region may be due to the fact that proliferative activty of the epithelium no longer keeps pace with the disintegrative changes. Maternal blood can be found in only small amounts in the glandular interstices and the supra-glandular blood reservoir is reduced lamellae of the hemophagous organ having usurped a considerable part of its space. A few basal segments of the glands can be seen and their lumina are filled with histotrophic secretion.

## DISCUSSION

From the foregoing account of the structure of the zonary placenta of the raccoon, two main features may be emphasized Firstly this placenta possesses two morphologically distinct regions providing an opportunity for exchange between mother and fetus, and secondly it undergoes a continuous change in form, structure and size throughout its existence

Because of these two features it is difficult to assign it to a category in any classification which has so far been proposed. The micro-anatomical classification of Grosser ('08, '09) extended by Mossman ('26, '37) is one in which the number of tissue layers between maternal and fetal blood is used as the criterion for grouping placentae and is a classification which has been favored over the last half century. According to Grosser's classification the placental labyrinth of the raccoon would be designated as being an endothelio-chorial placenta. Recently it has been suggested that, because of the possession among carnivores of a relatively thick PAS-positive basement membrane outside the maternal sinusoidal capillary endothelium, this should be classified as a vasochorial condition (Wislocki '55 Wislocki and Amoroso, '56). Whether the term endothelio-chorial or vasochorial be used either is applicable only to the earlier stages of the raccoon placental labyrinth. In the later stages because of the infiltration of fetal capillaries through the basement membrane and in between the cells of the maternal endothelium, maternal blood appears to be in contact with fetal capillary endothelium in many places (fig. 23) — a hemo-endothelial condition (Mossman '26).

The changes occurring throughout development in the labyrinthine part of the placenta are an increase in size of the maternal sinusoidal capillaries coupled with some decrease in the height of their cuboidal endothelium a disappearance of cytotrophoblast and a hyphae-like proliferation of fetal capillaries leading to their invasion towards and ultimately into the maternal capillary vessels. All these changes lead to a gradually increasing approximation of fetal and maternal blood and all should be borne in mind in committing this part of the placenta to any particular morphological category.

In the hemophagous organ it is clear that histologically the maternal fetal relationship is different from that of the labyrinth. According to Grosser a hemochorial placenta is one where maternal blood is directly in contact with fetal trophoblast. Such is the situation in this part of the raccoon placenta. We are as yet not in a position to tell whether the blood of the hemophagous organ is circulating. The very nature of the organ structure suggests that if there is circulation it is likely to be a slow one. It seems clear that maternal blood moves into the inter-lamellar spaces of the organ gaining access from the blood filled glands of a well defined sub-hemophagous region.

It is of interest to consider the development of the hemophagous organ. The earliest stages which have only recently become available have not yet been fully studied. It may however be conjectured from the present material that the invading fetal villi covered by cytotrophoblast, erode away the maternal uterine epithelium together with much of the endometrial glands. In the labyrinthine placenta the villi continue to invade to the very bases of the glands (fig. 18). In the area of the hemophagous organ, however maternal blood fills the glands and once their distal parts have been opened up by the erosive action of the villi further incursion ceases. Introversion of the cytotrophoblastic epithelium seems to follow and continued proliferation of this trophoblast gives rise to the essential part of the hemophagous organ. The line at which the invasive action of the villi ceases, and introversion commences can be seen in figures 5 and 6. By this means maternal blood is allowed to pass out into the interlamellar spaces of the hemophagous organ and bathe the columnar trophoblastic cells which in many respects are similar to those of the villous tips in the labyrinthine part of the placenta. Both the trophoblastic cells of the villus tips and those of the hemophagous organ possess great phagocytosing powers the former phagocytosing glandular secretions and histolytic material the latter phagocytosing primarily blood corpuscles but also some glandular material. The means by which maternal blood gains access to the glands of the sub-hemophagous region is so far not known.

Reference to the literature reveals three other members of the Carnivora possessing organs which may be similar to the hemophagous organ of the raccoon. These organs are the "blutbeutel" of the otter (Bischoff 1865) the central blood pouch

of the badger (Amoroso '52b) and the central hematoma of the wolverine (Wislocki and Amoroso '56). In the case of the otter Bischoff gives a brief account of the gross anatomy of the "blutbeutel" from two placentae of approximately the same developmental stage. Amoroso in a discussion of the hematoma of carnivores mentions the central blood pouch of the badger but gives no description, and Wislocki and Amoroso give an account of the gross and microscopic anatomy of one fairly advanced stage (fetal crown-rump length 75 mm) of the wolverine placenta. These authors were unable, however, to study the development of the placenta, and it is difficult to form a useful comparison between the hemophagous organ of the raccoon on the one hand and the "blutbeutel" of the otter, the central blood pouch of the badger, or the central hematoma of the wolverine on the other hand. Nevertheless the central hematoma of the wolverine possesses tall columnar phagocytic fetal epithelial cells similar in most respects to those of the raccoon hemophagous organ. These too appear to be hemophagous and to be bathed by maternal blood, and it seems that this type of cell is predominant in all carnivore hematomata which have been described. Rarely, however, has the origin and development of these hematomata been thoroughly investigated. Both Mossman ('37) and Amoroso ('52b) regard the central and marginal hematoma to be an atypical hemochorial placenta on the grounds that the maternal blood spaces actually lie between the uterine epithelium and the chorion, instead of in spaces lined entirely by trophoblast. Wislocki and Padykula ('60) for the same reason, namely that the hematomata consist of extensive extravasation of maternal blood between the chorion and the endometrium, on the other hand regard them as epithelio-chorial according to Grosser's classification. Differences therefore exist in the interpretation of Grosser's classification as applied to the hematomata. In the raccoon, however, the blood spaces throughout the hemophagous organ are lined by trophoblast and in the sub-hemophagous region, the maternal blood is contained by glandular epithelium (fig. 6). It may be argued that because endometrial glandular epithelium is ontogenetically a derivative of uterine epithelium, and trophoblast is a chorionic development, the situation in the raccoon is also epithelio-chorial; but one must not lose sight of the fact that considerable erosive action has taken place and that this has resulted in the removal of uterine epithelium and connective tissue, and brought about this maternal-fetal relationship in the raccoon. However, since maternal blood spaces are lined by fetal trophoblast in the raccoon hemophagous organ, it seems more reasonable to regard this organ as being a hemochorial placenta. Yet it is by no means clear as to whether, by comparison with the hematomata of other groups, this can be looked upon as being a typical or an atypical hemochorial condition.

The hematomata of carnivores have been regarded as accessory (Mossman, '37) or supplementary (Amoroso '52b) placentae. Whether the hemophagous organ at all stages of development, should be so regarded may be debatable. The size of the organ, relative to the labyrinthine part of the placenta, is impressive and, because of the complexity of its lamellae, the surface area of the hemophagocytic trophoblast is extensive. Furthermore morphological changes occurring in both parts of the placenta may possibly reflect changes in relative activity. Thorough discussion of the functional activity of the hemophagous organ would be premature at the moment and must await the outcome of

---

We have recently examined, through the courtesy of Dr. H. W. Mossman, sections of the placenta of another Procyonid — the olingo (Bassaricyon gabbi orinomus Goldman). This placenta was from an adult animal weighing 1.70 kg, which was obtained by Dr. W. A. Wimsatt in '49 in the Rio Canzo area, Palenque, Colon Province, Panama. We find that this animal also possesses an hemophagous organ.

Since this manuscript was completed, we have had an opportunity of preparing sections through the placentae of a wolverine and a river otter (Lutra canadensis). The wolverine specimen, killed in '53 at Skwentna, Alaska, was presented to us by Dr. H. W. Mossman. It possessed a placenta which was at a much earlier stage of development (fetal greatest length 17 mm) than that examined by Wislocki and Amoroso ('56).

The otter specimens from Western Montana were obtained in '66 and '67 by Vernon Hawley and Kenneth Greer of the Montana Fish and Game Department, and were sent to us by Dr. P. L. Wright. The placentae associated with 60 mm fetuses, each revealed a central antimesometrial structure equivalent to the "blutbeutel" of the European otter (Lutra vulgaris) as described by Bischoff ('865).

Histological examination confirms our belief that the central hematoma of the wolverine, the "blutbeutel" of the otter and the hemophagous organ of the raccoon are similar structures.

histochemical and electron micrographic studies now in progress. Nevertheless certain inferences may be made.

Until relatively recently it was generally supposed that nearly all substances which passed from mother to fetus did so by diffusion across the placenta, and that this diffusion was most efficiently performed at the thinnest parts of the chorio-allantoic placenta. Cunningham ('20 '22) recognized however a differential permeability of the placental barrier in experiments on cats and rabbits. Since then cytological and histochemical investigations of the mammalian placenta (Wislocki and Bennett, 43 Dempsey and Wislocki 44 46 Wislocki and Dempsey 45 46a 46b Wimsatt, 49) have shown the placental barrier to be more complex than hitherto supposed. Currently the general opinion is that Grosser's concept that the fewer the layers between the maternal and fetal blood the speedier is the diffusion rate may hold good only in the case of the more readily diffusible substances. On the other hand it seems likely that the more complex substances require chemical mediation and this may well take place only in thicker regions of the placental barrier

In the earlier stages of the raccoon placenta the maternal and fetal bloods are in closer proximity in the hemophagous organ than in the labyrinthine region, and if the maternal blood in this organ has readily diffusible substances to offer exchange may be more efficiently carried out here than in the labyrinth As pregnancy proceeds however fetal capillaries in the labyrinth become more extensive and invasive and the two bloods become closer together in the labyrinth than in the hemophagous organ, in some instances being separated only by fetal endothelium. This thinning of the barrier in the labyrinth is not however paralleled by the hemophagous organ where throughout pregnancy the fetal capillaries remain in sub-epithelial or basally intraepithelial positions with respect to the phagocytic trophoblast.

It has been reported (Wislocki and Padykula '60) that the hematomata of carnivores persist throughout gestation without apparent cytologic changes or any reduction in width or number of layers Although there may be no reduction in the width or number of layers in such carnivores as the dog and the red fox (Vulpes vulpes) (Creed '58) a great extension of the surface area of the phagocytosing layers occur In the raccoon hemophagous organ not only does the surface area of the phagocytosing trophoblast increase throughout most of gestation and decrease only towards the end of pregnancy but also distinct cytological changes take place The nuclei of the trophoblast cells migrate from a basal position in early pregnancy to a position at the free ends of the cells in late pregnancy The basal cytoplasm of the cells in the early stages is more basophilic than in the late stages In addition a progressive accumulation of crystals of orange-yellow pigment within the cells culminates eventually in a disgorging of these crystals back into the interlamellar maternal blood It is likely that this pigment is primarily bilirubin (Wise '62) The changes involved are indicative of great cellular activity and it may well be that these particular cells of the hemophagous organ play a most important role in transforming chemically the maternal blood contents together with some histotrophe, thereby mediating the passage of certain substances designed for fetal metabolism. Thus in this animal it is possible that readily diffusible substances may be exchanged through the placental labyrinth and more complex substances through the hemophagous organ Harrison and Young ('61) in discussing the placenta of certain species of Pinnepedia remark on the presence of anisotropic bilirubin crystals and cholesterol esters in the hematomata of *Phoca vitulina* L. and *Halichoerus grypus* Fabricius and suggest that a mechanism for transferring iron to the fetus is indicated In such regions however iron may not necessarily be the only fetal requirement being transferred

It seems quite clear at least in the case of the hemophagous organ of the raccoon and probably also in the case of the hematomata of other carnivores that these structures are of great importance in the supply of nutriment to the developing embryo. The condition of the blood entering these regions is still open to inquiry Generally past studies of erythrophagocytosis have been directed to the investigation of

the phenomenon as a means of destruction of unwanted erythrocytes (Essner '60) and there is a body of opinion that suggests that only aged or altered erythrocytes can be phagocytosed (Miescher '57). If this opinion is valid in all cases where erythrophagocytosis occurs presumably some change is wrought in, at least, the erythrocytes of the blood present in the hemophagous organ. This change may be brought about by the secretions of the glandular epithelium below the hemophagous organ, by secretions of the phagocytic fetal epithelium itself or in some other way. Alternatively there exists the possibility that non-effete blood cells can also be phagocytosed in this particular region.

The contingency that a complete circulation does not exist in the raccoon hemophagous organ or the hematomata of other carnivores is not a valid objection to their nutritive role since a one-way feed might be entirely satisfactory where tissues with great phagocytosing powers are present. Phagocytosis as a means of imbibition of food material is a well known phenomenon in a number of lower animal groups. The retention of this primitive potentiality and its manifestation in the activity of certain cells during early development in higher animals is therefore not surprising. Thus the concept that a kind of extra-fetal digestion occurs in hemophagous regions of the placenta may be of the greatest importance to the complete understanding of placental activity.

As reported elsewhere (Biggers and Creed, '62) the term hemophagous organ was proposed for this specialized placental structure because of its great blood phagocytosing activity. It may be equivalent to the hematomata of other carnivores, but as Amoroso ('52b) states "A thorough investigation of the hematoma has yet to be made. This applies particularly to the method of formation. The term hematoma has a pathological implication and conjures up the idea of accidental extravasation of blood. Phylogenetically the origin of such structures may have been "accidental," but the fundamental ability of certain mammalian cells to take over a phagocytic role in the presence of extravasated blood may well have led, during the course of evolution, to the establishment of constant pathways by which maternal blood can gain access to well defined hemophagocytic organs. These well defined and constant hemophagocytic regions such as some of the hematomata of certain mammals appear to be extremely active and the fact that a pathological term has been assigned to them may well be partly the reason for lack of investigation of, and interest in, them. The use of the term hemophagous, being more descriptive and functional, may help to stimulate interest in these regions of the placenta.


## SUMMARY

1. The material presented consists of a series of four developmental stages of the raccoon placenta. Appropriate measurements are tabulated.

2. An account of the gross morphological features of the four placentas is given. The placenta forms a complete zonary band or annulus around the equator of the allanto-chorionic sac, and is not incomplete as reported by previous authors.

3. Marginal hematomata as in the dog, fox, or coyote are not present but an outstanding feature of the placenta is the presence of an anti-mesometrially situated hemophagous organ.

4. A description of the histology of the placenta is given. Two distinct regions are recognized, a labyrinthine region and a hemophagous one.

5. In the labyrinthine part the maternal sinusoid-like capillaries are noteworthy for their atypical endothelium of cuboidal cells, and a thick surrounding basement membrane.

6. The hemophagous organ consists essentially of great areas of phagocytosing fetal epithelium whose main function appears to be that of ingesting the maternal blood by which it is bathed.

7. Changes in form, structure and size of the placenta throughout gestation are discussed.

8. The possible role of the hemophagous organ for fetal nutrition is stressed and the concept of its being an extra fetal digestive mechanism for complex substances is introduced.

9. The likelihood of the hemophagous organ being functionally equivalent to the

hematoma of other carnivores is considered The suggestion is made that the use of the term "hematoma because of its pathological implications could, with advantage, be discontinued and that the more descriptive and functional term "hemophagous be applied to such regions of the placenta.

ACKNOWLEDGMENT

The work was supported by generous grants from the Lalor Foundation and the National Science Foundation (grant no. N.S F G17658) One of us (R.F.S C.) also wishes to acknowledge a Fullbright Travel Fellowship We are greatly indebted to the Leptospirosis Unit of the School of Veterinary Medicine University of Pennsylvania under the direction of Dr L. G Clark for help in obtaining animals and to Dr H. W Mossman for the material he has placed at our disposal. We wish further to acknowledge the skilled technical assistance rendered by Mrs. Wilhelmina Harrell and Mrs. Nell Phillips and our thanks are due to H A. Burgess for taking all the photographs except those of figures 20 22, and 24

LITERATURE CITED

Amoroso, E. C. 1952a Allanto-chorionic differentiations in the Carnivora. J Anat. London, 86 481

——— 1952b In Marshall' Physiology of Reproduction, 3rd ed., Ed. by A. S. Parkes, Vol. II, Chap. 15 127–311 Longmans, Green & Co., London.

——— 1959 Comparative anatomy of the placenta Ann. N Y Acad. Sci., 75 855–872.

Biggers, J D and R. F S. Creed 1962 Two morphological types of placentae in the raccoon. N ture 194 103–104

Bischoff T L W 1865 U ber das Vorkommen eines eigenthümliches Blut und Hämatoidin enthaltenden Beutels an der Plazenta der Fischotter (Lutra vulgaris) Sitzungsb. König. bay Akad. Wissensch. München. 1 214–225

Bissonette T H and A G Csech 1937 Modification of mammalian sexual cycles VII. Fertile matings of raccoon in December instead of February induced by increasing daily periods of light. Proc Roy Soc B 122 246–254.

——— 1938 Sexual photoperiodicity of raccoons on low protein diet and second litters in the same season. J Mammal 19 342–349.

——— 1939 A third year of modified breeding behaviour with raccoons Ecology 20 156–162.

Creed, R. F S 1958 Unpublished observation

Cunningham, R. S. 1920 Studies in placental permeability I. The differential resistance to certain solutions offered by the placenta in the cat. Am. J Physiol., 53 439–456.

——— 1922 Studies in placental permeability II. Localization of certain physiological activities in the chorionic ectoderm in the t. Ibid 60 448–460

Dempsey E. W and G. B Wislocki 1944 Observations on some histochemical reactions in the human placenta with special reference to the significance of lipoids, glycogen and iron. Endocrinology 35 409–429.

——— 1946 Histochemical contributions to physiology Physiol. Rev 26 1–27

Duval, M. 1895 Le placent des carnassiers. J Anat., Paris, 31 38–80.

Essner E. 1960 An electron microscopic study of erythrophagocytosis. J Biophys. Biochem. Cytol., 7 329–333.

George, J L., and M. Stitt 1951 March litters of raccoons (Procyon lotor) in Michigan. J. Mammal., 32 218.

Grosser O 1908 Über vergleichende Placentation und die Einteilung tierischer Placenten. Zbl. Physiol., 22 198–199

——— 1909 Vergleichende Anatomie und Entwicklungsgeschichte der Eihäut und der Placenta. Braumuller W Wien-Leipzig.

Hamilton W J Jr 1935 The food and breeding habits of the raccoon. Ohio J Sci., 36 131–140

Harrison, R. J and B A. Young 1961 Specializations in the pinniped placenta. J Anat., Lond., 95 450.

Llewellyn, L. M. 1953 Growth rate of the raccoon fetus. J Wildlife Manag., 17 320–321.

Llewellyn, L. M., and R. K. Enders 1954 Transuterine migration in the raccoon. J. Mammal., 35 439

——— 1954b Ovulation in the raccoon. Ibid 35 440.

Matthews L. H. 1954 Remarks on the placenta of the spotted hyena Crocuta crocuta. Proc. Zool. Soc. Lond., 124 198.

McKeever S. 1958 Reproduction in the raccoon (Procyon lotor) in the southeastern United States. J Wildlif Manag 22 211

Miescher P 1957 In Physiopathology of the Reticuloendothelial system. Ed. by R. N. Halpern, B Benacerraf and J F Delafresnaye 147–171 Blackwell Scientific Publications, Oxford.

Morton, W R. M. 1959 Placentation in the Spotted Hyena (Crocuta crocuta Erxleben) J Anat. Lond., 91 374–382.

Mossman, H. W 1926 The rabbit placenta and the problem of placental transmission. Amer J Anat., 37 433–497

——— 1937 Comparative morphogenesis of the fetal membranes and accessory uterine structures. Contrib. Embryol. Carneg Instn., 26. 129–246

Pope C. H 1944 Attainment of sexual maturity in raccoons. J Mammal., 25 91

Ra A. S 1925 Contributions to our knowledge of the structure of the placenta of Mustelidae Ursidae and Sciuridae Proc Zool Soc Lond B 1027 1069

Rinker G. C. 1944 Os clitoridis from the raccoon. J Mammal., 25 91–92.

Sanderson, G. C. 1950 Methods of measuring productivity in raccoons. J Wildlife Manag., 14: 389–402.

——— 1951 Breeding habits and history of the Missouri raccoon population from 1941 to 1948. Trans. N Amer Wildlife Conf. no., 16 445–461.

Stuewer, F W 1943 Reproduction of raccoons in Michigan. J Wildlife Manag., 7 60–73.

Strahl, H and E. Ballman 1915 Embryonalhüllen und Plazenta von *Putorius furo*. Abh. preuss Akad. Wiss. Nr., 4 3–69

Watson, M. 1881 On the female organs and placentation of the Raccoon (*Procyon lotor*) Proc. Roy Soc. B 32: 272–298

Wimsatt, W A. 1949 Cytochemical observations on the fetal membranes and placenta of the bat, *Myotis lucifugus lucifugus* Am. J Anat., 84: 63–141.

Wise, C. D 1962 Personal communication.

Wislocki, G. B., and E. C. Amoroso 1956 The placenta of the wolverine (*Gulo gulo luscus*. Linnaeus) Bull. Mus. Comp. Zool. Harvard, *114* 91–100.

Wislocki, G B., and H. S. Bennett 1943 The histology and cytology of the human and monkey placenta with special reference to the trophoblast. Amer. J Anat., 73 335–449.

Wislocki, G. B., and E. W Dempsey 1945 Histochemical reactions of the endometrium in pregnancy Ibid., 77 365–403.

——— 1946a Histochemical reactions in the placenta of the cat. Ibid., 78 1–45

——— 1946b Histochemical reactions in the placenta of the pig. Ibid., 78 181–225

Wislocki, G B., and H. A. Padykula, Ed. by W C. Young 1961 In Sex and Internal Secretions, Vol. II, Chap., 15 883–957

*Abbreviations for plates*

B.M., basement membrane
B.S.G., basal segments of glands
C.E., cuboidal endothelium
C.T cytotrophoblast
F., fetus
F.B.V fetal blood vessels
F.C., fetal capillary
F.C.E., phagocytosing fetal columnar epithelium
F.M., fetal mesenchyme
F V fetal villi
G.E., glandular epithelium
H.M histotrophic material
H.O., hemoph gou organ
J.G junctional and glandular zone
L., labyrinth
M.B.C., maternal blood corpuscles
M.S C., maternal sinusoidal capillaries
P pigment granules
P.A., placental annulus
S., septum
S.G.R., supra-glandular reservoir
S.H., sub-hemophagous region
S.T syncytial trophoblast

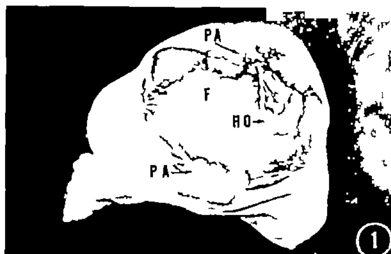
## PLATE 1

### EXPLANATION OF FIGURES

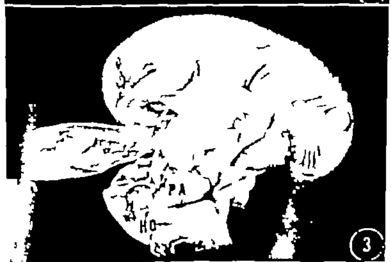
1 Photograph of one of the conceptuses of animal no. 97 A piece of the lateral wall of the uterus has been removed and reveals the fetu within it membranes lying in the allantoic cavity The placental annulus and the hemophagou organ are clearly shown × 2¼

2 A conceptus of animal no. 148 also opened in the same manner Note the increase in size of the fetus, the hemophagous organ and the annul s. × 1½

3 One of the fetuses removed together with the annulu from ani mal no. 209. The hemophagous organ in this example is reduced t mere plaque of ti sue × 8/9


PA
F
HO
PA
1


PA
HO
F
2


PA
HO
3

## PLATE 2

### EXPLANATION OF FIGURES

4 A higher magnification of the same hemophagous organ as shown in figure 3. Fetal blood vessels are converging on to the organ along the inside surface of the annulus. × 4

5 The early placenta (no. 97) Low power photomicrograph of sec tion cut transversely to the annulus, through the region of the hemophagous organ. This shows the placental l byrinth below which is the junctional and glandular zone. The hemophagous organ can be seen to consist of distal blood filled sac-like part and lamellated proximal part below which is the supra-glandular blood reservoir and the s b-hemoph gous region. Note the region of disintegration I tissues immediately below the supra-glandular reservoir × 6. Bouin fixation. Hematoxylin and eosin staining.


HO
5

PLATE 3

EXPLAN TION O FIGURES

All preparations figured in this plate were fixed in Boui s sol tion nd t ined with hematoxylin nd eosin.

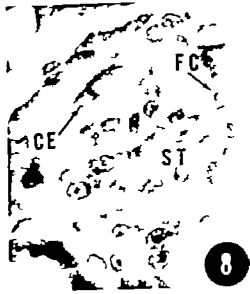
*Early placenta (no 97)*

6 A part of the same section in figure 5. Fetal villi project int the gl nd cavities below the labyrinth. Below the supra-glandular blood reservoir the glandular compartment of the sub-hemophagous region, separated by septa, are filled with maternal blood. Histotrophe only is present in the gland cavities of the functional and gl ndula zon Note the foldings f the septal walls and floors of the gland cavities Unmodified basal segments of the gland are present primarily below the functional and gl ndular zone. × 33.

7 A section through the placental l byrinth showing maternal sin soidal capillaries nd lacuna of fetal mesenchyme. × 140.

8 A section through the placental labyrinth to show a single maternal sinusoidal capillary with its endothelial wall of cuboidal cells, nd the surrounding yncytial trophoblast. Note that fetal capillaries have not penetrated far toward the maternal blood essel t thi stage.


MSC
FM
7


FC
CE
ST
8

## PLATE 4

### EXPLANATION OF FIGURES

All preparations figured in this pl te with the exception of figure 9 were fixed in Bouin solution nd stained with hematoxylin and eosin.

### *Early placenta (no 97)*

9 A section through a maternal sinusoidal capillary showing the cuboidal endothelium surrounded by well marked basement membrane Adjacent to this is syncytial trophoblast outside which is a layer of cellula trophoblast. × 1,200 and enlarged two and one-quarter times. PAS.

10 The tip of a single fetal villus can here be seen in the cavity of an endometrial gland Cytotrophoblast covers the vill tip and histotrophic material is present in the gland cavity × 140.

11 A section showing the floor and septa of the expanded part of an *endometrial gland in the junctional and glandular zone of the placenta.* Note histotrophe both in the gland cavity nd in the lumen of the unmodified basal segments of the gland. × 140.

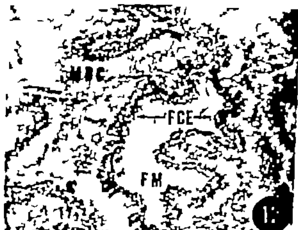
12 A section through the hemophagous organ. The lamellae consi t of fetal mesenchyme lined with phagocytosing fetal columnar epithelium. A few small accumulations of pigment granules can be seen within the epithelial cells. Maternal blood corpuscles fill the inter lamell r spaces. × 140.

13 Fetal phagocytosing epitheli m consists of columnar cell which have basal nuclei and cytoplasmic processes at their free ends. M ternal blood bathes these free ends and phagocytosed particles of blood and pigment granules can be seen in the supra nclear cytoplasm Fetal capillaries are immediately ub-adjacent to the cell bases 500


CT
ST
BM
CE
9


CT
HM
10


S
HM
11


MBC
FCE
FM


FC
MB
13

## PLATE 5

### EXPLANATION OF FIGURES

All preparation figured in this plat were fixed in Bouin sol tion.

*Two-thirds to three-quarter term placenta (no 148)*

14 A section cut tran versely t the nulus and through the hemopha gous org n. The relative sizes of the labyrinth nd the functional nd gl ndular zone can be seen Note the out tanding degree of proliferation of the glandular epithelium in the sub-hemophagou re gion 6. Hematoxylin d eosin.

15 A section through the labyrinth showing n increase in size of the matern l in soidal pillaries rel tive to those of the early placent (fig 7) 140 Hem toxylin nd eosin.

16 The l byrinth t how the basement membrane f the maternal pil l ries 330. PAS


15


BM
16

## PLATE 6

EXPLANATION OF FIGURES

All preparations figured in this plate were fixed in Bouin s solution and stained with hem toxylin and eosin.

*Two-thirds to three-quarter term placenta*

17 A section showing maternal sinusoidal capillary filled with maternal blood corpuscles. Fetal capillaries are present between the cuboidal endothelium of the maternal vessel and the syncytial trophoblast. Note the infiltration of one such capillary into an intra-endothelial position. × 800.

18 A part of the junctional and gl nd lar zone with fetal villi penetrat ing to the bases of the gland cavities. Little histotrophe can be seen in these cavities but histotrophe is contained in the basal unmodified segments of the gland. × 140.

19 A section through the hemophagou organ showing the phagocytosing fetal columnar epithelium bathed by m ternal blood. By comparison with the fetal columnar cells of the hemophagou organ of the early placent (fig. 12) an increase in pigment accumulation can be noted. × 140.

20 A section of phagocytosing fetal columnar epithelium showing nuclei to be no longer basal in position and the presence within the cell cytoplasm f blood corpuscles and fragments together with accumulation of pigment granules. Fetal capillaries are in basally intra-epithelial position. × 900 nd enlarged five times.


CE
FC
MD
17


18


19


P
FC
20

## PLATE

EXPLAN TION OF FIGURES

All preparations figured in this plate were fixed in Bouin s solution.

*Near full-term placenta (no 209)*

21 Section through the annulus and hemophagous organ Note the reduction in size of the hemophagou org n and the presence in it of large ccumulation of pigment. × 6. Masson.

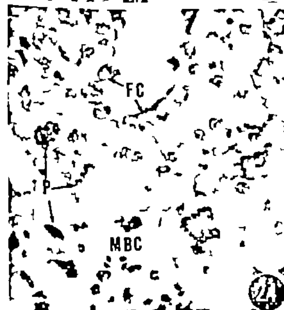
22 Section through the labyrinth showing the large size of the maternal sinusoidal capillaries. × 125 and enlarged five times. Hem toxylin and eosin

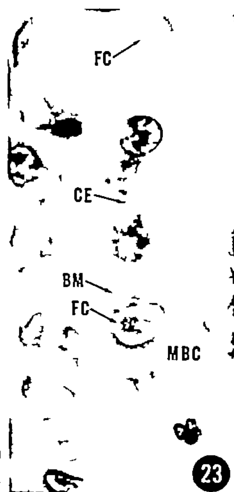
23 The wall of maternal sinusoidal capillary showing fetal capillaries which h infiltrated through the basement membrane and the endothelial cells and are bathed by maternal blood. × 1,200 and enlarged two and one-third times. PAS.

24 A section through the hemophagous organ showing the ph gocytosing fetal epithelium with fet l pillaries at its base The nclei re now t the free nd of the epithelial cells and pigment accumulation an be seen both in the cell cytoplasm and in the mat rnal blood 400 and enlarged fi times. Hematoxylin and eosi


HC
GE
GH
21


22


FC
P
MBC


FC
CE
BM
FC
MBC
23

# The Fetal Membranes of the Pocket Gopher Illustrating an Intermediate Type of Rodent Membrane Formation

## II. FROM THE BEGINNING OF THE ALLANTOIS TO TERM[1]

H. W. MOSSMAN AND FRITZ STRAUSS
*Department of Anatomy, The University of Wisconsin and Department of Anatomy, The University of Berne, Switzerland*

It was pointed out briefly by Mossman ('37) that the type of development of the fetal membranes of *Geomys* is intermediate between that of primitive and higher rodents. A detailed description of the early development of *Geomys* followed (Mossman and Hisaw, '40). Nielson ('40) discussed fetal membrane development of *Dipodomys* and other heteromyids. We now describe in detail the later morphogenesis of the membranes of *Geomys*, believing that it will aid in understanding the anatomical, and eventually the physiological nature and evolutionary sequence of the membranes of Rodentia.

In this paper we also present some thoughts about fetal membranes in general, as well as of rodents in particular, with the hope that they will suggest future lines of attack on problems of gestation.

For simple diagrams revealing the essential nature of different types of fetal membrane morphogenesis in rodents the reader is referred to Mossman ('37) or to Hamilton, Boyd, and Mossman ('62) figure 509.

As stated by Mossman and Hisaw ('40), most of the *Geomys* material studied is from the collection made early in the century by Dr. T. G. Lee, and from a later one by Professor F. L. Hisaw. We also wish to express our appreciation to Dr. Patricia DeCoursey, Department of Zoology, University of Wisconsin for her assistance in a new collection of *Geomys* material, and to Dr. Robert L. Rudd, Department of Zoology, University of California at Davis for his recent courtesy in supplying living pregnant *Thomomys*. For figures 1, 2, and 3 we are indebted to Mrs. Patricia Seeliger and for figure 4 to Miss Evelyn Lipman.

### DECIDUA

In all rodents so far studied, implantation is on the antimesometrial side of the uterus, and in all of them this is also the area of the first decidual reaction. The initial stage of this reaction appears while the zona pellucida is still intact, approximately concomitant with the achievement of spacing of the embryos, and preceding, possibly by several hours, the actual trophoblastic contact with the uterine lining. Invariably the decidual hypertrophy is less rapid in the mid-sagittal plane of the uterus directly between the embryo and the antimesometrial musculature than it is immediately surrounding this area. This results in the formation of an "implantation chamber" bulging antimesometrially from the uterine lumen, and of slightly greater diameter than the blastocyst. In the more primitive rodents, such as the Sciuridae, this is from the first relatively broad and shallow, i.e., spheroidal, to accomodate the large spherical blastocyst; in the more specialized ones, such as the Muridae and Caviidae, it is a narrow deep cylindrical space, at or near the blind end of which the very small precocious blastocyst implants.

In *Geomys* an intermediate condition occurs (Mossman, '37; Mossman and Hisaw, '40). Figure 1 shows the changes in shape of the uterine lumen brought about by the endometrial hypertrophy which results in the establishment in

[1] Supported in part by the Research Committee of the Graduate School from funds supplied by the Wisconsin Alumni Research Foundation, by the National Institutes of Health (grant H-3331), and by the American Swiss Foundation for Scientific Exchange, Inc., and the Swiss Academy of Medical Sciences.

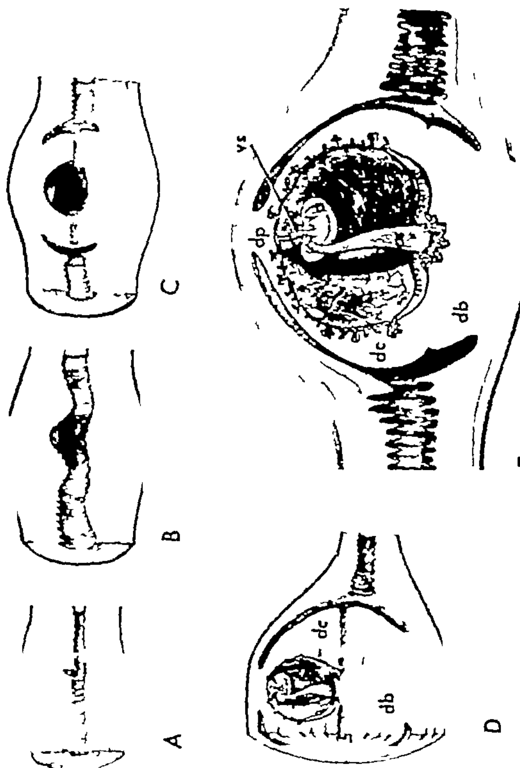



Figure 1

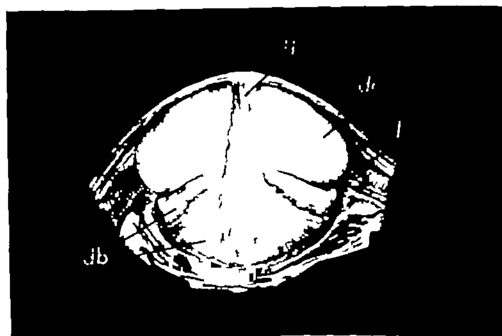



Fig. 2 Drawing of the decidua of gestation sac containing an embryo with very early limb buds. One-half of the uterine wall is dissected way db, decidua basalis; dc, decidua capsularis dp decidua parietalis; l, uterine lumen. × 5.

Geomys of buttresses of capsular and basilar decidua blocking the uterine lumen at both the cephalic and caudal entrances of the implantation chambers. It also shows how the relative extension of the uterine lumen from each end of a gestation sac toward the attachment region, and outside of the decidual masses maintains the band of parietal decidua as a narrow zone continuous with the mesometrially located basal decidua and in addition it shows how this extension of the lumen appears to cut the capsular decidua free from the parietal uterine wall. The extension of the uterine cavity around the capsularis is, of course the result of differential growth, and not of actual undercutting, as the parietal decidua is at least as wide at mid-term as in the beginning. The growth and differentiation of the basal decidua, although slower to start, soon becomes far more extensive and elaborate than that of the capsular and parietal regions (figs. 1D 2, 3 4 5 and 7) It, too becomes somewhat undercut by the uterine lumen, yet the basalis in *Geomys* at term still provides a relatively broad area of attachment for the placenta, about half the diameter of the placental disc (fig. 27)

The histological peculiarities of the decidua capsularis and parietalis will be dealt with in connection with the discussion of the yolk sac those of the decidua basalis will be taken up with the chorio-allantoic placenta. No histochemical studies of the decidua have been made

———

Fig. 1 Perspective diagrams of the development of the *Geomys* gestation sac to show the relations of the decidua to the embryo and uterine lumen. A, initial implantation of the morula (cf. I. [Mossman and Hisaw 40] figs. 1 and 10); B at the time of the bilaminar blastocyst (cf. I. figs. 2 and 14) C, at the time of the yolk sac inversion and amniogenesis (cf. I. figs. 3 and 25); D t the time of allantoic contact (cf. fig. 11), showing the nearly obliterated uterine lumen through the decidua, and the apparent extension of the uterine lumen; E, t the time of the placental hillock (cf. fig. 13) showing obliteration of the uterine lumen through the decidua, and the positions of the two villous areas of the yolk sac. D and E are drawn to smaller scale than A, B and C. a, amnion; aa, allantoic stalk; db, decidua basalis; dc, decidua capsularis; dp, decidua parietalis vs, vitelline stalk.

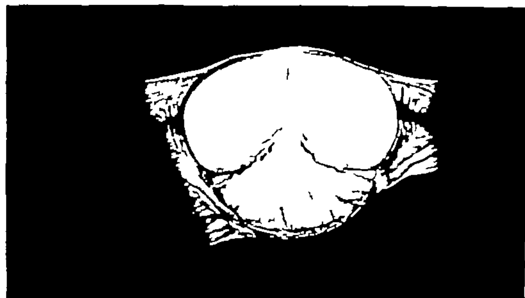


Fig. 3 Drawing f the decidua of gestation sac containing an embryo of 8 6 mm CR (late limb bud digit ridges with complete webs) 3 5.

INVERTED YOLK SAC PLACENTA DECIDUA CAPSULARIS AND PARIETALIS

The splanchnopleuric hemisphere of the yolk sac becomes completely inverted against the bilaminar abembryonic hemi sphere at the period of formation and closure of the neural folds (figs 4 and 5) and blood islands are scattered over most of its surface (cf fig 33 Mossman and Hisaw 40) By the time the limb buds appear (fig 7) *the sinus terminalis is well developed and the vitelline circulation has* certainly started The sinus terminalis immediately surrounds the small discoid plate of true chorion which separates the open epamnionic cavity from the exocoelom *in other words it is at the angle of* junction of the splanchnopleuric yolk sac with the bilaminar omphalopleure and the true chorion (fig 8)

At this period of limb bud formation when the mesodermal allantois has not yet reached the chorion the inverted yolk sac in the antimesometrial region and on all sides of the opening of the yolk duct (fig. 13) exhibits evaginations endodermal buds and true vascular villi penetrating into the adjacent decidua capsularis and into the narrow area of its attachment to the uterine wall the decidua parietalis (figs 1D 4C and 33) These villous structures soon become very numerous and cover at least the antimesometrial half of the inverted yolk sac, reaching nearly to the junction of the capsular with the basal decidua (figs 1E and 13) They are always most numerous and complex where the antimesometrial hemisphere of the capsular decidua is thickest which is the more antimesometrial portion.

Although at first sight the penetration of villous structures *into the capsularis appears* to concern only the splanchnopleuric yolk sac careful examination shows that the bilaminar yolk sac wall persists and at first lines the cavities formed in the decidua (figs 4C and 33) The very delicate *Reichert s membrane and the* small dark nuclei of the endodermal cells are readily seen at the limb bud period lining the pockets into which the villous structures fit

It is also apparent that most of the orig inal maternal stroma of the capsular decidua has disappeared by this time and is replaced by large mainly mononuclear trophoblastic giant cells which surround a rich network of sinusoidal maternal capil laries (figs. 4C and 33) Even much later when most of these giant cells appear to be degenerate intact blood-filled maternal capillaries can still be found (fig 4D)




Figure 4

A Drawing of sagittal section of gestation sac at neural groove stage comparable to figure 5, to show the relationships of the decidua and membranes a, amnion; bl, bilaminar omphalopleure with Reichert' membrane; c, chorion; db decidua basalis; dc, decidua capsularis; de, degenerating epithelium dp, decidua parietalis ec epamniotic cavity; ex, area of extravasation; iy inverted vascular segment of yolk sac l, uterine lumen; xc, exocoelom. Approx. × 25

B Enlarged portion of A, showing decidua capsularis, bilaminar omphalopleure and inverted vascular segment of yolk sac with its rich vascul ture The tissue of the capsularis is mixture of decidua (indicated as cells with clear cytoplasm) and invading cytotrophoblast (indicated as cells with granular cytoplasm) For photomicrograph of a similar stage see figure 32. Approx. × 100.

C Similar area of capsularis of late limb bu at the 8 mm CR, comparable to figure 33, showing disappearance of most decidual cells and the formation by the bilaminar omphalopleure of pits (p) which are occupied mainly by h low diverticul (d) f the ascular yolk sac, and occasionall by villi (yv) Approx. × 100

D Similar area at late fetal period, 30 mm CR comparable to figure 34 when only few remnants of the maternal vasculature and endothelium rema and the bilaminar omphalopleure and Reichert membrane hav dis p eared. pprox. 100.

*In rodents generally the most characteristically villous area of the inverted yolk sac is a zone next to the sinus terminalis* i.e. a zone adjacent to the remnant of true chorion if such remains, as it does in the Sciuridae (Mossman and Weisfeldt, '39); or if as in *Geomys* no true chorion remains a zone bordering the attachment of the inverted yolk sac to the placenta (figs. 13 15 16 21 and 27) In *Geomys* the villi begin to form in this zone at about 9 mm at which time those of the antimesometrial hemisphere are already well developed *They spread rapidly outward* beyond the region of junction of the basal and capsular decidua, so that for a short time at about 10 mm CR they become continuous or almost so with the antimesometrial villous area at least laterally where the parietal decidua blends with the basal decidua.

At either end of the gestation chamber where the capsular decidua fuses with the basal decidua the former is much thicker than it ever is at the antimesometrial side. Furthermore there is little invasion of trophoblastic giant cells into this area This thick region of capsular decidua remains to term (36 mm CR) as a flange extending outward from the basal decidua It resembles in its histology the latter although at its thin outer margin it grades into the typical degenerating capsularis (figs. 19 23 26 and 27) As mentioned previously most of the capsular decidua degenerates and with this process the villous structures of its adjacent yolk sac also largely disappear so that at term only a few very much compressed and scattered villi remain on the antimesometrial hemisphere (fig 35) and almost none in the broad equatorial zone Also this thinning and degeneration of the capsularis and of the yolk sac villi throughout the equatorial zone results in the permanent and wide separation of the two villous regions of the yolk sac (fig. 19)

The mesometrial villous zone continues to differentiate the villi becoming long and complex on that part of the yolk sac which fits snugly over the margins of the chorio-allantoic placenta (figs. 19 20 21 26 27 and 28) Villi also remain next to the persistent flange of decidua capsularis of the placental base but rapidly shorten as they approach its degenerate margin (fig. 27) In this whole mesometrial villous zone of the *Geomys* yolk sac only true villi occur there are none of the narrow mesothelium-lined evaginations so common at the opposite hemisphere In short this villous area is entirely typical of that of rodents in general but it follows the positional pattern of the more specialized types which like *Geomys* lack a persistent true chorionic ring and therefore have the inverted yolk sac attached directly to the allantoic placenta, so that the villi are closely associated *with its surface and margin and with* any remnant of the capsular decidua which may persist here As in other rodents these villi also persist to term (36 mm CR)

The history of the capsular decidua is perhaps best surveyed by examination of *the series of drawings* (figs 1 2 3 and 4) and of the photomicrographic figures 5 7 11 13 16 17 19 23 26 27 and 32 to 35 At first of course it is well vascularized (figs. 4A and B and 32 and 33) but as it is stretched by the developing conceptus, it rapidly loses its vasculature This vessel atrophy begins at the equatorial zone between the mesometrial and antimesometrial hemispheres which is the region farthest from its sources of feeder vessels in the zonary band of decidua parietalis and in the basalis. The capsularis persists throughout most of gestation in the area as a pair of circumferential bands, each attached to a margin of this zonary band of decidua Presumably these bands of capsularis persist because of the availability of feeder vessels. Since the lateral and antimesometrial area becomes more distended and more removed from the mesometrial source of blood supply as pregnancy advances it is understandable that in this area capsular degeneration would be greater than at the mesometrial side where it is attached to the well vascularized broad portion of the parietalis and to the basalis In fact, in the mesometrial area the rims of capsularis remain thick throughout gestation and their histological characteristics are essentially the same as those of the basalis (fig. 27)

Throughout the rest of the capsularis profound changes quite different from those of the basalis occur By 9 mm CR

both the capsularis and parietalis especially in the antimesometrial area, show uniform invasion by relatively small trophoblastic giant cells and disappearance of the decidual cells (figs. 4C and 33) These giant cells are interspersed between enlarged maternal capillaries and, as described above, by spaces lined by Reichert's membrane and thin endothelium-like cells derived from the endoderm of the bilaminar layer of the yolk sac. Many of these spaces are occupied by villi or by hollow villus-like evaginations of the inverted yolk sac. By 30 mm CR this antimesometrial portion of the capsularis has become completely disorganized, and most, if not all of the giant cells have degenerated, or are in the process of doing so (figs. 4D 34 and 35) At full term it is difficult to detect even a remnant of the capsularis in this region, although a very narrow thin band of parietalis can be found.

Histogenetically the decidua parietalis behaves like the capsularis except for its outer zone i.e. the portion closest the myometrium, which does not degenerate, and which, although very thin and narrow always resembles the outer zone of the basalis (figs. 4A and 32 to 35) In fact, this so-called parietal decidua is in its relation to the original implantation of the rodent blastocyst, actually a decidua basalis, and could perhaps be more logically thought of as the earlier portion of a signet ring-shaped basalis, the signet of which is the portion at the base of the definitive placenta, exactly opposite to the original site of implantation. The remainder of the uterine endometrium lining the gestation sac at either side of this central decidual ring is more properly homologous to the decidua parietalis of man. Because previously the zonary band has been called parietal decidua confusion can be avoided by continuing this usage The rest of the endometrium of the parietal wall of the gestation sac, the area most homologous to the human parietalis can best be designated simply the parietal endometrium since in rodents it does not show a decidual change and is not shed as a true decidua.

EPAMNIONIC CAVITY AND TRUE CHORION

As pointed out by Mossman and Hisaw (40) a distinct but open epamnionic cavity is present (figs 4A and 6 [illegible]) and the true chorion (extraemb[illegible] [illegible]matopleure exclusive of the amn[illegible]) [illegible]mited to a mere "drumhead" [illegible] the epamnionic cavity from th[illegible] [illegible]inous exocoelom. By the first appe[illegible]ance [illegible] the limb buds the epamnionic ca[illegible]ty h[illegible] been reduced to a shallow pit, and its [illegible]noblastic lining and adjacent chorionic [illegible]soderm are both hypertrophied [illegible] figs [illegible] 8) the trophoblast being from 5 to 15 [illegible] in thickness. The mesoderm is hypertrophied only on the "drumhead" proper not at its margins but some trophoblastic hypertrophy extends beyond the margin of the epamnionic aperture as far as the zone of junction of the basal and capsular decidua (figs. 7 and 8)

At the time of first appearance of the rear limb buds the allantois has just contacted and fused with the thickened mesoderm of the chorion, i.e., with the former "drumhead" of the epamnion. The epamnionic cavity has not been completely obliterated, and the trophoblast of its "drumhead" is in intimate contact with the degenerating epithelium of the mesometrial side of the uterine lumen (figs. 11 and 12) At this time also the uterine lumen has been obliterated just cephalad and caudad to this region, thus the conceptus is for the first time completely enclosed in decidua and thus entirely isolated from the uterine lumen (figs. 1E and 11) The obliteration of these narrow portions of the uterine lumen is brought about by atrophy of the epithelium and fusion of the subepithelial connective tissue

The former wall of the epamnionic drum, which is a narrow band of the bilaminar omphalopleure, is folded against the rim of the newly formed chorio-allantoic disc, and the two adjacent trophoblastic surfaces fuse (fig. 12). The significance of this is discussed under the chorio-allantoic placenta (p 454)

Even before the allantois attaches changes in the decidua are striking (fig. 7) Much of the capsularis is already thin and degenerate but especially near the zonary decidua parietalis it is being rapidly augmented by the addition of enlarging trophoblast cells, and near its attachment to the decidua basalis it is thick and histologically similar to the inner more

compact zone of the basalis. The innermost portion of the parietalis is also loosened and degenerate. Its outer juxtamuscular portion is compact and is continuous at its mesometrial ends with the similar very thin outermost zone of the basalis. This zone of junction with the myometrium consists of relatively "embryonic" stroma. Most of the basalis (roughly the outer two-thirds of its total thickness) is less compact because of numerous cyst-like remnants of uterine epithelium, more or less dilated venous and capillary spaces and considerable enlargement and vacuolar degeneration of its decidual cells. Through the center of the basalis a few *arterial channels surrounded by compact decidual cell sheathes* penetrate to the inner compact zone. Immediately subjacent to the epithelium lining the center of the mesometrial segment of the gestation chamber is an acidophilic mass of tissue consisting of extravasated blood and degenerating stroma (figs. 5, 7 and 8). The uterine lumen in this area contains much cellular debris which extends into the collapsing epamnionic cavity (figs. 7 and 8). The uterine epithelium is intact at both ends of this area where it continues as the lining of the very narrow uterine canals which connect with the immensely expanded juxtadecidual lumen of the gestation sac.

CHORIO-ALLANTOIC PLACENTA

*Allantoic growth and contact*

Development and growth of the allantois is similar to that of the rat and guinea pig, there being no endodermal diverticulum beyond the immediately proximal portion *which is destined to form the urachus* and urinary bladder. The allantoic anlage is first seen at about the time the fifth somite appears and there are blood islands in it as soon as it definitely projects into the exocoelom. A complete circulation appears to be present, as judged by vessel development, before it reaches the chorion. Contact with the chorionic disc (the former "drumhead" of the epamnionic cavity) occurs at about 5 mm and definite chorio-allantoic fusion at about 6 mm, which is during the period of epamnion collapse.

At about 6 mm, when fusion has just occurred, the hypertrophied chorionic mesoderm forms a distinct layer to the fetal surface of which a net of allantoic vessels is applied (fig. 11). Soon this net invades the chorionic mesoderm and contacts the fetal surface of the trophoblast (figs. 13 and 15). This obliteration of the chorionic mesoderm as a distinct layer should be thought of as the initiation of the true chorio-allantoic placentation.

*Allantoic bulb and placental hillock*

In the late limb bud period, between 6 and 9 mm CR, a rapid bulbous enlargement of the distal allantoic mesoderm occurs (figs. 13 to 16). This bulb is clothed by the chorionic trophoblast usually two to four cell layers in thickness, which is actually the expanded trophoblast of the epamnionic drumhead, and this in turn is surrounded by a mass of cellular trophoblast (fig. 13, t) forming a prominent hillock in which the above elements are embedded. This mass of cellular trophoblast extends well out from the base of the hillock, at least as far as the region of junction of the capsular and basal decidua (figs. 13 and 16).

The basal cytotrophoblast originates from the bilaminar omphalopleure just lateral to the open rim of the epamnion at about the time of the collapse of the epamnion, when the embryo is in the late gill-cleft stage. These trophoblast cells are almost certainly homologous to the trophoblastic giant cells which arise from the corresponding portion of the bilaminar omphalopleure in the squirrel and mice. Like the homologous cells of the latter they are destined to form not only the *basal giant cells but also the basal trophoblast* or trophospongium of the definitive placenta.

In *Geomys*, and in fact in Geomyoidea in general, these cells are small and difficult to distinguish as they migrate away from the blastocyst. However, their existence becomes very obvious as they invade the basal decidua on the mesometrial side of a mass of maternal extravasated blood and degenerating endometrial cells which forms opposite the epamnion (fig. 1). Unfortunately, with the material available

Direct embryo measurement for these specimens are not av[ail]able.

to us, we can characterize them only in the most general histological terms. They exhibit numerous mitoses and distinct cell boundaries. Their cytoplasm contains a coarse basophilic reticulum very different from the relatively acidophilic cytoplasm of most of the basal decidual cells. They cling to one another in grossly visible masses and strands surrounding similar masses and strands of decidua. Soon irregular channels filled with maternal blood appear within the larger trophoblastic masses. These are the anlagen of the venous network of the definitive trophospongium. Figures 13 16 and 17 show well the extent of this basal trophoblast, the way it builds up around the chorionic trophoblast of the chorio-allantoic bulb and, especially in figures 14 15 and 16 the numerous venous sinuses which it contains. Since this mass of tissue arises from the bilaminar omphalopleure just lateral to the chorio-allantoic bulb and builds up around the latter to form the placental hillock, its surface facing the original blastocyst (yolk sac) cavity is lined by the other component of the bilaminar omphalopleure the endoderm (fig. 15) There is also a very thin, and usually distinct, Reichert's membrane (barely visible on fig. 28) Figures 16 to 28 show the extent and structural importance of this zone as the placenta develops

The trophoblast of the true chorion i.e. of the epamnionic drumhead is in direct contact with the vascular net of the allantois as the allantoic bulb is formed. It is this layer of trophoblast which immediately clothes the developing allantoic villi as they differentiate in close association with the trophospongium just described (figs. 14 and 15) Soon contact is made between this layer and the maternal blood in the trophospongial channels The trophoblastic tubules of the labyrinth in fact all the maternal blood channels in the labyrinth are lined by this trophoblast of chorionic origin, not by that of bilaminar omphalopleure origin the trophospongium This difference in origin is evident in other rodents (Mossman, '37) The chorionic trophoblast at least of the more primitive rodents becomes syncytial but the omphalopleuric trophoblast usually remains cellular The chorionic trophoblast usually is the layer taking part in the placental membrane (barrier) the omphalopleuric portion usually does not. The only apparent exceptions to this are in the Dipodidae and Zapodidae where giant cells of omphalopleuric origin seem to take over the position and function of the chorionic trophoblast (Mossman and Conaway '54)

### *The gross anatomy of the placenta and of its relations to the yolk sac*

Examination of the figures especially of figures 13 16 17 19 21 23 26 and 27 will furnish a general image of the gross relationships in the region of the chorio-allantoic placenta. One notes how the development of the allantoic bulb and placental hillock initiates the inflected mushroom cap or pileate shape of the placenta, so characteristic not only of *Geomys* and *Thomomys* but of all Geomyoidea so far examined (Mossman, '37 Nielson 40)

As growth of the placenta proceeds the inflected edges become more and more infolded (fig 19) until finally the equatorial region is acutely bent and only a thin flange of vascular allantoic mesoderm separates the flattened inflected rim from the equally flattened placental base (top of the pileus ) (figs 26 and 27) Measured from stained sections the total diameter of the placental disc at term is approximately 20 mm. The width of one inflected margin is about 5 mm, approximately 25% of the total diameter of the placenta. The diameter of the opening between the inner edges of the inflected ring is about 10 mm that is just half of the total placental diameter Thus enables the peripheral allantoic vessels to supply both the inflected ring and adjacent base thus reducing significantly the vessel length that would be necessary if a placental labyrinth of the same thickness and volume were to be provided in the form of a simple flat disc. The maternal vessels must on the other hand be as long perhaps slightly longer than would be necessary if the margins were not inflected.

At term, again measured from stained sections the approximate thickness of the various layers at the center of the disk is as follows labyrinth 1 mm; trophospongium 1.5 mm decidua basalis 5 mm; myometrium 2 mm; making a total of 9.5 mm

excluding the irregular allantoic mesoderm and umbilical vessel branches covering the fetal surface. The labyrinth is remarkably uniform in thickness even on the inflected portion (fig. 28)

In longitudinal section (figs. 23 26 and 27) the definitive placental disc is seen to have two circumferential constrictions one between the trophospongium and the area of junction of the capsular and basal decidua, the other more basal between this decidual junctional area and the uterine wall This double constriction results in a flared or discus-like pedicle rather than the simple attachment area characteristic of placentas such as those of the squirrels, which have only the rudiments of a capsular decidua and those of the mice in which even the mesometrial portion of the capsularis disappears relatively early in development. The first constriction (internal *to the decidua capsularis*) is lined on its placental surface by a simple endodermal epithelium and on its outer surface by the degenerate bilaminar omphalopleure attached to the basal portion of the decidua capsularis. It is occupied by the vitelline cavity containing in later stages an amorphous presumably proteinaceous mass (figs. 27 and 28) and the deeply infolded and accurately fitted villous portion of the proximal splanchnopleuric yolk sac and of course by a thin ring of exocoelom within the vitelline fold. Although yolk sac villi are profuse on that part of the splanchnopleure facing the placenta they extend but a very short distance beyond the innermost angle of the constriction along only that part of the yolk sac facing the most basal part of the decidua capsularis (fig 24) Whatever the function of this villous region it seems to be associated almost entirely with the outer surface of the trophospongium of the projecting and of the inflected placental margin, i.e. the portion having no contact with decidua and also with the yolk sac contents which tend to collect in this reservoir

The area of the outer constriction is of course continuous with those portions of the uterine lumen not comprising part of the gestation chambers. It is covered by columnar epithelium on its outer or uterine wall surface and by more or less degenerated uterine epithelium on the surface of the pedicle and of the basal portion of the decidua capsularis. Here near term, the capsularis is highly degenerate and extends no farther than the margin of the placental disc

*Establishment of the labyrinth*

The first rudiments of mesodermal villi appear on the placental bulb at 9 mm (figs. 14 and 15) At 12.5 mm they are well formed so that a thin placental labyrinth is established This rests upon a trophospongial zone of generally somewhat greater thickness (figs. 19 and 20)

Figures 14 15 16 and 17 show how the originally smooth chorio-allantoic bulb (fig. 13) is roughened by the outgrowth into the surrounding trophospongium of buds of allantoic mesenchyme covered by chorionic cytotrophoblast. The latter is about two cell layers in thickness. Occasionally its outer layer appears to be syncytial but in none of the material available is it clearly so at any time during placental development *thus it may be that this group of rodents possesses a labyrinth of chorionic cytotrophoblast instead of syntrophoblast*

The villi are soon profusely and irregularly branched and maternal blood channels deriving their blood from the trophospongial channels are trapped between them, thus establishing the labyrinth A rank of large maternal channels is formed along the fetal surface of the labyrinth (figs. 19 and 20) These are undoubtedly supplied by arterial channels penetrating from the basal decidua and it i from them that maternal blood enters the functional trophoblastic tubules of th labyrinth

Another set of even larger and more confluent maternal blood spaces forms at the outer surface of the trophospongium (figs 19 and 20) All maternal blood that enters the labyrinth drains from its tubules through the trophospongial network into these. On the surface of the free placental margin these are bordered externally chiefly by Reichert s membrane and its accompanying endoderm (figs. 20 and 21) On the attached surface next the decidua basalis they are less confluent and drain by numerous connections to the decidual veins (fig 26)

During this period numerous mitoses of trophoblastic nuclei throughout the labyrinth and trophospongium attest to its rapid growth, and to its cellular nature. Growth of the placenta is certainly mainly interstitial at this time. The labyrinth, but not the trophospongium is almost as thick at the edge of the inflected rim as elsewhere and mitoses are no more numerous here which seems to rule out this area as a special growth region although the extensiveness of this inflected rim in later placentas might suggest such a behavior

Attention should be called to the often overlooked fact that in placental morphogenesis an organized fetal structure such as a villus, seldom actually invades organized maternal tissue. However individual trophoblastic wandering giant cells or groups of these may do this. It is of course true that fetal villi do invade uterine glands and crypts for appreciable distances, as in the squirrels, shrews and moles, and especially in the development of the placental cotyledons of ruminants. But even in these cases, concomitant growth of fetal and maternal tissues greatly exaggerates the apparent movement of one element past another At the beginning of this section it is stated that the smooth chorio-allantoic bulb is roughened by the outgrowth of the anlagen of chorio-allantoic villi into the trophospongium. Figures 14 15 18 and 20 show this process but it is obvious when one considers the rapid absolute increase in thickness of both the labyrinth and the trophospongium, that even here between two fetal tissues there is very slight invasion in the true sense The labyrinth is almost completely built up from the true chorionic trophoblast and the allantoic mesodermal structures, with maternal blood being led into its arterial channels and tubules *from* the trophospongium, not by invasion and surrounding of channels already in the trophospongium. Figure 18 represents about the deepest interdigitation of the chorio-allantoic villi and the trophospongium that occurs in this species, not over 0.2 mm

*The definitive placenta and basal decidua*

The placenta of a *Geomys* fetus of 18 mm CR has reached its definitive form and structure (figs. 23 and 24) but not its full size. Figures 25 and 29 show the irregular nature of the mesodermal villi and their characteristic tendency to lateral branching at right angles to their main axes. Since the stem villi themselves are short and closely set the profuseness of short horizontal branches gives the labyrinth an intricacy of pattern which is difficult to analyze microscopically Adding to this difficulty is the very narrow caliber of the trophoblastic tubules (narrower than the fetal capillaries) the thinness of the trophoblast of the placental membrane separating the two blood streams in the functional labyrinth (figs. 30 and 31) and the small and very similar diameters of the nuclei of the trophoblastic mesenchymal, and endothelial cells of this region In short, very characteristic features of the placental labyrinth of *Geomys* are the uniformity and "fineness of its microscopic architecture.

In view of this one would expect a very thin placental membrane, and this is the case. Although it is obviously of the hemochorial type at first, older placentas often show areas of tubule/capillary contact where only one extremely thin layer of cytoplasm is visible between the two blood streams (figs. 30 and 31) This is apparently the fetal endothelium. On this basis the *Geomys* placenta can tentatively be classed as hemo-endothelial, until electron microscopic observation establishes with certainty the presence or absence of a lamella of trophoblastic cytoplasm in these thin areas.

The trophospongium of the mature placenta contains a network of venous channels draining maternal blood from the labyrinth and delivering it to the large veins of the basal decidua. This is of course typical of the trophospongial layer in all species in which it is present. These venous channels are lined by a definite endothelium-like layer separated from the surrounding *trophoblast cells by a PAS* positive basement membrane containing reticulum fibers. The interpretation of this endothelium-like layer is a problem, for as one examines earlier specimens the endothelial" cells become progressively thicker and more and more like the surrounding trophoblast, until finally at the stage of

the allantoic bulb and the beginning of villus formation, only a few maternal blood spaces seem to be lined by other than perhaps somewhat flattened cytotrophoblast cells (figs. 14 15 and 18) Even at the time the labyrinth is first established, definite lining endothelium" is by no means always seen (fig 20) As so often happens in attempting to interpret the morphology of the placenta, here again one is confronted with the problem of whether this endothelium is of maternal or fetal origin. Classical histological techniques will never completely answer these problems sex chromatin determination might, but attempts to apply this method to rodents have been unrewarding.

The surface sinuses of the trophospongium of the free portion of the placenta show the same conditions but their outer surfaces seem to be lined only by scattered trophoblast cells of the bilaminar omphalopleure and in some places directly by the very thin Reichert's membrane. However even these trophoblast cells are often thin and endothelioid (fig 20)

A few large maternal arterial channels pierce the trophospongium centrally carrying blood to the fetal surface of the labyrinth (figs. 26 and 27). In the trophospongium these have a greater diameter and take a straighter and more direct course than the venous channels, and, of course they continue on through the labyrinth which the venous channels do not do. They also have as in most placentas a thick sheath or wall which appears to be composed mainly of modified trophoblastic tissue (fig 27) The trophoblastic nuclei and cells are very much flattened next to the lumen but every transitional cell type between them and the surrounding cells of the trophospongium or labyrinth occurs within three or four cell layers from the lumen. The inner layers are separated by lamellae of fibrin which become thinner and more irregular in the outer layers and finally disappear At no place in the labyrinth or trophospongium do these arterial channels possess a lining closely resembling an endothelium. Only in or just outside the myometrium does an apparently true endothelium occur and even here at least the inner portions of the arterial walls appear to be made up of modified trophoblast probably homologous to the trophoblastic giant cells which ensheath the placental arteries in the decidual region in many other rodents In fact, it may be that much of the "endothelium of this area in *Geomys* is actually modified trophoblast, comparable to the endovascular giant cells of the hamster (Orsini '54)

A detailed study of the nature and origin of the vessel walls in the placenta of *Geomys* was not attempted because of the relatively great difficulty in differentiating between cells of fetal and maternal origin in this species About all that can be done without an undue amount of effort, is to interpret what one sees here in the light of observations on other species, such as the hamster where the origin and migration of trophoblastic cells into corresponding situations is clearer

The changes in the decidua basalis and adjacent persistent portion of the capsularis are complex and without histochemical study are difficult to assess as to their significance. Therefore only a cursory description is attempted here.

At first the decidua basalis consists of two major zones (figs. 5 and 7) an outer two-fifths composed mainly of highly vacuolated decidual cells and containing relatively few large vessels and an inner three-fifths containing many dilated vessels along its junction with the former and characterized by compacted decidual cells with homogeneous acidophilic granular cytoplasm Many of these cells are binucleate and a few show three to four nuclei. In this zone directly opposite the open epamnion and immediately beneath the still intact uterine epithelium is a large area of extravasation containing many degenerating stromal cells. There are no gland remnants in the decidua for the *Geomys* uterus is aglandular

By the time of the obliteration of the epamnionic cavity and adjacent uterine lumen, and of the attachment of the allantois trophoblast cells have invaded the area of extravasation and are beginning to convert it into the first trophospongium (fig 12) The earlier zonation of the basalis is lost apparently by the disappearance of most of the vacuolated cells and

an increase everywhere of the nonvacuolated types. Figure 11 shows remnants of the zone of vacuolation.

With the attainment of the placental hillock (fig. 13) trophospongium has spread from the center to cover half of the radius of the disc of basal decidua, and forms a zone about one-half the thickness of the basalis. From this period on to at least the time of the 18 mm CR embryo (fig. 23) the zonation of the basalis is the reverse of the early period that is the outer zone tends to be compact with nonvacuolated cells and the inner zone next to the trophospongium tends to be loosely organized and contains many large vacuolated decidual cells. The large fluid-filled intercellular spaces of this area probably arise in part from degeneration of groups of decidual cells. These spaces may facilitate infiltration of the area by trophoblast cells at the maternal surface of the trophospongium. These no doubt correspond to the layer of trophoblastic giant cells which in other rodents so commonly lies between the trophospongium and the decidua basalis.

From 18 mm CR on to term (figs. 27 and 28) the basal decidua is of very loose and irregular composition, even near the myometrium. Compact areas still occur (fig 26) especially in the form of the thicker sheathes of arteries and the thinner ones of veins. Between these a loose framework of irregular and radiate cells of stromal origin, and prominent intercellular spaces forms a background occupied by a great variety of elements. These include intact and fragmenting decidual cells scattered single or groups of trophoblastic cells, rather characteristic oval cells with homogeneous eosinophilic cytoplasm and eccentrically located nucleus which are presumably a form of plasma cell lymphocytes and occasional polymorphonuclear leucocytes, and a great number and variety of unidentified cells and cellular debris. There is no obvious specialized zone of separation for the placenta at birth. Although we have no uteri that are certainly immediately post partum ones it is probable that separation of the placenta occurs very close to the myometrium.

## THE CIRCULATION WITHIN THE LABYRINTH

Although no injections of the circulation were made, the structure and arrangement of the maternal and fetal vessels of the labyrinth show quite clearly that this placenta has the typical fetal-maternal counterflow arrangement. However the length and exact pattern of the trophoblastic tubules and fetal capillaries is not entirely clear

The mesodermal villous cores are very closely spaced and complexly branched (figs 25 and 29). Whether these branches and hence the fetal capillaries and trophoblastic tubules chiefly take a course perpendicular to the placental surface or are horizontal to it, i.e. at right angles to the villous stems, has not been determined. In some areas of some later placentas the first appears to be the case but in other areas often of the same section the second situation appears to prevail. Only good colored vascular injections can demonstrate the actual pattern, and they are not available.

In a placenta with such a thin separation membrane one would expect relatively short "functional" capillary and tubule contacts. Presumably natural selection should have provided that the maternal and fetal blood streams remain in physiological contiguity only far enough to assure effective interchange in the time needed for the respective units of blood to traverse the area of contiguity The greater the interchange efficiency of the placental separation membrane, time-wise, the shorter would the length of the fetal capillary/maternal tubule units need to be. The evidence indicates that thin membranes in general make physiological transfers more quickly than thick ones, hence *Geomys* should possess relatively short exchange units. *Geomys* does have a thin placental membrane or "barrier" and relatively short areas of contiquity of maternal tubules and fetal capillaries. This is also true of all other Geomyoidea placentas so far studied.

## DISCUSSION

(Since no general discussion and summary were included in the first paper (I) of this series, which dealt with the female tract and implantation in *Geomys* (Moss-

man and Hisaw '40) they are included here.)

The unusually regular conical mass formed by the coiled isthmus of the *Geomys* oviduct has been found to be characteristic of all other Geomyoidea studied (*Dipodomys*, *Microdipodops*, *Perognathus* and *Thomomys*). This is another example of the relative conservatism typical of mammalian reproductive tract characters (Mossman, '53).

It was stated in I that the uterus of *Geomys* is probably duplex. New material shows that the uterus is duplex in both *Geomys* and *Thomomys*.

Fertilization obviously takes place in the ampulla, as in most other mammals. Numerous sperm may penetrate the zona pellucida. They often penetrate the polar bodies, a phenomenon not often described but which has little significance except to indicate a close physiological similarity between the polocytes and oocytes. Embryos enter the uterus as morulas of about 20 blastomeres.

Free uterine morulas of about 85 cells with intact zona pellucida seem to have not yet reached their site of implantation. Compared to rodents with more specialized membranes, such as the mice, rats and guinea pig, the number of blastomeres in the *Geomys* morula is very high. The more primitive groups, such as the squirrels, also have a comparably high number. Thus, in this respect *Geomys* appears relatively primitive.

The earliest implanting embryo had about 128 cells, but no blastocyst cavity. This is somewhat out of line with other rodents, for both the more primitive squirrels and the more specialized murids and caviids (guinea pig and porcupine) show no signs of cellular invasion of the endometrium until after the inner cell mass has separated. It indicates an early implantation relative to embryo development, a condition which seems to be correlated with the more specialized rodent groups.

The relatively large size of the *Geomys* blastocyst at the time it definitely becomes interstitial (I, figs. 2 and 17) and the tardiness of its inversion (I, figs. 3 and 25) indicates clearly the intermediate position occupied by this form, a position between the primitive method of membrane development in the rabbits and squirrels and the specialized conditions of the mice, rat, guinea pig and porcupine. The presence of an open epamniotic cavity and definite but small amniotic folds (I, figs. 3, 29, 30 and 32) are also distinctly intermediate characters.

It is well to compare the gross relations of the decidua in rodents with those of man, as there are major differences. In man the placenta forms on the side of the blastocyst that first contacts and attaches to the endometrium, in rodents it forms on the side opposite the first attachment. Hence in man the basal decidua is at the region of implantation, but in rodents it is opposite this region. As the capsularis forms around the human chorionic vesicle it is from the first attached only at the margins of the implantation area, that is, at the ring of junction of the decidua basalis and parietalis. In rodents it is likewise attached around the region of first implantation, but this is not the region where the basalis forms. In its early period the rodent capsularis has free "edges" projecting into the uterine lumen at each end of the implantation chamber. These, together with the hypertrophying basal endometrium, constrict the lumen, so tending to isolate each implantation chamber from the intergestational segments of the lumen. In the more specialized rodents these "edges" soon disappear by what may be called growth constriction or encroachment upon the lumen, which results in its obliteration at each end of the chamber; thus the capsularis becomes *secondarily* continuous with the "ends" of the basalis, a very different sequence of events from that in man. Laterally, however, the "edges" never develop, the decidua of this area is always continuous with the area of the basalis, thus a zonary band of "fixed" decidua, which includes the future basalis, extends completely around the uterus at the center of each gestation loculus. To each side of this band the two halves of the "free" decidua capsularis are attached.

Rapid growth of the "edges" and of the basalis soon results in the formation of two bulging thin hollow hemispheres of capsularis, each encircling an end of the implantation chamber and extending into the dilated uterine lumen. In the central

zone of the implantation chamber as mentioned above, the decidua is directly attached to the myometrium. This attachment is broad at the base of the placenta, the basalis. Laterally from each side of the basalis, the attachment tapers into two narrow bands which meet at the antimesometrial pole, where attachment first occurred. Thus the attached decidual band is signet ring-shaped the broad or signet portion of this band being the basalis, while the narrow part, after the placenta forms, is somewhat comparable to the parietal decidua of man, and has been so named. However in a sense the rodent parietalis is also "basal" decidua, since, at least the antimesometrial part of it lies deep to the first attachment. Furthermore the endometrium of the gestation sac facing the outer surface of the extensive capsularis is also comparable to the human parietal decidua. However in rodents this area undergoes very little decidual change, and hence it is not reasonable to speak of it as decidua. The terminology of the deciduas of rodents is defensible on grounds of homology with man and other forms in the case of the basalis and capsularis. The designation of only the narrow band of the parietal uterine wall as parietalis and of the nondecidual portion of the parietal wall as simply parietal endometrium is justifiable on the grounds of the respective presence and absence of true decidual tissue and on the necessity for distinguishing between these two portions of the parietal endometrium.

It is interesting to note that there are animals such as the hedgehog *Erinaceous* which implant antimesometrially as do rodents, but which form the placenta at this location and hence have decidual relations comparable to those of man. Also, at least one megachiropteran bat *Pteropus* has mesometrial implantation and a mesometrial placenta, hence decidua again comparable to those of man. In other words if the placenta develops at the area of implantation decidual relationships will be most comparable to the human but if the placenta forms elsewhere these relationships must be different.

The inverted yolk sac of *Geomys* is like that of *Thomomys* and *Perognathus* in having well developed villous processes on its antimesometrial hemisphere and in the fact that many of these are hollow vascular evaginations rather than true villi. These latter are more elaborately developed and apparently more persistent in *Thomomys* and especially in *Perognathus* (Nielson, 40) In *Dipodomys* and *Microdipodops* on the other hand we have seen only true villi, and these only on the mesometrial portion adjacent to the placenta. This is probably a more primitive condition, as it is characteristic of the Sciuridae. Very probably these differences in specialization of the inverted yolk sac have physiological significance This is another of a multitude of striking variations in placental morphology the functional significance of which is completely obscure.

The history of the capsular decidua wherever it occurs, is no doubt correlated with the nature and function of the fetal membranes apposed to it. In all cases so far known, the capsular decidua degenerates long before parturition, and thus allows functional contact of the adjacent membranes with the parietal endometrium.

In lagomorphs and rodents extraembryonic mesoderm never spreads beyond the embryonic hemisphere of the blastocyst and of course the exocoelom extends only as far as the mesoderm. In the lagomorphs and more primitive rodents (mountain "beavers and squirrels) approximately the abembryonic one-half to three-fourths of the spherical blastocyst wall remains as bilaminar omphalopleure at the time of greatest extension of the mesoderm. In the more specialized forms (mice and guinea pig) the mesoderm is far more restricted and hence a far greater portion of the sphere is bilaminar But in these, especially the guinea pig, this bilaminar portion itself tends to become rudimentary with little or no differentiation even of its endoderm and in the guinea pig it actually disappears as a distinct blastocyst wall while the blastocyst is still very minute and in the process of nidation.

As the result of this restriction of extraembryonic mesoderm it is only in the primitive forms that an appreciable ring of area vasculosa or chorio-vitelline placenta develops on the outer surface of the chorionic vesicle And when this is ended

Two-cell embryos are found in the transitional region between ampulla and isthmus. Eighteen to twenty cell embryos are in the lower isthmus.

Morulas of about 85 nuclei and with intact zona are still free in the uterine cavity Generalized predecidual change has occurred at this time throughout the endometrium with no local differences to mark the location of the morulas hence it is believed that they have not yet reached their definitive location.

Implantation is antimesometrial. A morula of about 128 cells has begun to implant. Later blastocysts are largely interstitial in position, but with the broad area of the incipient amnio-embryonic area exposed to the uterine lumen. The decidua capsularis forms in the same manner as in other rodents

Amniogenesis is by folding but an open *epamnionic cavity remains.*

Inversion of the yolk sac is completed at the five somite stage just prior to establishment of its circulation and at about the time of the appearance of the allantoic anlage

The narrow uterine lumen at each end of the implantation chamber is closed during the early limb bud period thus making the capsular decidua complete However by midterm most of the antimesometrial capsular decidua has atrophied.

The basal decidua is relatively massive and forms the signet of a signet ring shaped zonary band completed by the narrow decidua parietalis surrounding the central region of each gestation sac.

During limb bud formation true villi and hollow villus-like evaginations of the *antimesometrial hemisphere of the* inverted yolk sac occupy pits at first lined by the bilaminar omphalopleure in the well vascularized capsular decidua. Thus a complex inverted yolk sac placenta is formed. The capsularis is by this time heavily invaded by trophoblastic giant cells. This area of the capsularis soon disintegrates in approximately the following sequence degeneration of all decidual cells and the bilaminar omphalopleure; atrophy of maternal vessels atrophy of the giant cells Inversion is then complete the villous splanchnopleure having direct contact with the uterine contents and the parietal endometrium Meanwhile true villi have developed on the mesometrial hemisphere. These do not indent the capsularis or placenta and unlike those of the opposite hemisphere which become flattened and largely atrophic in late pregnancy these persist to term

There is no allantoic vesicle outside the body of the embryo.

The only true chorion is the small area roofing the epamnionic cavity In the early limb bud period the allantois contacts it and converts it into chorio-allantois.

Rapid proliferation of "träger" trophoblast at the time of chorio-allantoic contact produces a localized hillock with a high incurving rim surrounding the allantoic bulb. This results in the development of a placental disc with broad inflected margins typical of all Geomyoidea so far studied.

The mesometrial portion of the bilaminar omphalopleure with its Reichert's membrane clothes the entire free surface of the placenta, except that area immediately surrounding the attachment of the umbilical cord, which is covered by allantoic mesoderm.

The labyrinth is at first hemo-chorial and later so far as can be ascertained by light microscopy is hemo-endothelial Both the maternal tubules and fetal capillaries of the definitive period are very fine the trophoblast has unusually small nuclei and is always very thin

No vascular injections were made, but there is every evidence that a typical maternal/fetal counterflow system is present.

The development and morphology of the fetal membranes of *Geomys* is distinctly intermediate between the primitive and highly specialized rodent types.

## LITERATURE CITED

Hamilton, W J J D. Boyd and H W Mossman 1962 Human Embryology Third ed. W Heffer and Sons Ltd., Cambridge and Williams and Wilkins, Baltimore

Hillemann, H H., and Alta Gaynor 1961 The definitive architecture of the placentae of nutria, *Myocastor coypus* (Molina) Am J Anat *109* 299–317

Mossman H. W 1937 Comparative morphogenesis of the fetal membranes and accessory uterine structures. Contrib. Embryol Carnegie Inst 26 129–246.

——— 1953 The genital system and the fetal membranes as criteria for mammalian phylogeny and taxonomy J Mammalogy 34: 289–294.

——— 1957 Endotheliochorial placentation in the rodents, *Castor* and *Pedetes* Proc. Zool. Soc., Calcutta, Mookerjee Memorial Volume 183–189

Mossman, H. W and C. H. Conaway 1954 A new type of placentation demonstrating the phylogenetic and taxonomic significance of the fetal membranes. Anat. Rec., *118* 431–432.

Mossman, H. W and F L. Hisaw 1940 The fetal membranes of the pocket gopher illustrating an intermediate type of rodent membrane formation. I. From the unfertilized egg to the beginning of the allantois. Am. J Anat., 66 367–391.

Mossman, H W and A
The fetal membranes pı
thirteen-striped grour squı
64 59–109

Nielson, P ul E 1940 The fe
the kangaro rat, *Dipod*
tion of the phylogeny of the G
Rec., 77 10 127

Orsini, M. W 19 4 The t bo
and endovasc ar cells asoc
nancy in the h mster, Cri
J Anat., 94 273 331

Perrotta, Carmie A. 1959 Fetal
the Canadian porcupine, *E ethi*
Am. J Anat., *104* 35–60.

T bbutts, F D and H H. Hillemann
development and histology of
placentas. J Morph., 105 317 36

## PLATE 1

### EXPLANATION OF FIGURES

5 Sagittal section of gestation sac at neural groove tage The vascular segment of the yolk sac (iy) i fully inverted. The epamnionic cavity (ec) is wide open and partially filled with epithelial debris. The dark region of the mucosa opposit the epamnionic cavity is the area of extravasation (ex) The uterine lumen is narrow but still patent through the decidual area. Compare with figures 4 A and B. (Lee) 333 slide 14 × 9.5

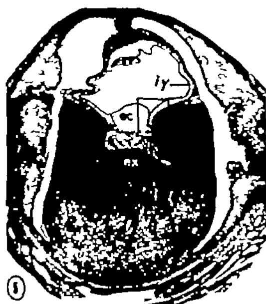
6 Area comparable to rectangle in figure 5 showing the true chorion (c) roofing the epamnionic cavity; the bil minar omphalopleure (bl); and a portion of the inverted yolk sac splanchnopleure with the marginal blood island destined to become the sinus terminali (st) ep uterine epithelium; R, Reichert s membrane; I, are of invading small trophobl st cells corresponding to the are of primary trophobla tic giant cell formation f more primitive species (Sciuridae) and to the area of the triger of higher groups (Hystricomorpha). Secondary trophobl stic gia t cells form from all of the rest of the attached bilaminar omphalopleuric trophoblast, and eventually oc cupy most of the capsular decidua. Compare with figure 4 A. (Lee) 333, slide 14 × 67

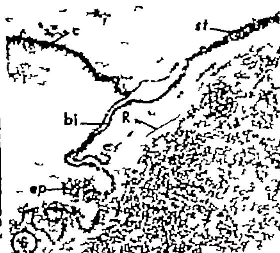
7 Sagittal section of gestation sac t early limb bud tag showi g thinning of decidua psularis thick true horion ( ) roofing the much reduced epamnionic cavity and persistent terine lumen (l) (Lee) 339 slide 19 × 9.

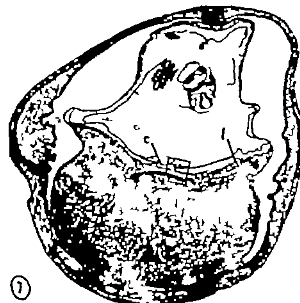
8 Are comparable to rectangle in figure 7 howing greatly thickened true chorion roofing epamnionic c vity and the hypertrophied trophobl st (t) of bilaminar omphalopleure. The primary trophoblastic in ding cells, which are homologou to giant cells of other rodent groups, arise from this region of the bilaminar omphalopleure st sin terminalis d cellular debris of epamnionic c vity; ex compact area of extravasation. (Lee) 339 slide 19. × 93

9 Interior view of early gestation sac from same terus figures 14 and 16 (embryo 9.5 mm CR) looking toward placental hillock (p) showing decidu capsularis (dc) with attached yolk sac on which it ascula network i visible nd decidua parietalis (dp) Retouched to m ke f at res more clear 31 × 2.

10 Interior iew of timesometrial portion of gestation sac hown in figure 9 showing ttachment of yolk stalk. Retouched for gre ter larity 31 2


ly
ec
ex
5


c
st
bl
R
ep
6


c
l
7


st


p



## PLATE 2

### EXPLANATION OF FIGURES

11 Sagittal section of gest tion sac containing an embryo of about 6 mm CR, showing first contact of the allantois (al) with the chorion. (Lee) 359 slide 48. × 7

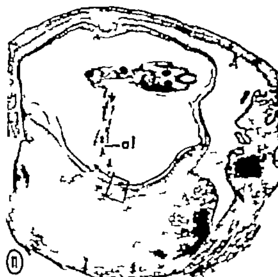
12 Area comparable to rectangle in figure 11 showing collapsed epam nion; close contact of chorionic trophoblast with cellular debris (d) of uterine lumen; and masses of cytotrophoblast (cy) (corresponding to primary giant cells of träger of other rodents) invading mesometrial extravasation area of the basal decidua. (Lee) 359 slide 48 × 114

13 Sagittal section f gestation sac with an embryo of bout 9 mm CR, showing the placental hillock before formation of villi; the broad thick zone of early trophospongium (t) formed by the invading cytotrophoblast; the allantoic stalk (al); and the yolk duct (yd) (Lee) 369 slide 50 × 7

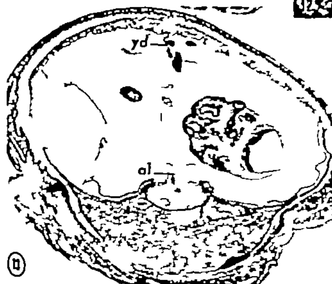
14 Area from the side of placenta from the same uterus s the one shown in figure 16 showing some of the allantoic villi bro ken way from their covering trophoblast; the beginning indentation of the trophospongium (t) by the latter; the matern l blood spaces of the trophospongium (m); and the endoderm (en) clothing the surface of the trophospongium. This endoderm rests upon very thin Reichert membrane which is not visible in the figure 31 slide 113. 100.

15 Detail of one-half of the placenta with djacent membranes at pproximately the tage shown in figure 16. Area of villus anl gen ( ) trophospongium (t) with maternal blood spaces (m); inus terminalis (st); yolk sac villus (yv); yolk sac ca ity (y); endoderm of bilaminar omphalopleure (en) 15 slide G × 62.

16 S gittal section of gestation sac from same uterus a figures 9 nd 10 nd slightly older than that of figure 13 showing placental hillock with anlagen of villi and the now broader nd thicker zone of trophospong um (t) 31 slide F × 6.


al
11




yd
al


st
yv
y
en


m


15

## PLATE 3

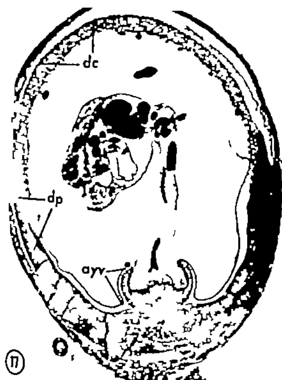
### EXPLANATION OF FIGURES

17 Slightly oblique cross section of gestation sac of embryo of about 10 mm CR approximately the same age as that of figures 13 15 and 16 showing the trophospongial and cytotrophoblastic tissue (lighter shade) comprising the bulk of the placental hillock and penetrating deeply into the decidua basalis. Approximately the mesometrial half of the sac is cut through the decidua parietalis (dp) and the opposite half through the adjacent capsularis (dc) Note the numerous yolk sac villi and diverticula of the antimesometrial hemisphere permeating the decidua capsularis the area of early yolk sac villi (syv) adjacent to the placenta and their complete absence from a wide band between these two areas. (Lee) 364 slide 104 × 7

18 Detail of a small portion from the side of the placenta shown in figure 17 showing the early villi (v) penetrating the trophospongium (t) (Lee) 364 slide 104 × 300.

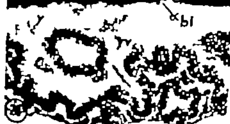
19 Sagittal section of gestation sac with an embryo of 12.5 mm CR showing the flattening of the placental disc and the incurving of its margin to form the characteristic pile te shape There is a conspicuous layer of vessels on the inner surface of the early labyrinth These vessels are mainly maternal arterial channels (ma) from which trophoblastic tubules carry the blood through the labyrinth to the channel in the trophospongium. These in turn empty the venous blood into a prominent rank of venous channels (mv) along the outer surface of the trophospongium. These unite and join the main trunks of the decidua basalis. 32, slide 0 × 5.

20 An area corresponding to the rectangle in figure 19 showing in more detail the maternal arterial channel (ma) the mesodermal villi (v) the early labyrinth (lb) the trophospongium (t); and the outer venous channel (mv) walled in part by the bilaminar omphalopleure (bl) and Reichert's membrane the yolk sac cavity (y) and portion of the mesometrial villous segment of the vitelline splanchnopleure (y ) 3* slide C Approx 150


dc
dp
ayv
17




mu
lb
mv
bl



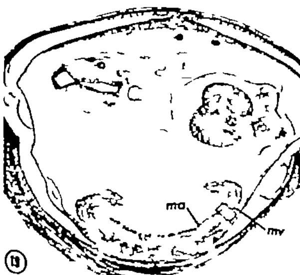

ma
mv
19

PLATE 4

EXPLAN TION OF FIGURES

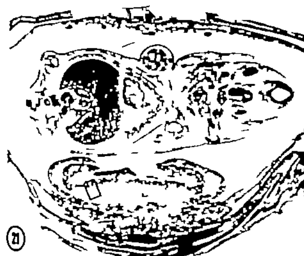
21 Sagittal section of gestation sac containing a fetus f 14 mm CR, having digits still webbed for about two-thirds of their length. Compared with figure 19 the labyrinth is thicker as are the trophospong i m and basal decidua, and the margins are more flattened against the disc. 33 slide E. × 6.

22 Rectangular are indicated on figure 21 showing the allantoic mesodermal villi (v); the labyrinth (lb); and the trophospongium (t) fc fetal pillaries; mt, maternal tubules; ma maternal arterial channel; mv maternal venous channel. 33, slide E. × 100.

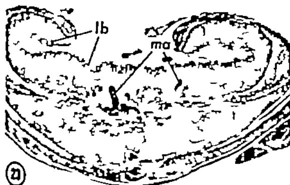
23 Sagittal section f the placent of n 18 mm CR fetus showing the well est blished labyrinth (lb) and portion of the maternal arterial channels (ma) that carry maternal blood to the fetal surface of the labyrinth. 35 slide C. × 6.

24 Right half of figure 23 enlarged. am allantoic mesenchyme with fetal vessel ; lb, labyrinth; t trophospongium; g, area corresponding t giant cell layer of other rodent placentas. 35 lide C. × 13.

25 Detail of labyrinth (lb) and inner trophospongium (t) of placenta from same uterus as figures 23 and 24 Note the trunk of the mesodermal villi ( ) from which the branch villi radiat most of them in roughly horizontal direction Note also the narrowness of the areas between the trunks allable to functional branch villi hence the relative shortnes f the later In sense thi placenta ex hibit primitiv type of lobulation 35, slide B. Approx. × 100.


21


mt
fc
mv
22


lb
ma
23


am



## PLATE 5

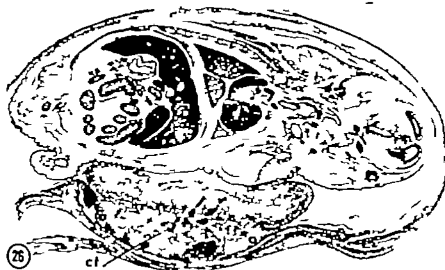
### EXPLAN TION OF FIGURES

26 Sagittal section of the gest tion sac of l te fetus, 30 mm CR show ing the flattened pile te shape of the placenta; its relatively thin labyri th and trophospongium; the thick decidua basali with its mottling (lighter areas) of invading cytotrophoblast (ct) and of edematou area of probable traumatic origin ( ) at the right and left. Note the almost complet disappearance of the decidua apsu- laris and of the ntimesometrial villous segment. Two large maternal arterial hannel can be seen penetrating the trophospongium and labyrinth. 28 slide 10. × 4

27 Sagittal section f placenta at nearly full term. Note the relatively uniform thickness of the labyrinth (lb) both in the main disc nd the incurved margins. A small rim of decidua c psularis (dc) till persist 26, slide F × 7

28 Detail of the right edge f the section shown in figure 27 A very thin Reichert membrane (R) till borders the trophospongium. Not also the amorphous coagul m occupying the yolk sac cav ty (y) and ften pparently concentrated (darker m sses) in the immediate neighborhood f the yolk sac villi (yv) and between them. 30 slide F × 8.

29 Obliquely horizontal section of a portion of the l byrinth f l t fetal tage 35 mm CR, showing the profuse lateral br nching nd interdigitation of the mesodermal allantoic villi ( ) 16 slide L- 75.


26
cf


lb
dc
27


y
R
yv


29

## PLATE 6

### EXPLANATION OF FIGURES

30–31 The labyrinth of an early fetal stage, showing the trophoblastic tubules (mt) filled with maternal red blood corpuscles of uniform size; and the fetal capillaries (fc) with the much larger nd more irregular fetal corpuscles, some of which are nucleated Note the thinness, even at this relatively early stage of the placental membrane (arrows) which usually seems to be double but in some places appears to consist of only a single cytoplasmic layer 37 slide C. × 400.

32 Uterine wall ( ); decidua parietalis (dp); and c psularis (dc) at the neural groove stage shown also in figures 4A and B and 5. The bilaminar omphalopleure (bl) is attached to the decidua, and invading trophoblast cells are present, but their small size makes them difficult to recognize. Notice that the uterine epithelium on the outer surface of the capsularis ha already degenerated. (Lee) 333, slide 8. × 66.

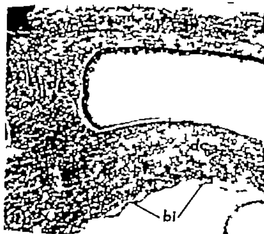
33 Uterine wall, decidua parietalis and capsularis at the late limb bud stage 9 mm CR, corresponding to figures 4C and 13. The large cells of the decidua are trophoblastic giant cells. These are much smaller than homologous cells in many other rodents. Mo t maternal decidual cells have already degenerated or are in the process of doing so, as is clear at the junction f the parietali and apsularis. Maternal vessels (mc) still mai tain their integrity Also shown is part of pit (p) lined by Reichert' membrane (R) and few adhering endoderm cells, and occupied by portion of yolk sac villus. 15, slide G × 66

34 Uterine wall decidua parietalis and capsularis at late fetal stage 30 mm CR, comparable to figures 4D and 28 showing the degeneration and breaking up of the trophoblastic cells of the capsularis. Intact maternal vessels are no longer found in this are of the capsularis, and there seems to be some leakage of blood into the uterine cavity from the vessels of the parietalis. This blood and the cellular debris can come into lose contact with the inverted splanchnopleuric yolk sac, since the bilaminar omphalopleure and Reichert' membrane no longer exist in this area However it is also true that the inverted yolk sac is relatively atrophic for its villi are small, compressed, nd scarce and it vessels are also small and widely separated. 21 slide G × 66.

35 Uterine wall decidua parietalis (dp) and capsularis (dc); yolk sac splanchnopleure with one remnant of illus (yv); yolk stalk (ys) and amnion ( ) of full term fetus 33 mm CR, comparable to figure 26 showing the atrophic nature f the decidua and membranes. Some trophoblastic giant cells (gc) still contain uclei. 16 slid II × 66

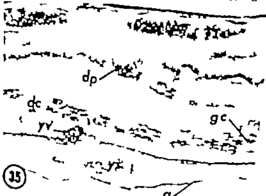



m
31


d
bl


mc
R
p
33


34


dp
gc
yv
gc
35
a

# Teratogenic Effects of Hypoglycemic Treatments in Inbred Strains of Mice[1]

MORRIS SMITHBERG AND MEREDITH N RUNNER
*Department of Anatomy University of Minnesota, Minneapolis Minnesota and Roscoe B Jackson Memorial Laboratory Bar Harbor Maine*

Congenital malformations have been produced by subjecting pregnant animals to diversified agents and procedures at various times during gestation. It is not unreasonable to presume that many of the treatments alter embryonic development by affecting the metabolism of the mother and/or embryo The reader is referred to the recent excellent review of this subject by Kalter and Warkany ('59)

Insulin, in concentrations which produce shock, has produced congenital malformations in the mouse (Smithberg et al. '56) and in the rabbit (Chomette '55; Brinsmade et al. 56) The sulfonamide tolbutamide produced some malformations in the rat (Tuchmann-Duplessis and Mercier Parot, '60) and in mice (Smithberg, '60) Fasting of the pregnant mouse for 16 to 30 hours resulted in congenital deformities (Runner '54 Runner and Miller '56 Miller '62)

The purpose of the present experiments was to determine (1) whether or not the three hypoglycemia producing treatments cause similar defects quantitatively and qualitatively within a single inbred strain of mice and (2) whether or not the various treatments produce similar defects among three strains of mice.

Toward this end each of three samples of mice of strain 129/Rr were subjected to one of the three hypoglycemic treatments; each of two lots of mice from a second strain, BALB cRr were given either insulin or tolbutamide and one lot from a third strain, C57BL/6J were treated only with tolbutamide. In this manner it was possible to compare the effects of tolbutamide upon mice of three strains; to compare the effects of insulin and tolbutamide upon mice of two strains; and to compare the effects of fasting within a single strain of mice. A second phase of the investigation was devoted to attempts to reverse the effects of insulin or tolbutamide by the administration of nicotinamide. The choice of nicotinamide was prompted by the experiments of Landauer ('48) who showed that the incidence of insulin-induced rumplessness following treatment at 24 hours incubation and that of micromelia after injection of insulin at the 96-hour stage was reduced by providing embryos with supplementary nicotinamide (Landauer '48 Landauer and Rhodes, '52) Nicotinamide protected against some of the teratogenic effects of insulin in the chick since some of the phosphopyridine nucleotides apparently play an important role in the morphogenesis of the chick embryo Similar experiments in the mouse seemed worthwhile.

## MATERIALS AND METHODS

Prepuberal and adult females of inbred strains 129/Rr BALB/cRr and C57BL/6J (B) were used They were mated to adult male mice of their respective strains.

### *Experimental animals*

*Prepuberal mice* Prepuberal females weighing 12–16 gm and about 30–35 days old were induced to ovulate and to mate following intraperitoneal injections of gonadotropic hormones according to the method described by Runner and Gates ('54) and Smithberg and Runner ('56) Beginning two days after mating subcutaneous injections of 1 or 2 mg progesterone[3] were given daily to insure main-

[1] This investigation was supported, in part, by PHS research grants RG-6 11 and RC-4437 from the National Institutes of Health, Public Health Service.

[2] Current address Department of Biology University of Colorado.

[3] Proluton, brand of progesterone was contributed through the courtesy of the Schering Corporation, Bloomfield, New Jersey

tenance of pregnancy (Smithberg and Runner '56) One day before term or at term i e on day 18 or 19 *post coitum* pregnant females were killed and fetuses were removed.

*Adult mice* Adult mice of strain 129 in spontaneous estrus were used in the ex periments on fasting and were carrying their third litters at the time of treatment. Adult females of the other strains were primigravid at the time of treatment either they mated spontaneously or they were induced to ovulate and to mate fol lowing injections of gonadotropic hor mones as indicated below

Females in spontaneous estrus after be ing placed into the cages of males in the late afternoon were observed for the pres ence of the copulatory plug on the follow ing morning The day of the observation of the copulatory plug was designated as day 0 of gestation.

*Induction of estrus in adult females*

Many of the adult females, particularly those of strains BALB/c and B were in duced to ovulate by a procedure similar to that described by Edwards and Fowler ('59) The females were given intraperi toneal injections of 6 I U of Pregnant Mares Serum and 4 I U of Human Chorionic Gonadotropic Hormone[4] spaced about 45 hours apart and were then in troduced into the male s cage Two days following mating the female mice each received a daily injection of 2 mg proges terone to insure that a larger proportion would carry fetuses to term (Runner '59a)

*Treatment procedures*

All treatments were performed on the ninth day of gestation

1 *Fasting Strain 129* Females were deprived of food for 24 hours following the technique described by Runner and Miller ('56) and by Runner ('59b) Food was removed on the morning of the ninth day and was returned the morning of the tenth day Water was always available Supplementary progesterone was not given to the adult mice in these experiments

2 *Insulin Strain 129 Strain BALB/c* Mated females received a single intraperi toneal injection of 0 1 unit of protamine zinc insulin (4–5 units/kg) in 1 ml dis tilled water Distilled water alone was given to the control animals Food but not water was withheld for six hours after treatment

3 *Tolbutamide Strain 129 Strain BALB/c Strain B* Females received ap proximately 1 mg/gm body weight of tol butamide (sodium salt) in a single in traperitoneal injection Prepuberal mice received 15 mg and adult mice received 20 mg tolbutamide in 0 5 ml 0.9% NaCl solution

4 *Nicotinamide All strains* An in traperitoneal injection of 10 mg nicotin amide (0 4–0 5 gm/kg) in 0 5 ml 0 9% NaCl solution was administered immedi ately after the injection of insulin or tol butamide Nicotinamide alone was given to other animals in control experiments.

*Autopsy procedures* All pregnant fe males were killed on day 18 or 19 *post coitum* Fetuses were removed from uteri and observed for obvious skeletal defects such as exencephaly or defective ribs The fetuses were fixed in 95% alcohol for 24 hours. Following maceration in 2% po tassium hydroxide the skeletons were stained with alizarin red and cleared in gradual changes of varying proportions of potassium hydroxide and glycerin. The skeletons were stored in pure glycerin until detailed observations were made for skel etal defects. No detailed observations were made on the soft internal tissues.

## RESULTS

*Physiologic effect on the pregnant mothers*

Although these experiment were ulti mately concerned with congenital malfor mations in the fetus a few remarks on the physiologic and lethal effect of the treat ments on the pregnant mouse are indi cated.

Only treatments employing insulin or tolbutamide singly or in combination with nicotinamide produced any obvious phys iologic effect on the mother Blood sugar

[4] Pregnant Mares Serum and Human Chorionic Gonadotropin was generously supplied by Dr A F Grieve of Ayerst Laboratories Montreal

Protamine zinc insulin, Eli Lilly and Company Indianapolis Indiana

Orinase brand of tolbutamide (as sodium salt), kindly supplied by the Upjohn Company Kalamazoo, Michigan

Nicotinamide Eastman Chemical Rochester New York

levels of some females were found to be abnormally low e.g., from a pretreatment average level of 171 mg per cent, sugar levels decreased in three to four hours following an injection of tolbutamide plus nicotinamide, to an average level of 59 mg per cent.

After receiving insulin or tolbutamide the females of all strains behaved in a similar, characteristic fashion. In about half an hour the animals became relatively motionless yet hypersensitive to tappings on the metal cage. They were lethargic for two to three hours and appeared quite helpless, occasionally jerking as though in convulsion. At the end of six hours most of the animals had spontaneously recovered and the food that had been withheld at the start of the treatment was returned to the cage. Generally the effects of tolbutamide were not as prolonged as those of insulin.

Data relating the lethal effects of the various treatments on mothers and litters are shown in table 1. It will be observed that treatments which included insulin or tolbutamide singly or in combination with nicotinamide produced 3 to 42% fatalities. All other treatments produced no deaths. The data in table 1 may be made most meaningful by considering one strain at a time relative to (1) effects of insulin as compared to those of tolbutamide and (2) effects of the addition of nicotinamide to insulin or to tolbutamide treatments.

*Strain 129.* The frequency of deaths produced by insulin or tolbutamide alone were approximately the same 17% and 23% respectively. The addition of nicotinamide to insulin increased the frequency of deaths to 42%. On the other hand, no such combined effect was found when nicotinamide was given with tolbutamide.

*Strain BALB/c.* The lethal effect of tolbutamide in this strain was considerably higher than that of insulin, 18% compared to 3%. The frequency of deaths decreased to 8% when nicotinamide was given in conjunction with tolbutamide while insulin plus nicotinamide increased the per cent of deaths to 25%.

*Strain B.* Tolbutamide produced 29% deaths which was approximately the same frequency found in the other strains of mice following the injection of this agent. Nicotinamide did not modify the lethal effects of tolbutamide. Insulin was not given to animals of this strain.

In summary it was found that tolbutamide produced a substantial proportion (18–29%) of deaths in the three strains. Deaths produced by insulin in the two strains tested strains 129 and BALB/c were 3 and 17% respectively. Nicotinamide consistently increased the lethal effect of insulin in strains 129 and BALB/c while it tended to decrease the adverse effect of tolbutamide in these same two strains of mice. Nicotinamide demonstrated no ameliorating effect on lethality of tolbutamide in strain B.

*Effect of treatment on litter production.* The per cent of mothers surviving treatments and their subsequent litters at term are also shown in table 1. The purpose of the tabulation was to evaluate whether the treatments caused any untoward loss of whole litters. Although there was considerable variation within and among strains ranging from 23–90% of mothers

TABLE 1

*Effect of treatments upon survival of mothers and litters in three inbred strains of mice*

| Treatment Group | Percentage of mothers dead after treatment | | | Number of survivors with litters at term Percentage in ( ) | | |
|---|---|---|---|---|---|---|
| | 129 | BALB/ | C57BL/6 | 129 | BALB/ | C57BL/6 |
| Insulin | 17 | 3 | — | 175(33) | 35(71) | — |
| Tolbutamide | 23 | 18 | 29 | 49(30) | 60(80) | 20(65) |
| Ins. and Nicotinamide | 42 | 25 | — | 48(53) | 18(73) | — |
| Tolb. and Nicotinamide | 16 | 8 | 31 | 66(53) | 37(71) | 12(67) |
| Nicotinamide | 0 | 0 | 0 | 26(65) | 27(90) | 5(80) |
| Fasting (Prepuberal) | 0 | — | — | 444(23) | — | — |
| Fasting (Adult) | 0 | — | — | 128(43) | — | — |
| Water (Prepuberal) | 0 | — | — | 79(33) | — | — |

producing litters an interesting pattern of results became apparent. In each strain the females that had received nicotin amide alone produced the highest propor tion of litters, as compared to any of the other treated or control groups of females within each strain More litters were produced by several groups of females receiv ing nicotinamide in combination with in sulin or tolbutamide than by those groups of females given insulin or tolbutamide alone In strain 129 for example litters were produced by 32% of females receiving insulin alone and by 52% of those receiving insulin plus nicotinamide. Simi larly 30% of the females produced litters following treatment with tolbutamide as compared to 53% after the combination treatment. In strain BALB/c 71% of females given nicotinamide in conjunction with tolbutamide produced litters com pared to only 50% of those given tolbut amide alone. No enhancing effect was seen in this regard with insulin alone or in combination treatment. Nor was any enhancing effect of nicotinamide seen in females of strain B receiving tolbutamide alone or tolbutamide plus nicotinamide.

It seems clear then that nicotinamide when given alone had an enhancing ef fect on litter production in all strains tested. Moreover nicotinamide had no deleterious effect on litter production when used in combination with other agents. In some strains an enhancing effect was found when used in combination with teratogenic treatments.

The two groups of strain 129 females, one group of prepuberal and a second of adult females that were fasted showed a litter production of 23 and 43% respec tively Prepuberal mice that received injections of water in control series produced 33% litters It is interesting that these data fall within the range of results obtained with strain 129 females given treatments which excluded nicotinamide

*Production of fetal abnormalities* The effect of various treatments upon produc tion and types of congenital malformation in mice of strain 129 are indicated in fig ure 1 The frequency (in per cent) of malformations of all types is given as the wide bars above the zero line

Abnormalities resulting from hypogly cemic agents varied from 33% after fast ing of prepuberal mothers to 85% after the combined treatment of tolbutamide and nicotinamide The remaining three hypoglycemic treatments namely insulin, tolbutamide and insulin plus nicotinamide produced abnormalities varying between 56 and 62% Statistical tests (Chi Square) revealed significant differences between fasting (prepuberal mice) and all other teratogenic treatments and between tol butamide plus nicotinamide and the other teratogenic treatments (see legend to fig. 1). It should be emphasized that all hypoglycemia-producing treatments save fast ing of adults produced a significant frequency of fetal malformations

The frequency of malformations result ing from fasting of adults (1%) was not significantly different from that obtained from control animals treated with water or nicotinamide (5 and 2%) The appar ent discrepancy of results obtained by fasting of adults (1%) and prepuberal mothers (33%) will be discussed later Treatments which did not produce hypoglycemia i.e. nicotinamide or water produced an insignificant percentage of mal formed fetuses, yet these showed rib vertebral and skull defects similar to those which followed treatments with teratogenic agents.

The per cent abnormalities resulting from insulin alone or tolbutamide alone was essentially similar 62 and 56% The addition of nicotinamide to these agents demonstrated that treatments with insulin plus nicotinamide were not significantly different from insulin alone (or tolbut amide alone) In contrast the addition of nicotinamide to tolbutamide significantly increased the per cent of malformation to 85% as compared to 56% for tolbutamide alone It is of some interest that the apparent enhancement of the nicotinamide to the tolbutamide effects was not a simple mathematical summation of their single effects

A few remarks are warranted concerning the type of defect produced by the various treatments Three major abnor malities were observed: (1) rib defects which included mainly fusion of two or more neighboring ribs anywhere along

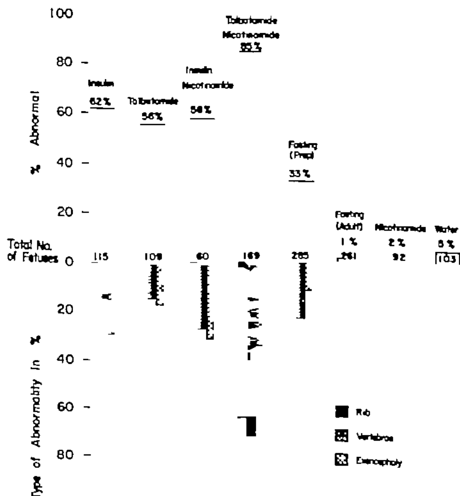



Fig. 1 Effects of treatments (day 9 of gestation) on production of malformations (Strain 129) $X_2$ test for significance between treatments Tolbutamide vs. Tolbutamide + Nicotinamide $P < .0005$. Insulin + Nicotinamide vs. Tolbutamide + Nicotinamide $P < .0005$. Fasting (Prep.) vs. all other teratogenic agents $P < .0005$.

their length. Occasionally entire ribs were fused or lacking. Rib defects occurred bilaterally in many animals but were also observed unilaterally (figs. 3 5 and 6) (2) vertebral defects involved fused neural arches between two or more vetebrae and abnormally ossifying centra were also found (figs. 4 and 6) The vertebral defects occurred in isolated sites along the entire spinal column but most often were found in the thoracic region. It should be borne in mind that the classification of vertebral defects (and other skeletal defects) was based solely on stained, calcified portions of the vertebrae. At the time of sacrifice individual vertebrae were not completely calcified; thus other bony vertebral defects might have appeared later This limitation was not a factor for classification of rib defects or for exencephalia (3) exencephaly or brain hernia resulting from absence of cranial bones, was the third major anomaly regularly observed following teratogenic treatments (fig 3)

The data for the per cent of abnormalities are shown as the "reflected" or downwardly directed bars in figure 1 It will be noticed that rib defects occurred most frequently and approximated the total per centage of malformed fetuses found for

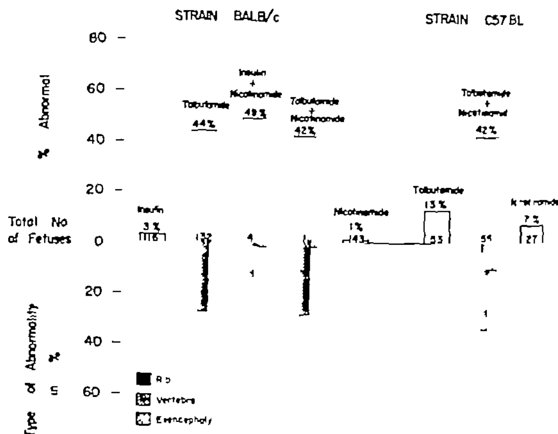



FIG. 2 Effects of treatment (day 9 of gestation) on production of malformation (Strains BALB and C57BL/6) X test for statistical significance between treatment Strain C Insulin vs. Tolbutamide $P < .0005$ Insulin vs. Insulin + Nicotinamide $P < .0005$. Strain B Tolbutamide vs. Tolbutamide + Nicotinamide $P < .0005$

each treatment with the possible exception of the most active teratogenic treatment. The most potent treatment tolbutamide plus nicotinamide revealed a slightly higher per cent of vertebral defects than rib defects. Almost as many vertebral as rib defects were found in the fasting experiments. The per cent of animals obtained with vertebral defects and exencephaly among the various teratogenic treatments was somewhat variable

From 10 to 35% of the total number of fetuses in each group showed exencephaly Exencephaly was found alone or together with other bony defects It should be evident from the data that most of the abnormal fetuses observed had multiple defects particularly those treated with highly potent teratogens

One of the remarkable results obtained in strain BALB/c mice (fig 2) was the relative ineffectiveness of insulin treatment in producing malformations 3% as compared to 62% in mice of strain 129 On the other hand tolbutamide produced 44% abnormalities in strain BALB/c mice as compared to 56% in strain 129 mice

No significant change in the per cent of malformations in strain BALB/c resulted from combining nicotinamide and tolbutamide compared with tolbutamide treatment alone 42% as compared to 44% It may be recalled (fig 1) that nicotinamide plus tolbutamide in mice of strain 129 produced a significant increase in the per cent of malformations over other teratogenic treatments Nicotinamide alone

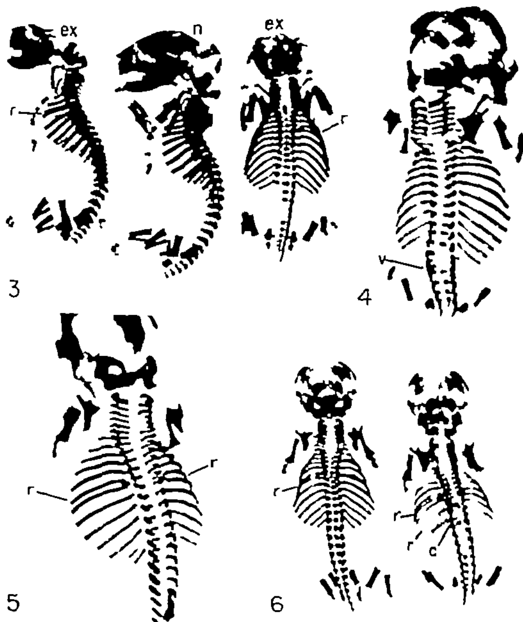



Fig. 3 Strain 129 insulin treatment. Three fetal skeletal preparation stained with alizarin red. The fetuses on the left and on the right show exencephaly (ex), (note absence of skull bones) compare to middle fetus which has normal (n) skull. Note unilateral rib fusion ( ) in fetus on the right.

Fig. 4 Strain BALB/ tolbutamide treatment. This fetus is norm l with th exception of fused vertebral arches ( ) in the lumbar region.

Fig. 5 Strain C57BL/6, tolbutamide treatment. A fetus which shows bilateral rib fusions ( ).

Fig. 6 Strain BALB c, tolbutamide plus nicotinamide treatment. Fetuses which exhibit various rib malform tions ( ). Fetu on right has multiple rib fusions and an bnormal curvature ( ).

was not teratogenic in either strain of mice

In striking contrast to the lack of enhancing potency of nicotinamide when added to tolbutamide in strain BALB/c nicotinamide markedly increased the proportion of malformations when given with insulin an increase from 3 to 44% was obtained No such increase was found in mice of strain 129 after this combined treatment.

The quantity and kind of defects found in mice of strain BABL/c were quite consistent (fig 2) Rib defects were most prevalent in fetuses after each potent treatment. Vertebral defects were also commonly found and were similar in quantity and kind after the three significant teratogenic treatments The type of defects obtained in mice of strain BALB/c was similar to that found in strain 129 mice. However unlike mice of strain 129 exencephaly was rarely seen in mice of this strain.

The small number of mice of strain C57BL/6 observed (fig. 2) suggested that developing ribs vertebrae and cranium were sensitive to teratogenic treatments. Treatment with tolbutamide plus nicotinamide produced a significant per cent of defective fetuses 42% when compared to treatments with tolbutamide alone 13% or with nicotinamide alone 7% The combination treatment was equal in potency to its effect on mice of strain BALB c but less potent than it was to mice of strain 129 (table 1)

Rib and vertebral defects occurred with equal frequency in C57BL mice The frequency of exencephaly 11% was greater than that found in strain BALB c 3% but less than that in strain 129 35%

## DISCUSSION

The results of the present experiments clearly demonstrate the ability of hypoglycemia producing treatments to produce congenital malformations in inbred strains of mice Hypoglycemia producing treatments including single treatment of insulin tolbutamide and fasting of prepuberal mice as well as combination treatments involving nicotinamide plus insulin or tolbutamide are potent teratogens in one or more inbred strains of mice Teratogenic treatments, with the exception of fasting also cause a variable proportion of deaths.

It is evident from the data obtained that the response of different strains of mice to individual treatments as regards teratogenicity or lethality was highly variable It is this variation of responsiveness elicited from each strain of mouse as a group which may be the most pertinent finding in these experiments. The use of highly inbred strains of mice minimizes the variability of response among animals of a single strain due to genetic heterogeneity At the same time this same constancy would exaggerate any differences between strains. The genetic background of each strain no doubt imparts a particular susceptibility or resistance to various environmental agents It follows then that the variation of responsiveness obtained between strains results from an interplay of the genetic background and the environment.

An example of the differential response to an environmental agent as indicated by the production of death was shown by insulin treatment in strain 129 as compared to strain BALB/c Each teratogenic treatment caused a greater proportion of deaths in mice of strain 129 than in other strains (table 1) Most noteworthy is the 3% mortality produced by insulin treatment in strain BALB/c as compared to 17% in strain 129 The resistance to insulin in strain BALB/c mice was overcome by the addition of nicotinamide which raised the death rate to 25% Nicotinamide also increased the lethal effects of insulin in strain 129.

Strain BALB/c mice and the other strains tested were relatively susceptible to tolbutamide Since tolbutamide presumably caused the release of endogenous insulin it is conceivable that exogenous insulin derived from a foreign species could account for the differential responses of inbred strains to insulin.

Nicotinamide may afford some protection against the lethal effects of tolbutamide in strains 129 and BALB c. The nature of the divergent responses after the addition of nicotinamide to insulin or to tolbutamide is not clear The enigma is further complicated by the results of

Heber and Manthei ('61) who reported that nicotinamide elevated blood sugar levels in insulin-treated male mice.

In passing, it should be mentioned that there was no direct relationship between the degree of severity of the treatment (as indicated by mortality percentage) and the per cent abnormalities which resulted. To cite one of several examples tolbutamide and *nicotinamide* which produced 85% abnormalities in strain 129 caused a lesser proportion of death than the other potent teratogens, tolbutamide, insulin or insulin plus nicotinamide.

One rather interesting incidental finding arose from the results regarding the effects of nicotinamide on litter production. In most cases a greater proportion of mice carried litters to term if they had received an injection of nicotinamide (plus daily injections of progesterone) either singly or in conjunction with insulin or tolbutamide. Further investigation of the possible litter-sparing effect of nicotinamide seems to be warranted.

The responsiveness of pregnant mice to teratogenic treatments seems to depend upon the potency of the teratogen and upon the inherent susceptibility of the particularly inbred strain involved. The validity of this statement is supported by the present study and by others mentioned below. Differential responsiveness implies differential susceptibilities of the particular strains of mice but by the same token it assumes that a number of other factors are similar or constant. Firstly it assumes that all embryos (as a group) in every strain had reached the same stage of development at the time of treatment. Secondly it assumes that the development of the skeletal system in each of the different strains was similar in time and in rate. Quite recently Miller ('62) has expressed the notion that not only different developmental rates but changes in the manner of nutritional derivation from the placenta may account for the different responsiveness of inbred strains to a particular teratogenic treatment.

There is no doubt that in mice some hypoglycemic agents are more effective teratogens than others. Fasting of prepuberal mice was not as effective a teratogen as the other hypoglycemic agents. Insulin was mildly teratogenic in strain BALB/c, yet it caused a high per cent of malformations in strain 129.

These results also demonstrate that a combined treatment in some cases can enhance the potency of single treatments. Divergent results between strains were obtained when nicotinamide was combined with insulin in strains 129 and BALB/c. *Enhancement (from 3 to 49%)* resulted in strain BALB/c but not in strain 129. Opposing results were obtained in these same strains with combinations of nicotinamide and tolbutamide. That is potentiation (from 58 to 85%) occurred in strain 129 but not in strain BALB/c. Enhancement from 13 to 42% was observed in strain B mice with these agents.

It is also of interest that two agents, each ineffective or weakly teratogenic when administered alone can be highly teratogenic when given in combination. In strain BALB/c insulin or nicotinamide neither of which produced more than 6% abnormal young when used singly produced 49% abnormal young when used together.

In none of the experiments involving combined treatments of nicotinamide and insulin or tolbutamide was any protection against skeletal deformity obtained. This result contrasts with that reported by Landauer ('48) who found that, in the chick, a portion of the skeletal syndrome of defects produced by insulin could be reversed with nicotinamide.

The kind of defect produced by teratogenic treatments is indicative of the inherent susceptibility of the skeletal system to malformation in the various inbred strains. The results demonstrate that the normal development of ribs and vertebrae can be upset by particular teratogens. All three strains of mice showed a high incidence of rib and vertebral defects varying only quantitatively among strains. The relatively high per cent of malformations of the skeletal system found in mice of strain 129 may be especially due to the inherent weakness of genes controlling normal rib and other skeletal parts. Mackensen and Stevens ('60) have recently reported a mutation causing rib and vertebral defects in this particular strain of mice. No such mutation has been reported

for the other two strains employed in the present study

Although ribs and vertebrae were subject to malformation in all the strains tested, exencephaly was common to only two of the three strains. Exencephaly was rarely found (less than 5% ) in offspring of strain BALB/c, but occurred in 11% of the fetuses of C57Bl mice and in as high as 35% of the young of strain 129

That the kind of malformation produced by various teratogenic agents is dependent on the strain of mice used seems to be demonstrated by these experiments and in investigations of others. Cortisone produced cleft palate in strain A/Jax, but had little effect in mice of strain C57BL/6 (Fraser and Fainstat '51 Kalter '54) Using riboflavin-deficient and galactoflavin-containing diets in 4 inbred strains of mice Kalter and Warkany ('57) showed that malformations produced were characteristic of the particular strain treated Recently Dagg ('60) showed specific strain responses after administration of 5-flourouracil

The results obtained after fasting of strain 129 mice for 24 hours were surprising It was found that only 1% of young were abnormal after fasting pregnant adults The low frequency of abnormalities was at variance with the well substantiated work of Runner ('54) and Runner and Miller ('56) who showed a 28–32% incidence of fetal abnormalities in fasted pregnant adult mice of strain 129 These differences have been reconciled on the realization of different scheduling used to count gestation age the mice in the present study were actually treated one day later even though both experimenters called the treatment day the ninth day

The variation of results between fasted prepuberal (33% malformations) and adult mice (1% malformations) in the present investigation may be explained on the basis of age and size differences of the two groups It seems likely that prepuberal mice being considerably younger and lighter in weight should be more affected by 24 hours of fasting than adult mice

The present study has raised the issue of differences in responsiveness to environmental treatments in inbred strains. Since methods are at hand to readily measure such parameters as blood sugar glycogen and other tissue and cellular components we are continuing our efforts to measure possible physiological and morphological differences in inbred mice following teratogenic treatments.

## SUMMARY

Pregnant females of three inbred strains of mice were treated with various hypoglycemia-producing agents Treatments were given on or during the ninth day of gestation The frequency of malformations of the skeletal system was investigated.

1 All of the treatments involving insulin or tolbutamide singly or in conjunction with nicotinamide produced death ranging from 3 to 42% of the treated mice Mice of strain 129 were most susceptible as a group and particularly to the combined treatment of insulin and nicotinamide

2 A significant increase in the frequency of malformations resulted in strain 129 following a single injection of insulin or tolbutamide or after combination injections of either drug with nicotinamide Malformations were also found after fasting of prepuberal mice for 24 hours. Abnormalities produced included rib and vertebral defects and exencephaly

3. Fasting of adult pregnant mice or injections of water or nicotinamide (10 mg animal) did not produce a significant frequency of malformations

4 Nicotinamide did not protect against the effects of insulin and it enhanced the teratogenic effects of tolbutamide in mice of strain 129

5 Insulin was mildly teratogenic in mice of strain BALB c Tolbutamide on the other hand produced malformations of the ribs and vertebrae Exencephaly was not commonly found in fetuses of this strain.

6 In strain BALB c nicotinamide alone or insulin alone produced but few abnormal young however when the two drugs were given in combination a high incidence of malformations resulted Nic

otinamide did not enhance the teratogenicity of tolbutamide.

7 Tolbutamide plus nicotinamide was teratogenic in mice of strain C57BL/6 Rib and vertebral defects and exencephaly were frequently found after teratogenic treatment.

8 A possible litter-sparing effect of nicotinamide is indicated

9 The frequency and type of defect produced following various teratogenic treatments involves an interplay of the inherent susceptibility (or resistance) and the potency of the environmental agent concerned.

## LITERATURE CITED


Brunnmade, A. F F Büchner and H. Rübsaamen 1956 Missbildungen am Kaninchenembryo durch Insulininjektion beim Muttertier Naturwiss., 43 259

Chomette, G 1955 Entwicklungsstörungen nach Insulinschock beim trächtigen Kaninchen. Beitr. path. Anat., 115 439–451

Degg, C. P 1960 Sensitive stages for the production of developmental abnormalities in mice with 5-fluorouracil. Amer J Anat., 106 89–96.

Edwards, R. G., and R. E. Fowler 1959 Fetal mortality in adult mice after superovulation with gonadotrophins. J Exp. Zool., 141 299–322.

Fraser F C., and T D. Fainstat 1951 Production of congenital defects in offspring of pregnant mice treated with cortisone. Pediatrics, 8 527–533.

Kalter, H. 1954 Inheritance of susceptibility to the teratogenic action of cortisone in mice. Genetics, 39 185–196.

Kalter H., and J Warkany 1957 Congenital malformations in inbred strains of mice induced by riboflavin-deficient, galactoflavin-containing diets. J Exp Zool., 136 531–566.

——— 1959 Experimental production of congenital malformations in mammals by metabolic procedure Physiol Rev 39 69–115.

Kleber H. P and R. W Manthei 1961 Influence of nicotinic acid and nicotinamide on insulin hypoglycemia Proc Soc. E p. Biol and Med. 107 975–977

Landauer W 1948 The effect of nicotinamide and ketoglutaric acid on the teratogenic action of insulin. J Exp. Zool 109 2?3–290

Landauer W and M. B Rhode 195? Further observations on the teratogenic nature of insulin and its modification by supplementary treatment. Ibid., 119 ?21–?6

Mackensen, J A., and L. C Stevens 19?? Rib fusions, new mutation in the mouse Hered., 51 264–268

Miller J R. 1962 A strain difference response to the teratogenic effect of maternal fasting in the house mouse Can J Genet and Cytol., 4 69–78.

Runner M. N 1954 Inheritance of susceptibility to congenital deformity — embryonic instability J Nat. Cancer Inst., 151 637–649

Runner M N and A. Gates 1954 Conception in prepuberal mice following artificially induced ovulation and mating. Nature 174 222–223.

Runner M. N and J R. Miller 1956 Congenital deformity in the mouse as consequence of fasting. Anat. Rec 124 437–438. (abst)

Runner M. N 1959a Embryocidal effect of handling pregnant mice and its prevention with progesterone Ibid., 133 330–331 (abst)

——— 1959b Inheritance of susceptibility to congenital deformity Metabolic clues provided by experiments with teratogenic agents. Pediatrics, 23 245–251.

Smithberg, M., H. W Sanchez and M. N Runner 1956 Congenital deformity in the mouse induced by insulin. Anat. Rec., 126 441 (abst)

Smithberg, M., and M. N Runner 1956 The induction and maintenance of pregnancy in prepuberal mice. J Exp. Zool., 133 441–457

Smithberg, M. 1960 Teratogenic effects of some hypoglycemic agents in mice. Anat. Rec., 136 280 (abst)

Tuchmann-Duplessis, H., and L. Mercier-Parot 1960 Influence of three hypoglycemic sulfamides, carbutamide $BZ_{55}$, tolbutamide $D_{860}$, and chlorpropamide on pregnancy and prenatal development of the rat. Ibid 136 294–295 (abst)

S M S MEDICAL COLLEGE LIBRARY

*DUE DATE SLIP*

*This book is to be returned on or before the date marked below :—*

A fine of annas four will be charged for each day the book is kept overtime.